JOURNAL OF TECHNICAL UNIVERSITY OF MOLDOVA
AND MOLDAVIAN ENGINEERING ASSOCIATION

MERIDIAN INGINERESC

Technical and applied scientific publication founded in

9 February 1995

2

2016

Typesetting and desktop publishing:
Dulgheru Valeriu

Cover: Podborschi V.
Trifan N.

ISSN 1683-853X
Published by Technical University of Moldova

C O N T E N T

REZUMATE

***Băjenescu, T.-M. I.,* Dispozitive memristive (cu memristoare).** Aceste dispozitive sunt comutatoare de rezistențe electrice care pot să-și amintească de starea rezistenței interne pe baza istoricului curentului și tensiunii aplicate. Ele pot înmagazina și trata informația oferind câteva caracteristici-cheie performante care depășesc tehnologia convențională a circuitelor integrate. O importantă clasă de memristoare sunt comutatoare de rezistență cu două terminale, bazate pe mișcarea ionilor, și sunt constituite dintr-un simplu teanc conductor/ izolant/conductor realizat dintr-un film subțire.

***Adascalitei A., Secrieru N., Todos P.* Tehnologie consolidată educațională la ingineria electrică în contextul proiectului TEMPUS CRUNT**. În cadrul proiectului TEMPUS CRUNT, a fost aplicată e-Pedagogia utilizării mediilor TIC (Tehnologii Informatice și de Comunicații) de învățare. Rețeaua inter-universitară E-learning din Moldova utilizează un mediu virtual de învățare cu scopul de a îmbunătăți procesul de formare a studenților în inginerie. Articolul prezintă câteva elemente metodologice care au contribuit la succesul proiectului TEMPUS CRUNT. Mai multe tipuri de cursuri web, bazate pe metodologia Blended Learning sunt evidențiate. Lucrarea de față prezintă materiale de instruire E-learning în inginerie dezvoltate pentru studenți în Mediul Virtual de Instruire a Universității Tehnice a Moldovei, la adresa http://elearning.utm.md/moodle/login/index.php/.
Modelul de Disciplină pentru Inginerie și Tehnologie Electrică (EET) utilizat reprezintă o nouă abordare a procesului de învățare a tehnologiilor electrice; conceptele ingineriei electrice sunt prezentate în mod logic și sunt ilustrate cu exemple de aplicații care interesează pe studenți. Resursele multimedia (de nivel introductiv până la avansat) aferente disciplinelor de Inginerie Electrică pot fi folosite și de profesorii și elevii din învățământul liceal și vocațional (profesional).

***Javgureanu V., Gordelenco P., Bors D.* Particularitățile deformării elasto-plastice și deteriorarea fragilă a acoperirilor electrolitice de fier.** În lucrare se analizează particularitățile de deformare elasto-plastice și deteriorarea fragilă a acoperirilor electrolitice de fier. Sa constatat ca condițiile de electroliza influențează proprietățile de deformare elasto-plastice a acoperirilor electrolitice de fier. Experimental sa demonstrat că cu schimbarea condițiilor de electroliză se schimbă dependența acoperirilor galvanice de fier, la deteriorarea fragilă.

***Mogoreanu N.* Problemele pieței energiei electrice în Republica Moldova: prevederi legale și realitatea.** Prioritățile cheie ale Republicii Moldova în sectorul energetic sunt determinate, în principal, de Strategia Energetică a Republicii Moldova până în a. 2030, adoptată în februarie 2013. Scopul Strategiei este crearea unui mediu energetic mai eficient și mai sigur în Republica Moldova, stabilind trei obiective cheie: securitatea aprovizionării țării cu energie și resurse energetice, dezvoltarea unei piețe energetice concurențiale și dezvoltarea durabilă a sectorului energetic în Republica Moldova. De asemenea, Moldova urmărește să se integreze în rețeaua europeană a operatorilor de sisteme de transport de energie electrică (ENTSO-E). În lucrare se demonstrează faptul că în anturajul energetic regional și cadrul legislativ - regulatoriu existent apariția relațiilor de piață este exclusă.

***Guţuleac E., Zaporojan S., Gîrleanu I., Cărbune V.* Reţele Petri stocastice hibride cu atribute matriceale pentru modelarea proceselor discret-continuie.** În lucrare este introdusă și studiată o nouă clasă de rețele Petri stocastice hibride cu atribute matriceale marcaj-dependente, numite HSMN, care permit de a descrie flexibil dinamica proceselor discret-continue ale sistemelor hibride. Aplicabilitatea acestei abordări este ilustrată prin câteva exemple de modele de HSMN cu diferite atribute matriceale. Un avantaj important al demersului propus constă în faptul că redarea grafică a acestui tip de modele este foarte compactă și flexibilă, deoarece atributele sale sunt matriceal parametrizate.

***Bradu A., Cazacu N.* Proprietățile mecanice ale betonului autocompactant.** Betonul autocompactant (BAC) a marcat o nouă etapă revoluționară în industria construcțiilor. Deși este confecționat din materiale similare betonului tradițional vibrat, caracteristicile reologice diferă esențial. Fluiditatea BAC este obținută ca urmare a introducerii unei cantități mai mari de pulberi și sporirea dozajului de superplastifiant. Aceste modificări ale compoziției și-au lăsat amprenta asupra caracteristicilor mecanice (rezistența la compresiune, rezistența la întindere, modulul de elasticitate), adoptate inițial similare betonului vibrat.

***Marusic G., Marusic D., Puțuntică A.* RiverPrut - Software pentru determinarea și managementul calității apei.** În lucrare se discută problema poluării și calității apei în sistemele de tip "*râu*". A fost creat RiverPrut - software pentru determinarea și managementul calității apei în baza Indicelui de Poluare a Apei.

***Javgureanu V., Gordelenco P., Bors D.* Proprietăţile elastoplastice şi determinarea caracteristicilor de porozitate al acoperirilor electrolitice de fier.** In lucrare se analizează proprietăţile elastoplastice (he; hp; h; Ae; Ap; A; Hh; H; P) şi caracteristicile de porozitate (K, ρ) al acoperirilor electrolitice de fier. Experimental s-a constatat ca proprietăţile elastoplastice al acoperirilor electrolitice de fier au o valoare extremală de variaţia condiţiilor de electroliza (Dk, T). S-a constat, că cu mărirea densităţii de curent (Dk) şi micşorarea temperaturii de electroliza (T), coeficientul care ia în consideraţie densitatea materialului (k) se micşorează, iar porozitatea acoperirilor de fier (p) se măreşte.

Chelmenciuc C., Musteață V., Tcaci L. **Avantajele termodinamice ale integrării cogenerării în cuptoarele de panificație.** În lucrarea dată este argumentată necesitatea reducerii ireversibilității proceselor cu gaze în cuptoare de panificaţie, şi anume este analizat procesul de amestecare a gazelor obţinute în camera de ardere cu gaze recirculate în scopul obţinerii temperaturii necesare a gazelor de ardere în canalele cuptorului. Sunt expuse argumentele în favoarea utilizării cuptoarelor cu gaze de tip tunel în panificaţie în comparaţie cu cele alimentate cu energie electrică. Sunt prezentate esenţa şi beneficiile implementării a două soluţii de cuptoare cu cogenerare integrată.

Kalașnikov V. **Metodă de proiectare a locuințelor de lux cu confort psihologic al colocatarilor de cameră cu diverse psihotipuri.** Articolul a descris în detaliu secvența unei metode de proiectare a unei locuințe psihologic confortabile de lux pentru colegi cu diverse psihopatii pe exemplul designului real al interiorului de lux cu doua dormitoare + kk pentru o familie formată din doi adulți și un copil. Conceptul a inclus o versiune funcțională și rațională a interiorului, care poate fi transformat cu ușurință într-un stil modernist, cu elemente de proiectare ecologică. Această metodă accelerează procesul de proiectare, iar rezultatul oferă un confort cuprinzător de ședere pentru toți colegii de cameră.

Bantea-Zagareanu V., Canja A. **Elaborarea concentratelor alimentare pentru mic-dejun destinate alimentației curative.** Prezenta lucrare se referă la elaborarea și cercetarea sortimentului de concentrate alimentare pentru mic-dejun, destinate alimentației curative. Scopul în sine al studiului de cercetare a fost de a elabora o rețetă de fabricație a concentratelor alimentare pentru mic-dejun destinate alimentației curative, în special persoanelor ce suferă de diabet zaharat sau alte afecțiuni metabolice și nutriționale și concomitent de a obține o caracteristică amplă a produselor respective, din punct de vedere al indicilor fizico-chimici și senzoriali. Se urmărește prin intermediul gamei sortimentale de produse obținute experimental de a îmbunătăți valoarea alimentară a produselor cerealiere în amestec: muesli și granola. Gama sortimentală propusă este una inovativă și unică pe piața autohtonă.

Cazac V. **Sistem de control al acționării de curent alternativ a bobinatorului liniei de trefilare.** În această lucrare sunt analizate modalitățile de utilizare a motorului asincron cu rotorul în scurtcircuit pentru acționarea mecanismelor de bobinare ale liniilor de trefilare a firelor, controlate cu convertor de frecvență. Pe baza metodelor teoretice şi practice este ajustată bucla sistemului de control automat al forței din sârmă la bobinare. Metoda de control propusă a mecanismului de bobinare a demonstrat o eficiență înaltă pentru linia de trefilare a sârmei și stabilitate în gamă largă de viteze de lucru (0-1200 m/min), de asemenea, o stabilitate ridicată la accelerare și decelerare a mașinii de trefilare fără șocurile mecanice care pot duce la ruperea firul procesat.

Nicolaev P. **Impedanţmetru cu rezonanţă simulată.** Lucrarea este dedicată problemelor de măsurare automată a componentelor impedanței în coordonate carteziene. În lucrare este prezentată structura şi principiul de funcţionare a impedanţmetru cu rezonanţă simulată caracterizat prin simplitate, precizie şi cost redus. O atenție deosebită s-a acordat componentelor impedanţ-metrului ce permit automatizarea procesului de măsurare şi prelucrarea datelor.

Cojuhari I., Izvoreanu I., Fiodorov I., Moraru D. **Sinteza algoritmului de conducere cu procesul termic în cuptor.** În lucrare se propune acordarea algoritmului tipizat PID în baza metodelor analitice şi experimentale în cadrul sistemului automat de reglare a temperaturii în cuptorul electric, unde reglarea temperaturii se realizează în baza controlerului industrial TRM-151, firma OWEN. S-a ridicat procesul tranzitoriu experimental al variaţiei temperaturii în cuptor şi prin procedura de identificare s-a determinat modelul matematic al cuptorului. Acordarea algoritmului PID s-a făcut în baza metodei gradului maximal de stabilitate şi metodei Ziegler-Nichols. Rezultatele obţinute s-au verificat experimental pe instalaţie şi în pachetul de programe MATLAB.

Bostan I., Piso I.M., Bostan V., Badea A., Secrieru N., Manciu G. V. **Perspectivele cooperării Universității Tehnice a Moldovei cu Agenția Spațială Română în domeniul tehnologiilor satelitare.** Acest articol reflectă viziunea autorilor asupra perspectivelor cooperării internaționale în domeniul tehnologiilor satelitare, care se dezvoltă vertiginos cu o extindere spectaculoasă în diverse domenii de interes științific, economic și social. În majoritatea țărilor europene preocupările în domeniul tehnologiilor satelitare câștigă tot mai mult teren în cadrul Centrelor Universitare și de Cercetare, atrăgând în sfera cercetării noi adepți, în special din rândul tinerilor cercetători. În ultimii ani spectrul tematic al cercetărilor științifice s-a extins vertiginos, au fost deschise noi școli științifice și structuri instituționale de cercetare-dezvoltare profilate pe domeniul tehnologiilor spațiale. Odată cu semnarea Acordului de Asociere a Republicii Moldova la Programul European pentru cercetare-inovare Orizont 2020, se deschid noi oportunități de participare a comunității academice moldovenești la Programele Europene de dezvoltare a tehnologiilor spațiale.

Bostan I., Piso I.M., Bostan V., Badea A., Secrieru N., Trusculescu M., Candraman S., Margarint A. **Arhitectura rețelei stațiilor terestre de comunicații cu sateliți.** Acest articol reflectă viziunea autorilor asupra perspectivelor cooperării internaționale în domeniul tehnologiilor satelitare, care se dezvoltă vertiginos cu o extindere spectaculoasă în diverse domenii de interes științific, economic și social. În majoritatea țărilor Europene preocupările în domeniul tehnologiilor satelitare câștigă tot mai mult teren în cadrul centrelor universitare și de cercetare, atrăgând în sfera cercetării noi adepți. Rețeaua de stații terestre pentru comunicații satelitare devine o platforma pentru o cooperare mai strânsă, în special în rândul tinerilor cercetători.

ABSTRACT

Băjenescu T.-M.I. **Reliability aspects of MEMS and RF Microswitches**. As MEMS technology is implemented in a growing range of areas, the reliability of MEMS devices is a concern. Understanding the failure mechanisms is a prerequisite for quantifying and improving the reliability of MEMS devices. This paper reviews the common failure mechanisms in MEMS and highlights some of the reliability concerns for both ohmic and capacitive MEMS switches. Ohmic switches fail catastrophically by stiction whereas dielectric charging leads to degraded performance of capacitive switches.

Adascalitei A., Secrieru N., Todos P. **Technology enhanced electrical engineering Education in context of CRUNT TEMPUS project.** In the CRUNT TEMPUS project, e-pedagogy of using ITC learning environments was used. E-learning inter-university network of Moldova uses a virtual learning environment for training and learning process improvement dedicated to engineering students. The article presents some methodological elements that contributed to the success of TEMPUS CRUNT Project. Several web courses, based on Blended Learning methodology are highlighted. This paper presents e-learning instruction materials for engineering undergraduates developed on the Virtual Learning Environment http://elearning.utm.md/moodle/login/index.php/. Electrical Engineering and Technology (EET) Discipline model is a new approach to learning electrical technology-one that presents concepts in the customary logically developed order but illustrates them with exemplars that reflect the applications students are interested in. Electrical Engineering Discipline resources are especially for secondary school teachers and students, with topics ranging from introductory to advanced Electrical Engineering and Technology.

Javgureanu V., Gordelenco P., Bors D. **Features elasto-plastic deformation and brittle fracture, electrolytic iron coatings.** The paper analyses the peculiarities of deformation and fragile damage elasto-plastic coatings electrolytic iron. It was found that the electrolysis conditions influence the elasto-plastic deformation properties of electrolytic iron coatings. Experimental, it was demonstrated that changing the electrolysis conditions changes the electroplating iron dependency at the fragile damage.

Mogoreanu N. **Moldovan electricity market problems: legal provisions and reality.** Moldovan energy sector key priorities are determined mainly by the Energy Strategy of the Republic of Moldova till year 2030, document adopted in February 2013. The Strategy aims to create a more energy efficient and safe environment in the country, establishing three goals: security of energy supply and of energy resources, development of a competitive energy market and sustainable development of the energy sector in Moldova. Moldova also aims to integrate into the European network of transmission system operators of electricity (ENTSO-E). This paper demonstrates that due to regional energy environment as well as to the existing legislative-regulatory framework, the emergence of market relations is impossible.

Guţuleac E., Zaporojan S., Gîrleanu I., Cărbune V. **Hybrid stochastic Petri nets with matrix attributes for modelling of discrete-continuous process.** This paper introduces a new class of hybrid stochastic Petri nets (called *HSMN*) with marked-controlled matrix attributes which allow high flexibility in describing the discrete-continuous processes dynamics of hybrid systems. The applicability of this approach is illustrated through a few examples of *HSMN* models with different matrix attributes. An important advantage of the proposed approach is that the graphic representations of these kinds of models are very compact and flexible because their attributes are matrix parameterized.

Bradu A., Cazacu N. **Mechanical properties of self-compacting concrete.** Self-compacting concrete (SCC) marked a revolutionary step in the construction industry. SCC components are similar to vibrated concrete but its rheological characteristics are different. SCC fluidity is achieved as result of introducing a larger quantity of powder and increased dosage of superplasticizer. The changes made in concrete composition affect its mechanical characteristics (compressive strength, tensile strength and modulus of elasticity); those were adopted similar with vibrated concrete.

Marusic G., Marusic D., Puţuntică A. **RiverPrut - Software for determination and management of water quality.** This paper discusses the problem of water pollution and water quality in river-type systems. RiverPrut, software for determination and management of water quality based on Water Pollution Index, was created.

Javgureanu V., Gordelenco P., Bors D. **The elasto-plastic properties and porosity characterizations of coatings electrolytic iron.** The paper analyses the elasto-plastic properties (He, Hp, H, A; Ap; A; Hh, H, P) and porosity characteristics (K, ρ) of electrolytic iron coverings. Experimental, it was found that the elasto-plastic properties of electrolytic iron coatings have an extremely value of variation electrolysis conditions (Dk, T). It was noted that with increasing current density (Dk) and decreasing temperature electrolysis (T) coefficient that takes into account material density (K) shrinks and coverings iron porosity (p) increases.

Chelmenciuc C., Musteaţă V., Tcaci L. **The thermodynamic benefits of the integration of cogeneration installations in bakery ovens.** The present work is motivated by the need to reduce the irreversibility of the process with combustion gas in bakery ovens, especially

it was analysed the process of the mixing of the obtained gases in the combustion chamber with the recycled gases in order to achieve the necessary temperature of the flue-gas in the oven channels. There are also exposed the arguments in favour of using gas tunnel ovens in the bakery compared with the electrical ovens. There are presented the essence and benefits of the implementation of two solutions of ovens with integrated cogeneration installation.

Kalashnikova V. **Method of designing of the elite dwelling for the cohabitants with different psychotypes.** The article described in details the sequence of method of designing of the elite dwelling for the cohabitants with different psychotypes on the example real interior design an elite three-room flat for a family consisting of two adults and a child. Described the concept and implemented a rational and functional interior variant that is easily transformed, into a modern style with elements of ecodesign. Using this method speeds up the design process, and the result has been providing complex comfort accommodation for all cohabitants.

Bantea-Zagareanu V., Canja A. **Development of breakfast food concentrates for therapeutic nutrition**. This paper refers to the development and research of the assortment of breakfast food concentrates, intended for therapeutic nutrition. The goal itself of this research study was to develop a recipe for breakfast food concentrates, that can be consumed especially by people suffering from diabetes or other metabolic disorders and nutrition and simultaneously to obtain a large characteristic of those products in terms of physico-chemical and sensorial indexes. It aims through this experimentally obtained product to improve the nutritional value of cereal mix: muesli and granola. The proposed assortment is an innovative and unique on our internal market.

Cazac V. **The Winder Control System with Alternative Current Drive of Wire Drawing Line.** In this paper are analysed the ways of using the asincron motor with rotor in short circuit for driving the winding mechanisms of the wire drawing machines controlled by frequency converter. Based on the theoretical and practical methods was adjusted the loop of the automatic control system of tension force in the wire. The proposed control method of winding mechanism demonstrated a maximum efficiency for wire driving machine and stability in wide range of working speeds (0–1200 m/min), also this method have a high stability at acceleration and deceleration of the wire drawing machine without mechanical shocks that can lead the processed wire to break.

Nicolaev P. **Impedance meter with simulated resonance.** The paper is dedicated to the problems of automatic measurement of the impedance components in Cartesian coordinates. In paper is presented the structure and the operating principle of the impedance meter with simulated that is characterized by simplicity, accuracy and low cost. A particular attention was given to the components of the impedance meter that enables the automation of the measurement and the processing of the results.

Cojuhari I., Izvoreanu I., Fiodorov I., Moraru D. **Synthesis of the control algorithm with thermal process in the oven.** In this paper was proposed to tune the typical PID controller by the analytical and experimental methods in the thermic automatic control system, where the temperature regime was proposed to control by the industrial TRM-151 controller. It was obtained the experimental curve of the temperature variation and using the identification procedures was obtained the mathematical model. The tuning of the PID controller was done by the maximum stability degree method and Ziegler-Nichols method. The obtained results were verified experimental by the installation and in the MATLAB.

Bostan I., Piso I.M., Bostan V., Badea A., Secrieru N., Manciu G. V. **Prospects for cooperation of the technical university of Moldova with Romanian space agency in the field of space technologies.** This paper reflects the vision of the authors on the prospects of international cooperation in the field of satellite technologies, which are developing rapidly with a spectacular expansion in various areas of scientific, economic and social interest. In most European countries the concerns in satellite technologies are gaining more ground in the universities and research centres attracting in research new adherents, especially among young researchers. In recent years the thematic variety of scientific research has expanded rapidly, new scientific schools and institutional structures of research - development in the area of space technologies were opened. The Republic of Moldova takes the first steps in this field. After signing the Agreement of Association of the Republic of Moldova to the European research – innovation programme – Horizon 2020 in June 2014, new opportunities open regarding the participation of Moldovan academic community in European programmes for the development of space technologies.

Bostan I., Piso I.M., Bostan V., Badea A., Secrieru N., Trusculescu M., Candraman S., Margarint A. **Architecture of the ground stations - satellites communication network.** This paper reflects the vision of the authors on the prospects of international cooperation in the field of satellite technologies, which are developing rapidly with a spectacular expansion in various areas of scientific, economic and social interest. In most European countries the concerns in satellite technologies are gaining more ground in the universities and research centres attracting new adherents in the research area. The network of ground stations for satellite communications becomes a platform for closer cooperation, especially among young researchers.

SOMMAIRE

in fours de boulangerie et ceux avec cogénération intégrée. Dans cet article, il est soutenu la nécessité de réduire l'irréversibilité du processus des gaz dans les fours de boulangerie, Il a analysé le processus de mélange du gaz produit dans la chambre de combustion avec gaz recirculés dans le but d'obtenir la température nécessaire du gaz de combustion dans les canaux du four. Ils sont exposés les arguments en faveur de l'utilisation de fours à gaz du catégorie tunnel en boulangeries par rapport à l'électricité. Ils sont présentés l'essence et les avantages de la mise en œuvre des deux solutions des fours avec cogénération intégrée.

Kalashnikova V. **Méthodes de conception de confort psychologique des logements de luxe à un colocataire avec différents psychotypes.** L'article décrit en détail la séquence d'un procédé de conception d'un logement de luxe psychologiquement confortable pour cohabitants avec divers psycho sur l'exemple de la conception réelle de l'intérieur de luxe de deux chambres pour une famille composée de deux adultes et un enfant. Le concept et la mise en œuvre d'une version fonctionnelle et rationnelle de l'intérieur, qui peut être facilement transformé dans, un style moderniste avec des éléments de l'écoconception. Cette méthode accélère le processus de conception, et le résultat offre un confort complet à résider pour tous les colocataires.

Bantea-Zagareanu V., Canja A. **Développement de petit-déjeuner concentrés alimentaires pour la nutrition thérapeutique.** Ce document se réfère à la mise au point et la recherche de l'assortiment de produits concentrés de petit déjeuner, destinés à l'alimentation thérapeutique. Le but même de cette étude était de développer une recette pour les concentrés alimentaires, qui peut être consommé en particulier par les personnes souffrant de diabète ou d'autres troubles métaboliques et nutrition et simultanément pour obtenir une grande caractéristique de ces produits en termes de propriétés physico -chimiques et indices sensoriels. Il vise, à travers ce produit obtenu expérimentalement pour améliorer la valeur nutritionnelle du mélange de céréales : muesli et granola. L'assortiment proposé est une société innovante et unique sur notre marché intérieur.

Cazac V. **Système de contrôle des actionnaires du courant alternatif de mécanisme d'enroulement de la ligne de tréfilage.** Ce document a analysé l'utilisation du moteur à induction à cage d'écureuil pour d'actionnement les mécanismes d'enroulement de lignes de tréfilage de fils, contrôlées avec convertisseur de fréquence. Basé sur des méthodes théorique et pratique est ajustée de la boucle du système de contrôle automatiquement force du fil de bobinage. La méthode de contrôle proposée mécanisme d'enroulement a démontré une efficacité élevée de ligne de tréfilage de fil et de la stabilité dans la large plage de vitesse (0-1200 m/min), aussi, une grande stabilité sur l'accélération et la décélération de tréfilage de la machine sans chocs mécaniques qui peuvent entraîner la rupture du fil traité.

Nicolaev P. **Impédance mètre avec la résonance simulée.** Le travail est dédié aux problèmes de la mesure automatique des composants d'impédance en coordonnées cartésiennes. Le travail présente la structure et le principe de fonctionnement de l'impédance mètre avec la résonance simulée, caractérisé par la simplicité, précision et à faible coût. Une attention particulière été donné aux composants de la impédance mètre qui permet l'automatisation de la mesure et le traitement des résultats.

Cojuhari I., Izvoreanu I., Fiodorov I., Moraru D. **Synthèse des algorithmes de réglage des régimes thermiques d'un four.** Dans ce travail est proposée une méthode de mis en calcul des paramètres de l'algorithme PID typique, en utilisant des méthodes analytique et expérimentale de recherches pour un système de réglage automatique des régimes thermiques d'un four électrique où la régulation de la température est réalisée sur la base du régulateur industriel TRM-151 (la société OWEN, Russie). Pour la température du four a été déterminée la réponse indicielle sur la base duquel, en utilisant la procédure d'identification, était construit un modèle mathématique du four. Pour calculer des paramètres de l'algorithme PID était utilisés les critères du degré maximum de stabilité et de Ziegler - Nichols. Ces résultats ont été vérifiés expérimentalement dans une usine expérimentale et modélisées dans MATLAB.

Bostan I., Piso I.-M., Bostan V., Badea A., Secrieru N., Manciu G. V. **Les perspectives de la coopération de l'Université Technique de Moldavie avec l'Agence Spatiale Roumaine dans le domaine des technologies spatiales.** Ce papier reflète la vision des auteurs sur les perspectives de la coopération internationale dans le domaine des technologies satellitaires, qui se développent rapidement avec une expansion spectaculaire dans divers domaines d'intérêt scientifique, économique et social. Ces dernières années, la variété thématique de la recherche scientifique a augmenté rapidement, de nouvelles écoles scientifiques et les structures institutionnelles de la recherche - développement dans le domaine des technologies spatiales ont été ouvertes. La République de Moldova prend les premiers pas dans ce domaine. Après la signature de l'accord d'association de la République de Moldova à la recherche européenne - programme d'innovation - Horizon 2020 en Juin 2014, ouvre de nouvelles possibilités en ce qui concerne la participation de la communauté universitaire moldave dans les programmes européens pour le développement des technologies spatiales.

Bostan I., Piso I.M., Bostan V., Badea A., Secrieru N., Trusculescu M., Candraman S., Margarint A. **L'architecture des réseau stations au sol de communication de satellites.** Cette papier reflète la vision des auteurs sur les perspectives de la coopération internationale dans le domaine des technologies satellitaires, qui se développent rapidement avec une expansion spectaculaire dans divers domaines d'intérêt scientifique, économique et social. Dans la plupart des pays européens, les préoccupations en matière de technologies satellitaires gagnent plus de terrain dans les universités et les centres de recherche d'attirer de nouveaux adeptes dans le domaine de la recherche. Le réseau de stations terrestres pour les communications par satellite devient une plateforme pour une coopération plus étroite, en particulier chez les jeunes chercheurs.

РЕЗЮМЕ

Бэженеску Т. М. И. **Устройства пизастор (с пизасторами).** Эти устройства представляют собой переключателями электрических резисторов которые могут вспомнить состояние внутреннего сопротивления на базе истории и текущего приложенного напряжения. Они могут хранить и обрабатывать информацию, предлагая некоторые ключевые характеристики, превосходящие обычные технологии интегральных схем. Важным классом мемристоров являются переключатели сопротивления с двумя терминалами, основанные на перемещении ионов, и состоят из простого стека проводник / диэлектрик / проводник, выполненного из тонкой пленки.

Адаскалицей А., Секриеру S., Тодос Р. **Усовершенствованная технология электрического инженерного образования в контексте проекта CRUNT TEMPUS**. В проекте CRUNT TEMPUS использованы методы электронный педагогике с использованием среды обучения ИТК. Межвузовская сеть электронного обучения Молдовы использует виртуальную среду обучения для совершенствования учебного процесса и обучения, посвященный студентов инженерных факультетов. В статье представлены некоторые методологические элементы, которые внесли свой вклад в успех проекта TEMPUS CRUNT. Некоторые веб-курсы, основанные на методологии смешанного обучения, выдвинуты на первый план. В статье представлены учебные материалы электронного обучения для инженерных студентов, разработанных на Virtual Learning Environment http://elear-ning.utm.md/ moodle/login/index.php/. Модель дисциплины «*Электротехника и технологии (EET*)» представляет собой новый подход к изучению электрической технологии, который представляет концепции в обычном логическом порядке, но иллюстрируется примерами, интересных для студентов. Ресурсы электротехнической дисциплины могут быть использованы учителями и студентами среднего образования, начиная от начального до продвинутого уровня электротехники и технологии. Модули электронного обучения используют визуализацию электротехнических концепций.

Жавгуреану В., Горделенко П., Борщ Д., **Особенности упругопластической деформации и хрупкого разрушения, электролитических железных покрытий.** В статье анализируются особенности упругопластической пластической деформации и хрупкого разрушения электролитических железных покрытий. Было установлено, что условия электролиза влияют на упругопластическую деформацию и свойства покрытий электролитического железа. Экспериментально было продемонстрировано, что с изменением условия электролиза изменяются зависимость электролитических железных покрытий к хрупкого разрушению.

Могоряну Н. **Проблемы рынка электрической энергии Республики Молдова: законодательные предпосылки и реальность.** Ключевые приоритеты энергетического сектора Республики Молдова определены Энергетической Стратегией Республики Молдова до 2030 года, утвержденной Правительством в феврале 2013 года. Основной задачей Стратегии является создание эффективной и надежной энергетической среды в республике, определив три ключевых направления: надежность обеспечения страны энергией и энергетическими ресурсами, развитие конкурентного энергетического рынка и развитие энергетического сектора. Одновременно преследуется цель интегрироваться в европейскую энергетическую систему транспортных операторов электрической энергии (ENTSO-E). В предлагаемой работе показано что при существующем региональном энергетическом антураже и при нынешней законодательной базе возникновение рыночных отношений в секторе электрической энергии исключается.

Гуцуляк Е., Запорожан С., Гырляну И., Кэрбуне В. **Гибридные стохастические сети Петри с матрицными атрибутами для моделирования дискретно-непрерывных процессов.** В работе представлен новый класс гибридных стохастических сетей Петри с маркировочно-контролируемых матрицными атрибутами (ГССПМ), которые позволяют гибко описывать динамику дискретно-непрерывных процессов гибридных систем. Применимость такого подхода иллюстрируется несколькими примерами моделей ГССПМ с различными матрицными атрибутами. Важным преимуществом предлагаемого подхода состоит в том, что графические представления этих видов моделей очень компактны и гибки для исследования.

Браду А., Казаку Н. **Механические свойства самоуплотняющегося бетона.** Самоуплотняющийся бетон (СУБ) ознаменовало новый революционный шаг в строительной отрасли. Несмотря на то, что он состоит из аналогичных материалов традиционно вибробетона, его реологические характеристики существенно отличаются. Высокое подвижности бетонный смеси обеспечивается за счет увеличенной долей мелкого заполнителя, и повышении дозировки суперпластификатора. Эти изменения в составе оказывают воздействие на механические свойства (прочность на сжатие, прочность на растяжение, модуль упругости), каторые первоначально были приняты аналогичными вибробетона.

Марусик Г., Марусик Д., Пуцунтикэ А. **RiverPrut – программное обеспечение для определения и управления качеством воды.** В данной статье рассматривается вопрос загрязнения и качества воды в реках. Было разработано программное обеспечение для определения и управления качеством воды на основе Индекса Загрязнения Воды.

Жавгуреану В., Горделенко П., Борщ Д., **Упругопластические свойства и определение характеристик пористости железных электролитических покрытий.** В данной работе представлены экспериментальные исследования упругопластических свойств (he; hp; h; Ae; Ap; A; Hh; H; P) и характеристики пористости (K, ρ) железных электролитических покрытий. Экспериментально установлено, что упругопластические свойства железных электролитических покрытий имеют практическое значение с изменением условий электролиза (Dk, T). Установлено также, что с увеличением плотности тока (Dk) и уменьшением температуры электролиза (T), коэффициент, учитывающий степень уплотнения материала, уменьшается, а пористость (ρ) увеличивается.

Chelmenciuc C., Musteață V., Tcaci L. **Эксергетический анализ процессов производства газов в туннельных печах для выпечки хлеба и в печах с внедрённой когенерацией.** В данной работе мотивирована необходимость уменьшения необратимости газовых процессов в хлебопекарных печах, т.е. анализирован процесс смешения газов из камеры сгорания с рециркулируемыми газами в камере смешения для того чтобы получить требуемую температуру дымовых газов в каналах печи. Представлены аргументы в пользу использования газовых печей, туннельного типа в пекарнях, по сравнению с печами с электрическим подогревом.

Калашникова В. **Метод проектирования психологически комфортного элитного жилья для сожителей с различными психотипами.** В статье подробно описано последовательность метода проектирования психологически комфортного элитного жилья для сожителей с различными психотипами на примере реального проектирования интерьера элитной трехкомнатной кватиры для семьи, состоящей из двух взрослых и ребенка. Разработана концепция и реализовано функциональный и рациональный вариант интерьера, который легко трансформируется, в стиле модерн с элементами экодизайна. Использование этого метода ускоряет процесс проектирования, а результат обеспечивает комплексный комфорт проживания для всех сожителей.

Бантя-Загареану В., Канжа А. **Разработка пищевых концентратов для завтрака**, **предназначенных для лечебного питания**. Статья относится к исследованию ассортимента продуктов питания для завтрака в виде пищевых концентратов, предназначенных для лечебного питания. Цель исследовательской работы было разработать продукты питания для завтрака в виде пищевых концентратов предназначен-ные особенно людям, страдающим от диабета или других нарушений обмена веществ и питания. Одновременно исследуется общая характеристика этих продуктов с точки зрения физико-химических и сенсорных показателей. Также рассматривается ассортимент продукции выпускаемой экспериментально с точки зрения повышения питательной ценности зерновых продуктов в смешанном виде: мюсли и гранола. Предлагаемый ассортимент является инновационным и уникальным на внутреннем рынке.

Казак В. **Система управление электроприводом переменного тока намоточного механизма волочильной линий.** В работе анализируются способы использования асинхроного двигателя с короткозамкнутым ротором для приведения в действие намоточного механизма волочильного стана для проволоки, управляемым преобразователем частоты. На основе теоретических и практических методов настроили систему автоматического контроля силы в проводе при намотки. Предлагаемый способ управления намоточного механизма продемонстрировал высокую эффективность для волочильного стана и стабильность в широком диапазоне рабочих скоростей (0-1200 м/мин). Способ имеет высокую устойчивость при ускорении и замедлении волочильного стана, без шоков, которые могут привести к разрыву обработанной проволоки.

Николаев П. **Измеритель импеданса с имитированной резонанса.** Работа посвящена проблемам автоматического измерения составляющих импеданса в декартовой системе координат. В статье представлена структура и принцип работы измерителя импеданса с имитированной резонанса, который характеризуется простотой, точностью и низкой стоимостью. Особое внимание было уделено компонентам измерителя импеданса, который позволяет автоматизировать измерения и обработку результатов.

Кожухарь И., Изворяну Б., Фёдоров И., Морару Д. **Синтез алгоритма управления температурным режимом в печи.** В работе предлагается метод определения параметров настройки типового ПИД-алгоритма, используя аналитические и экспериментальные методы на примере автоматической системы управления температурным режимом в электрической печи, реализованной на базе промышленного регулятора ТРМ-151, фирмы OWEN. Для печи была снята переходная характеристика изменения температуры, на основе которой, используя процедуру идентификации, была построена математическая модель печи. Полученные результаты были проверены экспериментально на промышленной установке и смоделированы в MATLABe.

Бостан И., Писо И.М., Бостан В., Бадя А., Секриеру Н., Манчу Г. **Перспективы сотрудничества Технического Университета Молдовы с Румынским Космическим Агентством в области космических технологий.** Статья отражает видение авторов о перспективах международного сотрудничества в области спутниковых технологий, которые развиваются быстрыми темпами с захватывающим расширения в различных областях научного, экономического и социального интереса. В большинстве европейских стран озабоченность в спутниковых технологий приобретают все больше пространства в университетах и научно-исследовательских центров, привлекающих в исследованиях новых приверженцев, особенно среди молодых исследователей. В последние годы тематическое многообразие научных исследований быстро расширяется, новые научные школы и институциональные структуры исследования - были открыты разработки в области космических технологий. Республика Молдова делает первые шаги в этой области. После подписания Соглашения о ассоциации Республики Молдова к Европейскому исследования – инновационной программы - HORIZON 2020 в июне 2014 года, новые возможности открываются в отношении участия молдавских академического сообщества в европейских программах развития космических технологий.

Бостан И., Секриеру Н., Бостан В., Бадя А., Секриеру Н., Трускулеску М., Кандраман С., Маргаринт А. **Архитектура сети наземных станций спутниковой связи.** Эта статья отражает видение авторов о перспективах международного сотрудничества в области спутниковых технологий, которые развиваются быстрыми темпами с захватывающим расширения в различных областях научного, экономического и социального интереса. В большинстве европейских стран озабоченность в спутниковых технологий приобретают все больше пространства в университетах и научно-исследовательских центров привлечения новых сторонников в области научных исследований. Сеть наземных станций спутниковой связи становится платформой для более тесного сотрудничества, особенно среди молодых исследователей.

MEMRISTIVE DEVICES

Titu-Marius I. Băjenescu, prof.
Switzerland

1. INTRODUCTION

The emergence of the Internet of Things (IoT) and the insatiable demand for smart devices in every aspect of life is driving a complete overhaul of traditional wisdom in the microcontroller and embedded memory markets. The driving force behind the semiconductor industry is twofold: *(i)* Develop new material systems which exhibit novel or superior properties which can be exploited in various applications and devices. *(ii)* Decrease the size of constituent devices in order to make them more powerful and accessible to society.

The industry is currently facing barriers which will stall the scaling of memory and storage. In order to overcome these barriers, new materials and methods must be considered.

The NAND structure was introduced in 1987 by Dr. Fujio Masuoka from Toshiba. This structure uses a string of Electronically Erasable Programmable Read Only Memory (EEPROM) transistors connected in a series. NAND Flash technology has been serving the storage memory applications market for several decades – thus creating a dependency that has steadily increased due to its scaling technology.

Flash memory is a form of non-volatile EEPROM. Flash memory arrays consist of a grid of columns and rows, with two transistors at each intersection. A thin oxide layer separates the two transistors, known as the floating gate and control (external) gate (Figure 1). Flash memory cells work via the application of an electric field to the control gate. The field causes electrons to become trapped at the oxide-floating gate interface. A value of 0 or 1 is assigned to the memory cell based off of the shift in threshold voltage caused by the presence of electrons[1]. However, in recent years, further scaling of this technology has shown profound limitations.

Currently, it is widely accepted that scaling below 25 nm has significantly degraded performance and reliability, thus, resulting in significant overhead complexity and computational power-demand from the system controller. System manufacturers as well as NAND Flash manufactures have begun the quest for a new technological solution. For several years now, companies[2] have focused on developing a next generation memory technology that will lead to significant improvements in reliability, performance, low power operation and scalability compared to existing non-volatile memories.

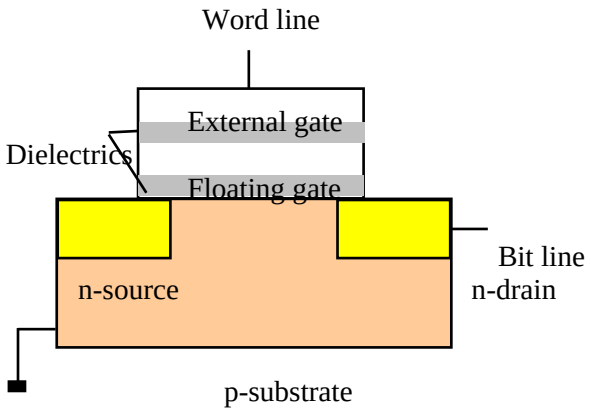

Figure 1. *Flash memory cell (after [1]).*

Several non-volatile memory device structures such as Ferroelectric RAM (FeRAM), Magneto-resistive RAM (MRAM), Organic RAM (ORAM) and Phase Change RAM (PRAM) have been proposed [3]. Resistive Random Access Memory, (RRAM or ReRAM), shows superior switching speeds, requires less power, exhibits high endurance, and is compatible with current CMOS manufacturing processes.

[1] However, current models of flash store a limited number of electrons within the thin oxide layer. Because the system is sensitive to fluctuations in charge density, the loss of a single electron from thermal contributions can lead to loss of retention. Further scaling of Flash technology will only exacerbate losses.

[2] RRAM-based disruptive technologies have been sited and chosen by major R&D corporations as the best potential replacement for NAND Flash. At IEDM 2010, Sungjoo Hong from Hynix stated that *"RRAM can be one of the suitable candidates for a storage application due to its possibility of multi-stackable crosspoints."* During the 2011 Flash Summit, SanDisk CTO Yoram Cedar presented this message: *"3D RRAM technology development shows the best promise for a scalable post-NAND technology".* Again, at the 2013 ISSCC, Tz-Yi Liu from SanDisk presented *"32 Gbit RRAM Memory Device in 24 nm Technology," where he stated that "RRAM has been considered one of the potential technologies for the next generation non-volatile* memory, given its fast access speed, high reliability, and multi-level capability." [2].

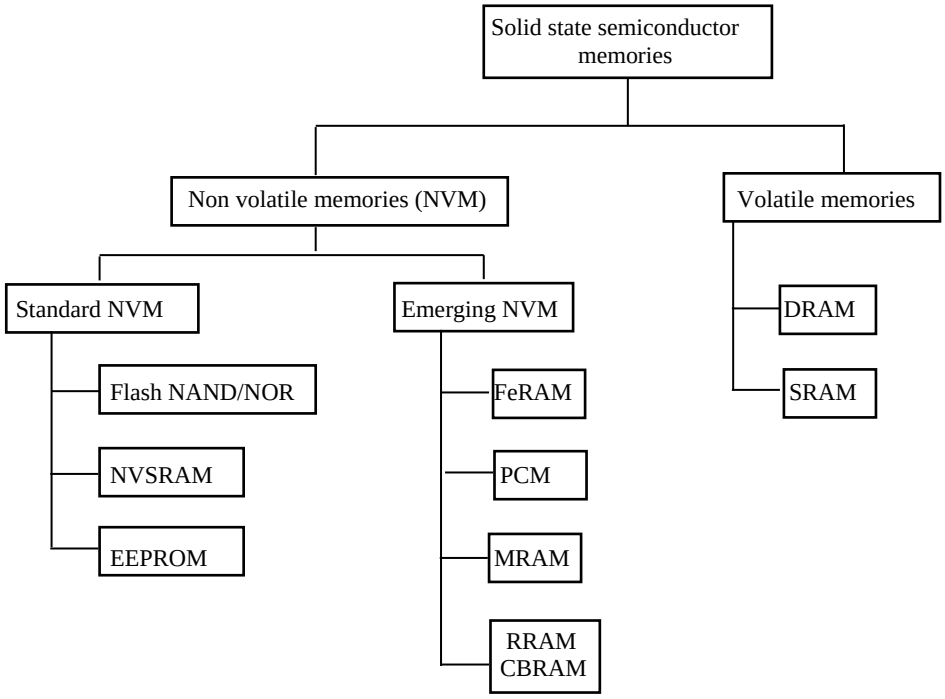

Figure 2. The solid state semiconductor family of memories. *CBRAM = Conductive Bridge RAM; DRAM = Dynamic RAM; FeRAM = Ferro Electric RAM; MRAM = Magnetic RAM; PCM = Phase Change Memory; RRAM = Resistive RAM [It can be also called Resistance Chance Memory (RCM)]; SRAM = Static RAM.*

Table 1. Comparison of memory and storage technologies [4**]**. Note that circuit-level overheads for the listed performance metrics are in general different among different device technologies and could often dominate individual device performance.*****

	Memristor	**PCM**	**STTRAM**	**SRAM**	**DRAM**	**Flash (NAND)**	**HDD**
	Prototypes				Commercialized technologies		
Reciprocal density (F2)	<4	4–16	20–60	140	6–12	1–4†	2/3
Energy per bit (pJ)	0.1–3	2–25	0.1–2.5	0.0005	0.005	0.00002	1–10 × 109
Read time (ns)	< 10	10–50	10–35	0.1–0.3	10	100,000	5–8 × 106
Write time (ns)	~10	50–500	10–90	0.1–0.3	10	100,000	5–8 × 106
Retention	years	years	years	As long as voltage applied	<< second	years	years
Endurance (cycles)	10^{12}	10^{9}	10^{15}	> 10^{16}	> 10^{16}	10^{4}	10^{4}

* The energy to operate NAND Flash is typically hundreds of picojoules (pJ) per bit primarily because accessing the memory cells requires charging word and bit lines to high voltages. †Smaller number represents an effective area for multi-level cells. PCM = phase-change memory; STTRAM = spin torque transfer random access memory; SRAM = static RAM; DRAM = dynamic RAM; HDD = hard disk drive.

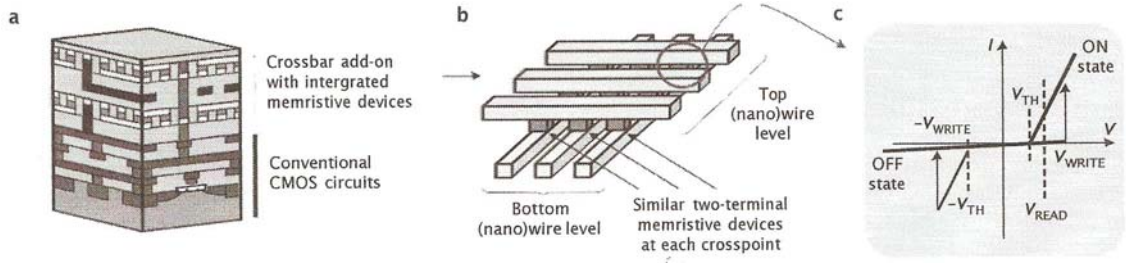

Figure 3. Hybrid CMOS/memristor circuits (**a, b**). *Owing simple functionality of memristors most practical approaches rely on combining memristors with sparse but more powerful conventional CMOS circuits **(a)** for example, by integrating memristive devices into crossbar structures on top of a CMOS subsystem. **(b)** Crossbar structures enable very high density in large-scale circuits, with devices defined by the overlap area of the two electrodes. **(c)** Schematic I-V curve for a nonlinear memristive device. V_{TH} denotes a threshold voltage below which current is negligible [5].*

2. SHORT HISTORY OF MEMRISTOR

Leon Chua - professor at UC Berkeley - discovered, in 1971 [6], a missing link in the pair wise mathematical equations that relate the four circuit quantities - charge, current, voltage, and magnetic flux - to one another. These can be related in six ways. Two are connected through the basic physical laws of electricity and magnetism, and three are related by the known circuit elements: resistors (connect voltage and current), inductors (connect flux and current), and capacitors (connect voltage and charge). But one equation is missing from this group: the relationship between charge moving through a circuit and the magnetic flux surrounded by that circuit - or more subtly, a mathematical double defined by Faraday's Law as the time integral of the voltage across the circuit [7]. Chua demonstrated mathematically that his hypothetical device would provide a relationship between flux and charge, similar to what a nonlinear resistor provides between voltage and current. In practice, that would mean the device's resistance would vary according to the amount of charge that passed through it. And it would remember that resistance value even after the current was turned off.

3. MEMRISTANCE

We now know that memristance is an intrinsic property of any electronic circuit. Its existence could have been deduced by Kirchhoff or by Maxwell, if either had considered nonlinear circuits in the 1800s. But the scales at which electronic devices have been built for most of the past two centuries have prevented experimental observation of the effect. It turns out that the influence of memristance obeys an inverse square law: memristance is a million times as important at the nanometre scale as it is at the micrometer scale, and it's essentially unobservable at the millimetre scale and larger [7]. As we build smaller and smaller devices, memristance is becoming more noticeable and in some cases dominant.

4. THE CROSSBAR

The crossbar (Figure 3) is an array of perpendicular wires. Anywhere two wires cross, they are connected by a switch. To connect a horizontal wire to a vertical wire at any point on the grid, you must close the switch between them. The HP idea was to open and close these switches by applying voltages to the ends of the wires. Note that a crossbar array is basically a storage system, with an open switch representing a zero and a closed switch representing a one. You read the data by probing the switch with a small voltage.

Like everything else at the nanoscale, the switches and wires of a crossbar are bound to be plagued by at least some non-functional components. These components will be only a few atoms wide, and the second law of thermodynamics ensures that we will not be able to completely specify the position of every atom [7]. However, the crossbar architecture builds in redundancy by allowing you to route around any parts of the circuit that don't work. Because of their simplicity, crossbar arrays have a much higher density of switches than a comparable integrated circuit based on transistors.

5. RESISTIVE MEMORY

The most promising emerging technology is Resistive Memory. In terms of nonvolatile memory (Figure 2), it is generally believed that transistor based Flash memory will approach the end of scaling within about a decade. As a result, novel, non-FET based devices and architectures will likely be needed to satisfy the growing demands for high performance memory and logic electronics applications. In terms of memory applications, it is generally believed that transistor based Flash memory will approach the end of scaling within about a decade. Hence one of the most important challenges in semiconductor industry is the need of a new memory technology which combines the best features of current memories such as high density of DRAM, fast speed of SRAM and non-volatile property of Flash with a CMOS compatible fabrication technology.

Resistive RAM, although behind the others in development, is very promising. This type of circuit element behaves as a memristor (a term derived from memory and resistor), a device that was predicted to exist in 1971 as the fourth circuit element (in addition to the resistor, capacitor, and inductor). Memristive devices are attractive for a number of reasons: they are nonvolatile, they have fast switching speeds, and they can be integrated into a crossbar memory structure that offers the potential to scale to very high densities (Figure 3b).

Nonvolatile memories with ultimate density near 1 terabit/cm^2 are predicted because the individual memristor bits are envisioned to be densely packed and addressed by nanocrossbar arrays using a 10 nm x-y pitch. The memristor bits may be incorporated heterogeneously into a

conventional CMOS process, which is used to address, read, and write the memory array. Commercial devices based on this technology are currently in development and should be on the market within one or two years. These devices, although early in their development cycle, may provide a new high-density nonvolatile memory technology for future systems developers. The individual memristors have been shown to be radiation hard to both total ionizing dose and displacement damage; however, reliability and the integration with underlying CMOS must be evaluated further before these devices can be introduced into critical applications.

The search for new computing technologies is driven by the continuing demand for improved computing performance, but to be of use a new technology must be scalable and capable.

Memristor or memristive nanodevices seem to fulfil these requirements [they show excellent resistance switching properties such as fast switching time (<50 ns), high on/off ratio (>10^6), good data retention (>6 years) and programming endurance (>10^5)] they can be scaled down to less than 10 nm and offer fast, non-volatile, low-energy electrical switching. Memristors[3] are two-terminal 'memory resistors', regardless of the device material and physical operating mechanisms, that retain internal resistance state according to the history of applied voltage and current. They are simple passive circuit elements, but their function cannot be replicated by any combination of fundamental resistors, capacitors and inductors [3, 8]. Moreover, their microscopically modified internal state is easily measured as an external two-terminal resistance. Memristors were originally defined as components that linked charge and magnetic flux [3], but they can be more usefully described as devices with a pinched-hysteresis loop whose size is frequency dependent[3]. The natural computing application for such devices is resistive random access memory (ReRAM or RRAM), but their dynamical nonlinear switching also suggests that they could be used to develop alternative computer logic architectures.

Memristive devices can be classified based on switching mechanism, switching phenomena or switching materials. Here we loosely group all ionic switching devices into two categories - anion devices and cation devices - to simplify the discussion of their mechanisms.

Research activity in resistance switching has been primarily driven by the search for an ideal memory device. Indeed, hybrid CMOS/ memristor circuits, and in particular those with the passive crossbar architecture, could potentially combine all the desired properties of 'universal memory' - high speed, low energy and high endurance of static random access memories, and high density, low cost and non-volatility of lash memories (Table 1).

RRAM is a two terminal device that the switching medium is sandwiched between top and bottom electrodes (Figure 4) and the resistance of the switching medium can be modulated by applying electrical signal (current or voltage) to the electrodes.

The resistance switching effect has been observed in a broad range of materials such as perovskite oxide (e.g. $SrZrO_3$, $LiNbO_3$, $SrTiO_3$) [9-11], binary metal oxide (e.g. NiO, CuO_2, TiO_2, HfO_2) [12-18], solid electrolytes (e.g. AgGeS, CuSiO) [19, 20] and even in some organic materials [21-23].

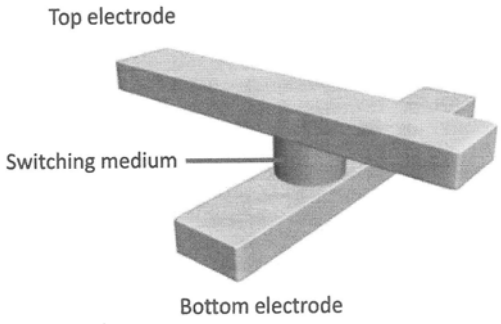

Figure 4. Two terminal RRAM structure. The resistance of a switching medium determines the state of the device [2].

The crossbar structure (Figure 5) consists of an array of parallel bottom nanowire electrodes, an array of parallel top nanowire electrodes with 90° degree with respect to the bottom electrodes and the switching medium between the electrodes. Each cross-point formed at the intersections of the top and bottom electrodes corresponds to an individual RRAM cell [2].

As digital memory devices, the devices are ideally suited in the crossbar architecture which offers ultra-high density and intrinsic defect tolerance capability. As an example, a high-density (2 Gbits/cm^2) 1 kb crossbar memory was demonstrated with excellent uniformity, high yield (>92%) and on/off ratio (>10^3), proving its

[3] Any two-terminal electronic device devoid of internal power source and which is capable of switching between two resistances upon application of an appropriate voltage or current signal, and whose resistance state at any instant of time can be sensed by applying a relatively much smaller sensing signal, is a *memristor* [6].

promising aspects for memory and reconfigurable logic applications. Properly designed devices can exhibit controlled analog switching behaviour and function as flux controlled memristor devices [2].

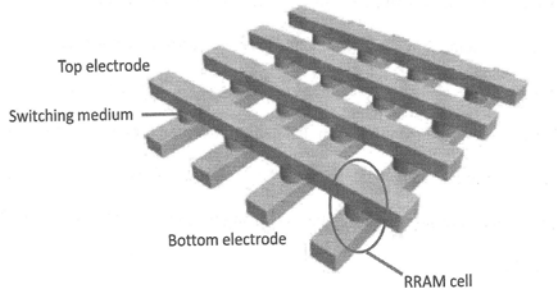

Figure 5. The schematic of a crossbar array (after [2]).

In essence, memristors operate as resistors the resistance of which can be changed and maintained in a non-volatile manner. This feature (and their compact size) is basically what makes them highly attractive not only for memories and computing systems in general, but also for building too neuromorphic systems. However, memristance is not necessarily restricted to two-terminal devices. It is well known that it is possible to use three (or four) terminal FETs (Field Effect Transistor) as resistors, current sources, or (volatile) memory elements. If the same nano scale principles that give rise to memristance in two-terminal devices could be extrapolated to three or four terminal FETs, then the adaptive memristive circuits presented so far could be extrapolated to more generic FET-based circuits as well. FETs have more terminals and consequently will result in less dense structures than their two-terminal counterparts. However, FETs can present very wide tuning ranges. For example, imagine a (nano)FET transistor in which the threshold voltage could be tuned through some memristive-like mechanism [24].

6. REQUIREMENTS TO FUTURE NON-VOLATILE DEVICES [25]

- *Energy efficiency*: Reset: < 100 μA; voltage$_{\text{-set, reset}}$ < 3 V
- *On/off ratio* >10
- *CMOS compatibility*: Read: ~1 μA, ~1V; J>10^6A/cm^2
- *Scalability*: <10 nm
- *Reliability*: Retention: 85°C 10 years; Endurance: >10^5@1 μs pulse

7. SOME RECENT APPLICATIONS

Memristive computing is a new area of research, and many of its fundamental questions still remain open. For example, it is yet unclear which applications would benefit the most from the inherent nonlinear dynamics of memristors. In any case, these dynamics should be exploited to allow memristors to perform computation in a natural way instead of attempting to emulate existing technologies such as CMOS logic. Examples of such methods of computation, presented in [26], are memristive stateful logic operations, memristive multiplication based on the translinear principle, and the exploitation of nonlinear dynamics to construct chaotic memristive circuits.

The main conclusion of [26] is that memristive computing will be advantageous in large-scale, highly parallel mixed-mode processing architectures. This can be justified by the following two arguments. First, since processing can be performed directly within memristive memory architectures, the required circuitry, processing time, and possibly also power consumption can be reduced compared to a conventional CMOS implementation. Second, intrachip communication can be naturally implemented by a memristive crossbar structure [26].

CMOS/memristor hybrid architectures combine conventional CMOS processing elements with thin-film memristor-based crossbar circuits for high-density reconfigurable systems. These architectures have received an explosive growth in research over the past few years due to the first practical demonstration of a thin-film memristor in 2008. The reliability and lifetimes of both the CMOS and memristor partitions of these architectures are severely affected by temperature variations across the chip. Therefore, it is expected that dynamic thermal management (DTM) mechanisms will be needed to improve their reliability and lifetime [27].

In order for CMOS/memristor architectures to become commercializable, several of their reliability concerns must be addressed. Due to their close proximity, memristor partitions of the architectures will be affected by thermal gradients in CMOS partitions. Due to their small feature sizes, temperature variations will have a significant effect on memristor crossbar circuits' performance and reliability. Therefore, these architectures will require dynamic thermal management (DTM) schemes to maximize device lifetimes and mitigate reliability concerns. DTM in traditional CMOS architectures has become a well established research domain. Currently, however, no work exists on thermal

management in next-generation CMOS/memristor hybrid architectures. Thesis [28] explores one aspect of thermal management–thermal profiling - in a CMOS/memristor hybrid memory architecture.

Memory circuit elements (namely memristive, memcapacitive and meminductive systems), are gaining considerable attention due to their ubiquity and use in diverse areas of science and technology. Their modelling within the most widely used environment, SPICE, is thus critical to make substantial progress in the design and analysis of complex circuits. Paper [29] presents a collection of models of different memory circuit elements and provides a methodology for their accurate and reliable modelling in the SPICE environment. The authors provide codes of these models written in the most popular SPICE versions (PSpice, LTspice, HSPICE) for the benefit of the reader. This will be of great value to the growing community of scientists interested in the wide range of applications of memory circuit elements.

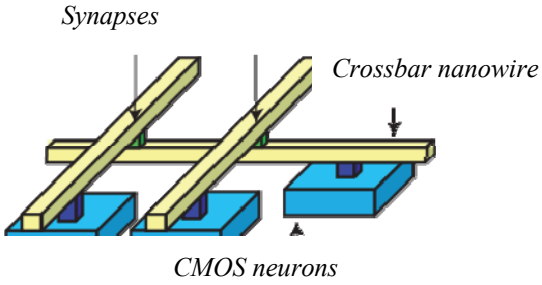

Figure 6. Bio-inspired and mixed-signal information processing: hybrid CMOS/memristor circuits may also enable efficient analogue dot-product computation, which is a key operation in artificial neural networks [5].

The idea of using resistance switching devices in artificial neural networks (Figure 6) and for mixed signal computing, in general, has a long history and can be traced back to at least the 1960s.

Synchronous memristive Spike-Timing-Dependent-Plasticity (STDP) learning architectures were proposed by Snider [30, 31], assuming voltage/flux driven memristors, and recently demonstrated by the group at Michigan University [32]. In that proposal each neural spike is mapped into a sequence of precisely spaced fixed amplitude digital pulses which must maintain global synchronization to separate the integration phase of neural activity from the synaptic weight update phase. This global synchronization requirement imposes severe difficulties when the system scales up to very large sizes.

8. CONCLUSION

Resistive RAM, although behind the others in development, is very promising. The development of memristive devices has recently witnessed remarkable progress. Nevertheless, it remains to be seen if memristive devices can combine all these characteristics in a single commercially competitive device design. Further research into device mechanisms - particularly the microscopic processes of the initial and subsequent switchings - is crucial to achieve reliable and predictable nanodevices at the wafer scale [5, 27].

References

1. http://www.siliconfareast.com/flash-memory.htm

2. Sung Hyun Jo, *Nanoscale Memristive Devices for Memory and Logic Applications, Ph. D. Thesis, University of Michigan, 2010.*

3. H. Goronkin, Y. Yang. *High-Performance Emerging Solid-State Memory Technologies. MRS Bull.* ***29****(2004), p. 805.*

4. ITRS International Technology Roadmap for Semiconductors*, 2011 edition; http://www.itrs.net*

5. J. Joshua Yang, Dmitri B. Strukov, Duncan R. Stewart. *Memristive Devices for Computing. Nature Nanotechnology, vol. 8, January 2013, pp. 13-24.*

6. Chua, L. O. *Memristor - missing circuit element. IEEE Trans. Circuit Theory* ***CT-18,*** *507–519 (1971).*

7. R. Stanley Williams. *How We Found the Missing Memristor. IEEE Spectrum, 28.11.2008.*

8. H. Kanaya, K. Tomioka, T. Matsushita, M. Omura, T. Ozaki et al. *A 0.602 μm^2 Nestled 'Chain' Cell Structure Formed by One Mask Etching Process for 64 Mbit FeRAM. VLSl Tech. Dig., 150, 2004.*

9. Y. Watanabe, J. G. Bednorz, A. Bietsch, Ch. Gerber, D. Widmer et al. *Current driven Insulator–Conductor Transition and Nonvolatile Memory in Chromium-Doped SrTiO3 Single Crystals. Appl. Phys. Lett.* ***78****, 3738, 2001.*

10. C. Y. Liu, P. H. Wu, A. Wang, W. Y. Jang, J. C. Young et al. *Bistable Resistive Switching of a Sputter-Deposited Cr-Doped SrZrO3 Memory Film. IEEE Electron Device Lett.* ***26****, 351, 2005.*

11. A. Beck, J. G. Bednorz, C. Gerber, C. Rossel, D. Widmer et al.. *Reproducible Switching Effect in Thin Oxide Films for Memory Applications. Appl. Phys. Lett. 77, 139, 2000.*

12. I. G. Baek, M. S. Lee, S. Seo, M. J. Lee, D. H. Seo et al. *Highly Scalable Nonvolatile Resistive Memory Using Simple Binary Oxide Driven by*

Asymmetric Unipolar Voltage Pulses. IEDM Tech. Dig, 587, 2004.

13. M. -J Lee, S. Han, S. H. Jeon, B. H. Park, B. S. Kang et al. *Electrical Manipulation of Nanofilaments in Transition-Metal Oxides for Resistance-Based Memory. Nano Lett.* ***9****, 1476, 2009.*

14. A. Chen, S. Haddad, Y.C. Wu, T.N. Fang, Z. Lan et al. *Non-Volatile Resistive Switching for Advanced Memory Applications. IEDM Tech. Dig, 746, 2005.*

15. J. J. Yang, M. D. Pickett, X. Li, D. A. A. Ohlberg, D. R. Stewart et al. *Memristive Switching Mechanism for Metal/Oxide/Metal Nanodevices. Nat. Nanotechnol.* ***3****, 429, 2008.*

16 I.-S. Park, K.-R. Kim, S. Lee, J. Ahn, *Resistance Switching Characteristics for Nonvolatile Memory Operation of Binary Metal Oxides. Jpn. J. Appl. Phys.* ***46****, 2172, 2007.*

17. S. Lee, W. -G. Kim, S. -W. Rhee, K. Yong, *Resistance Switching Behaviors of Hafnium Oxide Films Grown by MOCVD for Nonvolatile Memory Applications. Journal Electrochem. Soc.* ***155****, vol. 92, 2008.*

18. R. Waser, and M. Aono. *Nanoionics-Based Resistive Switching Memories. Nat. Mater.* ***6****, 833, 2007.*

19. M. N. Kozicki, C. Gopalan, M. Balakrishnan, M. Park, M. Mitkova. *Non-Volatile Memory Based on Solid Electrolytes. NVMTS, 2004*

20. T. Sakamoto, S. Kaeriyama, H. Sunamura, M. Mizuno, H. Kawaura et al. *A Nonvolatile Programmable Solid Electrolyte Nanometer Switch. ISSCC, 2004.*

21. W. L. Kwan, R.J. Tseng, W. Wu, Q. Pei, Y. Yang et al. *Stackable Resistive Memory Device Using Photo Cross-linkable Copolymer. IEDM Tech. Dig., 237, 2007.*

22. R. J. Tseng, C. Tsai, L. Ma, J. Ouyang, C. S. Ozkan et al. *Digital Memory Device Based on Tobacco Mosaic Virus Conjugated with Nanoparticles. Nat. Nanotechnol.* ***1****, 72, 2006.*

23. Y. Chen, G. Y. Jung, D. A. A. Ohlberg, X. M. Li, D. R. Stewart et al. *Nanoscale Molecular-Switch Crossbar Circuits. Nanotechnol.* ***14****, 462, 2003.*

24. C. Zamarreño-Ramos, L. Camuñas-Mesa, J. A. Pérez-Carrasco, T. Masquelier, T. Serrano-Gotarredona, and B. Linares-Barranco. *On Spike-Timing-Dependent-Plasticity, Memristive Devices, and building a Self-Learning Visual Cortex. https://capocaccia.ethz.ch/.../stdp_memr_final.pdf, 2011.*

25. Hyunsang Hwang. *Electrical and Reliability Characteristics of RRAM for Cross-point Memory Applications. http://www.sematech.org/meetings/ archives/fep/ 9064/Pres/ 28%20H%20Hwang.pdf*

26. Eero Lehtonen. *Memristive Computing, Ph. D. Thesis, University of Turku, 2012.*

27. Cory Merkel. *Thermal Profiling in CMOS/ Memristor Hybrid Architectures, Ph. D. Thesis, Rochester Institute of Technology, New York, 2011.*

28. Leon Chua. *Resistance Switching Memories are Memristors. Applied Physics A (2011) 102, pp. 765–783.*

29. Dalibor Biolek, Massimiliano Di Ventra, Yuriy V. Pershin. *Reliable SPICE Simulations of Memristors, Memcapacitors and Meminductors. Radioengineering, vol. 22, no. 4, December 2013, pp. 945-968.*

30. G. S. Snider. *Self-organized Computation with Unreliable, Memristive Nanodevices. Nanotechnology, 18:365202, 2007.*

31 G. S. Snider. *Spike-Timing-Dependent Learning in Memristive Nanodevices. IEEE Int. Symp. Nano Architectures, pp. 85-92, June 2008.*

32. S. H. Jo, T. Chang, I. Ebong, B. B. Bhadviya, P. Mazumder, W. Lu. *Nanoscale Memristor Device as Synapse in Neuromorphic Systems. Nano Lett., 10 (4), pp. 1297–1301, 2010.*

33. Davide Sacchetto, et al. *Applications of Multi-Terminal Memristive Devices: A Review. IEEE Circuits and Systems Magazine, second Quarter 2013, pp. 23-41.*

34. A. Caspani, et al. *Dynamic Nonlinear Behavior of Torsional Resonators in MEMS. J. Micromech. Microeng.* ***24*** *(2014) 095025 (9pp).*

35. Allyson Hartzell, et al. *Design for Reliability in MEMS-Based Systems. e-ISBN 978-1-4419-6018-4.*

36. Andreas C. Fischer, et al. *Integrating MEMS and ICs. Microsystems & Nanoengineering (2015) 1, 15005; doi:10.1038/micronano.2015.5.*

Recommended for publication: 24.02.2016.

TECHNOLOGY ENHANCED ELECTRICAL ENGINEERING EDUCATION IN CONTEXT OF CRUNT TEMPUS PROJECT

[1]Adrian Adăscălitei, professor, [2]Nicolae Secrieru, [3]Petru Todos, professor,
[1]"Gh. Asachi" Technical University, Iaşi, România,
[2]Department of Information Technologies, TUM, Chişinău, Republic of Moldova,
[3]Electro-Mechanics Department, TUM, Chişinău, Republic of Moldova

1. INTRODUCTION

Teaching Engineering as one of the components in the foundation technological program has been a challenging task to electrical engineering lecturers. A course webpage was constructed with the Moodle software system that utilizes various applications such as forum discussions, on-line assessments, accessing course information and learning resources including videos and useful links. The web application is not a duplicate of classroom content but serves as a complementary to further provide guidance and assistance to students' learning outside the classroom. Therefore, the research will investigates students' perception on the usefulness of the course webpage in terms of content, accessibility, satisfaction and whether the experience stimulated their interest towards learning Engineering. The hybrid approaches offer flexibility and provide adequate support to students in learning EET.

The principles of ICT integration in engineering education are expressed as seven specific learning objectives for Teaching Engineering by using Blended Learning:

1. Critically apply the pedagogical principles of ICT integration in education.
2. Develop and facilitate ICT-based learning activities in the context of teaching EET.
3. Analyze and evaluate appropriate content and context for the use of ICT in EET teaching.
4. Use appropriate and varied communication and multimedia tools (emails, websites etc) in teaching and learning EET.
5. Use ICT efficiently in research, problem solving and project-based learning in EET.
6. Use ICT efficiently for professional development in the context of teaching and learning EET.
7. Integrate ICT appropriately into EET curriculum activities that will foster students ownership of their ICT-rich learning environment.

Methodology. Electrical Technology courses in higher education have traditionally been composed of lectures, problem-solving sessions, and laboratories. This study was aimed at developing a freshmen Web-based EET course and investigating the performance of the students who use it. The course Web site included the following elements:

- Weekly problem sets, for which solutions were provided a week later
- Hyperlinks to Web sites that provide information about topics in EET that are relevant to the course, including historical and philosophical background
- Hyperlinks to sites that provide access to free computerized electrical circuits and drives modeling software
- An electronic forum that enables students to pose questions and instructors to answer them

An optional, individual CMM project. The Capability Maturity Model project was originally developed as a tool for objectively assessing the ability of government contractors' *processes* to implement a contracted software project.

2. USING THE MOODLE PLATFORM IN CLASS

Moodle is a tool which enables teachers to create a website environment for your class with online activities such as forums and quizzes.

"Moodle is a Course Management System (CMS), also known as a Learning Management System (LMS) or a Virtual Learning Environment (VLE). It is a free web application that educators can use to create effective online learning sites." (http://moodle.org/)

Course Webpage Design and Description by using Moodle platform (VLE, Virtual Learning Environment)

The blended learning environment was designed for a course entitled "*Electrical Engineering and Technology, EET*", which was a core module offered to engineering students. The front webpage provides the overall course content of the EET module with the names of the chapters,

followed by the activities in a drop-down list for each chapter. The activities involved in each chapter include: course materials, additional materials, quizzes, open forum/chat and latest news message/calendar.

Figure 1. Blended Learning course developed at the Technical University of Moldova, Chişinău, Republic of Moldova.

Course materials. There are a total of nine chapters in EET with topics of namely, Each of these chapters has plenty of information and activities related to the topic. This includes the course materials in the form of PowerPoint slides and Acrobat PDF documents, which are the duplicates of hand-outs that the students received in class. It is important to provide a softcopy to the students, as it is colored compared to their hardcopy and helps better in comprehending complex diagrams or figures.

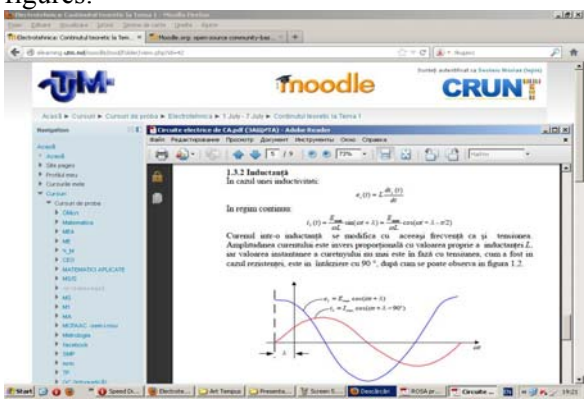

Figure 2. The Content Presentation of "*Electric Drive and Automation of Industrial Mechanisms*"

Additional Materials. Nowadays students are very much visual learners. The majority of the students expressed the strongest preference to visual learning style compared to other learning style dimensions. This implies that engineering students are strongly depending on visual learning environment. Video is clearly a valuable additional learning activity that provides a sensory experience that allows concepts and ideas to actually become alive and connected. It has the option to rewind and review a particular section of the video to ensure students understand the key concept. Thus, free educational video sharing websites that explained the EET theories were uploaded in the webpage. In addition to this were video links from You Tube. Apart from this, problems and solutions as well as simplified diagrams explaining complex concepts, taken from textbooks or take-home questions which were not discussed in class, were made available online for students. In each of these adapted materials, references were stated clearly in order to allow students to seek the original sources if the need arises, apart from avoiding copyright infringement.

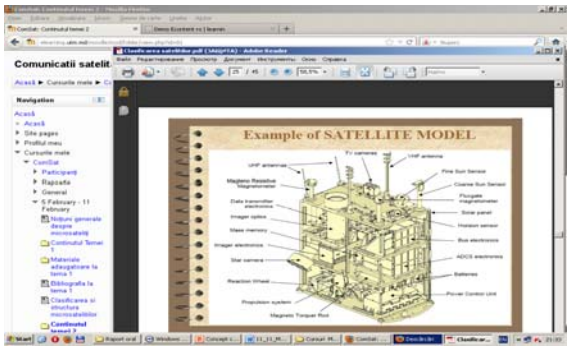

Figure 3. The Content Presentation in "*Satellite Communications*"

Quizzes. Quizzes were incorporated in each chapter for students who were keen to self-test their knowledge and learning after the revision of a chapter. Short quizzes in the form of true/false, multiple choice, short answers or numerical questions were assigned, depending on the chapter content. The majority of the questions were of problem solving type that involved calculation with pre-determined specific units and significant figures of the numerical answers. Two attempts were allowed for each question and the students received immediate feedback if they failed in their first attempt. Positive responses were provided if the students were successful in answering the questions. However, there was no time limit to answer each question as the students were given sufficient time to read and understand the questions, and to answer calmly at their own pace. Since the quizzes were not part of the students' assessment, it was considered, as an independent study at the students' own will. Hence, the quizzes were designed with a due date of two weeks, in order to encourage the students to have a constant revision and to avoid last-minute cramming before examination.

Open Forum. Open forum serves the purpose of allowing a student to post his/her questions or doubts and can be viewed by their fellow peers. This

allows the lecturer to disseminate the answered questions to the whole class without repeating in the classroom. Hence, each of the chapters was constructed with their very own Open Forum. Students were also encouraged to use the chat function that facilitated live discussion and interaction with their instructors and peers.

Latest news Message/Calendar. Another interesting feature of Moodle is the function on the right of the webpage which allows the lecturers to post any new messages. It also comes with the list of recent activities so that students can keep-track with any updates. General announcements such as due date of assignments, examination dates and venues, replacement classes etc. were posted at this section and these were linked to the students' email accounts, so that they were notified of every update.

3. GENERAL PRESENTATION OF OPEN EDUCATIONAL RESOURCES AND MOOCS

Open Educational Resources (OER) have the potential to broaden access to education and to improve the quality and cost-effectiveness of teaching and learning in Europe. The best way to put OERs into practice is through Massive Open Online Courses (MOOCs). MOOCs are large-scale courses that represent one of the latest developments in open education, an initiative that is always trying to improve quality, access and equality in education and training. MOOCs can be implemented in formal, informal and non-formal learning, and make learning ubiquitous.

Project will use leading-edge technology to create a combined Moodle MOOC platform– based on individual platforms and resources provided by project partners – making it possible to combine and transfer pilot activities in all the hubs involved.

Project will contribute to increasing awareness of the advantages of open education in Europe. The project will prove the potential of MOOCs (courses and communities) for breaking down technological barriers in learning across people with special needs or at risk of exclusion.

MOOCs adopted definition: MOOC is an online course designed for large number of participants that can be accessed by almost anyone anywhere as long as they have an internet connection, is open to everyone without entry qualifications and offers a full/complete course experience online free.

A MOOC includes educational content, facilitation interaction among peers (including some but limited interaction with academic staff), activities/tests, including feedback, some kind of (nonformal) recognition options and a study guide / syllabus.

4. UTILISING THE VIRTUAL LESSONS AND LABORATORY RESOURCES FOR ELECTRICAL ENGINEERING

Teaching electrical engineering laboratory procedures by means of a virtual laboratory on a personal computer will be much welcome by educational institutions for whom maintaining a hands-on electric engineering lab is not viable due to various reasons. Instructional laboratory simulations can be incorporated in the virtual laboratory resources where students are free to make the decisions they would confront in an actual laboratory setting. *Electrical Engineering and Technology eLearning Resources*

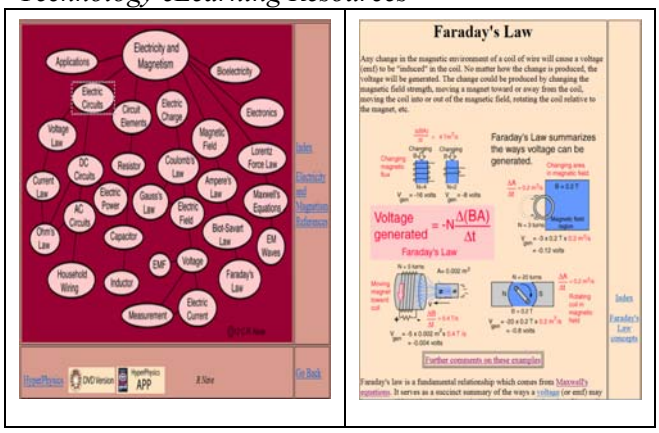

Figure 4. Hyperphysics, Electricity and Magnetism, *http://hyperphysics.phy-astr.gsu.edu/hbase/emcon.html#emcon*

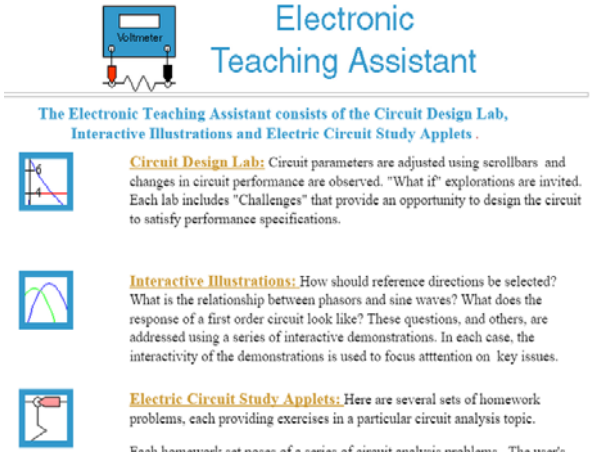

Figure 5. The Electronic Teaching Assistant: the Circuit Design Lab, Interactive Illustrations and Electric Circuit Study Applets.

Real-life situations and problems are faced by them, where they have to make/take decisions and face the consequences thereof.

The available links to following websites are given below as examples for the teachers to have an idea of such virtual laboratories.

CONCLUSIONS

This paper is a synthesis that presents the conception of a project devoted to use moodle Virtual Learning Environment for the development of MOOC courses which mainly contains OER materials in order to educate the Engineering Students.

Engineering School teaching and students' learning are moving through transition processes that use education technology in support of academic work. There exists a greater acceptance of the online mode of instruction as an adjunct to learning. Nevertheless, the results of our work showed that most students preferred a moderate use of e-learning in their courses. Their positive attitude was observed towards the model of blended learning approach, and Moodle platform did create a positive impact on students' learning experiences in terms of the accessibility of learning materials and the support of online assessment activities. Students reported that the most valuable benefits of using Moodle platform in learning EET were the convenience of accessing the course materials and completing the online assessment tasks. Overall, the majority of the students perceived the use of course website as an opportunity to enhance their academic experience.

Although the students agreed that the hybrid learning provided them with the needed assistance, one of the drawbacks observed was that this method of delivery was prone to become a one-way communication. Responses to this study showed that the number of the students' email correspondences to the lecturers were minimum. The students were expecting to be "spoon-fed" with information, announcements and notes. Thus, a more interactive learning is needed to promote a two-way communication. Communication tools such as forum discussion and online chat room have the features that create interaction with instructors and among the peers. However, as mentioned earlier in the study, most students are likely to participate in the learning practices only if the activities are considered as part of the evaluation of their academic performance. It is therefore necessary to assign grading procedure in e-learning activities to increase students' participation. With the improvements at these loose ends, Moodle application in Electrical Engineering will be an invaluable and imperative tool for the instructors as well as for the students.

REFERENCES

1. *EECS Course WEB Sites, http://inst.eecs. berkeley.edu/classes-eecs.htmlhttp://media.pear soncmg.com/ph/chet/chet_electronics_student_1//*

2. Svoboda J.A. *The Electronic Teaching Assistant: the Circuit Design Lab, Interactive Illustrations and Electric Circuit Study Applets . http://people. clarkson.edu/~jsvoboda/eta/*

3. Špaldonová D., Guzan M. *Application of Excel in three-phase circuit analysis. Acta Electrotechnica et Informatica No 6.1,4. 2006: http://aei.tuke.sk/papers/2006/4/Guzan.pdf*

4. Ivanov S. *E-Learning tools for Electrical Engineering, http://em.ucv.ro/elee/ro/realisations/ CircuitsElectriques/index.htm*

5. Enache S., Campeanu A., Enache M. A., Ivanov S. *E-learning tools for education in asynchronous machines. WSEAS transactions on advances in engineering education, 4(11), 2007, pp. 238-241.*

6. *JAVA Applets for Electrodynamics, www.walter-fendt.de/ph14ro*

7. *Learning objects that cover a broad-based electromechanical engineering program, http://electronics.wisc-online.com/; and https://www.wisc-online.com/learn/technical/*

8. *Engineering Open Educational Resources, http://guides.oer.hawaii.edu/engineeringOER*

9. *Interactive simulations, http://phet.colorado.edu/ en/simulations/translated/en*

10. *Open Courseware Consortium, www.ocwconsortium. org/*

11.*Online Repositories for Open Educational Resources, http://www.cincinnatistate.edu/online/ faculty-resources/online-repositories-for-open-educational-resources*

12. *MIT Open Courseware (OCW), Electrical Engineering and Computer Science, http://ocw.mit.edu/courses/electrical-engineering-and-computer-science/*

13.*Moodle e-learning, Electrical Engineering Faculty, Technical University "Gh. Asachi" Iași, România http://moodle.ee.tuiasi.ro/*

14. Jingyan L., Nancy Wai Ying Law*. Understanding collaborative learning behavior from Moodle log data. Interactive Learning Environments 20.5 (2012): 451-466.*

15. Filipovic M.D. *Understanding Electronics Components,http://www.mikroe.com/old/books/keu/ 00.htm*

16. *College Open Textbooks. Engineering & Electronics http://collegeopentextbooks.org/textbook-listings/textbooks-by-ubject/engineeringandelectronics*

Recommended for publication: 12.04.2016

FEATURES ELASTO-PLASTIC DEFORMATION AND BRITTLE FRACTURE, ELECTROLYTIC IRON COATINGS

[1]PhD, professor Vasile Javgureanu, [2]PhD, associate professor Pavel Gordelenco, [3]Lecturer Diana Bors
[1]Technical University of Moldova, Chisinau
[2]Technical University of Moldova, Chisinau
[3]Technical College, Chisinau

1. INTRODUCTION

Electrolytic iron coatings are used for hardening and restoring of machine elements in the industry in order to increase their durability. Terms of electrode position have a significant impact on the physical and mechanical properties of the coatings. Knowledge of the physical and mechanical characteristics of composite coatings of iron needed to make informed choices deposition process conditions, depending on the operating conditions of the recovered parts of the work, as well as for strong calculations.

2. GENERAL INFORMATION

Actual problems of the study of physical and mechanical properties of materials in surface and near-surface layers due to the fact that the deformations associated with contact with modern methods of treatment, hardening and the metal connection.

The importance of determining the elasto-plastic characteristics (he, hp, h), the work required for deformation (Ae, the Ap, A), unreduced and dynamic hardness (Hh, Hd), modulus of elasticity (E) coating the critical load indentation diamond spherical indenter, in which begins the process of brittle fracture (Pcr), the ratio of non-reduced and dynamic hardness to elastic modulus (Hh/E, Hd/E), yield strength (σ_f), the true tensile strength (σ_{vtr}), tensile strength (σ_{tr}), toughness (α_n), the extent of material deformation in the contact zone (φ) is invaluable.

An important parameter of the iron composite coating is brittleness. This property of the coatings is undesirable because the increase in brittleness affects important characteristics such as wear resistance [2].

It is known that the brittleness of coatings envy of pretreatment conditions of the substrate and electroplating. It can be caused by the inclusion of hydrogen coverage, surface active substances (surfactants), metals and other foreign particles.

To determine the brittleness of precipitation, it is mainly used a method based on bending of the plate, with the application of the coating layers. Before the appearance of cracks in the sediment, and the angle of bending the plate appreciate the fragility of the coating [2]. In this case, the test results can depend upon the nature of the material and thickness of the substrate plate. Moreover, using this method, researchers have information about the relative brittleness of coatings without the applied voltage necessary for the formation of cracks in the coating. To this end, it was an attempt to use a method of pressing [1-4] allows you to determine the breaking stress. On the fragility of the coating has a significant influence of electrode position conditions: to increase their stiffness (increased current density, decreasing the temperature of the electrolyte) is significantly increased. The electrolyte composition may have a different impact on the considered properties of the coatings.

We present elasto-plastic properties and their tendency to brittle fracture of electrolytic iron coatings obtained from the electrolyte 1 (2, 59). The samples used rollers diameter 30 mm, thickness of 0.5 tmm and a length of 100 mm, which were processed under optimal conditions of grinding. Physical and mechanical properties were determined at the facility for the study of the hardness of materials macro volume equipped with inductive sensor and a differential amplifier, allows you to record the chart indentation diamond spherical indenter and restore print after unloading.

The dynamic hardness (Hd) was determined as the ratio of the total work (A) consumed for elasto-plastic deformation to the deformable volume indentation (V) under load in all studied electrolytic iron coatings.

On the plastic deformation of the coating associated with the preparation of destruction, spent is spending the work (the An).

At present, the theoretical and experimental issues associated with the assessment of the

properties of brittle materials indentation of a spherical indenter, well developed [1-10].

Studies [2] have shown that when a spherical indentation gradually increasing the load on the indenter can reach a critical state in which cracks form a ring, with a diameter approximately the same fingerprint from coatings obtained under all conditions of electrolysis. [2] However, the critical condition occurs when the elasto-plastic deformation. Due to the small residual strain coating great difficulties arise when measuring the diameter of the indentation, so it is locked at the boundary contact area. Furthermore, in this case, to form a continuous circumferential crack occurs occurrence of new cracks arbitrary direction [2].

When scratching the critical load was fixed at cracking perpendicular to the direction of movement of the indenter. As with a spherical indentation, brittle fracture occurred in the presence of plastic deformation. Due to fracture during the test, the coatings were formed as separate new cracks located at different angles to the direction of displacement of the indenter [2].

Analysis of the results showed that in spite of the plastic deformation of the coating for all the studied sediments as under static indentation and scratching at the critical load is proportional to the radius of the sphere. With increasing current density, the critical state occurs at lower loads. [2]

For comparison, the theoretical and experimental values of the ratio of the critical load slip (Pcr) to the critical load under static indentation (Pst) was used formula derived from the condition that the critical stress upon occurrence of failure in the case of static and dynamic indentation.

$$\frac{\mathrm{P}cr}{\mathrm{P}st} = \frac{1}{(1+3Af)^3},$$

where: *Pcr* and *Pst* - critical load, respectively, with scratching and static indentation.

f - coefficient of friction between the indenter and the sample in scratching.

To determine the value but to use the expression:

$$A = \frac{3\pi(4+\mu)}{8(1-2\mu)},$$

where: μ - Poisson's ratio of coatings.

Studies have shown that using macropressingin selection of load and the diameter of the sphere is possible to determine the physical and mechanical properties of the coatings.

Despite the value of information, which can be determined by pressing, when it is used there are difficulties associated with determining the diameter of the indentation and the beginning of brittle fracture, which affects the elasto-plastic deformation of coatings by immersing the indenter. Furthermore hardness measuring method based on determination of the diameter of the print does not allow to obtain information about the nature of the elastic deformation of the materials. Therefore, to study the hardness of the coatings was used microvolume hardness TKC-1, you can record a chart indentation diamond spherical indenter and restore print after unloading. As the indenter used artificial diamond sphere with a radius of 1 mm.

As a result of measurement of physical and mechanical properties of iron coatings with different loads on the indenter (P) found that when the initial load (up Pcr) ratio $P/\pi\Delta h$ is constant. With further increase of the load, this value increases sharply, indicating a deviation from the mechanical similarity. In the considered pattern is significantly influenced by the conditions of electrolysis. With the increase in the current density of the original violation of laws takes place at lower loads on the indenter (2).

The study of the (hy) elastic and plastic (Hp) features strain coatings showed that the responsibility for the results is the change in the character of elastic deformation, depending on the loading conditions. Regardless of the conditions for obtaining coatings with increasing load on the indenter deformation elastic component coatings increases sharply at first, then it rises slightly (2).

The main reason that causes a mechanical violation of the law of similarity, associated with the beginning of brittle fracture surfaces.

Comparing this critical loads with their values determined from observations of the formation of a ring crack, one could argue that the beginning of brittle fracture surfaces can be determined much more accurately measure the depth of indentation and the critical load (Pcr) as to form a ring crack growth is possible starting cracks the formation of new, behind which is difficult to observe. The critical stress can be taken as a criterion for assessing the tendency to brittle fracture surfaces.

3. DISCUSSION OF EXPERIMENTAL STUDIES

Studies have shown that the elasto-plastic properties and the tendency to brittle fracture of electrolytic iron coatings vary with electrolysis conditions (Table 1-5).

With increasing current density (Dk) of $5\text{x}10^{-4}$ to $80\text{x}10^{-4}$ kA/m^2 at a constant temperature

Table 1. Elasto-plastic properties of iron-nickel composite coatings and their tendency to brittle fracture.

Conditions electrolysis		*H_h, N/ mm²*	*H_d, N/ mm²*	*Elasto plastic properties*						*P, N*	*Pcr, N*
$D_к$, x10⁻⁴ кA/m²	*T, ⁰C*			*h_e, μm*	*A_e, N·mm*	*h_p, μm*	*A_p, N·mm*	*h, μm*	*A, N·mm*		
5	40	3505	2694	0.65	47.66	0.35	25.66	1.0	73.32	22.0	200
10	40	3729	2868	0.66	51.48	0.34	26.52	1.0	78.00	23.4	175
20	40	3855	2963	0.67	54.05	0.33	26.62	1.0	80.67	24.2	150
40	40	3220	2451	0.71	47.81	0.29	19.53	1.0	67.34	20.02	120
20	20	2600	1996	0.76	42.93	0.24	13.04	1.0	55.97	16.3	105
20	60	2750	2118	0.55	31.71	0.45	26.97	1.0	57.68	17.3	225

electrolysis (40^0C), the plastic indentation depth (hp) and critical load indentation (Pcr) on the diamond spherical indenter reduced accordingly by 0.35 to 0.29 (μm) and 200 to 120 (N) and the elastic component of penetration depth (hy) increases from 0.65 to 0.71 (μm), total indentation depth (h) is 1.0 μm.

The work expended on elastic (Ae), plastic (Ap), elasto-plastic deformation (A) and unreduced (Hh), dynamic (Hd) hardness iron coatings, the load pressing the diamond spherical indenter (P) are the extreme value with the change of the current density (Dk) from $5x10^{-4}$ to $40x10^{-4}$ kA/m^2 at a constant temperature of electrolysis (40^0C), table 1.

Elasto-plastic deformation and fracture characteristics of electrolytic iron coatings determined for several indentation depth h = (1,0 ÷ 4,0) μm by a known procedure (2).

Providence studies have shown that an increase in the current density of $5x10^{-4}$ to $20x10^{-4}$ kA/m^2 at a constant temperature electrolysis (40^0C) work expended on the deformation of the iron coating increased from $47.66x10^{-5}$ to $54.05x10^{-5}$ (N·mm), the work spent on the plastic deformation (Ap) coatings increased from $25,66x10^{-5}$ to $26,62$ $x10^{-5}$ (N·mm), unrestored coating hardness (Hh) increased from 3505 to 3855 (N·mm), the dynamic hardness (Hd) coatings increased from 2694 to 2963 (N·mm), and the load of pressing the diamond spherical indenter (P) is increased from 22 to 24,2(N).

Since ancient increase in current density (Dk) of $20x10^{-4}$ to $40x10^{-4}$ kA/m^2 at a constant temperature electrolysis (40^0C), the work expended on elastic (Ae) coatings increased by deformation $47.81x10^{-5}$ (N·mm) to $54.05x10^{-5}$ (N·mm), the work spent on the plastic deformation (Ap) decreased from 26.62 $x10^{-5}$ to $19.53x10^{-5}$, the work spent on the elastic-plastic deformation of the coating (A) decreased by $80,67x10^{-5}$ to $67,34x10^{-5}$ (N·mm), unrestorationed coating hardness (Hh) decreased from 3855 to 3220 (N/mm^2), the dynamic hardness of the coating (Hd) decreased from 2963 to 2451(N·mm^2) and the load pressing the diamond spherical indenter (p) decreased from 24,2 to 20,02(N).

According to the survey can be seen that the work spent on the elastic (Ae) plastic (Ap) elastic-plastic (A) deformation of coatings not restored (Hh), dynamic (Hd) hardness and the load pressing the diamond spherical indenter (P) with the change of the current density (Dk) at a constant temperature electrolysis (T) from 20^0C to 60^0C (table 1) at a constant current density ($20x10^{-4}$ kA/m^2), the critical load indentation (Pcr) the diamond spherical indenter characterizes the beginning of electrolytic iron brittle plastic component coatings (hp) the depth of indentation and the work spent on the plastic deformation of the coating (Ap), respectively, increased from 105 to 225 (N), from 0.24 to 0.45 (N·mm) and from $13.04x10^{-4}$ to 26.97 $x10^{-4}$ (N·mm), and the elastic component (hy) of penetration depth of a spherical indenter diamond decreased from 0.76 to 0.55 (μm).

The character of changes in the work expended on elastic (Ae), plastic (Ap), elasto-plastic deformation (A) coating and the indentation load (P) of the diamond spherical indenter at a depth of 1.0 microns is also extreme. With increasing temperature (T) of the cell from 20 to 40^0C at a constant current density ($20x10^{-4}$ kA/m^2), work spent on deforming the elastic coating (Ae) is increased by $42,93x10^{-5}$ up to $54,05x10^{-5}$ (N·mm), the work spent on the elasto-plastic deformation of the coating (A) is increased by up to $55,97x10^{-5}$ $80,67x10^{-5}$ (N·mm), unreduced hardness (Hh) coatings increased from 2600 to 3855 (N·mm^2), dynamic hardness (Hd) coatings increased from 1996 to 2693 (N·mm^2), and the indentation load (P) on a spherical diamond indenter is increased from 16.3 to 24.2 (N).

With further increase of the temperature (T) of electrolysis from 40 to 60°C at a constant current density (Dk) 20 $x10^{-4}$ kA/m^2, the work spent on the elasto deformation (Ae) coatings decreased from $80,67x10^{-4}$ to $57,68x10^{-5}$ (N·mm), unreduced

hardness (Hh) from 3855 to 2750 (N·mm^2), the dynamic hardness of the coatings (Hd) decreased from 2963 to 2118 (N·mm^2) and load indentation (P) on the diamond spherical indenter decreased from 24.2 to 17.3 (H, table 1).

Table 2. Elasto-plastic deformation and fracture characteristics of electrolytic iron coating.

Conditions electrolysis		*H_h, N/mm^2*	*H_d, N/mm^2*	*Elasto plastic properties*						*P, N*	*Pcr, N*
$D_к$, x10^{-4} кA/m^2	*T, ^{0}C*			*h_e, μm*	*A_e, N·mm*	*h_p, μm*	*A_p, N·mm*	*h, μm*	*A, N·mm*		
5	40	3560	2737	1.30	193.6	0.70	104.3	2.0	297.9	44.7	200
10	40	3760	2902	1.32	208.6	0.68	107.4	2.0	316.0	47.4	175
20	40	3920	3012	1.34	219.8	0.66	108.2	2.0	328.0	49.2	150
40	40	3280	2522	1.42	195.0	0.58	179.5	2.0	374.5	41.2	120
20	20	2650	2051	1.52	169.7	0.48	53.6	2.0	223.3	33.5	105
20	60	2800	2155	1.10	129.1	0.90	105.6	2.0	234.7	35.2	225

Table 3. Elasto-plastic deformation and fracture characteristics of electrolytic iron coatings.

Conditions electrolysis		*H_h, N/mm^2*	*H_d, N/ mm^2*	*Elasto plastic properties*						*P, N*	*Pcr, N*
$D_к$, x10^{-4} кA/m^2	*T, ^{0}C*			*h_e, μm*	*A_e, N·mm*	*h_p, μm*	*A_p, N·mm*	*h, μm*	*A, N·mm*		
5	40	3620	2784	1.95	443.3	1.05	3.0	682.0	68.2	68.2	200
10	40	3840	2951	1.98	477.2	1.02	3.0	723.0	72.3	72.3	175
20	40	3970	3053	2.01	501.2	0.99	3.0	748.0	74.8	74.8	150
40	40	3330	2559	2.13	445.2	0.87	3.0	627.0	62.7	62.7	120
20	20	2700	2486	2.28	386.8	0.72	3.0	509.0	50.9	50.9	105
20	60	2840	2200	1.67	294.3	1.35	3.0	535.1	53.9	53.9	225

Table 4. Elasto-plastic deformation and fracture characteristics of electrolytic iron coatings.

Conditions electrolysis		*Elasto plastic properties*						*H, N/mm^2*	*Hh, N/mm^2*	*P, N*	*Pcr, N*
Dk, x10^{-4} kA/m^2	*T, ^{0}C*	*h_e, μm*	*Ae x10^{-5}, Hmm*	*hp, μm*	*Ap x10^{-5}, Hmm*	*h, μm*	*A, x10^{-5}, Hmm*				
5	40	2,60	800,8	1,40	431,2	4,0	1232	2829	3680	92,4	200
10	40	2,64	862,4	1,36	444,3	4,0	1306,7	3000	3900	98	175
20	40	2,68	904,1	1,32	445,3	4,0	1349,4	3098	4030	101,2	150
40	40	2,84	803,7	1,26	356,6	4,0	1160,3	2599	3380	89,9	120
20	20	3,04	861,3	0,96	245,1	4,0	1106,4	2345	3050	76,6	105
20	60	3,20	530,3	1,80	453,8	4,0	964,1	2213	2880	72,3	225

With the change of penetration depth (h) of the diamond spherical indenter electrolytic iron coatings behavior of the stored elasto-plastic deformation (table 2-4), only to change the indentation depth, the work spent on the elastic and plastic deformation, unrestored (Nh), dynamic (Hd) Hardness and the indentation load (P) on the diamond spherical indenter.

The study of the effect of the current density (Dk) and the electrolysis temperature (T) of electrolytic iron propensity to brittle fracture surfaces showed that, with increasing current density (Dk) of 40x10^{-4} up to 5x10^{-4} kA/m^2 at a constant temperature of electrolysis (T=40^{0}C) critical load pressing the diamond spherical indenter (Pcr) is reduced from 200 to 120 (N), which indicates the increasing tendency of electrolytic iron coating brittle fracture (table 5).

With increasing temperature, the electrolysis of 20 to 60 seconds at a constant current density (20x10^{-4} kA/m^2), the critical load (Pcr) pressing the diamond spherical indenter increases from 105 to 225 (H), indicating that the decrease in inclination of electrolytic iron coatings brittle fracture.

Table 5. Elasto-plastic properties of electrolytic iron coatings in a critical state (early brittle fracture).

Conditions electrolysis		*Elasto plastic properties*				*V,* x10^{-5} *mm³*	*Pcr, N*	*Hh_{cr}, N/mm²*	*Hd_{cr}, N/mm²*	*E,* x10^{-5} *N/mm²*	*Hh_{cr}/E*	*Hd_{cr}/E*
Dk, x10^{-4} *kA/m²*	*T,* ^0C	*Ae* x10^{-5}, *Hmm*	*Ap* x10^{-5}, *Hmm*	*h, μm*	*A,* x10^{-5}, *Hmm*							
5	40	800,8	431,2	4,0	1232	18,10	200	3981	2997	1,95	0,0204	0,0151
10	40	862,4	444,3	4,0	1306,7	12,20	175	4347	3066	1,85	0,0235	0,0168
20	40	904,1	445,3	4,0	1349,4	9,08	150	6188	3194	1,75	0,0354	0,0183
40	40	803,7	356,6	4,0	1160,3	8,5	120	5028	2700	1,60	0,0314	0,0169
20	20	861,3	245,1	4,0	1106,4	8,5	105	3498	2600	1,50	0,0269	0,0113
20	60	530,3	453,8	4,0	964,1	34,37	225	6022	2400	2,10	0,0287	0,0124

It causes great interest to determine the beginning of the destruction of the fragile iron coatings in the test indentation. For most of the materials of the theoretical limit strength at shear Gmax. This is due to the fact that the sliding connection between atoms perpendicular to the sliding plane periodically reversed. The degree of recovery of these connections and more flexibility. Unrestored bond equivalent to the appearance of new elementary surface, the creation of which is spent on the job. From this point of view, we consider the change elasto-plastic properties of electrolytic iron coatings at the beginning of brittle fracture surfaces (Pcr, table 5).

With increasing current density (Dk) of 5x10^{-4} to 40x10^{-4} kA/m^2 at a constant temperature electrolysis (40^{0}C), elasto-plastic properties (Ae, Ap, h, A) decreased respectively by 35300x10^{-5} to 15200x10^{-5} (N·mm) from 1800x10^{-5} to 7260x10^{-5} (N·mm), from 8.0 to 5,6 (μm) and from 53300x10^{-5} to 22400x10^{-5} (N·mm). The volume of prints (V) at the load also reduced by up 18.1x10^{-5} to 8.5x10^{-5}(mm^3).

The results obtained show that the process of electrolytic iron brittle coatings started (table 5). Work spent at elastic (Ae), plastic and elasto-plastic (Ap) deformation of the iron coatings with critical indentation load (Pcr) significantly higher (table 5) than in the previous cases (table 1-4). This shows that the elastic, plastic and general deformation of electrolytic iron coatings spent considerably more work (Ae; Ap; A), which is connected with the beginning of brittle fracture surfaces.

With increasing current density (Dk) of 5x10^{-4} to 40x10^{-4} kA/m^2, at a constant temperature electrolysis (40^{0}C), unrestored critical hardness (Hh_{cr}), a critical dynamic hardness (Hd_{cr}), and their relationship Hh_{cr}/E have both before the extreme nature (table 5). Since the beginning of the achievements of brittle fracture electrolytic iron coatings under various conditions of the electrolysis (Dk, T) critical load varies from 105 to 225 (N) and the indentation depth of the diamond spherical indenter (h) also varies from 5.6 to 11.0 (μm).

Studies have shown that an increase in current density (Dk) of 5x10^{-4} to 20x10^{-4} kA/m^2, at a constant temperature electrolysis (40^{0}C) unrestored critical hardness (Hh_{cr}) increased from 3981 to 6188 (N/mm^2), the dynamic critical hardness (Hd_{cr}) increased from 2997 to 3194 (N/mm^2), and the ratio Hh_{cr}/E and Hd_{cr}/E increased, respectively, from 0.0204 to 0.0354 and from 0.0151 to further 0,0183. Current density of 20x10^{-4} to 40x10^{-4} kA/m^2, at a constant current density (40^{0}C) unrestored critical hardness (Hhcr) decreased from 6188 to 5028 (N/mm^2), the critical dynamic hardness (Hd_{cr}) decreased from 3194 to 2700 (N/mm^2) and the ratio of Hh_{cr}/E and Hd_{cr}/E of 0.354 to 0.314 and from 0.354 to 0.314 and from 0.183 to 0.169.

With increasing temperature, the electrolysis of 20 to 60^{0}C (see table 5) at a constant current density 20x10^{-4} kA/m^2, the critical load indentation (Pcr) characterizing the beginning brittle iron coatings, elasto-plastic properties (Ae; Ap; h; A) increases respectively from 105 to 225 (N) from 16800x10^{-5} to 44600x10^{-5} (N/mm^2), from 5300x10^{-5} to 37900x10^{-5} (N/mm^2), from 8.5 to 34.37 (μm), and from 22100x10^{-5} to 82500x10^{-5} (N/mm^2).

With increasing temperature electrolysis (T) from 20 to 40^{0}C, at a constant current density 20x10^{-4} kA/m^2 unrestored critical hardness (Hh_{cr}) increased from 3498 to 6188 (N/mm^2), the critical dynamic hardness (Hd_{cr}) increased from 2600 to 3194 (N/mm^2), the ratio Hh_{cr}/E and Hd_{cr}/E increased, respectively, from 0.0269 to 0.0354 and from 0.0113 to 0.0183 and volume the footprint volume under load (V) decreased from 8,5x10^{-5} to 9,08x10^{-5} (N/mm^2).

With further increase in temperature electrolysis from 40 to 60^{0}C at a constant current density (Dk) 20x10^{-4} kA/m^2 unrestored critical hardness (Hh_{cr}) decreased from 6188 to 6022 (N/mm^2), the dynamic critical hardness (Hd_{cr}) decreased from 3194 to 2400 (N/mm^2), the ratio Hh_{cr}/E and Hd_{cr}/E decreased respectively from

0.0354 to 0.0287, and from 0.0183 to 0.0124, and volume the fingerprint volume under load (V) increased from 9.08 to 34.37 (N/mm^2). In this case, the results obtained confirm the beginning of the destruction of the fragile iron coatings (Table 5).

With increasing temperature electrolysis (T) of 20 to 60^0C at a constant current density ($20x10^{-4}$ kA/m^2) coating the propensity to brittle fracture is reduced, since the critical load (Pcr) at which brittle fracture starts coating increases from 105 to 225. This is confirmed and in that the work expended on the elastic and plastic deformation of the overall coating (table 5) is significantly higher than in the previous cases (see table 1-4). This proves that the higher elastic (Ae), plastic (Ap) and elasto-plastic work (A) associated with the start of electrolysis of iron brittle coatings.

Comparing the experimental data may claim (5-11), which begin the process of brittle iron coatings can be determined by measuring the elasto-plastic indentation depth of the diamond spherical indenter, elasto-plastic characteristics (he; hp; h; Ae; Ap; A) the critical indentation load (Pcr), the beginning of brittle fracture, critical stress iron coatings (Hh_{cr}; Hd_{cr}). The critical voltage (Nh_{cr}; Hd_{cr}) can be taken as a criterion for assessing the tendency to brittle fracture surfaces.

The study of the influence of electrolysis conditions (Dk, T) on the tendency to brittle fracture surfaces showed that the critical condition of the coating occurs at higher current densities (Dk) and less than the electrolysis temperature (T).

Studies have shown that the maximum values of elasto-plastic characteristics (Ae; Ap; A; Hh; P, table 1-4) iron coatings can make a selection of coatings obtained under different conditions of the electrolysis (Dk, T) in terms of maximum resistance to wear.

This will significantly reduce the time of the experiments, increasing the amount of research that will significantly extend the effective use of iron-nickel coatings industry.

4. CONCLUSION

It was established experimentally that the unreduced hardness dynamic hardness (Hh), the dynamic hardness (Hd), the work expended on elastic (Ae), plastic (Ap), elasto-plastic (A) and the load deformation of the diamond spherical indenter (at h=1-4 μm) have an extreme character with a change in the conditions of the electrolysis (Dk, T) for the study of iron coatings, provided that (P<Pcr).

Experimentally established the beginning of the destruction of the iron coating on the critical load extrusion (Pcr) and recovery of critical hardness (Hh_{cr}), with a change in the conditions of the electrolysis (Dk, T). Critical load indentation (Pcr) diamond spherical indenter and the critical stress (hardness Hhcp) can be taken as a criterion for assessing the tendency to brittle fracture surfaces.

It was established experimentally that since the beginning of brittle iron coatings (at P=Pcr) work expended on elastic (Ae), plastic (Ap), elasto-plastic deformation (A), the load on the diamond spherical indenter (P = Pcr) and the depth of the indentation (hp; h) decreases with increasing current density (Dk) and the decrease in the temperature of electrolysis (T).

It was established experimentally that with the beginning of brittle iron coating (at P=Pcr) work expended on elastic (Ae), plastic (Ap) and elasto-plastic (A) strain significantly increased in value than when (P<Pcr). This shows that the increase in the work expended on elastic (Ae), plastic (Ap) and elasto-plastic (A) of the strain associated with the beginning of the brittle iron coatings.

It is found that with increasing the current density (Dk) and the decrease in the electrolysis temperature (T) increases the tendency of iron coatings to brittle fracture.

It was established experimentally that the critical unreduced hardness (voltage Hdkp), a critical dynamic hardness (Hdkp), the ratio Hhkp/E and Hdkp/E has an extreme character with a change in the conditions of the electrolysis (Dk, T) for the study of iron coatings. Extreme values Hhcp, Hdcp, relations Hhkp/E and Hdkp/E coincide with our earlier recommendation for iron coatings in terms of optimum durability.

Extreme values are reduced hardness (Hh), dynamic hardness (Hd), the work expended on elastic (Ae), plastic (Ap), elasto-plastic deformation (A) and the load indentation on diamond spherical indenter (P) coincide with our earlier recommendations. Coatings for railways in terms of ensuring their optimum durability.

Bibliography

1. Bulychev S.I., Alokhin V.N. *Ispytanie materialov nepreryvnym vdavlivaniem. Moskva, mashinostroenie, 1990, 224 s.*

2. V. F. Gologan, V. V. Azhder, V. N. Zhavguryanu. *Povyshenie dolgovechnosti detalej mashin iznosostojkimi pokrytiyami. Kishinev, Izd-vo Shtiincza, 112 s, 1979 (in Russian).*

3. Markovets M.P. *Opredelenie mexanicheskix*

svojstv materialov po tverdosti. Moskva, Mashinostroenie, 1979, 191s.

4. Grigorovich V.K. *Tverdost' i mikrotverdost' metallov. Moskva, Izdatel'stvo ''Nauka", 1976, 230 s.*

5. Javgureanu V., Gordelenco P., Elita M*. The work of deforming wear – proof iron-nickel plating in microsquelging. The Annals of University "Dunarea de Jos" of Galati, Fascicle 8, 2004, Tribology, Romania, pp. 65-68.*

6. Javgureanu V., Gordelenco P., Elita M. *Relationship of the restored and unrestored micro hardness of chromium coating. The Annals of University "Dunarea de Jos" of Galati, Fascicle 8, 2004, Tribology, Romania, pp. 48-51.*

7. Zhavguryanu V.N., Gordelenko P.V. *Sootnoshenie vosstanovlennoj i nevosstanovlennoj mikro tverdosti xromovyx pokrytij. Mezhdunarodnaya NTK "Mashinostroeniye i Texnosfera 21 veka", Sevastopol', 2005, r. 205-208.*

8. Zhavguryanu V.P. *Issledovanie raboty deformaczii iznosostojkix gal'vanicheskix pokrytij pri mikrovdavlivanii. Mezhdunarodnaya NTK "Novye proczessy i ix modeli v resurso- i energosberegayushhix texnologiyax". Odessa, 2003, s. 7-8.*

9. Javgureanu V., Gordelenco P. *Elasto-plastic properties and definition of porosity characterizes composite iron-nikel coatings. International conference of hydraulics and Pneumatics - Hervex-2014, Romania, Călimănești-Căciulata, 2014, p.126-131.*

10. Javgureanu V., Gordelenco P. *Elasto-plastic properties and tendency of iron-nikel composite coatings to brittle fracture. International conference of Hydraulics and Pneumatics - HERVEX-2014, Romania, Călimănești-Căciulata, 2014, p. 148-155.*

Recommended for publication: 28.02.2016

MOLDOVAN ELECTRICITY MARKET PROBLEMS: LEGAL PROVISIONS AND REALITY

PhD, associate professor Nicolae Mogoreanu
Technical University of Moldova, Chişinau

The structure of Moldovan electricity market

Currently, the Moldovan electricity market comprises two segments:

1. Electricity based on regulated prices, produced by CHPs whose operating regime is determined by heat load;
2. Wholesale market electricity based on non-regulated prices (about 75% of annual consumption volume) from *"Moldovan Thermal Power Plant - Ukraine"* duopoly, meaning that these prices do not result from unregulated competition.

Clearly, the so-called "*market power*" is missing in Moldova and competition in this energy sector will exist only when:

- New generating capacity will be built on the right bank of the river Nistru;
- Moldova will actually interconnect with ENTSO-E.

With regard to new generating capacity:

- Relatively low electricity consumption cannot provide sufficient incentives for investment in generating capacity from private business;
- The presence of a new plant with 2500 MW capacity at a distance of 100 km, with only 30-40% of capacity load employed is a risk factor for new capacity;
- Legislative-regulatory deficiencies together with disintegration of the Transmission Operator make high-risk obstacles for investors.

Therefore, only the construction of interconnections with European Energy Community is the way to solve the problem of market relations in the electricity system of the Republic of Moldova.

Let us assume that the problem interconnections is already solved and analyze to what extent the national legislative and regulatory framework favors the promotion of "supplier-consumer" relations typical for competitive market.

Directive2009/72/EC concerning common rules for the internal market in electricity

Art. 36, General objectives of the regulatory authority.

a) "promoting,…, a competitive, secure and environmentally sustainable internal market in electricity …, and effective market opening for all customers and suppliers …";

g) "ensuring that customers benefit through the efficient functioning of their national market, promoting effective competition and helping to ensure consumer protection".

Moldova's Energy strategy until year 2030 comprises three general objectives including:

2) development of competitive markets and their regional and European integration;

Art. 56 from the Strategy:

"…new players will be interested to enter the market ... once it is fully ***competitive and has a transparent and predictable regulatory framework****"*.

Law no. 124 on electricity**:**

The preamble *"This law establishes the framework necessary for the implementation of Directive 2003/54/EC of the European Parliament and of the Council of 26 June 2003 concerning common rules* ***for the internal market in electricity****..."*.

Art. 1.

"The purpose of this law is the establishment of legal framework for the effective operation, regulation and gradual opening of the electricity market ...".

Essentially, at first glance, the introductory statements as well as Art. 30 of the Law, named "*Electricity Market Rules*", legal -, technological - and organizational matters regarding the operation of electricity market from the Law are designed in strict accordance with the provisions of Directive 2009/72/EC.

Provision (8) from Art. 30 of the Law is in strict accordance with Directive 72.

*"Electricity suppliers, ...****eligible consumers*** *... **are obliged** to purchase electricity based on volumes established by the Agency in accordance with the Rules of electricity market ... The supplier designated by the Government ... delivers electricity purchased from CHP plants and from plants generating electricity from renewable energy based on the tariff approved by the Agency".*

Also, the manner this provision is enforced has become an obstacle to the emergence of market

relations in the electricity sector of the Republic of Moldova, even if there were interconnections with Romania or new production capacities on the right bank of the river Nistru.

Art. 30 (8) is repeated in the Electricity market rules:

"Eligible consumers that concluded bilateral contracts for supply of electricity and electric power ..... must necessarily ***conclude bilateral contracts for supply of electricity and electric power produced from sources regulated by ANRE*** *... . The share of electricity supplied to Eligible Consumers from sources regulated by ANRE is subject to annual approval by ANRE...."*.

In terms of practical enforcement of this provision, ANRE Board of Directors annually issues corresponding decisions.

ANRE BOARD OF DIRECTORS
Decision no. 536
of November 26, 2013
On the distribution of electricity.

Acting under Art. 7 and Art. 8, par. (1), let. m) of the Law on Electricity No. 124 of 23.12.2009, considering the priority status assigned to domestic marketing of electricity produced at domestic cogeneration power plants as well as the provisions of Electricity market rules, ANRE Board of Directors decides:

1. Starting with January 2014, the following approach for distribution of electricity **produced** at domestic CHP plants in cogeneration regime is approved:

a) CET-1 S.A., CET-2 S.A., CET Nord S.A.:
Î.C.S. ,,RED Union Fenosa" S.A. – 72,57 %
RED Nord S.A. – 20,82 %
RED Nord - Vest S.A. -- 4,11 %
Eligible consumers -- 2,50 %

The decision of ANRE Board of Directors contradicts the law provision:

❖ Law no. 124 only provides for: *„...electricity* ***purchased*** *from power plants ..."*;

❖ ANRE decision provides for *„...electricity* ***produced*** *from sources regulated by the Agency"*.

What's the difference? About 12%. In 2014 CET-1 produced 70.2 mil. kWh and supplied (the operator bought) 58 mil. kWh, CET-2 produced 765 mil. kWh and supplied 655 mln. kWh, CET Nord produced 70.0 mil. kWh and delivered 58 million. kWh. Extra 2.5% of 135 mln. kWh, which is 5 mln. lei, have to be paid. What are the reasons for operating with electricity that was not delivered to the grid, thus unreasonably increasing costs for bilateral contracts? Is it a mistake?

The results of this provision have been noticed without occurring in practice and are confirmed by a **case study for year 2014**.
Input data:

- Annual electricity consumption – 100 mil. kWh;
- Purchase price of electricity under bilateral contract – 0,82 lei/kWh;
- Based on ANRE decision no. 536 of 26.11.2013, eligible customer must purchase 2.5% of the electricity **produced** by CHP plants;
- Comparison of results was made only by **comparing purchasing costs of electricity** for an eligible consumer according to the Electricity market rules and to the competitive Bilateral contract, without the obligation to purchase expensive energy.

Table 1. Calculation results are shown in the table, where the following can be observed.

Based on current Electricity market rules					Based on competitive bilateral Contract		
Pro-ducer, supplier	Volume produced, mil. kWh	**2,5 %** from volume produced, mil. kWh	Tariff approved, lei/kWh	Total cost of electricity, mil. lei	Contracted volume, mil. kWh	Contract-based price, lei/kWh	Total cost of electricity, mil. lei
CET – 1	44	1,1	1,66	1,83			
CET – 2	616	15,4	1,586	24,42			
CET – N	50	1,25	1,371	1,71			
Total		**17,75**		**27,96**			
Contract		**82,25**	0,82*	**67,45**	**100**	0,82*	**82**
		100,00		**94,41**			

1. By signing the contract directly, under current conditions the total annual cost of electricity consumed would have been 82.0 mil. lei;

2. By respecting the market Rules, the total annual cost of electricity would have been 94.4 mil. lei;

3. The difference between 2014 cost results was 12.4 mil. lei;

How these aspects of tariff policy promoted around 20 years in the Republic of Moldova can be explained?

The aim is to reduce the cost of one Gigacalorie for Chișinău and Bălți residents connected to district heating systems.

For this purpose:

1. About 60% of energy production costs (electricity and heat) at CHPs are embedded in the cost of electricity and about 40% are embedded in heat production costs;
2. That is why the cost of electricity produced by CHP-2 (1,586 lei/kWh) is twice higher than the cost of imported electricity (0,708 euro/kWh);
3. All inhabitants of the country consume electricity and pre-school institutions and schools, hospitals and some 250-300 thousand families, etc., from Chișinău and Bălți employ the district heating system only. As a result, all people from the country, including most vulnerable household consumers, through electricity consumption contribute to cheaper thermal energy for district heating systems users in Chișinău and Bălți (subsidizing of district heating systems occurs). Thus, a local issue has become an issue of national scale;
4. The cost of 1 Gcal (2011) was: in Chișinău - 898 lei, in Bălți - 1047 lei (only these cities have heat and power plants and district heating systems), in district centers: Ştefan-Vodă - 1466 lei, Călăraşi - 1766 lei, Criuleni - 2870 lei, etc. The difference is obvious.

Provision 30 (8) of Law no. 124, slightly camouflaged, was transcribed into Art. 79 (4) of the draft new Law on electricity.

Article 79. *Bilateral contracts electricity market.*

(4) *Notwithstanding the provisions of paragraph (2) from this Article, within the bilateral contracts market the central electricity supplier* ***purchases*** *electricity from eligible power plants that produce electricity from RES,* ***electricity produced in high efficiency cogeneration regime and electricity produced by district heating power plants****, and resells it ..... according to the algorithm established by the Agency based on Electricity market rules, at regulated tariffs approved by the Agency.*

Let us recognize the fact that by purchasing electricity from renewable energy sources promotion of this type of generation is aimed for the future, and it is necessary to support the provisions of the preamble 43 of the Directive 2009/72/EC:

„Member States should have the possibility, in the interests of environmental protection and the promotion of ***new infant technologies****, of tendering for new capacity on the basis of published criteria. Such new capacity includes, inter alia, electricity from renewable energy sources and combined heat and power".*

However:

1. Combined energy production capacities – for electricity and heat are far from „**new infant technologies**" in the Republic of Moldova, more than that – these technologies are obsolete and outdated having considerable problems in terms of operation and maintenance;
2. Even if energy production is combined, both cycles are inefficient due to outdated equipment;
3. The method of cost allocation (heat/ electricity) is flawed and discriminatory against all categories of consumers, in particular against the vulnerable consumers.

If this provision is included in the new version of the Law, market relations in the electricity sector of the Republic of Moldova shall never develop.

The separate opinion of Moldovan Energy Consumers Association regarding Art. 79 (4) is currently examined by Energy Community Secretariat experts.

Another example related to possible market relations in Moldovan electricity sector.

When executing energy companies' privatization program in 2000, part of 110 kV electricity grid with transmission features and system connection were privatized by a private distribution operator.

When drawing up the contract for sale of distribution networks this mistake was detected, but could not be corrected because of changes in the Law on energy companies' privatization program that should be operated. As a result, based on the consent of parties, component 8 was introduced in the contract, stipulating the transfer of 110 kV power grids with transmission features and system connection to the Transmission Operator "*Mold-electrica*", which until present has not been done.

Power grids with transmission features and system connection owned by a private operator having a distribution license is against the rules promoted by European Directives, affects the energy security of the country and contributes to discrimination of consumers connected to these grids. In addition, two power plants release their electricity into the National Energy System through these networks, thus affecting sector safety and possible privatization of power plants in the future.

CASE STUDY

An eligible consumer connected to 110 kV grid within the private distribution operator ownership announced his intention to conclude a direct contract with the commercial operator S.A. "Energocom" aiming possible tariff reduction from 1.17 to 1.07 lei/kWh. In such case, the consumer would reduce annual electricity expenditures by 2.0 mil. Lei.

As a result, immediately appeared a letter signed by an ANRE director informing the consumer that if the contract was signed directly, the consumer should additionally pay both the cost of electricity transmission service through these grid sections (308 km of 110 kV network, tariff 8.13 bani/kWh) and the energy losses (0,41%). At that time the tariff for transmission service was 6.72 bani/kWh (the length of transmission network - over 4 000 km).

Calculations have demonstrated that signing of a direct contract while respecting the conditions imposed on the consumer will not bring any advantage. Figures from the letter (8.13 bani/kWh and 0.41%) with high precision covered the 2,0 mil. lei of economic- and legislative-based advantage.

It was also found, that in reality, ANRE's Board of Directors has not discussed this issue during a hearing and has not approved any decision regarding this subject; it was a simple letter, which at that time was treated as an official document.

During the last tariff setting procedure ANRE approved as "legal" the cost of transmission service through sections of transmission grids owned by the distribution operator, in the amount of 15 bani/kWh. The cost of transmission service through the national transport grid was established 14.5 bani/kWh. Both the ratio of figures 15,0/14,5 bani /kWh and of responsibilities and obligations (converted into costs) is incomprehensible

In fact, partial liberalization of the electricity market has been declared in 2002 and total liberalization - in 2014. Until present, no economic agent has been able to enjoy the benefits of a real electricity market.

CONCLUSIONS

1. Presently, the establishment of market relations in the energy sector of the Republic of Moldova in current conditions became a criterion, which for many years demonstrates that regardless of political color and government composition the policy pursued in this sector is subordinated to politics for social reasons with a strong electoral sub-stratum;

2. Even if members of the Board of Directors (ANRE) are appointed by the Parliament, this fact in no way contributes to ensuring the independence (conceptual) in the elaboration of documents and approval of tariffs (in terms of values and policies). A number of events from recent years confirms the declarative independence of ANRE only;

3. The examination of legislative and regulatory framework done by specialized international organizations is limited to the assessment of legal framework. It is also known that laws are enforced by means of a package of sub-legislative acts. These acts namely are the largest obstacles for carrying out legislative concepts, which at first glance, are formulated in compliance with European Directives; one such example is the problem regarding the electricity market;

4. The Energy Community Secretariat is informed by the Energy Consumers Association about the content of this paper (about the disintegration of country's electricity trasnmission system – during the last 2 years, about obstacles to market relations – during the last 8 months), but it only acknowledges the fact and hopes that the Ministry of Economy shall take care of the mentioned problems;

5. The existing situation offers unreasonable economic income to distribution and supply operators, thus exceeding 250-300 million lei annually, and these funds could decrease electricity payments as well as could be spent for activities increasing the economic effectiveness of a large group of enterprises in terms of GDP and jobs contribution.

References

1. *Directive 2009/72/EC of the European Parliament and of the Council of 13 July 2009 concerning common rules for the internal market in electricity.*

2. *Directive 2005/89/EC of the European Parliament and of the Council of 18 January 2006 concerning measures to safeguard security of electricity supply and infrastructure investment.*

3. *Regulation (EC) no. 714/2009 of the European Parliament and of the Council of 13 July 2009 on conditions for access to the network for cross-border exchanges in electricity.*

4. *Law on electricity no. 124 of 23.12.2009.*

5. *Electricity market rules, ANRE Decision no. 75 of 12.12.2002*

Recommended for publication: 15.03.2016.

HYBRID STOCHASTIC PETRI NETS WITH MATRIX ATTRIBUTES FOR MODELING OF DISCRETE-CONTINUOUS PROCESS

Emil Guţuleac, dr. hab, prof. univ., Sergiu Zaporojan, dr., conf. univ., Ion Gîrleanu, drd., Viorel Cărbune, drd.
Technical University of Moldova

INTRODUCTION

Hybrid systems (*HS*) are a class of systems which incorporates discrete-continuous process, such that the discrete dynamics and continuous dynamics are intertwined with each other. They arise in numerous important applications in CAD, real-time computing, computer networks, safety analysis, robotics and automation, flexible manufacturing systems, transport systems, fault tolerant control systems, mechatronics process control, biological systems, fluid systems, etc., and have recently been at the center of intense research activity in the computer systems and networks, control theory, computer-aided verification and artificial intelligence communities. Thus, *HS* have received increasing attention in the last few years, due to the ubiquitous trend of employing digital controllers in traditionally analogous environments, for example, manufacturing systems. For various applications and modeling of *HS* we refer to [1].

Discrete-continuous modelling and simulation is concerned with the description, analysis and performance evaluation of the dynamic behaviour of *HS* [3, 6, 7]. This approach is a research area that becomes more and more interesting and is due to the fact that most systems of real world applications are not purely discrete nor purely continuous and often both parts influence each other.

In the past several years, methodologies have been developed to model *HS* with stochastic behavior, to analyse their dynamic properties and asses their performance specifications [4, 5].

The generalized stochastic Petri nets (*GSPN*) provide a convenient and concise formalism for describing the discrete event dynamics of *HS* (computer systems, manufacturing systems, communication systems, biological systems, etc) [3, 7]. However, the underlying state space of *GSPN* models tends to be extremely large in practical modeling applications, often forcing us to seek approximate solution methods [4]. An alternative modeling paradigm for the purpose of analysis and simulation of *HS* is based on stochastic fluid models (*SFM*). The *SFM* paradigm allows the aggregation of multiple events into a single event associated with a “significant change” in the system dynamics. This offers the possibility of integrating, in a natural way, continuous and discrete dynamics in a single model.

Among the most *SFM* popular formalisms that are used for modelling of *HS*, there are the timed hybrid Petri nets (*THPN*) [4], fluid stochastic Petri nets (*FSPN*) [2, 6, 8] and hybrid stochastic Petri nets (*HSPN*) [5]. In such models the some places may hold a discrete number of tokens while others contain a continuous quantity represented by real quantities. However, for real *HS* visually modelling and simulation, it is possible that some attributes of these systems should take specific multiple different values; that cannot be easily described in *HSPN* or *FSPN* since their modelling will significantly increase graphical complexity of the system model. For example, in order to evaluate the performance measures of some hybrid systems processes for a specific simulation task considering thousands of services with different values, a high number of places, transitions and arcs will be needed in *HSPN* model in order to be able to obtain desired load value for each specified time interval. This brings a considerable higher structural complexity of this type model, so it is difficult to analyse such a complex structure, for example the amount of states introduces a complexity in global computing and because of that we have a longer simulation time. However, it should also to enhance this formalism in order to be able to fully represent, more concise and flexible describe *HS* systems with complex discrete-continuous stochastic process.

In order to address such issues, we introduce the model definition, behavior rules and the graphical representation for a new kind of *HSPN* formalism with matrix attributes, called bellow as *HSMN*, similarly as they were used in [6] through introducing *database arcs* with matrix weight, that makes possible the use of real data in the simulation process, assuring the validity of the obtained results.. This extension allows the modeling of high complexity systems without the danger of having a very graphically complicated *HSPN* model that is too difficult to represent and hard to understand. In the same context, we consider some examples to

graphically represent *HSMN* and them unfolding with *HSPN* models that whose behaviours are equivalents.

An important advantage of proposed approach is the fact that *HSPN* model representation is very concise and flexible, because majority of its attributes are parameterized and can take various marking-dependent values.

1. HSPN WITH MATRIX ATTRIBUTES

1.1. Formal definition

Let the IN_+ and IR are the sets of non-negative natural and real numbers, respectively.

The definition of a *HSPN* with matrix attributes, called *HSMN*, is derived from [3, 5, 6, 8] and it inherits most of the features of *GSPN*, *THPN* and *FSPN*. In a *HSMN* net the matrix attributes of objects (arcs, place capacities, transition guard and priority functions, transition firing rates, etc.) type *z*, depending on current network state *s*, are defined by a set of matrix $\boldsymbol{A}^z = [a^z_{ij}(s)]_{k\times n}$, $\boldsymbol{A}^z \in \mathbf{A}$. The value of elements $a^z_{ij}(s)$ are constants, variable or functions of specified type, eventually they can be depending on current network state *s* of a *HSMN*.

The dimension $k \times n$ and the localisation of current element $a^z_{ij}(s)$ of matrix $\boldsymbol{A}^z$ is specified by a discrete control place set $P^z_A \subset P_D$. For example, for specification $\boldsymbol{A}^z$ and current computing of its element it should be a control place p_l set $P^z_A = \{p_l, p_v\}$. So, the current number of tokens $i = m_l = M(p_l)$ and $j = m_v = M(p_v)$ of control places p_l and p_v respectively shows the element's position in the $\boldsymbol{A}^z$ matrix, and its values needs to be imported and taken in consideration when executing and analysing the model. Moreover, the capacity of control place $p_l \in P^z_A$ and place $p_v \in P^z_A$ should be specified to $K^p(p_l) = k$ and $K^p(p_v) = n$, respectively.

Formally, a *HSMN* is specified as a 14-tuple $H\Gamma = < P, T, Pre, Post, Test, Inh, K_p, K_b, G, Pri, M_0, \Lambda, W, V >$, where:

- P is the finite set of places consisting of a set of discrete places P_D and a set of continuous places P_C, $P = P_D \cup P_C$, $P_D \cap P_C = \varnothing$. A discrete place p_i is drawn with a single circle and can contain a number of tokens, $m_i = M(p_i) \in IN_+$, non-negative integer values. A continuous place (buffer) b_k is drawn with two concentric circles and can contain a real number of fluid $x_k = x(b_k) \in IR$. The marking (the *state*) $s=(M, \boldsymbol{x})$ of the $H\Gamma$ is given by pair of vector-columns, M and $\boldsymbol{x}$, describing the contents value of each type place, $(M, \boldsymbol{x}) \in \hat{S} = IN_+^{|P_D|} \times IR^{|P_C|}$, respectively. We call $\hat{S}$ the "potential state space", as opposed to the "actual state space" $S \subseteq \hat{S}$, the set of marking actually reachable during the evolution of the $H\Gamma$. The current marking $s = (M, \boldsymbol{x}) \in S$ evolve in time, which we indicate by τ, so, formally, it is a stochastic process $\{(M(\tau), \boldsymbol{x}(\tau), \tau \geq 0)$.
- T is a finite set of transitions, $T \cap P = \varnothing$, that is partitioned into a set T_D of discrete timed transitions and a set T_C of continuous timed transitions, that $T = T_D \cup T_C$, $T_D \cap T_C = \varnothing$. A continuous timed transition $u_k \in T_C$ is drawn as an empty rectangle. The set of discrete transitions T_D is partitioned into $T_D = T_0 \cup T_\tau$, $T_0 \cap T_\tau = \varnothing$ so that: T_τ is a set of timed discrete transitions and T_0 is a set of immediate discrete transitions.
- *Pre*, *Test* and $Inh: P \times T \times \hat{S} \times IN_+^{|P_A|} \to Bag(P)$ respectively are a backward flow, test and inhibition functions incidence mappings. $Bag(P)$ is a discrete or continuous multiset over *P*. The forward flow function incidence mappings in the multisets of *P* is a $Post: T \times P \times \hat{S} \times IN_+^{|P_A|} \to Bag(P)$ describe the set of arcs A with the marking-dependent cardinality, connecting transitions with places and vice-versa.
- $K_p: P_D \times IN_+^{|P_D|} \to IN_+ \cup \{\infty\}$ describe the capacity bound K_{p_k} on each discrete place $p_i \in P_D$, $0 \leq K^{\min}_{p_i} \leq M(p_i) \leq K^{\max}_{p_i} < +\infty$, which can contain an *integer* number of *tokens*, respectively. By default, the $K^{\min}_{p_i} = 0$ and $K^{\max}_{p_i}$ is set to infinity.
- The $K_b: P_C \times IR^{|P_C|} \times IN_+^{|P_A|} \to IR$ describe the fluid bound on each continuous place $b_k \in P_C$, such that $-\infty < x^{\min}_k \leq x(b_k) < x^{\max}_k < +\infty$, where the $x^{\min}_k$ describe the lower fluid bound and x_i^{max} upper bounds of of b_k. By default the $\forall\, x^{\max}_k$ is set to infinity, and it no effect. An implicit lower bound of continuous place is 0.
- $G: T \times \hat{S} \times IN_+^{|P_A|} \to \{True, False\}$ describe the marking-dependent *guard function* of each transition. For $t_j \in T$ a guard function $g_j(s)$ will be

evaluated in each marking s, and if it is *true* (the default value is *true*), the transition may be enabled, denoted $t_j \in T(s)$, otherwise t_j is disabled.

- $Pri: T \times \hat{S} \times IN_+^{|P_A|} \to IN_+$ defines the dynamic priority function for the firing of each transition. The firing of a transition with higher priority potentially disables all the transitions with the lower priority. By default, the $Pri(T_0) > Pri(T_\tau)$.

Figure 1 summarizes the representation of all the $H\Gamma$ graphical primitives.

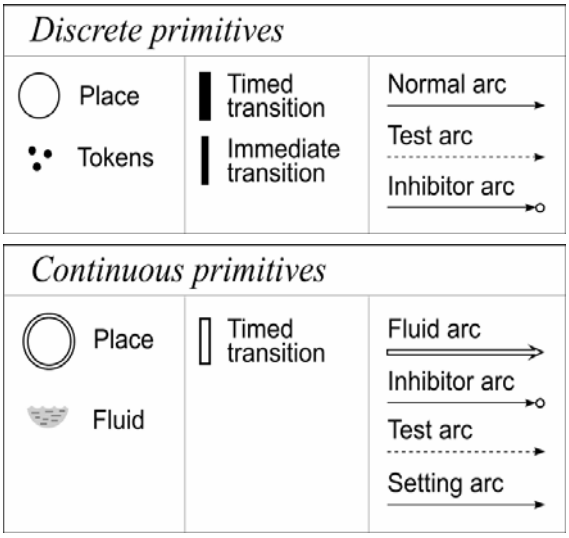

Figure 1. All the graphical primitive of the $H\Gamma$.

- The current marking (*state*) $s=(M, \boldsymbol{x}) \in S$ value of a $H\Gamma$ net depends on the kind of place. The $m_i = M(p_i)$ describes the number of tokens in discrete place p_i, and it is represented by black dots. The $x_k = \boldsymbol{x}(b_k)$ describes the fluid level in continuous place b_k and it is a real number, also allowed to take negative real value. The initial marking of net is $s_0 = (M_0, \boldsymbol{x}_0)$. Graphically, the initial marking is represented by writing the value of m_i^0, or x_k^0, inside the corresponding place. If the number m_i^0 is small it is common to drawn m_i^0 tokens inside the place p_i, represented by dots. A missing value indicates zero.
- A timed discrete transition $t \in T_\tau$ is drawn as a black rectangle and has an exponentially distributed firing time which marking - dependent firing rate $\Lambda : T_\tau \times \hat{S} \times IN_+^{|P^A|} \to IR_+$.
- $W : T_i \times Bag(P) \times IN_+^{|P^A|} \to IR_+$ is the weight function of immediate discrete transitions $t_k \in T_0$, and this type of transition is drawn with a black thin bar and has a zero firing time.
- $V : T_C \times \hat{S} \times IN_+^{|P^A|} \to IR_+$ is the marking dependent fluid rate function of timed continuous transitions T_c. These rates appear as labels next to the continuous timed transitions. If $u_j \in T_c$ is enabled in *tangible* marking *M* it fires with rate $V_j(M)$, that continuously change the fluid level of continuous place P_C. ■

Figure 2 summarizes the all possible ways placing of arcs in a $H\Gamma$ net for discrete transition and continuous transition with the discrete places and continuous places, respectively.

Given a transition $t_j \in T$, we denote by ${}^\bullet t_j$ and $t_j^\bullet$ the directed preset places and postset places and by ${}^\circ t_j$ and ${}^* t_j$ the *inhibition* set places and *test* set places connected respectively with transition t_j.

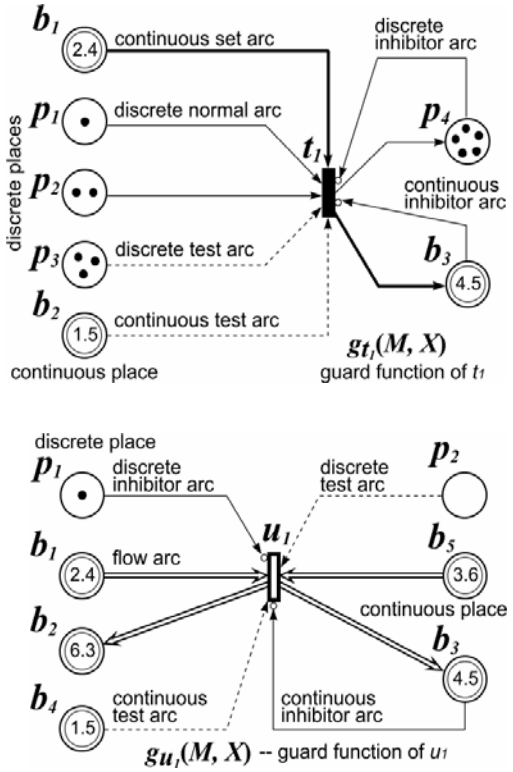

Figure 2. All kinds of arcs and their possible ways for placing in a $H\Gamma$.

1.2. The HSMN dynamics

The dynamics of the *HSMN* combines both time-driven and event-driven dynamics. We define *macro-events* the events that occur when [3]:

The evolutions of *HSMN* in current marking $s = (M, x)$ are determined by the following rules:

1. Localization of the elements $a_{i,j}^z(s) \in \boldsymbol{A}^z$ for $i = M(p_l)$ and $j = M(p_v)$, $p_l, p_v \in P_A^z$ of type z;

2. Computing the current value of $a^z_{i,j}(s)$, obtaining the respective constant values. If $i = M(p_l) = 0$ and/or $j = M(p_v) = 0$ then the cardinality value of a respective attribute type z is given by default;

3. For theses values obtain the enabling set of transitions $T(s) = T_D(s) \cup T_C(s), T_D(s) \cap T_C(s) = \varnothing$;

4. Firing of selected transition $t \in T(s)$ and change the current state: $s[t > s'$.

Enabling and Firing rules. As already described [??], two types firing of enabled transition, called *discrete firing* and *continuous firing*, govern the state evolution of the net.

Let $T(s)$ be the set of enabled transitions in current state $s=(M, x) \in S$.

We say that a *discrete transition* $t_j \in T_D(s)$ is enabled in current state s if the following logic (Boolean) expression (enabling condition $ec_D(t_j)$ of t_j is verified:

$$ec_D(t_j) = (\underset{\forall p_i \in {}^\bullet t_j}{\wedge} (m_i \geq Pre(p_i, t_j)) \,\&\, (\underset{\forall p_k \in {}^\circ t_j}{\wedge} (m_k < Inh(p_k, t_j)) \,\&\, (\underset{\forall p_l \in {}^* t_j}{\wedge} (m_l \geq Test(p_l, t_j)) \,\&\, (\underset{\forall p_n \in t_j^\bullet}{\wedge} ((K_p - m_n) \geq Post(p_n, t_j)) \,\&\, (\underset{\forall b_i \in {}^\bullet t_j}{\wedge} (x_i \geq Pre(b_i, t_j)) \,\&\, (\underset{\forall b_k \in {}^\circ t_j}{\wedge} (x_k < Inh(b_k, t_j)) \,\&\, (\underset{\forall b_l \in {}^* t_j}{\wedge} (x_l \geq Test(b_l, t_j)) \,\&\, (\underset{\forall b_n \in t_j^\bullet}{\wedge} ((K_b - x_n) \geq Post(x_n, t_j)) \,\&\, g_j(s).$$

The transition $t_j \in T_d(s)$ may fire if no other transition $t_k \in T_d(s)$ with higher priority is enabled, and yielding:

$$M' = M + C(\cdot, t_j), \text{ there}$$

$$C(p, t_j) = Post(p, t_j) - Pre(p, t_j), \ \forall p \in P_D.$$

The stochastic evolution of the *HSMN* in *tangible* marking is governed by a race [2, 3]: the timed discrete transition *t* with the shortest firing time is the one chosen to fire next. If an immediate discrete transition is enabled in current marking *s*, it is *vanishing*. Otherwise, the marking is tangible and any timed discrete transition is enabled in it [3, 5]. If several enabled immediate transitions $t_j, t_k \in T_D(s)$ are scheduled to fire at the same time in *vanishing* marking *s*, the transitions t_k, with the respective weights w_k , fire with probability:

$$q(t_k, s) = w(t_k, s) / \sum_{t_j \in T_0(M)} w(t_j, s).$$

Also, we say that a continuous transition $u_j \in T_C(s)$ is enabled and continuously fires in current marking *s* if the following logic expression (the enabling condition $ec_C(u_j)$) is verified:

$$ec_C(u_j) = (\underset{\forall b_i \in {}^\bullet u_j}{\wedge} (x_i > 0) \,\&\, (\underset{\forall p_k \in {}^\circ u_j}{\wedge} (m_k < Inh(p_k, u_j)) \,\&\, (\underset{\forall p_l \in {}^* u_j}{\wedge} (m_l \geq Test(p_l, u_j)) \,\&\, (\underset{\forall b_k \in {}^\circ u_j}{\wedge} (x_k < Inh(b_k, u_j)) \,\&\, g_j(s) \,\&\, (\underset{\forall b_l \in {}^* u_j}{\wedge} (x_l \geq Test(b_l, u_j)) \,\&\, (\underset{\forall b_n \in u_j^\bullet}{\wedge} ((K_{b_n} - x_n) \geq V_j \cdot Post(x_n, u_j)),$$

and no other transitions with higher priority are enabled in current state.

If the state *s* is tangible, fluid flow could continuously through the flow arcs of enabled continuous transitions into or out of continuous places. As a consequence, if transition t_c is *enabled* in current state it *enabling degree*, for every $b \in {}^\bullet u$ and $x(b)>0$, is:

$$Enab(u, s) = \min_{b \in {}^\bullet u} \{x(b)/Pre(u, b)\}.$$

Given two time instants τ and τ', the evolution of the fluid level in buffer $b_i \in P_C$ is given as:

$$x(b_i, \tau) = x(b_i, \tau') + \vartheta(b_i, u, \tau, \tau'), \text{ there}$$

$$\vartheta(b_i, u, \tau, \tau') := \sum_{u_j \in {}^\bullet b_i} Post(b_i, u_j) \cdot \int_{\tau'}^{\tau} \upsilon_{u_j}(\theta) d\theta - \sum_{u_k \in b_i^\bullet} Pre(b_i, u_j) \cdot \int_{\tau'}^{\tau} \upsilon_{u_k}(\theta) d\theta, \upsilon_{u_j}$$

and υ_{u_k} denote the firing speeds of u_j and u_k at time θ respectively.

Upon firing, the discrete (continuous) transition removes a specified number (quantity) of tokens (fluid) for each discrete (fluid) input place, and deposits a specified number (quantity) of tokens (fluid) for each discrete (fluid) output place. The levels of fluid places can change the enabling/disabling of transitions.

2. HSMN EXAMPLES

In the following, we illustrate the power and flexibility representation of proposed *HSMN* formalism with a few examples.

We allow the firing rates and the enabling functions of the timed discrete transitions, the enabling functions and firing speeds of the timed

continuous transitions, and arc cardinalities to be dependent on the current states of the $H\Gamma$.

Graphically, a matrix attribute of *HSMN* will be presented in a way that it will contain the matrix name in square brackets. So, for example, a direct arc matrix cardinality [2, 3, 5], denoted by  , can take values that are contained in a specified matrix **A**. To well understand the meaning of this model type, an example of *HSMN*1 is presented in figure 3 with the following initial state $s_0 = (M_0, x_0)$ with:

$$M_0 = (2,\ 3,\ 0,\ 1,\ 4) = (2p_1 3p_2 p_4 4p_5),$$

$$x_0 = (17.4,\ 3.25,\ 4.18) = (17.4b_1,\ 3.25b_2,\ 4.18b_3).$$

The mean matrix cardinality values of a discrete arc (t_1, p_3), setting continuous arcs $\{(b_1, t_1), (t_1, b_3)\}$ and fluid arc (u_1, b_2) in *HSMN*1, controlled by $P^A = \{p_1, p_2\}$, are given by following specified matrices:

$$\mathbf{A1}=\begin{bmatrix} 3 & 2m_1+m_3 & 1 & 1+m_3 \\ m_4 & 7 & m_2+2m_5 & 3+m_2 \\ 1 & 4 & 8 & m_2+4m_3 \end{bmatrix},$$

$$\mathbf{A2}=\mathbf{A3}=\begin{bmatrix} 3.0 & 2x_3 & 3.65 & 0.85+x_3 \\ 1.75 & 2.35 & 3.25+x_3 & 3.27 \\ 1.25 & 1.40 & x_3 & 2.15+m_4 \end{bmatrix},$$

$$\mathbf{A4}=\begin{bmatrix} 0.25 & x_3 & 3.65 & 0.85 \\ 0.75 & 2.35 & 0.32+x_3 & 3.27 \\ 1.25 & 1.40 & x_2 & 2.15+x_3 \end{bmatrix},$$

where $m_i = M(p_i), i = 1,2,3,4,5$ is the number of tokens in discrete place p_i in current state, and $x_k = x(b_k), k = 1,2,3$ is the quantity of a fluid level in buffer b_k.

Control place p_1 has the specified capacity $K^p(p_1) = k = 3$, but the capacity of place p_2 is $K^p(p_2) = n = 4$.

For *HSMN*1 in figure 3a the selected $a^z_{i,j}$ element position in matrix $\mathbf{A}^z$, the value must to be imported, is realized by information about the current token number contained in control place set $\{p_1, p_2\}$, that specify the index row $i = m_1$ and index column $j = m_2$. So, for $i = m_1^0 = 2$ and $j = m_2^0 = 3$ we obtain: the cardinality value of arc (t_1, p_3) is equal to $a^1_{2,3} = m_2 + 2m_5 = 10$, of arcs (b_1, t_1) and (t_1, b_3) its are equal to $a^2_{2,3} = a^3_{2,3} = 3.25 + x_3 = 7.43$, respectively, but for arc (u_1, b_2) it is equal to $a^4_{2,3} = 0.32 + x_3 = 4.5$. For these corresponding current values of arc cardinality the enabled set of transitions is $T(s_0) = \{t_1, u_1\}$.

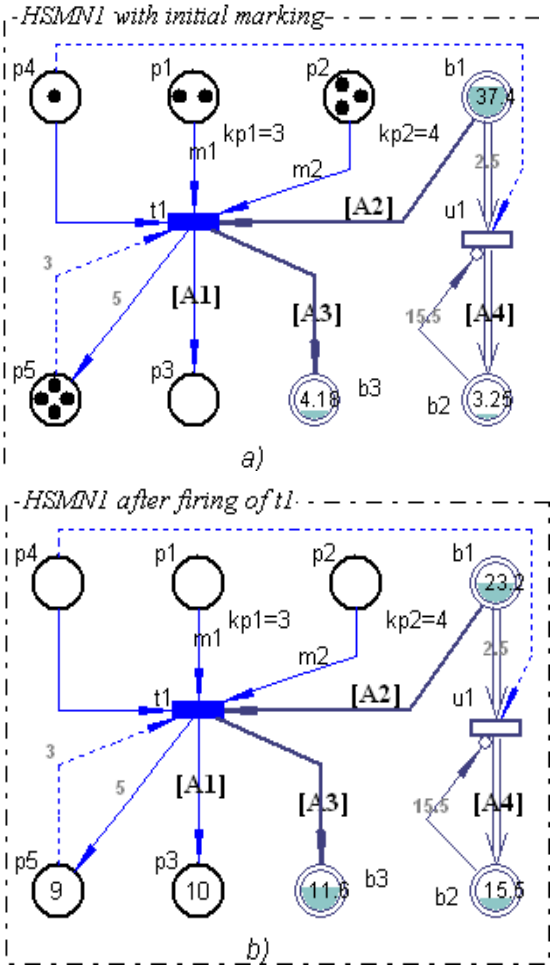

Figure 3. A *HSMN*1 with matrix arc cardinality: a) initial state; b) final state.

Let the firing speed of continuous transition u_1 is υ_1=1 and firing rate of timed transition t_1 is $\lambda_1 = 0.25$, that it mean firing delay is $\tau_{t1} = 4$ t.u.

Because the cardinality of $Inh(b_2, u_1)$=15.50, then the transition u_1 continuously fire only during $\tau_{u_1} = (15.50 - x_2)/a^4_{2,3} = 2.72 < \tau_{t1} = 4$ t.u., so it is disabled and the fluid level x_1' of buffer b_2 become: $x_1' = x_1 - (2.5 \cdot \tau_{u_1} + a^2_{2,3}) = 23.17$.

Figure 3b presents the state of HSMN1 network after t_1 fires, from where we can observe that place p_3 has a number of tokens equal to 9, because the element $a_{3,4} = m_2 + 4m_3 = 8$ was selected. As

a result the firing of t_1, we yield the new state $s' = (M', x')$ with:

$$M' = M_0 + a^1_{2,3} = (10\,p_3, 9\,p_5),$$

$$x'_2 = x_2 + a^2_{2,3} \cdot \tau_{u_1} = 15.50,\ x'_3 = x_3 + a^3_{2,3} = 11.61.$$

In a similar way all *HSMN* nets attributes can be parameterized using matrix cardinality, for example, see the following attributes [3]:

- Guard function of transitions $\boldsymbol{G}^{z1}$, $\boldsymbol{G}^{z1} = [g^{z1}_{i,j}(s)]_{k\times n}$, $z1 \in \{t, u\}$;
- Place capacity $\mathrm{K}^{z2} = [k^{z2}_{i,j}(s)]_{l\times n}$, $z2 \in \{p, b\}$;
- Firing rate $\boldsymbol{R}^{z3} = [r^{z3}_{i,j}(s)]_{k\times n}$, $z3 \in \{\lambda, w, \upsilon\}$;
- Priority firing of transitions T $\Gamma^{z4} = [\gamma^{z4}_{i,j}(s)]_{k\times n}$, $z4 = Pri$;

The most important benefit we get from using *HSMN* when describing and verifying discrete-continuous processes of hybrid systems is that the structure of these models' is very concise and is very flexible when modifying it parameters in real time, because most of its attributes are parameterized. This permits assigning in a current state controlled mode, alternative values of *HSMN* attributes. Also, using proposed approach matrix attributes, real time data can be easily imported in simulating model, and in this way we can ensure results correctness.

Moreover, the modelling the same system through the other kind of Petri net, for example *GSPN* or *THPN*, to drive the structure of this models it is necessity for each matrix attribute to use additional $2k \times n$ arcs and $k \times n$ additional transitions (respective places), and this means that the model's complexity grows significantly. To illustrate the usage advantages of *described approach*, we present a simple example of *HSMN*2 shown in figure 4a, that a matrix cardinality of direct arc $(t_5,\ p_6)$ is parameterized by matrix **A**:

$$\mathbf{A} = \begin{bmatrix} 5+m_1 & 3 & 2 \\ 4 & 2+m_2 & 1+2m_2 \end{bmatrix}.$$

In this model control places are $P^{A5} = \{p_l, p_v\}$ with $K^p(p_2) = 2$ and $K^p(p_3) = 3$ respectively. Selection of respective row $i = m_2$ and column $j = m_3$ of element $a^5_{i,j}(M)$, $i = 1, 2$; $j = 1, 2, 3$ from matrix **A** is done in a dynamic way by current marking of places p_2 and p_3, respectively.

The unfolding of the model *HSMN*2 trough *GSPN*2 attributes approach, that whose behaviours are equivalents, is shown in figure 4b.

In order to show it in such mode, we need to substitute in *HSMN*2 attributes as bellow:

1) The transition t_5 is substitute by $k \times n = 6$ transitions $t_{5,l}$, $l = 1,..., k \times n$, that whose guard functions are respectively:

$$g_{5,1}(M) = (m_2 = 2)\,\&\,(m_3 = 3),$$
$$g_{5,2}(M) = (m_2 = 2)\,\&\,(m_3 = 2),$$
$$g_{5,3}(M) = (m_2 = 2)\,\&\,(m_3 = 1),$$
$$g_{5,4}(M) = (m_2 = 1)\,\&\,(m_3 = 2),$$
$$g_{5,5}(M) = (m_2 = 1)\,\&\,(m_3 = 3),$$
$$g_{5,6}(M) = (m_2 = 1)\,\&\,(m_3 = 1);$$

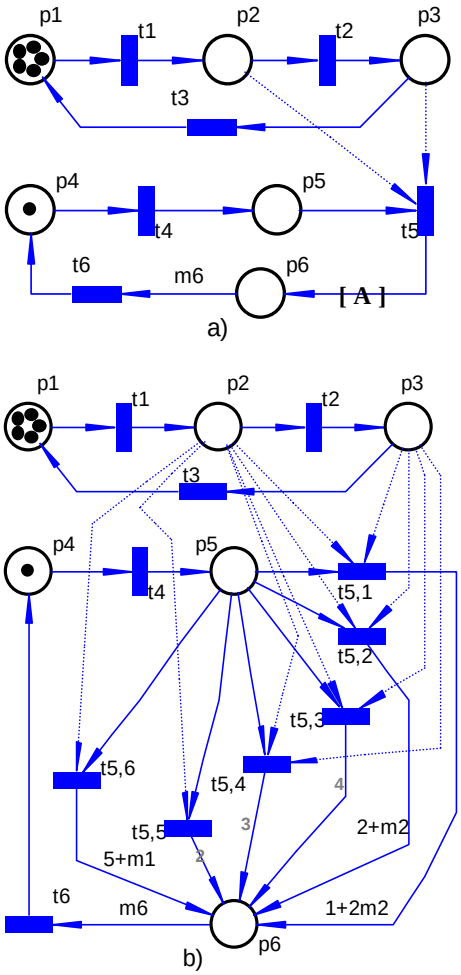

Figure 4. Behavioural equivalent Petri net: *a*) model *HSMN*2 and *b*) model *GSPN*2.

2) The direct matrix arc $(t_5,\ p_6)$ with matrix cardinality **A** is substitute by $k \times n$ direct arcs $(t_{5,l}, p_6)$, $l = 1,..., 6$ with weight's value from respective **A** matrix's elements;

3) To connect place p_5 with each introduced transition $t_{5,l}$ through arcs $(p_5, t_{5,l})$, $l = 1,...,6$;

4) Place p_2 (respectively p_3) is connected with each introduced transition $t_{5,l}$ through test arcs $(p_2, t_{5,l})$ (respectively $(p_3, t_{5,l})$).

In addition, it is to mention, that the real hybrid system is modelled by a *HSMN* approach, were contain multiple matrix attributes $\mathbf{A}^z$ with different sizes, the behavioural equivalents resulting *HSPN* model is still too complex to be of practical use for conveying the system behaviour visually. For example, the equivalents resulting *HSPN*1 model of *HSMN*1 shown in figure 3, may contain potentially at least $3N_1$ graphical elements (transitions, places and arcs), there:

$$N_1 = (\sum_j^4 (k_j \cdot n_j)) = 3^4 \cdot 4^4 = 20736 \cdot$$

Proposed framework is generic and can be applied to a numerous system types with discrete-continuous process. Additionally, with minor changes and additions, described approach can be generalised for studying domains with similar characteristics. Presented analysis shows that *HSMN*, which were defined and studied in this paper, can be used as a much promising instrument for modelling and evaluating of hybrid system performance indicators.

This work is supported by National Institutional Applied Reserche Project under grants 15.817.02.28A, Republic of Moldova.

3. CONCLUSIONS

In this paper, a new framework *HSMN* was introduced, as a derivative of *GSPN* and *HSPN*. Modelling and performance evaluation of stochastic discrete-continuous process is illustrated.

The *HSMN* approach is very efficient for representing, modelling, verifying and analysing of hybrid system performance, because *HSMN* use has the following advantages: 1) there are additional visualisation features for modelling and simulating procedures, that permits to create a string environment for validation and evaluation; 2) it is possible to visualise in the same model attribute's dynamic change; 3) the real data can be easily imported in simulation process, assuring correctness and validity of obtained results.

The applicability of this approach is illustrated through a few examples of *HSMN* models with different matrix attributes. Moreover, this approach with rather few modifications and additions may be further generalized to study a reconfigurable hybrid system from areas with similar enhanced characteristics.

We aim to elaborate and develop a software product for visual simulation and analysis of *HSMN* models that describe the evolution of hybrid systems with discrete-continuous process.

Bibliography

***1*. Bujorianu M.L., Lygeros J.** *Towards modelling of general stochastic hybrid systems. Stochastic Hybrid Systems: Theory and Safety Critical Applications. LNCIS, vol. 337, Springer, Heidelberg, pp. 3–30, 2006.*

***2. Ciardo G., Nicol D.M., Trivedi K.S.** Discrete-event simulation of fluid stochastic Petri nets, IEEE Transactions on Software Engineering, 2, (25), pp. 207–217, 1999.*

***3. Chiola G., Ajmone- Marsan M., Balbo G., Conte G.** Generalized stochastic Petri nets: A definition at the net level and its implications. IEEE Transactions on Software Engineering, 19(2), pp. 89-107, 1993.*

***4. David R., Alla H.** Discrete, Continuous, and Hybrid Petri Nets. Springer-Verlag, Berlin, 2010. - 568 p., DOI 10.1007/978-3-642 -10669-9.*

***5. Guţuleac E.** Descriptive compositional HSPN modeling of computer systems. Annals of the Craiova University, România, vol. 3 (30), no.2, pp.82-87, 2006.*

***6. Katsigiannis Y. A., Georgilakis P. S. Tsinarakis G. J.** Introducing a coloured fluid stochastic Petri net-based methodology for reliability and performance evaluation of small isolated power systems including wind turbines. IET Renewable Power Generation, Vol. 2, No. 2, pp. 75–88, 2008.*

***7. Herajy M., Schwarick M., Heiner M**. Hybrid Petri Nets for modelling the eukaryotic cell cycle. ToPNoC VIII, pp. 123–141, 2013. Doi: 10.1007/ 978-3-642- 40465-8/7.*

***8. Horton G., Kulkarni V. G., Nicol D. M., Trivedi, K. S.** Fluid Stochastic Petri Nets: Theory, Application, and Solution Techniques. European Journal of Operations Research, 105 (1), pp. 184-201, 1998.*

Recommended for publication: 26.05.2016.

MECHANICAL PROPERTIES OF SELF-COMPACTING CONCRETE

Aurelia Bradu, drd. ing., Nicolae Cazacu, drd. ing.
Tehnical University „Gheorghe Asachi" from Iassy

1. INTRODUCTION

Concrete is the most commonly used structural material in the construction (buildings, bridges, roads, dams, etc.). Self compacting concrete also referred as "Self-consolidating concrete" was discover in 1986 by Japanese prof. Okamura as a solution to improve the concrete durability, decreased due to the lack of skilled workers. This new material is able to flow and consolidates itself without additional mechanical compaction. The elimination of vibration reduces labor, shortened construction time, diminished equipment costs and improve working environment. The workability of SCC makes it convenient for placing in difficult conditions (complicated shapes, narrow sections, congested reinforcement). The self compactibility properties require high deformability of mortar and resistance to segregation when the concrete flows through confined zones. The procedures to determinate its fresh properties and allowable values are described in "European Guidelines for self-compacting concrete" [1].

The properties of hardened SCC were less studied despite of its importance in design concrete structures, they were conventionally adopted the same as for the vibrated concrete.

2. GENERAL FEATURES OF SCC

SCC components are similar to vibrated concrete (cement, mineral admixtures, aggregates, mineral and chemical admixtures, water), but the final composition of the mixture and its fresh characteristics are different (fig.1).

SCC requires a larger proportion of powder materials and higher quantities of high range water-reducing admixtures. The correct choice of cement and its quantity is determined by each application and must conform to EN 197-1 and EN 206-1. In order to keep the necessary paste volume without cement excess, in the composition of SCC is added mineral admixture, usually they represent industrial by-products: limestone filler, fly ash, silica fume, blast furnace slag.

Limestone filler is chemically inert and is the most commonly mineral addition, due to its particles size improves the mobility of fresh concrete and fills the gaps between cement grains.

Figure 1. Slump flow test of SCC.

Fly ash is a by-product of burning pulverized coal in an electrical generating station, it use increases the flowability, reduces the cement hydration heat and enhances the viscosity of fresh concrete. Fly ash have a pozzolanic activity, in the presence of moisture chemically reacts with calcium hydroxide, and form silicate hydrate and cementititous compounds.

Silica fume is also very effective in reducing or eliminating bleeding and this can solve the problem of rapid surface crusting. The high level of fineness and almost spherical shape its particles lead to a good cohesion and an improved resistance to segregation.

The passing ability of SCC is evaluated by its capability to flow through tight openings including spaces between reinforcing bars. The maximum aggregate size should generally be limited to 12 – 20 mm. In order to obtain a more consistent product is recommended to use washed aggregates.

Viscosity modifying admixtures (VMA) improve the cohesion of the SCC without significantly altering its fluidity. These admixtures are used in SCC to minimize the effect of variation in moisture content, making the SCC more robust.

The superplasticisers are the most important admixtures improving concrete performance; for SCC is recommended to use polycarboxylate ether based (PCE).

Typical range of mix design SCC according to the study ICECON S.A [2]:

- volume of paste varies between 32-42% of concrete volume;
- volume of coarse aggregate varies between 28-38% of concrete volume;
- the content of powder varies between 445-605kg/m³;
- the water powder ratio varies between 0,26-0,28;
- the content of fine aggregate varies between 38-54% of binder volume;
- the maximum aggregate size should be limited to 16 – 20mm;
- the most used cement type is Portland cement and the addition is mineral fillers.

SCC is produced with a low water/cement ratio and higher paste volume. To maintain the homogeneity and resistance to segregation, the aggregate is chosen more rigorous by shape, origin, nominal maximum size.

3. ESSENTIAL MECHANICAL CHARACTERISTICS

The modifications made in the mix design of SCC affect its mechanical behavior as compared to NVC in hardened state.

The main requirements which SCC (according to EN 206-1) must correspond are mechanical strength and durability.

Durability represents the capability of a concrete structure to withstand environmental aggressive situations during its design working life without impairing the required performance [EN 206-1]

The study of the mechanical characteristics of SCC became one of the research objective for the last years. The most important mechanical properties of the concrete are: compressive strength, tensile strength, the modulus of elasticity.

3.1. Compressive strength

Compressive strength is one of the most important mechanical characteristics of the concrete. Many of the other mechanical properties (e.g. tensile strength, modulus of elasticity, compressive strain) and physical properties (e.g. related to durability) of concrete are moreover expressed as a function of this parameter [1].

The compressive strength of concrete is affected by: W/C, cement compressive strength, properties of the aggregates (shape, grading, surface texture mineralogy, strength, stiffness, and maximum grain size), air-entrainment, curing conditions, testing parameters, specimen parameters, loading conditions, and test age.

In Eurocode 2, concrete is classified solely on the basis of its compressive strength, in accordance with EN 206-1 where cylinders 150/300 mm and cubes 150 mm are used as a reference.

The values $f_{c,cub,x}$ and $f_{c,cyl,d}$, represent the compressive strength determined on cubes side x and cylinders with diameter d. According to Domone [3], the ratio $f_{c,cyl,d}/f_{c,cub,x}$ for SCC increases from 0.8 to near 1.0 with increasing strength. The mean value of the strength ratio $f_{c,cyl,d}/f_{c,cub,x} = 0{,}9$. The experimental conversion of this factors for VC are generally situated within the region of 0.70–0.90.

Self-compacting concrete with a similar water cement or cement binder ratio will usually has a higher strength compared to the traditional vibrated concrete, this is due to the use of powder material, with particle size smaller than 0.125 mm, that improves the microstructures of concrete, complements the aggregate distribution and thus, the pores become extremely small. Additionally, absence of external vibration improve the bond between paste and aggregate. It should be taken in account, that SCC have reduced porosity and interfacial transition zone of higher quality compared to NVC due to the use of smaller aggregate.

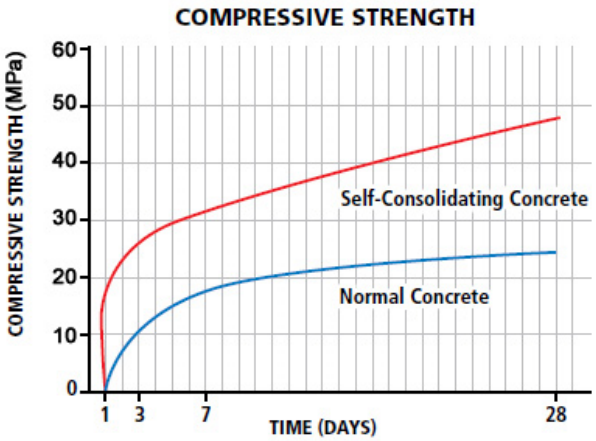

Figure 2. Compressive strength of SCC vs vibrated concrete [10].

At a constant W/C, a higher C/P leads to lower strengths. It is probably expected to the fact that increasing the cement content also requires the increase in water content to maintain the W/C, thus leading to a higher W/P. More water in the mixture leads to a higher capillary porosity and lower compressive strength.

The speed with which it gains strength also eliminates the need for steam or heat curing of concrete to facilitate early strength gain. SCC can attain significantly higher early and 28-day strengths

Coarse aggregates can have an influence on

the compressive strength due to their shape, nominal maximum size, surface texture, and origin. Crushed aggregate mixtures have higher cube strengths. It is similar to the behaviour of VC, but the average difference between the two best-fit curves for SCC was found to be small (4 MPa) compared with VC(8 MPa).

3.2 Tensile strength

The tensile strength of the concrete is used to evaluate the cracking moment and to draw the curvature diagrams. Its value is less than the compressive strength (from 1/6 up to 1/20) as result of the concrete heterogeneous nature. Cement stone contains numerous gaps: pores, micro cracks that favor concentration of tensions in a small volume.

There are three methods to assess the tensile strength: direct tensile test, the splitting tensile test and the bending tensile test.

Direct tensile strength tests are rather scarce due to its difficult setup. Splitting tensile strength is generally greater than direct tensile strength and lower than flexural strength.

Volume paste has no significant influences on the tensile strength. The tensile strength for self compacting concrete is similar to vibrated concrete for the same class.

The structure of SCC an vibrated concrete can be analyzed after splitting tensile test, (fig.3, fig.4). The effect of the Cement/ Powder is shown in the Fig.5 where SCC mixtures with a C/P less than 0.75 tend to lie beneath the mean values proposed by the Eurocode2 and the design code Model Code 2010.

Tensile strength of the concrete depends essentially on the tensile strength of cement stone, and its cohesion with the coarse aggregate, its value slightly increases with the cube compressive strength development.

Figure 3. Structure of SCC.

Figure 4. Structure of vibrated concrete.

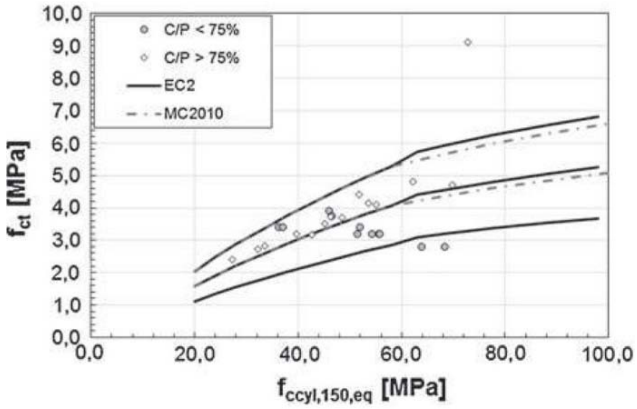

Figure 5. Direct tensile strength vs cylinder compressive strength and C/P [4].

3.3 Modulus of elasticity

The modulus of elasticity E-value, represents the ratio between stress and strain. This value is influenced by the elastic modulus of the aggregate and volumetric proportion of aggregate in the concrete.

As the aggregate is the bulk of the concrete volume, the type and amount of aggregate as well as its E-value have the most influence. Aggregate usually has a modulus of elasticity higher than that of cement stone. Selecting an aggregate with a high E-value will increase the modulus of elasticity of concrete. This dependence is due to the biphasic nature of concrete.

The modulus of elasticity of the tested SCC mixtures was lower than that of VC mixtures, with a similar compressive strength. Pineaud [4] studied the effect of the paste volume and W/C. By varying the paste volume between 359 and 452 l/m3 a decrease in E-value was found for an increasing paste volume. A survey by Domone [3] indicates that the difference

between SCC and VC in the modulus of elasticity is greater for lower compressive strengths.

The best fit line for the VC data is very close to that of the approximate relationship given in EC2, but the stiffness of the SCC mixes is on average about 40% lower than those of the VC mixes at low strength levels, with the difference reducing to less than 5% at high strengths. This behaviour is consistent with the lower coarse aggregate quantities in SCC (fig.4).

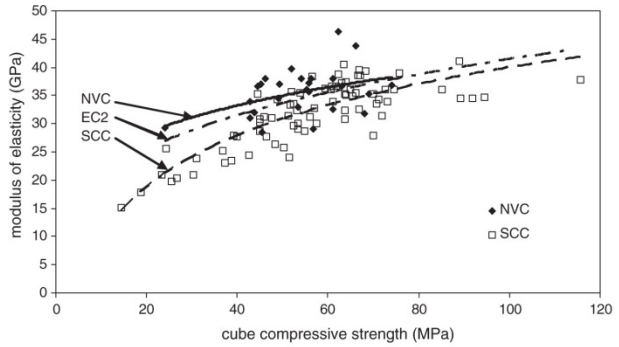

Figure 6. Elastic modulus vs cube compressive strength [12].

4. CONCLUSIONS

SCC is a relatively new material in the concrete industry. The mechanical properties of SCC were conventional adopted according to VC of a similar class. The results of research of the last years proved the existence of difference of properties in hardened state between VC and SCC:

- Compressive strength of SCC has higher strength comparated with VC, the main reason for the increase of is that packing density in SCC mix increases with increase of powder content.
- The tensile strength of SCC may be assumed to be the same as the one for a VC
- The elastic modulus of the SCC can be up to 40% lower than of VC at low compressive strength, but the difference reduces to less than 5% at high strengths
- The properties of the hardened SCC and its behavior over time represent a new direction for research.

References

1. The European Guidelines for Self-Compacting Concrete Specification*, Production and Use, May 2005.*

2. ICECON S.A. *Beton autocompactant – cercetare (prenormativă). februarie 2012.*

3. *Domone P.L. A review of the hardened mechanical properties of self compacting concret. Cement and Concrete Composites; 29(1), pag.1-12, 2007*

4. Khayat K.H., De Schutter G. *Mechanical properties of Self Compacting Concrete., State-of-the-Art Report of the RILEM Technical Committee 228-MPS on Mechanical Properties of Self-Compacting Concrete, 2014*

5. Sheinn A.M.M., Tam C.T., Rodrigo F.L. *Comparative study on hardened properties of self compacting concrete (scc) with normal slump concrete (nsc). 29th Conference on "Our world in concrete & structures" Singapore, pag. 485-494, 2004*

6. Almeida F., Barragánb B.E., Casasb J.R. *Hardened Properties of Self-Compacting Concrete — A Statistical Approach. Construction and Building Materials nr 24, pag.1608–1615, 2010*

7. Terec L, Szilágyi H. *Beton autocompactant (bac) pentru industria de prefabricate în construcţii. Revista „Urbanism. Arhitectură. Construcții", vol.1 nr.1, pag. 79-86, 2010.*

8. Vieira M., Bettencourt A*. Deformability of hardened SCC. In: Wallevik, O., Nielsson, I.(eds.) Proceedings of the 3rd International RILEM Symposium on SCC, Reykjavik, RILEM Publications S.A.R.L, Bagneux, pag. 637–644, 2003*

9. Okamura H., Outchi M. *Self compacting Concrete. Journal of Advanced Concrete Technology, vol 1, nr.1 pag. 5-15, april 2003*

10. Heirman G., Vandewalle L., Van Gemert D., Boel V., Audenaert K., De Schutter G., Desmet B., Vantomme J. *Time-dependent deformations of limestone powder type self compacting concrete. Eng. Struct. 30, pag.2945–2956, 2008*

11. Gesoglu M., Guneyisi E., Ozbay E. *Properties of self-compacting concretes made with binary, ternary,and quaternary cementitious blends of fly ash, blast furnace slag,and silica fume. Journal Construction and Building Materials 23, pag. 1847–1854, 2009*

Uysal M. *The influence of coarse aggregate type on mechanical properties of fly ash additive self-compacting concrete. Journal Construction and Building Materials 37, pag. 533–540, 2012.*

Recommended for publication: 18.03.2016.

RiverPrut - SOFTWARE FOR DETERMINATION AND MANAGEMENT OF WATER QUALITY

[1]Galina Marusic, PhD, [2]Diana Marusic, student, [3]Anatolie Puţuntică, PhD
[1]Technical University of Moldova
[2]"Ion Creangă" Theoretical Lyceum, Chisinau, Republic of Moldova
[3]Tiraspol State University, Republic of Moldova

INTRODUCTION

Water quality is a primary problem for every country's sustainable development. Nowadays there is a continuous process of water quality degradation in the majority of regions around the world. To stop this process, complex studies and actions are needed to be initiated by specialists from various fields.

Water quality has diminished dramatically as a result of human activity. Water quality evaluation of several bodies of water in Europe, according to the requirements of the Water Framework Directive, denotes a satisfactory or unsatisfactory environmental status. In order to rehabilitate and maintain water systems in a "very good" condition [1], there is a need of a thorough analysis of them.

In the majority of cases, water from rivers is used for human necessities such as water supply, irrigation, power generation etc.

Water quality is increasingly being influenced by pollution with various chemical, physical and biological substances. According to specialty literature, there are multiple analytical methods of determination of water quality, depending on the parameters and standards set out in the field. Usually, these methods include: parameter selection, adjustment of measurement units to the same scale, weight establishment of each parameter, water quality index calculation and others [2, 13-15].

An important criterion for water quality determination is the ratio of the amount of substance discharged and the normative limit of discharges. This is described by the Water Pollution Index (WPI), which value is calculated according to a fixed number of parameters (6): ammonium nitrogen, nitrite nitrogen, petroleum products, phenols, dissolved oxygen, biochemical oxygen for each 5 days. WPI is calculated according to the following formula [3]:

$$WPI = \sum \frac{C_i}{MAC_i / 6} \qquad (1)$$

where: C_i – average concentration of parameters, MAC_i - maximum admissible concentration of parameters, 6 – number of parameters taken into account.

1. A SHORT DESCRIPTION OF THE SOFTWARE

Mathematical modeling and numerical modeling are essential tools for water quality class calculation, as well as for determination of spatio-teporal evolution of pollutants for the purpose of preventing exceptional situations. Proper choice of the mathematical model and and simulation program allow a proper assessment of water quality [4, 5, 8-10].

According to bibliographical sources examined, at present there are several attempts and proposals of water quality modeling in rivers. These papers suggest variuos approaches to mathematical model combinations, GIS systems and software techniques [6, 7, 9, 11, 12].

RiverPrut, a software for determination of water quality class according to WPI, was created using Java programming language. The logical scheme of the program is presented in the Fig. 1.

RiverPrut software allows users to determine water quality of the Prut River according to WPI values, in each sector examined. The main window of the program is presented in the Fig. 2. At the top it is situated the scale of water quality classes, correlated with respective colors. In the upper right corner there is a drop-down list for the selection of the year of data to be presented. In the left part there are eight buttons – corresponding to studied sectors and a button with the image of Prut River map. Depending on the occurred event (year or sector changing), the color that indicates respective water quality class of the sector is initialized according to WPI.

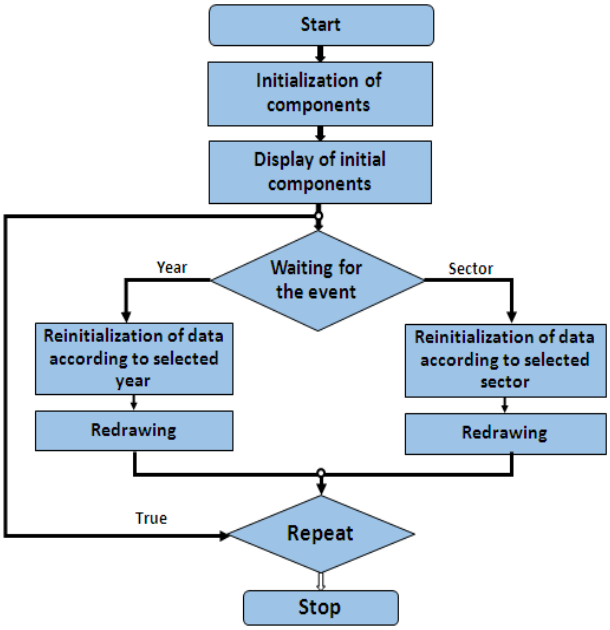

Figure 1. Logical scheme of the software.

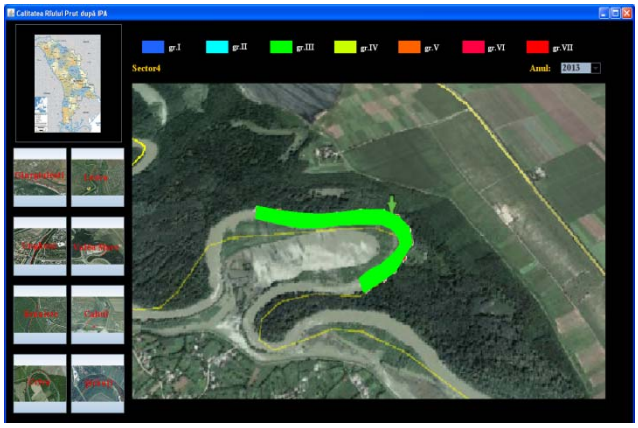

Figure 2. Water quality in the sector of Prut River from Valea Mare locality in 2013.

II. CASE STUDY - APPLYING SOFTWARE FOR RiverPrut WATER QUALITY DETERMINATION

The developed software was applied for determination of water quality in the Prut River. WPI values were examined for eight sectors of Prut River: villages Criva, Şirăuţi, Branişte, Valea Mare, Giurgiuleşti; cities Ungheni, Leova, Cahul –Fig 3. Information about WPI was provided by the State Hydrometeorological Service. From Fig. 3 it can be observed that River Prut water quality in Criva locality for the 2009-2011 period and 2013 year was placed in the second class(clean), and in 2012 year in the third class (moderately polluted); water quality in

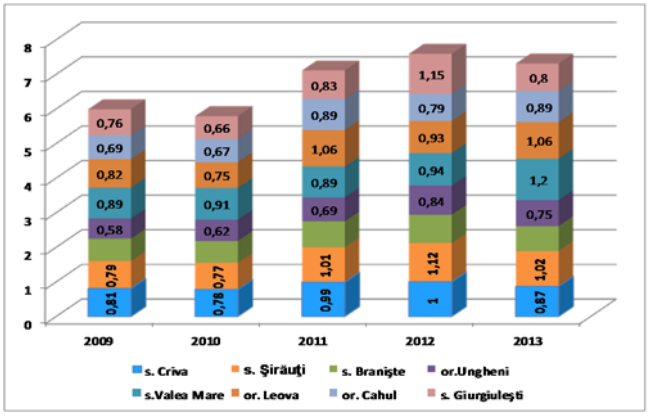

Figure 3. WPI values for the examined sectors of the Prut River.

Şirăuţi in the 2009-2010 period was placed in the second class(clean) and in the 2011 – 2013 period in the third class(moderately polluted); in Braniştе and Ungheni localities it was placed in the second class (clean) for the entire 2009-2013 period; in Valea Mare and Leova it was clean for the 2009-2012 period and in 2013 moderately polluted; in Cahul locality, for the entire examined period, it was clean; in Giurgiulesti water quality was placed in the second class(clean) for the 2009-2011 period, in 2012 – in the third class(moderately polluted) and in 2013 – again in the second class(polluted).

Water quality in Şirăuţi locality in 2013 year can be observed in the Fig. 4.

Figure 4. Water quality in the sector of Prut River from Şirăuţi locality in 2013.

It is possible to view the water quality in the entire sector of the Prut River on the territory of Moldova by accessing the picture of the Prut River and selecting the option Year. This allows to monitor the water quality in the entire Prut River and to undertake proper management of water quality. For example, the water quality in Prut River in 2012 year is presented in the Fig. 5, and in the 2013 year – in the Fig. 6.

Figure 5. Water quality of Prut River in 2012.

Figure 6. Water quality of Prut River in 2013.

CONCLUSIONS

Water quality based on WPI was determined in the river-type systems by designing and creating a software program for this purpose – RiverPrut. This will allow to actively and rapidly store information about water quality.

The water quality based on WPI was determined in 8 sectors of the Prut River. According to the results of analysis it can be affirmed that for the majority of analyzed sectors water quality falls within the second class (clean) and only in some cases and for some sectors it is moderately polluted.

The software that was created can be customized for other river-type systems, by changing configuration files, sector names and map. Also, the system offers a tool for determining the coordinates of river sector polygons on the map, which can be used to determine the coordinates for any other sectors and rivers.

It has been observed that the mathematical model is useful if the water quality is examined during a longer period of time, minimum 5 days.

If analyzing water quality daily, then it is necessary to model turbulent water flow in river-type systems and, accordingly, pollutant transport and dispersion processes.

References

1. **** European Parliament and Council Directive EU 2000/60/EC establishing a framework for Community action in the field of water, 2000.*

2. *http://www.justice.gov.md/file/Centrul%20de%20armonizare%20a%20legislatiei/Baza%20de%20date/Materiale%202010/Legislatie/32000L0060-Ro.PDF*

3. Ionuş O*. Water quality index - assessment method of the Motru River water quality (Oltenia, Romania). In: University of Craiova, Series Geography, 2010, Vol. 13, pp. 74-83.*

4. *ANUAR. Starea calităţii apelor de suprafaţă conform elementelor hidrobiologice pe teritoriul Republicii Moldova în anul 2013, Chişinău, 2014, 145 p.*

5. *http://www.meteo.md/monitor/anuare/2013/anuarhidro_2013.pdf*

6. Marusic G*. Study on numerical modeling of water quality in „river-type" systems. In: Meridian Ingineresc, 2013, Nr. 2, pp. 38 – 42.*

7. Mannina G*. Uncertainty Assessment of a Water-Quality Modelfor Ephemeral Rivers Using GLUE Analysis. In: Environmental Engineering, 2011, Vol. 137, no. 3, pp. 177-186.*

8. Marusic G., Sandu I., Moraru V., Vasilache V. *ş. a. Software for modeling spatial and temporal evolution of river-type systems. In: Proceedings of the 11th International Conference on Development and*

Application Systems, Suceava, Romania, May 17-19, 2012, pp. 162 – 165.

***9. Marusic G**. A study on the mathematical modeling of water quality in "river-type" aquatic systems. In: Journal Wseas Transactions on Fluid Mechanics, Issue 2, Vol. 8, April 2013, pp. 80 – 89.*

***10. Marusic G., Sandu I., Vasilache V., Filote C., Sevcenco, N.** Modelling of Spacio-temporal Evolution of Fluoride Dispersion in "River-type" Systems. Revue Roumaine de Chimie, Vol. 66 (4), pp. 503-506, December 2015.*

***11. Vasilache V., Filote C., Cretu M., Sandu I., Coisin V., Vasilache T., Maxim C.** Monitoring of groundwater quality in some vulnerable areas in Botosani county for nitrates and nitrites based pollutants. Environmental Engineering and Management Journal, Vol. 11 (2), pp. 471-479, February 2012.*

***12. Marusic G., Filote C., Ciufudean C.** The spatial-temporal evolution of iron dispersion in „river-type" systems. Proceedings of the 17th WSEAS International Conference on APPLIED MATHEMATICS (AMATH '12), Montreux, Switzerland, pp. 95-98, December 2012.*

***13. Vasilache V., Gutt S., Gutt G., Vasilache T., Filote C., Sandu I.** Studies of hardness for the electrodeposited nickel from watts baths with addition of polyvinyl pyrrolidone (PVP). Revue Roumaine de Chimie, Vol. 54 (3), pp. 243-246, March 2009.*

***14. Batrinescu G., Birsan E., Vasile G., Stanescu B., Stanescu E., Paun I., Petrescu M., Filote C.** Identification of the Aquatic Ecosystems Integrating Variables in the Suceava Hydrographic Basin and their Correlations. Journal of Environmental Protection and Ecology, Vol. 12 (4), pp. 1627-1643, January 2011.*

***15. Romanescu G., Hapciuc O-E., Sandu I., Minea I., Dascalita D., Iosub M.** Quality Indicators for Suceava River. REVISTA DE CHIMIE, Vol. 67, Issue 2, pp. 245-249, February 2016.*

***16. Romanescu G., Iosub M., Sandu I., Minea I., Enea A., Dascalita D., Hapciuc O-E.** Spatio-temporal Analysis of the Water Quality of the Ozana River. Revue Roumaine de Chimie, Vol. 67, Issue 1, pp. 42-47, January 2016.*

***17. Romanescu G., Tirnovan A., Cojoc G., Juravle D., Sandu I.** Groundwater Quality in Suha Basin (Northern Group of Eastern Carpathians). Revue Roumaine de Chimie, Vol. 66, Issue 11, pp. 1885-1890, November 2015.*

Recommended for publication: 15.03.2016.

ELASTO-PLASTIC PROPERTIES AND POROSITY CHARACTERISTICS OF DEFINE RAILWAY ELECTROLYTIC COATINGS

[1]PhD, professor Vasile Javgureanu, [1]PhD, associate professor Pavel Gordelenco, [2]Lecturer Diana Bors
[1]Technical University of Moldova, Chisinau
[2]Technical College, Chisinau

1. INTRODUCTION

The paper presents some features of the elasto-plastic deformation (Ae, Ap, A, Hh, H, P) and the porosity characteristics (K, ρ) of electrolytic iron coatings on various indentation depth of the diamond spherical indenter (1-6μm). It is found that the parameters (Ae, Ap, A, Hh, H and P) have an extreme character, which coincide with the guidelines for choosing the electrolysis conditions for optimal composition electrolytic iron coatings in terms of wear resistance.

The experimentally determined coefficient takes into account the degree of compaction of the material (k) and porosity (ρ) of electrolytic iron coatings with the change of conditions of electrolysis (Dk, T).

2. GENERAL INFORMATION

When electrodepositing iron coatings which included a large number of foreign particles significantly affect the structure of residues and, consequently, their physical and mechanical properties. High-voltage internal coatings depends on the characteristics electro crystallization precipitation. These features are the main reason for defining the properties of the coatings such as hardness, porosity, fragility, fatigue resistance of coatings. [1]

Under the influence of the internal stresses in the coatings appear porosity which can be divided into three groups:

- macropores occur depending on the structure of the coatings which is formed under the influence of electrolysis conditions;
- micropores arise depending on the coating structure which is influenced by the conditions of the electrolysis;
- channel porosity; type (network of cracks) arising due to the presence of large internal stresses.

In all cases an increase of internal stresses in the coating causes an increase in porosity [1]. Education has channel porosity; type coatings contributes to higher wear resistance of coatings with their work in the boundary lubrication conditions.

The electrolysis conditions have a significant impact on the density of the coating [1]. This is due to the change in porosity sediments. Perhaps, however vary within wide limits and elastic characteristics of the coatings.

Drinking Hh/H is almost independent of the nature of the pressure distribution in print, and is determined only by the medium pressure, normalized to the resulted P in the elastic modulus.

Analysis of elastic deformations in typo, followed by calculating the ratio of reduced and unreduced hardness is important for the study and the subsequent development of experimental methods of testing kinetic hardness and micro hardness.

Drinking Hh/H - important experimental parameter and its deviation from the calculated value may characterize a necessary measure to materials and hardening of the surface layers and coatings, as porosity. Analysis of this relationship a number of papers [2], which is also in the presence of two elastic displacement of the contacting bodies (one of them is the indenter) applied load is distributed over the area of the plastic print.

To assess the porosity of the surface layers of the material the technique of estimating the degree of porosity of the material for his seal indentation. The seal appears to change the height of the print roll around and leads to a reduction ratio Hh/H. Therefore to quantify and seals need to measure both hardness (Hh - unreduced hardness, H - restored hardness).

In the absence of material porosity ratio Hh/H in the first approximation, to be constant.

Due to the high localization of the local plastic deformation test with continuous recording of process parameters pressing spherical indenter can give more information than the tensile test at preserving its main advantage as a method of non-destructive and express control of material properties.

One of the defining characteristics of the powder coating materials is their porosity (ρ), touted

as the overall level and nature of the pore size distribution. The latter is very important because the pores being stress raisers, reduce the plastic properties of the material.

The influence of porosity on the process of indentation is dependent on the size of the fingerprint. If the pore size and the distance between them is greater than the print size, the probability of entering the pores in the print zone, and hence the local fluctuation of density of the material is subject to static laws.

If the print size significantly greater than the distance between the pores, the print area is saved middle static density of the material, depending on the total porosity of the material.

The total porosity of the indentation determines the change in the modulus of elasticity E and the relationship Hh/H.

The porosity of the material is determined by the formula:

$$\rho = 2(1 - \kappa);$$

where:

k - factor takes into account the degree of compaction of the material;

$$\kappa = (H_h/H)^{0,5}$$

where:

Hh- unreduced hardness of the material;

H - restored hardness of the material;

Meaning of E and Hh/H depend on pore shape. Offset pores according Krivoglaz give a lower modulus of elasticity E. In addition, they are easier to heal in the plastic zone under imprinted as spherical pores to heal a higher degree of hydrostatic compression. In connection with these flattened pores easily compacted, and thus have a lower ratio Hh/H ratio and higher strain hardening.

We present elastoplastic properties and porosity characteristics of iron coatings produced from the electrolysis of 1 [1, p.59]. The samples of 30 mm diameter rollers, coating thickness 0.5 mm and a length of 100mm, which were processed under optimal conditions of grinding.

Physical and mechanical properties were determined at the facility for the study of the hardness of materials macro volume, equipped with inductive sensor and a differential amplifier, you can record a chart indentation diamond spherical indenter and restore print after unloading [1].

3. DISCUSSION OF THE EXPERIMENTAL STUDY

Studies have shown that the studied elastoplastic properties and porosity characteristics electrolytic iron coatings vary with the conditions of electrolysis (table 1-6).

Table 1. Elastoplastic properties and porosity of electrolytic iron coatings (h=1 μм).

Conditions electrolysis		*Elastoplastic properties*						*H, N/mm²*	*Hh, N/mm²*	*Hh/H*	*E, N/mm²*	*P, N*	*K*	*ρ*
Dк, x10⁻⁴ кА/m²	*T, ⁰C*	*he, μм*	*Ae, x10⁻⁴ N•mm*	*hp, μм*	*Ap, x10⁻⁵ Nmm*	*h, μм*	*A, x10⁻⁴ Nmm*							
5	40	0,65	47,66	0,35	25,66	1,0	73,30	10009	3505	0,350	1,95	22,00	0,59	0,82
10	40	0,66	51,48	0,34	26,62	1,0	78,00	11437	3729	0,330	1,85	23,40	0,57	0,86
20	40	0,67	54,05	0,33	26,62	1,0	80,66	13288	3855	0,290	1,75	24,20	0,54	0,92
40	40	0,71	47,81	0,29	19,53	1,0	67,33	10993	3220	0,290	1,60	20,02	0,54	0,92
20	20	0,76	42,93	0,24	13,04	1,0	54,33	10815	2600	0,240	1,30	16,30	0,49	1,02
20	60	0,55	31,71	0,45	25,97	1,0	57,66	6079	2750	0,245	2,10	17,30	0,67	0,66

Table 2. Elastoplastic properties and porosity of electrolytic iron coatings (h=2 μм).

Conditions electrolysis		*Elastoplastic properties*						*H, N/mm²*	*Hh, N/mm²*	*Hh/H*	*E, N/mm²*	*P, N*	*K*	*ρ*
Dк, x10⁻⁴ кА/m²	*T, ⁰C*	*he, μм*	*Ae, x10⁻⁴ Nmm*	*hp, μм*	*Ap, x10⁻⁵ Nmm*	*h, μм*	*A, x10⁻⁴ Nmm*							
5	40	1,30	193,6	0,70	104,3	2,0	298	10168	3560	0,350	1,95	44,7	0,590	0,820
10	40	1,32	208,6	0,68	107,4	2,0	316	11101	3760	0,339	1,85	47,4	0,580	0,840
20	40	1,34	219,8	0,66	108,2	2,0	328	11870	3920	0,233	1,75	49,2	0,570	0,860
40	40	1,42	195,1	0,58	79,5	2,0	274,7	11312	3280	0,290	1,60	41,2	0,538	0,924
20	20	1,52	169,7	0,48	53,6	2,0	285,3	11115	2650	0,238	1,30	33,5	0,448	1,104
20	60	1,10	129,1	0,90	105,6	2,0	234,6	6228	2800	0,450	2,10	35,2	0,670	0,660

Table 3. Elastoplastic properties and porosity of electrolytic iron coatings (h=3 μм).

Conditions electrolysis		*Elastoplastic properties*						*H, N/mm²*	*Hh, N/mm²*	*Hh/H*	*E, N/ mm²*	*P, N*	*K*	*ρ*
$D_к$, x10^{-4} кА/м²	*T, ^0C*	*he, μм*	*Ae, x10^{-4} Nmm*	*hp, μм*	*Ap, x10^{-5} Nmm*	*h, μм*	*A, x10^{-4} Nmm*							
5	40	1,95	44,33	1,05	23,87	3,0	68,20	10343	3620	0,35	1,95	68,2	0,592	0,816
10	40	1,98	47,72	1,02	24,58	3,0	72,30	11286	3840	0,34	1,85	72,3	0,583	0,834
20	40	2,01	50,12	0,99	24,68	3,0	74,80	12032	3970	0,33	1,75	74,8	0,574	0,852
40	40	2,13	44,52	0,87	18,18	3,0	62,70	11475	3330	0,29	1,60	62,7	0,539	0,922
20	20	2,28	38,68	0,72	12,22	3,0	50,90	11256	2700	0,24	1,30	50,90	0,490	1,020
20	60	1,67	29,43	1,35	24,08	3,0	53,50	6310	2840	0,45	2,10	53,90	0,671	0,658

Table 4. Elastoplastic properties and porosity of electrolytic iron coatings (h=4 μм).

Conditions electrolysis		*Elastoplastic properties*						*H, N/mm²*	*Hh, N/mm²*	*Hh/H*	*E, N/ mm²*	*P, N*	*K*	*ρ*
$D_к$, x10^{-4} кА/м²	*T, ^0C*	*he, μм*	*Ae, x10^{-4} Nmm*	*hp, μм*	*Ap, x10^{-5} Nmm*	*h, μм*	*A, x10^{-4} Nmm*							
5	40	2,60	80,08	1,40	43,12	4,0	123,2	10509	3680	0,350	1,95	92,4	0,592	0,816
10	40	2,64	86,24	1,36	44,43	4,0	130,7	11474	3900	0,34	1,85	98,0	0,583	0,834
20	40	2,68	90,41	1,32	44,53	4,0	134,9	12208	4030	0,33	1,75	101,2	0,575	0,850
40	40	2,04	80,37	1,26	35,66	4,0	113,2	10707	3380	0,31	1,60	84,0	0,560	0,880
20	20	3,04	86,13	0,96	24,51	4,0	102,1	12705	3050	0,24	1,30	76,6	0,490	1,02
20	60	2,20	53,03	1,80	43,38	4,0	96,4	6396	2880	0,45	2,10	72,3	0,671	0,658

With increasing current density (Dk) of $5x10^{-4}$ to $40x10^{-4}$ kA/m^2 at a constant temperature electrolysis (40°C) plastic component (hp), spherical indentation depth of a diamond indenter, the ratio (Hh/H), the coefficient takes into account the degree of compaction of the material (K) and modulus of elasticity (E) are reduced respectively from 0.35 to 0.29 (μm), from 0.350 to 0.290, from 0.59 to 0.54 and from 19500 to 1600 (N/mm^2), and the elastic component (hy) of penetration depth and porosity of electrolytic iron coating increases, respectively, from 0.65 to 0.71 (μm) and from 0.82 to 0.92. Overall, while the depth was 1 μm time (h). The work expended on elastic (Ae), plastic (Ap), the total deformation (A), restored the hardness (H) is not restored hardness (Hh) and the load pressing the diamond spherical indenter (P) are the extreme value with the change of the current density (Dk) from $5x10^{-4}$ to $40x10^{-4}$ (kA/m^2), electrolysis at a constant temperature (40°C) (tables 1-5).

Studies have shown that an increase in current density (Dk) of $5x10^{-4}$ to $20x10^{-4}$ (kA/m^2) at a constant temperature electrolysis (40°C), the work spent on the elastic deformation of the iron coating (Ae), increased by $47.66x10^{-5}$ to $54.05x10^{-5}$ (N*mm) work spent on the plastic deformation of the coating increased from $25.66x10^{-5}$ to $26.62x10^{-5}$ (H·mm), and the total work spent on the elasto-plastic deformation of the coating increased from $73.3x10^{-5}$ to $80.66x10^{-5}$ (H·mm). With further increase of the current density of up $20x10^{-4}$ to $40x10^{-4}$ (kA/m^2) at a constant temperature electrolysis (40°C) the work spent on the elasto-plastic deformation of the coating decreased by $54.05x10^{-5}$ to $47.81x10^{-5}$ (H·mm) the work spent on the plastic deformation of the coating decreased by $26.62x10^{-5}$ to $19.53x10^{-5}$ (H·mm), and the total work spent on the elasto-plastic deformation of the coating decreased by $80.66x10^{-5}$ to $67.33x10^{-5}$ (H·mm). From the results of research it is clear that the work spent on the elastic (Ae), plastic (Ap), and elastic-plastic deformation (A) iron coatings have an extreme character with a change in the current density (Dk) at a constant temperature electrolysis (T,^{0}C). The nature of the changes restored (H), unreduced (Hh) hardness and indentation load (P) of the diamond spherical indenter at different penetration depth (1-6) microns to increase the current density of up to $5x10^{-4}$ - $40x10^{-5}$ (kA/m^2), at a constant temperature electrolysis (40^{o}C) have extreme character (table 1-6).

With increasing current from $5x10^{-4}$ to $50x10^{-5}$ (kA/m^2), at a constant temperature electrolysis (40^{o}C) restored the hardness (H) increased from 10009 to 13288 (N/mm^2), unreduced hardness (Hh) has increased from 3505 yes 3855 (N/mm^2) and a load of pressing the diamond spherical indenter has increased from 22 to 24.2 (N).

Table 5. Elastoplastic properties and porosity of electrolytic iron coatings (h=5 μм).

Conditions electrolysis		*Elastoplastic properties*						*H, N/ mm²*	*Hh, N/mm²*	*Hh/H*	*E, N/ mm²*	*P, N*	*K*	*ρ*
$D_к$, x10⁻⁴ кА/ m²	*T, ⁰C*	*he, μм*	*Ae, x10⁻⁴ Nmm*	*hp, μм*	*Ap, x10⁻⁵ Nmm*	*h, μм*	*A, x10⁻⁴ Nmm*							
5	40	3,25	126,56	1,75	68,31	5,0	194,87	10655	3730	0,350	1,95	117,1	0,592	0,816
10	40	3,30	136,73	1,70	70,44	5,0	207,17	11643	3960	0,340	1,85	124,3	0,583	0,834
20	40	3,35	143,38	1,65	70,66	5,0	214,00	12551	4090	0,330	1,75	128,4	0,571	0,858
40	40	3,55	140,46	1,45	57,37	5,0	196,66	13035	3780	0,290	1,60	118,7	0,539	0,922
20	20	-	-	-	-	-	-	-	-	-	1,30	-	-	-
20	60	2,75	84,06	2,25	68,38	5,0	152,83	6573	2920	0,440	2,10	91,7	0,667	0,666

Table 6. Elastoplastic properties and porosity of electrolytic iron coatings (h=6 μм).

Conditions electrolysis		*Elastoplastic properties*						*H, N/ mm²*	*Hh, N/mm²*	*Hh/H*	*E, N/ mm²*	*P, N*	*K*	*ρ*
$D_к$, x10⁻⁴ кА/ m²	*T, ⁰C*	*he, μм*	*Ae, x10⁻⁴ Nmm*	*hp, μм*	*Ap, x10⁻⁵ Nmm*	*h, μм*	*A, x10⁻⁴ Nmm*							
5	40	3,90	184,73	2,10	99,47	6,0	284,2	10775	3770	0,350	1,95	142,1	0,592	0,816
10	40	3,96	199,98	2,04	103,02	6,0	303,0	11289	4020	0,340	1,85	151,5	0,582	0,836
20	40	4,02	224,32	1,98	110,48	6,0	334,8	13463	4500	0,330	1,75	167,4	0,578	0,844
40	40	-	-	-	-	-	-	-	-	-	-	-	-	-
20	20	-	-	-	-	-	-	-	-	-	-	-	-	-
20	60	3,30	122,65	2,70	100,35	6,0	223,0	6576	2960	0,450	2,10	111,5	0,671	0,658

With further increase of the current density from $20x10^{-4}$ to $40x10^{-5}$ (kA/m^2), at a constant temperature electrolysis (40^{o}C), restored the hardness (H) decreased from 13288 to 10993 (N/mm^2), unreduced hardness decreased from 3855 to 3220 (N/mm^2) and the indentation load on the diamond spherical indenter (R) decreased from 24,2 to 20,02 (N).

With increasing temperature electrolysis (table 1-6) at a constant current density ($20x10^{-4}$ kA/m^2), up from 20°C to 60°C the plastic component (hp) penetration depth, the ratio of Hh/H modulus of elasticity (E) coefficient taking into account the degree of compaction of the material (K) increases, respectively (table 1-6) from 0.24 to 0,45 (μm), from 0.240 to 0.452, from 13000 to 21000 (N/mm^2) and from 0.49 to 0.67.

The character of changes in the work expended to another (Ae), plastic (Ap) and elastoplastic (A) deformation of electrolytic iron coating with temperature electrolysis of 20°C to 60°C at a constant current density ($20x10^{-4}$ kA/m^2) has an extreme character for all depths spherical diamond indenter indentation (h from 1 to 6 μm), table 1-6).

With the increase of electrolysis temperature of 20°C to 40°C at a constant current density ($20x10^{-4}$ kA/m^2) robot spent on elastic (Ae), plastic (Ap) and elasto-plastic (A), respectively, of the deformation increased from $54.05x10^{-5}$ to $42.93x10^{-5}$ (N·mm), up from $13.05x10^{-5}$ $26.62x10^{-5}$ (N·mm), and from $54.33x10^{-5}$ to $80,66x10^{-5}$ (N·mm).

With further increase of the electrolysis temperature of 40 to 60°C at a constant current density ($20x10^{-4}$ kA/m^2), the work expended on elastic (Ae), plastic (Ap) and elasto-plastic deformation of electrolytic iron coatings increased respectively by $54.05x10^{-5}$ up 31.71 $x10^{-5}$ (N/mm^2), from $26.02x10^{-5}$ to $25.97x10^{-5}$ (N·mm) and from $80.66x10^{-5}$ to $57.66x10^{-5}$ (N·mm).

Character changes unreduced hardness (Hh), reduced (H), the hardness and load of pressing the diamond spherical indenter (P) for all penetration depth of 1 to 6 microns with increasing temperature electrolysis of from 20°C to 60°C with constant toke $20x10^{-4}$ (kA/m^2) also has an extreme character. With increasing temperature electrolysis from 20°C to 40°C at a constant current density $20x10^{-4}$ (kA/m^2) is not restored hardness increased from 2600 to 3855 (N/mm^2) from 10815 to 13288 (N/mm^2) and a load of pressing the diamond spherical indenter increased from 16.3 to 24.2 (N). With further increase in temperature electrolysis from 40°C to 60°C at a constant current density ($20x10^{-4}$ kA/m^2), unreduced hardness decreased from 3855 to 2750 (N/mm^2), from 13288 to 6079

(N/mm^2) and the load indentation diamond spherical indenter has decreased from 24.2 to 17.3 (N).

Studies have shown that the unreduced hardness (H), the work expended on elastic (Ae), plastic (Ap), elasto-plastic (A) deformed, the load on the diamond spherical indenter (with all the indentation depth of 1 to 6 μm) have an extreme character with change in the conditions of the electrolysis (Dk, T) for the study of electrolytic iron coatings and coincide with the earlier recommendations in terms of their optimal wear resistance.

Experimentally proved (table 1-6), the ratio Hh/H, K - factor takes into account the degree of compaction of electrolytic iron coatings and elastic modulus E decreases with increasing current density (Dk) and a decrease in temperature electrolysis (T).

With increasing current density (Dk) and the decrease in the electrolysis temperature (T) increases the porosity of electrolytic iron coatings (tables 1-6). This proves that the conditions of the electrolysis (Dk, T) has a significant impact elastoplastic properties, density and porosity of electrolytic iron coatings.

4. CONCLUSION

It is experimentally established that the recovered hardness (H) unreduced hardness (Hh), the work expended on elastic (Ae), plastic (Ap), elasto-plastic deformation (A) and the load (P) is not the diamond spherical indenter (with all the indentation depth of 1 to 6 microns) are the extreme nature of the changes to the conditions of the electrolysis (Dk, T) for the study of electrical iron coatings.

The experimentally determined coefficient takes into account the degree of compaction of electrolytic iron coatings (K) and porosity (***ρ***) with a change in the conditions of the electrolysis (Dk, T);

It was established experimentally that an increase in current density (Dk) and a decrease in temperature (T) of the electrolysis for electrolytic iron coatings coefficient taking into account the degree of compaction of the material (K) is decreased, and coating porosity increases (***ρ***).

Experimental (maximum) value of the recovered hardness (H), not reduced hardness (Hh) work expended on elastic (Ae), plastic (Ap) elasto-plastic deformation (A) of the load on the diamond spherical indenter (P) coincide with the received recommendations for electrometric iron coatings in terms of ensuring their optimum wear resistance.

Physical and mechanical properties (Ae; Ap; A; Hh; P) of electrolytic iron coatings have a good correlation with the intensity of wear of these coatings.

Bibliography

1. Markovets M.P. *Opredeleniye mekhanicheskikh svoystv materialov po tverdosti. Moskva, Mashinostroyeniye, 1979, 191s.*

2. Grigorovich V.K. *Tverdost' i mikrotverdost' metallov. Moskva, Izdatel'stvo ‘’Nauka”, 1976, 230 s.*

3. Javgureanu V., Gordelenco P. *M. Elita, The work of deforming wear – proof iron-nickel plating in microsquelging. The Annals of University “Dunarea de Jos” of Galati, Fascicle 8, 2004, Tribology, Romania, pp. 65-68.*

4. Javgureanu V., Gordelenco P. *M. Elita. Relationship of the restored and unrestored micro hardness of chromium coating. . The Annals of University “Dunarea de Jos” of Galati, Fascicle 8, 2004, Tribology, Romania, pp. 48-51.*

5. Zhavguryan V.N., Gordelenko P.V. *Sootnosheniye vosstanovlennoj i nevosstanovlennoj mikro tverdosti khromovykh pokrytiy. Mezhdunarodnaya NTK “Mashinostroyeniye i Tekhnosfera 21 veka”, Sevastopol', 2005, r. 205-208.*

6. Zhavguryanu V.P. *Issledovaniye raboty deformatsii iznosostoykikh gal'vanicheskikh pokrytiy pri mikrovdavlivanii. Mezhdunarozhnaya NTK “Novyye protsessy i ikh modeli v resurso i energosberegayushchikh tekhnologiyakh”. Odessa, 2003, s. 7-8.*

7. Javgureanu V., Gordelenco P. *Elasto-plastic properties and definition of porosity characteries composite iron-nikel coatings. International conference of hydraulics and Pneumatics - Hervex-2014, Romania, Căimănești Căciulata, 2014, p.126-131.*

8. Javgureanu V., Gordelenco P. *Elasto-plastic properties and tendency of iron-nikel composite coatings to brittle fracture. International conference of Hydraulics and Pneumatics - HERVEX-2014, Romania, Călimănești-Căciulafa, 2014, p. 148-155.*

Recommended for publication: 22.11.2015

THE THERMODYNAMIC BENEFITS OF THE INTEGRATION OF COGENERATION INSTALLATIONS IN BAKERY OVENS

Corina Chelmenciuc, Valentin Musteață, dr. hab. prof., Larisa Tcaci
Technical University of Moldova

INTRODUCTION

The bread industry is one of the main branches of the food industry in Moldova, which offer the population the vital food –the bread. The food industry has a considerable share in the entirely industrial sector - about 51,6%, according to statistics, [1].

Baking industry share in total industrial production is approx. 4% [2], and in the total food production – 8,8%, but that does not diminish its importance in the development of industrial sector. Bakery branch has been, it is and will be one of the most needed, because this branch assure the vital human needs.

Recently, prices of bakery products were increased by approx. 15%. An important argument was put forward by the bakers- to increase of tariffs in august by 39,3% for electricity and 15% for natural gas. This has increased energy share in the cost price of bread from 10% to 11,5% [3].

In the mentioned context, the increasing energy efficiency of processes in bakery ovens is a significant concern and necessary.

The continuous increase of the price of the used fuel demonstrates the need to rationalize the energy consumption.

The researches devoted to developing a method and optimal schemes of fuel utilization are very important, not only in the bakery processes but in all technological industrial processes.

In the technological process of baking, in bakeries are used practically all forms of energy: warm water – for the preparation of the dough and for cleaning of the equipment; steam - for steaming bread in ovens and for drying of pasta; natural gas – for ovens; electricity - for ovens and for different electrical equipment; compressed air and cold - in auxiliary processes.

In general, there is a detailed analysis of the bread-making process by steps made in order to highlight the energy-intensive operations. The analysis results are shown in tab. 1, [4].

As it is shown in the tab. 1, the highest consumption of energy takes place in the cooking process, practically the entire heat introduced in the process of production of bread (approx. 93,8%) is used in the cooking chamber. Therefore, the present work will approach especially the issue of the increasing energy efficiency of the process of baking the bread.

Table 1. The analysis of share of the energy consumption in the bread bakery process.

Nr.	***The step of technological process***	***Share, %***	
		electricity	***heat***
1	Reception and storage of raw materials	1,5	0,3
2	Reception and dosing of raw and auxiliary materials	4,5	0,8
3	Preparation of dough	13,8	1,4
4	Processing of dough	23	2,4
5	Final rising	22,6	1
6	Baking	33,7	93,8
7	Receive product	0,5	0,2
8	Storage	0,4	0,1

1. COGENERATION – THE MEASURE TO INCREASE ENERGY EFFICIENCY OF PANIFICATION

At the moment, most bakeries in Moldova use electric bakery ovens. The main argument is simplicity of installation and their exploitation, compared with natural gas ovens, especially if it is the lack of access to a gas pipe. At the same time, in the use of electric ovens, there is no problem with the evacuation of combustion gases, because they aren't.

Actually, the country at the moment, deals with essential increase of the price of electricity, and it is absolutely necessary to pass the ovens from the electrical supply to the natural gas.

In [5] there were presented the detailed essence and benefits of implementing the measures to improve energy efficiency in the process of baking bread. A particular attention is paid to method of transition of ovens from the electric to natural gas supply and the cogeneration application in bakeries.

An electrical oven whose surface of baking is 50 m^2, has the average working power of 200 kW, and with the same surface and the same productivity, in the use of natural gas - the average consumption of natural gas– 23 m^3/h. Considering the operating schedule – 16 hours per day and 330 days per year, the ovens consume respectively 1056 MWh/year and 121,4 thousands m^3 of natural gas per year. For generating the indicated quantity of electrical energy, at the power plant are consumed 313 thousands m^3 of

natural gas. The transition from electrical supply to natural gas supply of ovens will be reduced the expenses for energy resources, at the current fares [6], by over one million lei per year, or 20 thousand lei per m^2 per year.

The bakeries operates entire year at a practically constant productivity. It slightly varies the electrical and thermal load. Therefore, an installation with cogeneration, based on piston engine on natural gas, at the same bakery can operate with a high coefficient of the use of the installed power, which would reduce the cost of the produced energy.

In the case of using the cogeneration installations result a fuel economy, in comparison with separate generation of electricity and heat, from 25% to 40 %.

2. THE BENEFITS OF TUNNEL OVENS WITH GASES

Lately, the tunnel ovens with gases became widespread in bakeries. The benefits of the tunnel ovens, in comparison with other types of gas ovens, are:

- mechanization of the processes of loading and unloading the products;
- continuous production process;
- uniform distribution of the heat in 4-5 areas of baking;
- more efficient automation of the baking and steaming areas;
- disappearance of the "gas" flavor of bread, because the flue gases flowing through the gas channels and don't enter in the baking chamber of the oven;
- viewing the baking processes through special viewfinders.

These are the arguments favoring the choice of tunnel oven. But the arguments in favor of the supply option to natural gas of the ovens, comparing with the electrical supply, are:

- the electric ovens have a higher thermal inertia and an expensive function, due to higher tariff for electricity;
- the taste of the bread baked in the gas ovens is better than that obtained in electric ovens;
- the probability of the interruption of electricity supply at the factory (in case of damage or repairs to electrical networks)is much higher than for natural gas.

In addition, some researches [7], demonstrated that total equivalent emission of greenhouse gases, generated by ovens, to produce 1 kg of bakery products, is greater than 2 times in electrical ovens than in the case of gas ovens. But environmental problem is very acute today, at national and global level.

In the above context, the purpose of this paper is to analyze the efficiency of the installation of oven by integrated internal combustion engine.

Thus, this installation will produce electricity and the flue gases evacuated from the cogeneration installation, will be used to perform the technological processes baking in the oven.

3. EXERGETIC ANALYSIS – RELEVANT METHOD TO ASSESSMENT THE ENERGY EFFICIENCY

In baking ovens take place baking processes of bread. For this purpose, it is consumed a certain amount of energy. It is important to understand how effectively this process from the energy point of view is.

A method of analysis would be one based on balance and energy efficiency of the oven.

Energetic analysis is the classic method of assessing the energy efficiency of an installation or process. But this method does not take into account the following important factors: thermodynamic state of the system, form of energy consumption, the degree of perfection of the process (the degree of irreversibility), the state of environment. That's why, this method leads to the difficulty of interpreting the energy efficiency level.

This has caused the scientists to search the new methods, more complex, for technological processes analysis, in sequence with the second law of thermodynamics, which would allow qualitative assessment of different forms of energy. So, the exergetic analysis was developed.

In concordance with the second law of thermodynamics, energies with limited capacity of transformation, can be converted partially into mechanical work, - in exergy, the rest of these energies is anergy.

The economic value of energy is so great then the suitable energy is greater, therefore the exergy can be used to assess circulating energies, and the quality of processes which take place in the installation.

In concordance with the second law of thermodynamics, the sum of the input exergy into the ovens is equal to the sum of the output exergy plus exergy losses.

The thermodynamic perfection of the oven is expressed through the efficiency of the thermodynamic perfection of this installation γ_{ex}^{cupt} and constitutes the report between the amount of

exergy output of the oven $\sum_{i=1}^{n} E_{xi}^{e}$ and the amount of exergy input the oven $\sum_{i=1}^{n} E_{xi}^{i}$ [8]:

$$\gamma_{ex}^{cupt} = \frac{\sum_{i=1}^{n} E_{xi}^{e}}{\sum_{i=1}^{n} E_{xi}^{i}} = 1 - \frac{\sum_{i=1}^{n} P_i}{\sum_{1=1}^{n} E_{xi}^{i}}, \quad (1)$$

in which $\sum_{i=1}^{n} P_i$ are the exergy losses of the oven.

That's why, knowing and the calculation need of the losses of exergy have considerable importance to determine the methods to reduce the irreversibility of the processes which take place in the studied oven.

To calculate these losses it can be used the entropy method, which requires the calculation of exergy losses in each process separately using Guy-Stodola theorem::

$$P_{ex} = T_o \cdot \Delta S, \quad (2)$$

where: T_0 is the thermodynamic temperature of the environment; ΔS - increase of entropy in examined process because of the irreversibility.

From the last relationship it follows that the question of exergetic losses calculation in any process is reduced to calculation of variation of entropy.

4. WHY DO WE NEED OF THE INSTALLATION OF OVENS WITH INTEGRATED COGENERATION?

That's why the real processes from the oven are irreversible; in this processes take place destruction of exergy. The improvement of the processes, ie reducing their irreversibility, can be achieved by improving of ovens in order to reduce losses of exergy, which may lead to a decrease of operating costs (due to the reduction of primary energy consumption).

One of the most irreversible processes resulting in the oven is the process of mixing of the gases to the combustion chamber with the recirculated gases.

For example, the oven *PPP 3 54 211ST* is equipped with combustion chamber with the gas burner. Gas temperature in the combustion chamber is approx. 1630 °C, while necessary temperature of the gases in the channels of oven is about 450 °C (fig. 1).

There is a huge difference between the gas temperature in the combustion chamber and the required temperature in the channels of baking chamber. The reduction of the gas temperature in the combustion chamber is achieved after mixing of hot gases with the cold gases recycled from the channels of the baking chamber, whose temperature is 268 °C.

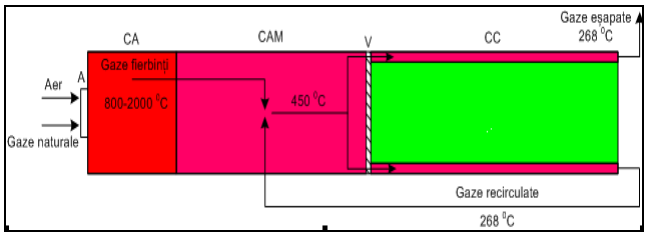

Figure 1. Heat flow diagram of the oven: *A – burner; CA – combustion chamber; CAM – mixing chamber; V – fan; CC – baking chamber.*

In case when currents, which are mixed, are the same ideal gas, with the same constant of gas *R*, and the same specific heat capacity c_p, is valid the following relationship for calculating entropy variation (were the term 1 refer to the parameters of the hot combustion gas in the combustion chamber, 2 – the parameters of the recirculated exhaust gases in the oven and 3 – the parameters of the gas mixture resulting from the mixing of the first two), [9]:

$$\frac{\Delta \dot{S}}{\dot{m}_3} \approx x(1-x)\left(\frac{T_1 - T_2}{T_1}\right)^2 + x\frac{R}{c_p}\left(\frac{p_1 - p_3}{p_3}\right) + (1-x)Rc_p\left(\frac{p_2 - p_3}{p_3}\right) \geq 0 \quad (3)$$

where $x = \dot{m}_1 / \dot{m}_3$ is the ratio between the flow rate of the hot flue gas in the combustion chamber and the flow rate of the gas mixture.

As it is shown in the equation (3), thermal irreversibility, increase of entropy and losses associated of mixing processes increase with the square of difference of the two gases mix of mixing temperature difference of the two mixed gases.

A measure to increase the energy efficiency of the process of baking bread would be the reducing the irreversibility of the process by replacing the process of mixing by a heat transfer process, which is less irreversible.

The essence of this technology involves „integrating" a cogeneration installation (based on the internal combustion engine, or a gas turbine installations) in an ovens installation.

The flue gases after expansion in internal combustion engine will be debited in a heat exchanger for the heating of the air taken from the environment and its subsequent circulation in baking channels of the oven (fig. 2).

Exergy losses after irreversibility of heat transfer will be determined by the relation, [9]:

$$P_{ex} = E_x^g - E_x^a = Q\frac{T_o}{T_{med}^a} \cdot \frac{1}{\left(1 + \left(T_{med}^a / \Delta T\right)\right)}, \quad (4)$$

where: T^a_{med} is the average thermodynamic temperature of the air in the heat exchanger;

ΔT - mean difference of the ambient temperature which environment are cooled and heated;

Q - the flow of heat exchanged in the heat exchanger, between the two fluids.

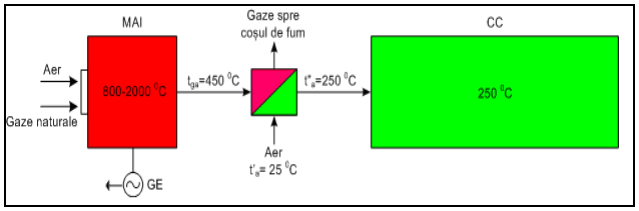

Figure 2. Schematic diagram of integrated cogeneration installation with heat exchanger:
MAI - internal combustion engine;
GE – electric generator; CC – cooking chamber.

As it is shown in equation (4), the loss of exergy is increased by the increase of the difference, but not square as in the case of mixing processes.

Applying this technology, the working agent for heating the baking chamber will be the air heated in the heat exchanger. This solution is welcome for ovens in which thermal agent is debited directly in the baking compartment, as the exhaust gas from the engine can contain drops of oil used to lubricate the engine and cannot be debited in the baking chamber because it can contaminate the bread.

In the exposed technology, are diminished the irreversibility of the process for the preparation of the heat by replacing the mixing process to heat transfer process, with a lower degree of irreversibility. The disadvantage of this solution lies in the fact that the heat exchanger can be larger, leading to an increase in the massiveness in the entire installation.

In case of the ovens tunnel, the thermal agent is not charged directly to the baking chamber, but circulates through the channels made in the walls of the chamber (so they have no contact with the bread), the flue gases discharged from internal combustion engine can be handled the cannels. Thus, are totally exhausted the losses of exergy associate with the made process of the heat (fig.3).

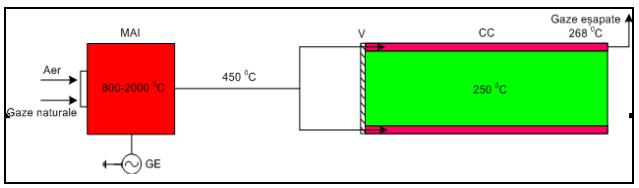

Figure 3. Schematic diagram of integrated cogeneration installation without heat exchanger

At the same time, it will significantly simplifies the installation by excluding the heat exchanger from its composition, in comparison with the solution described above.

Even if the combustion of fuel in the combustion chamber of the internal combustion engine, anyway there will be irreversibility and respective loss of exergy, they will be associated to the process of producing electricity (as the main product) and the exhaust gas evacuated from the internal combustion engine and subsequently used for the process of baking, they will result, in effect, as a waste.

The internal combustion engine is chosen depending on the thermal capacity of the baking chamber of the oven so that the oven heat load – Q, must correspond to the flow of the exhausted gases of internal combustion engine. Also, the combustion gas flow out of the internal combustion engine must provide the necessary flue gas- V_{gt} in baking channels of the oven.

In tab. 2, are presented the basic parameters of the ovens PPP required for selecting the type of internal combustion engine.

Table 2. The total volume of flow gases and heat load of the ovens PPP.

Oven type, [10]	**Capacity,** kg/h	**V_{gt},** m^3/s	**Q,** kW
PPP 2,1 18,9	342	0,56	163
PPP 2,1 25,2	450	0,74	216
PPP 2,1 31,5	558	0,84	245
PPP 2,1 37,8	684	1,02	297
PPP 2,1 44,1	792	1,21	353
PPP 2,1 50,4	900	1,40	408
PPP 2,1 56,7	1008	1,58	461
PPP 2,5 30,0	540	0,84	245
PPP 2,5 37,5	684	1,02	297
PPP 2,5 45,0	810	1,30	379
PPP 2,5 52,5	954	1,49	435
PPP 2,5 60.0	1080	1,67	487
PPP 3,0 54,0	972	1,49	435
PPP 3,0 63,0	1134	1,76	513
PPP 3,0 72,0	1296	2,05	598
PPP 3,0 81,0	1458	2,23	650
PPP 3,0 99,0	1782	2,79	814
PPP 3,0 108	1944	3,07	895

CONCLUSIONS

In the above article, we can conclude that the technology of integrated cogeneration installation in ovens is very relevant from the thermodynamic point of view, respectively, in terms of energy efficiency.

This measure allows the minimization of the exergetic losses associated to the process of securing the necessary temperature of thermal agent (by mixing), by replacing it with a heat transfer process, which is less irreversible than the mixing process (solution shown in Fig.2) or total avoidance of these exergy losses (the solution shown in Fig. 3).

The production of two forms of energy, after retrofitting of installation, will contribute to the increase of the amount of the flow exergy from the modernized installation (because the exergy work is equal to the work done and exergy of electricity also is equal to the value of produced electricity), by increasing the thermodynamic efficiency of the installation calculated the equation (1).

It should be noted that the proposed technology can be implemented in any enterprise equipped with natural gas oven, it doesn't matter with the type of products cooked, especially in cases where the required temperature of the flue gas for performing the processes is much lower compared with the temperature of combustion natural gas.

However, the result of implementing the cogeneration installations at the enterprise, it will be ensured with the electricity needed to carry out other processes or utilities, and coolants agents can be then used to require thermal energy consumption for preparing blanks or cleaning the equipment.

References

1. *Statistical yearbook of the Republic of Moldova 2013. Biroul Naţional de statistică al R. Moldova. Chişinău, 2013.*

2. Stecla ru D., Mamaliga V. *Analiza volumelor de producere şi desfacere în industria de panificaţie. Meridian Ingineresc Nr. 3, Chişinău, pag. 70-74, 2009.*

3*. http://ziarulnational.md/decis-painea-se-va-scumpi-din-15-august-cu-aproximativ-15-explicatia-brutarilor-din-r-moldova/*

4. Alexandru R. et al. *Economia de energie în industria alimentară// Bucureşti: Editura Tehnică, 1991, 354 p.*

5. Chelmenciuc C., Guţu C. *Sporirea eficienţei energetice în brutării// Conferinţa Tehnico-ştiinţifică a Colaboratorilor, Doctoranzilor şi Studenţilor UTM, Chişinău, pag. 320-323, 2011.*

6. *Hotărâre privind tarifele la gazele naturale. Nr. 425 din 29 septembrie 2011// Monitorul Oficial al Republicii Moldova, 30.09.2011, nr. 160-163/1459.*

7. Shevchenko R. i. d. *Sravnitel'ny'j e'kologicheskij analiz hlebopekarnyh pechej// Harchova nauka i tehnologiya Nr. 1(14), pp. 80-84, 2011.*

8. Musteaţă V. *Termodinamica tehnică şi procese tehnologice// Chişinău: Editura UTM, 2006, 88 p.*

9. Bejan A. *Termodinamica tehnică avansată// Bucureşti: Editura Tehnică, 1996, 848 p.*

10.*http://www.j4.cz/RJ/html/pekarskepece.htm#standard*

Recommended for publication: 23.03.2016

METHOD OF DESIGNING OF THE ELITE DWELLING FOR THE COHABITANTS WITH DIFFERENT PSYCHOTYPES

Victoria Kalashnikova, PhD student
National aviation university, Ukraine

INTRODUCTION

Relevame of the topic: Modern technologies and methods of designing elite dwelling offer many different ways to achieve the best results for stays of comfort for potential buyers and owners. But the effort largely aimed at physiological comfort, psychological aspect is very rarely included. If psychology is still considered, anyway, it focuses on the psychological characteristics of the so-called "*common man*", and individual characteristics psychotype specific buyer or owner does not count at all.

And if you live in one dwelling several cohabitants with with different psychotypes, as they pick a good design solution that would satisfy everyone, and at the same time was correct in terms of design and architecture.

It is therefore extremely important method is to create a single design solution of choice of elite dwelling to be psychologically comfortable for several cohabitants with different psychotypes.

Analysis of latest research: J.N.Kovalev and N.M.Mkhitaryan developed a design methodology psychologically comfortable residential property for various psychotypes, but not treated task create a single design solution of choice of elite dwelling to be psychologically comfortable for several cohabitants with different psychotypes.

Aim: consists in the development and implementation in practice of of designing a single design solution of choice of elite dwelling to be psychologically comfortable for several cohabitants with different psychotypes.

Tasks: describe the sequence of method of designing of the elite dwelling for the cohabitants with different psychotypes on the example real interior design an elite three-room flat for a family consisting of two adults and a child.

Expected scientific novelty: to determine for the first time method of selecting a single design solution of choice of elite dwelling to be psychologically comfortable for several cohabitants with different psychotypes.

Expected practical implementation: the results can be used in the formation of elite psychologically comfortable of elite dwelling in the city and outside it, with the development of normative documents, teaching handbooks for designing different types of elite dwelling.

1. DEFINITION OF THE PSYCHOTYPES OF SEVERAL COHABITANTS

The method begins with the definition of the psychotypes of several cohabitant of elite dwelling. This procedure can be conducted as short and expanded ways.

Short way is testing two types (Psyho-heometry test "*Definition of the psychotypes*" test "*Comprehensive assessment of psychotype according to the level of interaction in the system "man-dwelling-environment'*"". As a result of this testing, determined psychotypes of several cohabitants and individual coefficients to refine the formula for you. The disadvantage of this method is a percentage error of the reliability of the result, and advantage of speed, because not all potential customers are willing to take on extensive psychological study of personality. Short way often used to determine the psychotypes, among many respondents, during the various opinion polls that need quick results, as the time limit.

If the definition of psychotypes concise short way is not enough, there is a need for comprehensive testing and there is enough time to appropriately use the expanded way.

Expanded way includes comprehensive assessment of a human personality [6]. We evaluate a person's ways of communication with the external world - either directly or through the indirect indicators by identifying the motivations. Let us use complex tests first, and then we shall supplement them with the methods of identification of individual characteristics.

1. The scale of the significance of emotions by Dodonov. Life should bring joy, i.e. positive emotions, which the everyday life so often lacks. What are those emotional states that are able to

bring pleasure? They can be determined by ranking emotional preferences.

2. Evaluation of egoism. A short explanation. The easiest way to determine the degree of the development of egoism is the egotism, the verbal expression of self-centeredness when a person continually uses the word "*I"*, "*My*", "*I have"*, etc. The more often these expressions are used, the greater the person is concerned with his or her persona.

3."Aggressiveness" method (the modification of the Rosenzweig test). The test described further is designed to assess the degree of development of aggressiveness in a human being, understood as a tendency, which is not caused by the objective circumstances, to react with hostility to the majority of statements, actions and behavior of other people. Aggressiveness is a personality trait, which expresses itself in more or less constant hostility of a human against a human, animals and objects of nature and material culture, the tendency to their destruction and unprovoked aggressive actions.

4. Intelligence assessment. H. Eyesenck IQ Test. Perhaps it is one of the most famous tests. In general, the higher score you get the better. However, it isn't worth giving an "absolute" value to the achieved results. Testing methodology is not perfect; in real life there is an integral person who acts, not a separate intelligence that doesn't have a definition. As a result, for example film actresses and boxers, who, according to the public (prejudiced?) opinion, don't have high level of mental ability, join the prestigious international club for "*those who score higher than 160*". Therefore, we present two more rather simple tests.

5. Testing the sense of time-space organization. On rectangular sheets the drawings of "*Tree*", "*Elephant*, "House", etc. are made. Based on the location, details, proportions and compositional principles, the emotional characteristics, activity/passivity and time-space preferences are determined.

6. Sensation-Seeking Scale (test by M. Zuckerman). The test is designed to research the risk taking tendency, estimation of the level of personal need in seeking different new sensations. The search for new feelings is of great importance for a person as it stimulates emotions and imagination, develops creativity.

7. Evaluation of resistance to negative external influences. Scale of situational anxiety by Spielberger. Anxiety - the tendency of a person to experience the emotional state which manifests itself in anticipation of adverse events.

Personal anxiety and situational anxiety are distinguished. This is important when considering the possibilities of compensation of such a state during the design of a dwelling.Situational (reactive) anxiety – this is the behavior that looks like the one mentioned above but which, however, is not associated with the presence of personal anxiety displayed by people in certain (but not all) situations. In unfavorable circumstances, reactive anxiety can develop into personal one, i.e. the anxiety can become a stable trait of personality. It is obvious that the means of compensation should prevent such course of events.

That is why the study of such types is very important life-related task.

8. The scale assessing the level of personal anxiety by Spielberger. Personal anxiety - a basic personality trait which is formed and fixed in early childhood and becomes apparent in sustainable situational anxiety of a person expressed by a state of increased anxiety in a threatening or seemingly threatening situation. Obviously, in this case only minimal compensation is possible.

9. Assessment of stress tolerance of a person. Conflicts, as well as a number of other negative life factors, create nervous state and often lead to stress.The proposed test will help to assess stress tolerance. For an objective result, sincere answers are necessary.

Thanks, psychotypes expanded by definition can not only more accurately determine the psychotypes owners, but also to choose the specific measures to achieve an integrated comfort with regard to the results for each component of comprehensive assessment of personality.

In this case, we determined psychotypes cohabitants expanded way. So, psychotype of husband is "*Up-and-coming Researcher*", psychotype of wife is "Contemplator", psychotype of child is "*Fighter*".

1. DEFINITION OF COMPLEX PROFILE OF COMMON PSYCHOTYPES

Defining psychotype each cohabitants, to analyze that psychotype stands dominant and which secondary. Summarizing the results of a comprehensive evaluation of psychotype according to the level of interaction in the system "man-dwelling-environment», obtain a complex profile of the common profiles as follows.

At fig. 1 shows a profile of the first cohabitant. Considering the figures for the level of interaction in the system "*man-dwelling-environment"* apparently the husband belongs to psychotype "*Up-and-coming Researcher"* [6]. He rather likes predictability, order and stability:

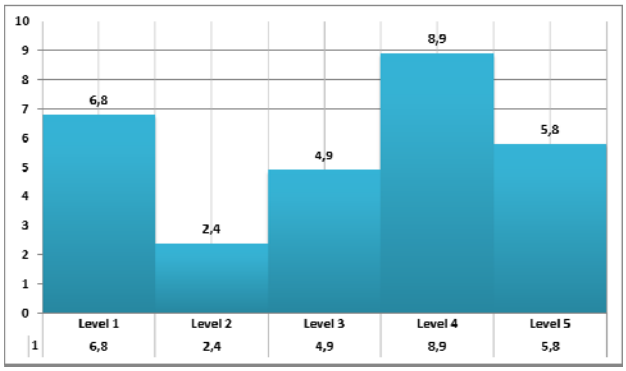

Figure 1. Profile of the husband.

"*Money loves peace and quiet*". But within these limits, he can be quite vigorous, energetic and intelligent (mind prevails over will), both in business and in science. "*Strengthening of the mind*" takes place mainly at the expense of the senses, and some people even know how, consciously or not, to sublimate sexual energy for "*creative goals*", which was noted by Freud. Demands for the dwelling are as follows: a strict and conservative style, clear and time-tested solutions, and calm tones of the interior – however.

At fig. 2 shows a profile of the second cohabitan.

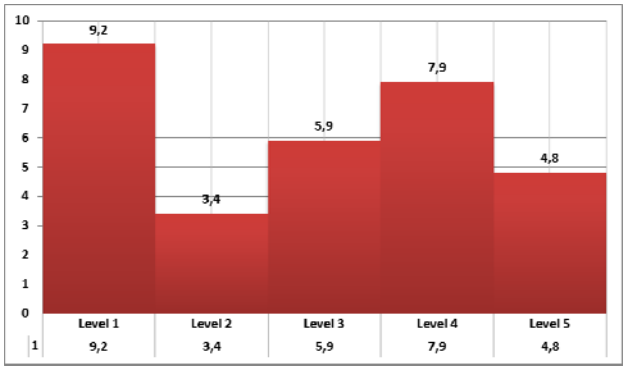

Figure 2. Profile of the wife.

Considering the figures for the level of interaction in the system "*man-dwelling-environment*" apparently the wife belongs to psychotype "*Contemplator*" [6]. Here, the same as for the other types, the balance between the levels is already broken. Since the total value of the potential is constant, the increase of certain qualities - in this case, intuition - will be at the expense of others - above all, the ego and will. Therefore, contemplators are inclined to have a quiet way of life. As for the dwelling, their requirements are minimal: it should be located in a quiet, beautiful and, if possible, deserted place and meet their biological needs. The next aspect is its adjustment in accordance with the mood and health of the owners. Here, both psychological and physiological research is needed, plus improved management programs. In addition, the progress in the creation of new building materials and technologies must be made. We will return to this topic in the section "*Dwelling of the future*".

At fig. 3 shows a profile of the third cohabitan.

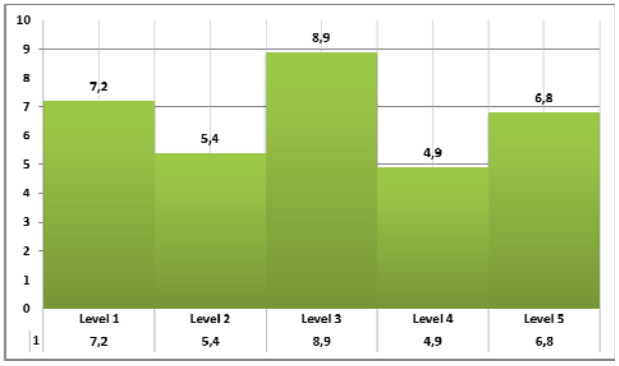

Figure 3. Profile of the child.

Considering the figures for the level of interaction in the system "*man-dwelling-environment*" apparently the child belongs to psychotype "*Fighter*" [6] is characterized by high inclination for self-realization, also by conflict character and aggression (will prevails over mind), which cannot but lead to both physical and mental disorder, because intuition, ego and intellect are oppressed. This is the "*Martian*" type, whose motto, like that of Porthos, is "*I fight because I fight*". The vigorous and varied activity puts excess demands for the dwelling's transformability. The corresponding emotional state should also be encouraged - for example, by bright colors in the interior, etc.

Compare the indicators of of the three profiles at fig. 4.

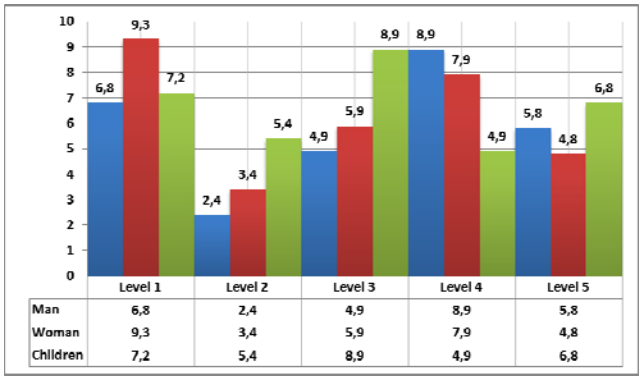

Figure 4. Compare profiles.

Is now depicted complex profile of common psychotypes of two adults and a child at fig. 5.

Define its indicators of (this is the arithmetic mean of the three indicators on each of the levels of interaction in the system "*man-dwelling-environment*"). Thus, the priority for the family is the next level of interaction in the system "*man-dwelling-environment*".

1. Level 1 – integrity. Here a man and the environment are not isolated from each other as separate parts yet; however, the possibility of their separation already exists as some potential of free resources, which can be used for this. Physically,

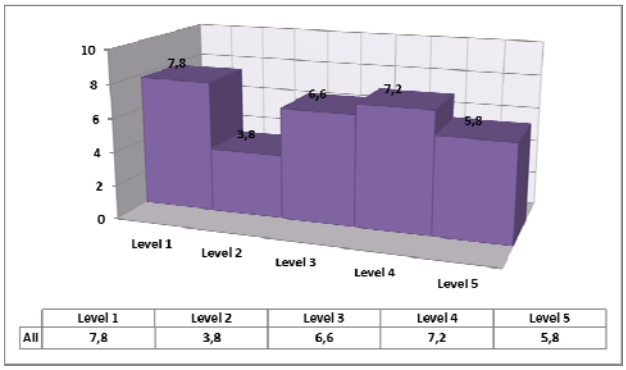

Figure 5. Complex profile.

the unity of the man and the environment is expressed, for example, in the fact that the man's body consists of the same elements and follows the same laws as the Universe. Mathematically, this unity is expressed through self-similarity, different symmetries and corresponding to them conservation laws, harmonic relations based on the "*golden section*" and Fibonacci numbers etc. If such relation did not exist, no interactions with the environment would be possible [6].

2. Level 2 – space and time. Appearance of actions and reactions is followed by their arrangement in two categories (inheriting characteristics of the previous level, linked with number 2) which are generally called space and time. Based on the self-organization theoretical scenario, three parameters should be given to each of them. So it is indeed: space is three-dimensional; time includes past, present and future. Ternary divisions are just as characteristic for our consciousness as the binary ones. For instance, we distinguish energy, information and entropy, three months of summer, three social estates, etc. [6].

3. Level 3 – actions and reactions. The existence of not only oneself, but also of the environment is realized, as well as impacts on it and feeling its feedback. For a man the reaction may be favorable and unfavorable, which is perceived in categories "*good*" and "*bad*". The "*knowledge of good and evil*" takes place with the natural need to make and fulfill decisions, regulate wishes, etc., for which decisiveness and will are needed. For this level, generally, binary divisions are characteristic. Thus, for a man, there is a distinction between bodily and psychic components, left and right halves, male and female sex. For the Universe, substance and field, attraction and repulsion, space and time, etc. are distinguished [6].

The adapted ***"formula of comfort"*** for this family, is the following:

$$p=0,78*o_1+0,38*o_2+0,66*o_3+0,72*o_4+0,58o_{5\text{-}6}, \quad (1)$$

where p – general assessment;
o_1-$o_{5\text{-}6}$ – assessment for the levels.

2. SELECTING THE CONCEPT OF INTERIOR

Results of complex profile of common psychotypes needs owners, their life style, family members, personal aesthetic preferences and tastes, along with the vision of the authors of the project - defined concept design of the apartment at fig. 6.

Figure 6. The concept of the interior.

3. DEVELOPING OF PLANNING AND STYLISTIC DECISIONS OF INTERIOR

The style and planning. The desire for open spaces identified the unifying nature of the existence of the living room, the dining room are the kitchen fig.7 [8]. And ease of interpenetration of space hallway and living room**.**

Expanded one of the bathrooms - the state of "*spacious*" with spacious spa bath and shower. The hall is mounted semicircular closet. In fact organized dressing room. A similar approach is used when creating the office - in place of the balcony and the bedroom. In both cases, the wings open or closed spaces the adjacent premises or combine or disconnected. This is - an example of the transformed spaces. Streamlined wardrobe

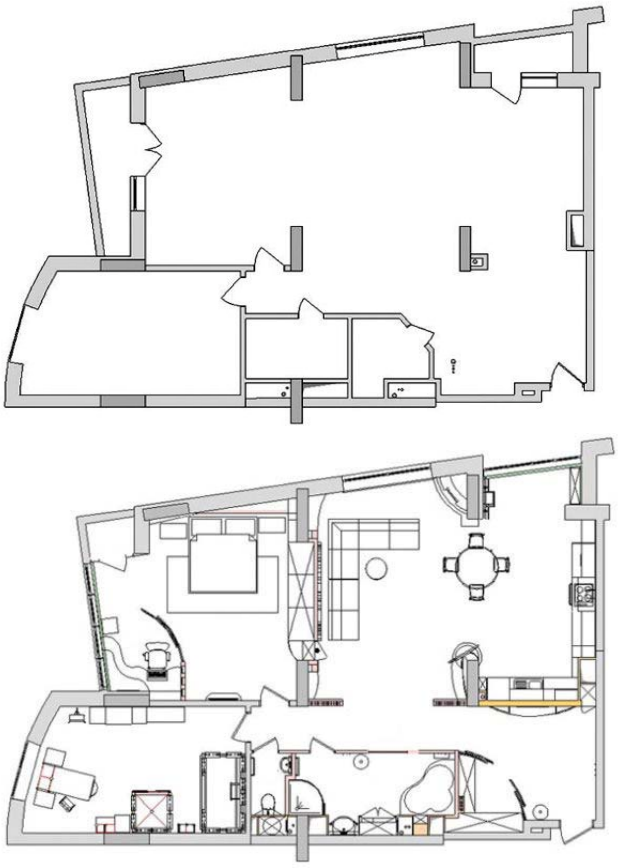

Figure 7. Plan apartments before and after redevelopment.

cabinet and also create a sense of ease interpenetration of spaces, while claimed total "*flexible*" style of the interior of the apartment.

Zones of common-use developed taking into account of complex profile of common psychotypes. Living room - dining room - kitchen at fig.8 [8] equipped beautifully decorated fireplace, a column posted on the TV, easy to view from almost all points, and that is very important - full plenitude of living plants and their images. Worth paying attention to special zoning means that space. With wood flooring, different colors formed "track" and "islands" supported structures hanging and suspended ceilings and placement of fixtures. In the middle of all the space - a round table at him, almost in the same shape - a round ceiling design with round shapes as chandeliers.

Decorative pylons, separate corridor transit zone of living space. Embedding they asked stylistic stained glass fabric around the interior - the curved shape of pylons, curved stained glass, flexible forms its own image - the same graphics we see a completely different elements of the interior of the apartment. Living room at fig. 9 [8] has its own flavor - edged with decorative stone panorama favorite places. By itself, the stone already sets a special mood, something wistful in the past, and so real. In the partition that separates the kitchen from

Figure 8. The interior of the kitchen-dining room.

the hallway, stained glass mounted. In most of the kitchen work surface placed decorative panel that carries the hostess home in flood meadows at times when not thought about spices and proportion.

All this creates a feeling the owners - comfortable, at home cozy as on the desert island.

Figure 9. The interior of the living room

In the bathroom at fig.10 [8] there was a "*window on the island*" - the same stained glass with a favorite theme and "*plant*" flexible mosaic mosaic inserts in the same wall. In cases as simple function - to hide the washing machine and put everything you need on the shelves.

Is worth mentioning that the selection and texture, and color mosaics already creates a special mood associated adjusting to "*island*" system. The same applies to the leisure, lime green toilet, which besides toilet hidden behind a console so necessary in the summer boiler.

Individual zones are developed based on individual profiles of psychotypes of several cohabitant. As a parent bedroom at fig. 11 [8] wall in the head of the bed covered with paintings of weeping willows. The ceiling is made of stretch and suspended structures, is the secret symbols merger

Figure 10. The interior of the bathroom room.

of the two areas and the center of the composition is crowned with a chandelier, wonderfully reminding crystal bouquet of flowers.

Figure 11. The interior of the bedroom room.

In children room at fig. 12 [8] all the walls are covered with paintings on the the same theme, but here's flowers, bees and dragonflies have children do better perception - a fantastic character. A blue sky over your head (tension ceiling) floating lights - white clouds children's world in the materials and colors.

Figure 12. The interior of the children room.

Design project of the apartment interior designed by the method of designing of the elite dwelling for the cohabitants with different psychotypest, by studio of architecture and design studio "*Zlatograf Interior*" (authors: Anatoliy Bilonoha - chief architect of studio, Oksana Novoshytska - designer).

CONCLUSION

The article described in details the sequence of method of designing of the elite dwelling for the cohabitants with different psychotypes on the example real interior design an elite three-room flat for a family consisting of two adults and a child. Defined of the psychotypes of several cohabitants (husband, wife, child). Depicted complex profile of common psychotypes of two adults and a child, according to the level of interaction in the system "*man-dwelling-environment*". Described the concept and implemented a rational and functional interior variant, that is easily transformed, into a modern style with elements of ecodesign. Using this method speeds up the design process, and the result has been providing complex comfort accommodation for all cohabitants.

Bibliography

1. Kovalyov Yu. N. *Geometric simulation of ergatic systems: hardware development. Kyiv: KMUGA, 1996. 134 p.*

2. Kovalyov Yu. N. *Ergonomic optimization of management based on C-space models. Kyiv: KMUGA, 1997. 152 p.*

3. Mkhitaryan N. M. *Ergonomic aspects of complex systems/ Mkhitaryan N.M., Badeyan G.V., Kovalyov Yu.N. – Kyiv: Naukova Dumka, 2004. 599 p.*

4. Mkhitaryan N. M. *Man and Comfort. Kiev. Naukova Dumka, 2005. 394 p.*

5. Mkhitaryan N. M. *Comfort and Energy. Kiev. Naukova Dumka, 2011. 442p.*

6. Mkhitaryan N. M. *Man and Dwelling. Kiev. Naukova Dumka, 2012. 310 p.*

7. Leroux R. *Human Ecology: the Science of Housing Construction. M.. Publisher of Construction Literature. 1970. 264 p.*

8. http://www.zlatograf-interior.com/

Recommended for publication: 11.04.2016.

DEVELOPMENT OF BREAKFAST FOOD CONCENTRATES FOR THERAPEUTIC NUTRITION

Bantea-Zagareanu Valentina, PhD, assoc. prof., Canja Ana, MA student
Technical University of Moldova

INTRODUCTION

Scientific and technical progress and implementation of next-generation technologies around the world has enabled the creation of a number of utilities that facilitate human's existence, but unfortunately have increasingly affected everyone's health. Perhaps the most plausible explanation consists in human's eating habits that have changed simultaneously with the constant evolution in all areas of life. Scientific researches have established that with decreasing consumption of cereals has been recorded an increase in the frequency of XXI century diseases such as: cancer, obesity, diabetes, hypertension, cardiovascular disease, etc. Very important are the studies which proved that cereals contain protease inhibitors and antioxidants, this fact aiming to inactivate carcinogens [1-3]. So a very efficient solution would be to return to the old and simple foods that have fed our ancestors - cereal products rich in dietary fiber.

1. MATERIALS AND METHODS

The main raw materials and auxiliary materials used for the research were: No.1 and No.2 oatmeal cereals, wheat bran and oats, coconut flakes, margarine, agave syrup "*AGAVENSIRUP*", fructose, cinnamon, walnuts, egg yolk, sugar-free dark chocolate. All this materials were grouped from the start according to their principles of action and characteristics that are transposed on the characteristics of the final product. So, we can distinguish: texture enhancer (oatmeal, wheat bran and oat, walnuts grits), flavor enhancers (taste and odor: coconut flakes, cinnamon, dark chocolate) and ligands (agave syrup, margarine, fructose, egg yolk).

The main methods of physicochemical analysis that were used for the research are: determination of the content of dry substances in food concentrates, determination of total content of carbohydrates, determination of titrable acidity, ash content in food concentrates and the sensorial methods of analysis - assessing quality through 0... 5 points scale and profile diagram. It was also established the energy value for the obtained product, baking and drying losses.

2. RESULTS AND DISCUSSIONS

Following the scientific and practical research, it was established a basic recipe that allowed the development of three kinds of food concentrates for breakfast: muesli, cereal bars "*Granola Bar*" and glazed with chocolate cereal clusters. The distinctive feature of these products is the target market, represented by people with diabetes or metabolic disorders. The products were subjected to physical and chemical analyzes and the results are shown in table 1. Due to a more sophisticated recipe composition of "*Granola Crunch*" product (coated with chocolate cereal clusters), suitable methods for determining physicochemical indexes for food concentrates used before are not compatible with this product.

It was therefore performed a simple determination of the semi product, which was later cooked and presented as glazed cereal clusters, the obtained results are shown in table 2.

Because the researched and realized products are innovative, there are currently no technical documents, nor standards which might stipulate the physical and chemical indicators. However, according to studies achieved by Americans [4, 5], we can estimate the moisture content in the finished product within 2-6%. Therefore, this physicochemical index for "*Muesli*" and "*Granola Bar*" products can be included in that range.

Unlike the physicochemical analyzes that were performed for this three types of food concentrates; the sensory analysis was accomplished separately because the appearance, texture and flavor itself make the difference.

Products were rated called: Diabetic muesli, cereal bars "*Granola Bar*" and glazed cereal clusters "*Granola Crunch*".

Sensory characteristics were examined in the following order: appearance, texture, color, smell and taste and the results are presented in table 3 below.

Tabel 1. Physicochemical characteristics of food concentrates for diabetes.

Nr.	Characteristics / Product	Muesli	Granola Bar
1	Humidity content W, %	5,2	4,8
2	Ash, %	1,61	
3	Carbohydrates, g/100 g product	56	
4	Titrable acidity, degree of acidity	5,3	
5.	Energy value, kcal/100 g product	422	424
6.	Baking losses, %	0,7	1,1
7.	Drying losses, %	1,4	1,1

Tabel 2. Physicochemical characteristics of ”*Granola Crunch*” semiproduct.

Nr.	Characteristics / Product	Granola Crunch (unglazed semiproduct)
1.	Humidity content W, %	5,1
2.	Ash, %	1,63
3.	Glucide totale, g/100 g product	48
4.	Energy value, kcal/100 g product	422
5.	Baking losses, %	3,9

Tabel 3. Sensory characteristics of food concentrates for diabetes.

Nr.	Characteristics / Product	Muesli	Cereal bar ***”Granola Bar”***	Glazed cereal clusters ***”Granola Crunch”***
1.	Appearence and color	Well defined appearence, visible outline, dark brown color	Upright appearence, slightly caramelized color	Upright appearence, dark brown color, specific for chocolate
2.	Texture	Brittle, slightly crispy during mastication	Crispy, sonorous during mastication	Crispy and slightly gummy
3.	Smell and taste	The smell of caramel syrup, coconut flakes and cinnamon, harmonious and fine taste	The smell of caramel syrup and muesli, pleasant, slightly astringent	Pleasant smell of chocolate and cinnamon, sweet taste but slightly astringent

To assess the characteristics based on the 0...5 points scale, was organized a product tasting which was attended by students and teachers who had previously been examined on sensory skills.

For each researched feature of food concentrates was offered a score with values between 0 and 5 points. Based on average scores of sensory analysis it was developed a centralized sheet of the results, considering the total average score, based on weighted average scores. Variation of total average scores is presented in figure 1 below.

Assessing the data from figure 1 it is clear that preferential product is Muesli, tasters characterizing it as "an attractive colored product, flavorful, soft and sweet, with a pleasant taste". Although the opinions for different products were impartial, products gained a high total average score and tasters had been interested about the new assortment of food concentrates and their importance in human’s daily diet.

The graphical presentation of average scores was shown in figure 2 named Profile Diagram. Analyzing the data presented in the profile diagram we can distinguish three features that make the difference between samples: color, texture and taste.

Default texture can influence the taste and preferences of consumers. In decreasing order of the obtained score for color we have: „*Granola Crunch*” - 4.85 points, the most prefered one, followed by „*Granola Bar*” - 4.7 points and last place „*Muesli*” - 4.5 points.

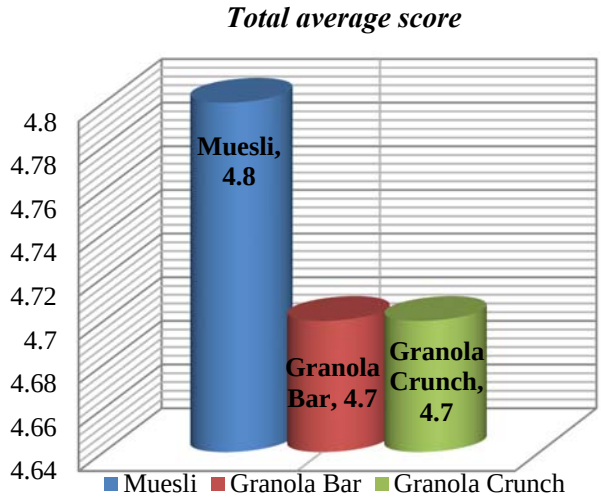

Figure 1. Variation of total average score of food concentrate's samples.

Analysing the taster's observations it was determined that they preferred a color uniformity throughout the entire mass of muesli, noticing some particles being more caramelized than others. For texture, the score in order of decreasing values were: „*Muesli"* - 4.77 points, „*Granola Crunch*" - 4.62 points and „*Granola Bar*" - 4.42 points. Tasters noted a crisp texture and specific sound for each product during mastication. Because the product "Granola Bar" is represented by a pressed cereal mass, it's quite tenacious and difficulty while biting. This makes it difficult to consume and that has led to downgrading to. And not least, the appreciation of taste: „*Muesli*" again obtained the highest score 4.92 points, followed by „*Granola Bar*" - 4.77 points and "Granola Crunch" - 4.50 points.

Following the profile diagram we can determine that the product with the most optimal sensory characteristics, is „*Muesli*", while both „*Granola Bar*" and „*Granola Crunch*" need to be improved; for the first one mentioned - texture and appearance, and the second one - taste and appearance.

CONCLUSIONS

After studying about food concentrates for breakfast in general, and different varieties of cereal mixture (muesli and granola) in particular, there were revealed a list of their nutritional and dietary benefits on human's body, which have helped with choice of product and production technology.

So it was performed a wide new assortment (muesli, cereal bars "*Granola Bar*" and clusters of grains coated with chocolate "*Granola Crunch*"), all food concentrated for breakfast being intended for curative nutrition (people suffering from diabetes).

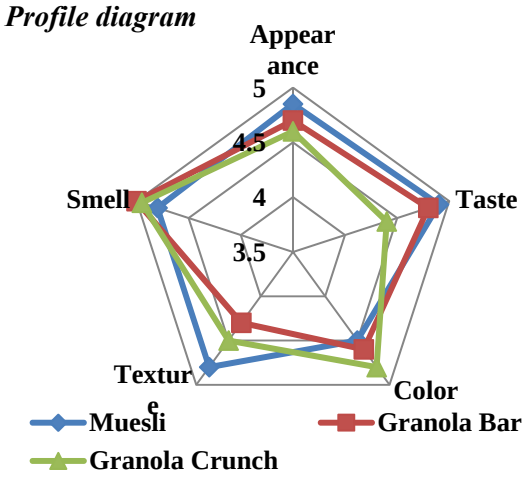

Figure 2. Profile diagram of food concentrates for diabetes.

Based on the analysis and evaluation of sensory profile diagram, the highest average scoring was obtained by muesli-type product, defining its sensory characteristics: flavor (smell and taste), color and texture. The products "*Granola Bar*" and "*Granola Crunch*", although accumulated a similarly total average score should be improved, especially some characteristics (color and texture). Thus, we can say that the entire range of products that was developed has a nutritional and special curative purpose, which offer innovativeness and will certainly cause interest among buyers.

Bibliography

1. ***Bivolaru G.*** *Alimentaţia şi terapia naturistă cu cereale. Ed. DAKINI, 2001, pp.200.*
2. ***Segal R. ş.a.*** *Alimentele funcţionale – alimentele şi sănătatea. Galaţi: Ed. Academica, 1999, pp. 356.*
3. ***Segal R. ş.a****. Produse cerealiere pentru micul dejun – o trecere în revistă. BIMP, 5(4), 1994, pp.27-42.*
4. ***Johnson et al.*** *No Bake Granola and methods of preparation. United States Patent Applications Publication, US 2013/0316063 A1, 2013, pp.11.*
5. ***Mesu et al****. Manufacture of Granola and Snack-food products. United States Patent, US 7,169,422 B2, 2007, pp.6.*

Recommended for publication: 25.02.2016.

THE WINDER CONTROL SYSTEM WITH ALTERNATIVE CURRENT DRIVE OF WIRE DRAWING LINE

Cazac Vadim, lecturer
Technical University of Moldova

INTRODUCTION

For high speed wire drawing machine, coordination of speed between the wire drawing machine and winding mechanism is very important. Further, because of a wide range of processing diameters the demands on dynamic response of the speed controlling AC drives are critical. The article attempts to present a review on the a winding mechanism of wire drawing machine working up to 1200 m/min using high performance variable speed AC drive.

In an wire drawing process one of the biggest challenges is to keep the tension force of the wire almost constant or the maximum allowable, variation of the tension force may be within the range of 4 to 5% of the desired value.

1. THE ELECTRICAL DRIVE ISSUE OF WINDING MECHANISMS

During of the wire drawing process along with the electrical noise and transients process, the disturbances are too much and some of the essential controlled parameters like the wire thickness, wire straining may unnecessarily show variations which are highly unacceptable in industrial process control.

The main purposes in this paper are:

- the best mode to control identifying of three-phase motor with rotor in short circuit for winding mechanism using the frequency converters.
- the mathematical model and transfer function identification of the control system
- tension force loop parameter set for winding mechanism.
- the setting methodology identification of PID controller on the real frequency converter used for wire drawing machine drive.

The developed control system of the technological process must ensure following requirements:

- quick start of the wiredrawing machine without shocks of tension force,
- tension force keep constant for excluding the breaking of the wire at high speeds of winding.

The driving control systems typically have two working modes: motor speed control and torque control. The choosed control system of wire tensioning force must ensure the precisely and constant force about 3-10% depending on the destination (Fig.1).

In practice frequency converter can be used in three modes for winding function:

- Wind mode 1: In this mode, frequency converter can realize simple winding function. Generally, frequency converter can run normally with correct wiring and there is no need to configure any mechanical parameter.
- Wind mode 2: When frequency converter is in this mode, roll diameter can be calculated automatically to realize better tension control. Relevant mechanical parameters are required to be input.
- Wind mode 3: When frequency converter is in this mode, it's not necessary to acquire the speed of host, but winding frequency converter must start before drawing out wire [3], [4].

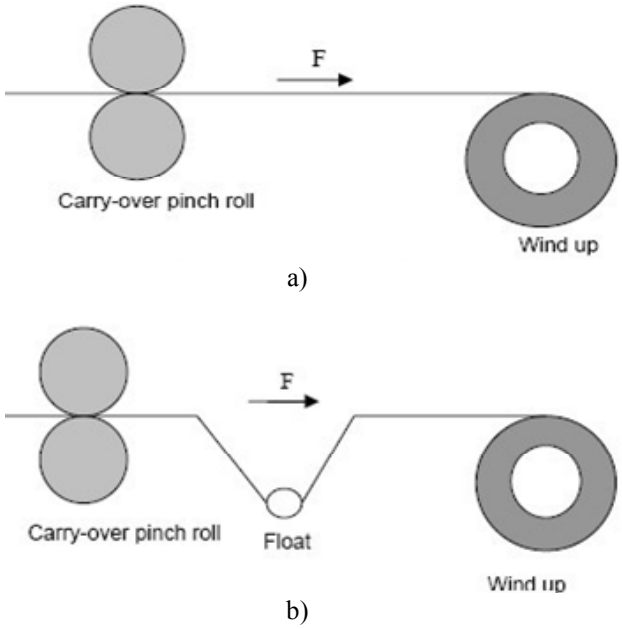

Figure 1. The diagrams of typical winding modes [3]: *a-without feedback; b - with tension force feedback.*

The process of wire drawing is carried out at speed of 50m/s (average 20–25m/s) [11]. Force for wire drawing thru dies is developed by drawing drums and friction force that occurs at the contact between the drum and processed wire. This largely depends of the friction coefficient in the dies of the wire drawing machine Drive system of wire drawing machine must develop the power necessary

to overcome the drawing force and prescribed working speed [1], [2], [5].

The system consists of MA1 asynchrony motor, frequency converter with vector control CF1. Since the wire drawing machine does not require a drive with high dynamic parameters, the motor MA1 operates on frequency characteristics, without feedback loops.

For excluding wire breakage, drive system of the winder ensure prescribed speed and tension force. Therefore it contains a MA2 asynchrony motor and frequency converter with vector control CF2.

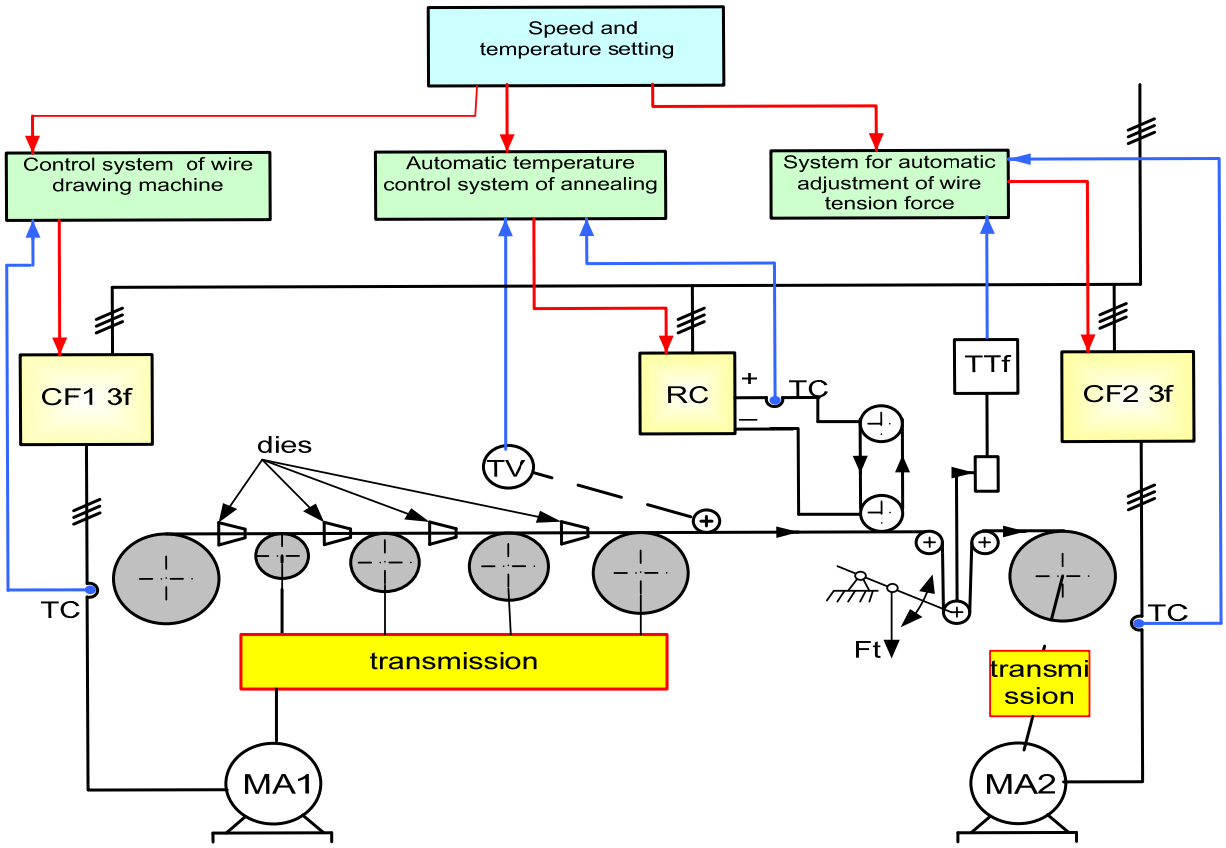

Figure. *2*. Block diagram of power and control system of the wire drawing machine with annealing module and winder [8].

2. THE MATHEMATICAL MODEL OF WINDING MECHANISM

Tension force adjusting at winding can be do in two ways: direct measurement of the force from wire or by modifying some parameters indirectly [6].

2.1. The matehmatical model of the spool

Spool diameter changes in time, depending upon linear velocity of the wire. The radius of spool any time can be estimate using following relationship [4], [8], [6]:

$$R_b = \sqrt{R_0^2 + \frac{d^2}{\pi \cdot L_b} \int V_l dt} \qquad (1)$$

where: Ro– the initial radius of the spool, d–the diameter of wire, L_b– spool length.

The spool inertia according to quantity of material that has been spooled can be determined by (2) [6]:

$$J = J_0 + \frac{\pi L_b \rho}{2}(R_b^4 - R_0^4), \qquad (2)$$

where: J_0– the empty spool moment of inertia, ρ– the wire density, taking into account filling factor.

2.2. The torque of winding mechanism

The value of wire tension force depends on its section and shall not exceed the amounts that would cause its thinning and breakage during the work. The tension force in the wire drawing machine is made by a pneumatic cylinder fed with compressed airflow through a pressure regulator that enable to set the stretch force.

The tension force calculus in the wire at winding:

$$T = \frac{\sigma_{Al.}}{\nu_{rez.}}\left[\frac{N}{mm^2}\right] \quad (3)$$

where: σ_{Al} – the tensile strength of the metal, $\nu_{rez.}$ – reserve ratio.

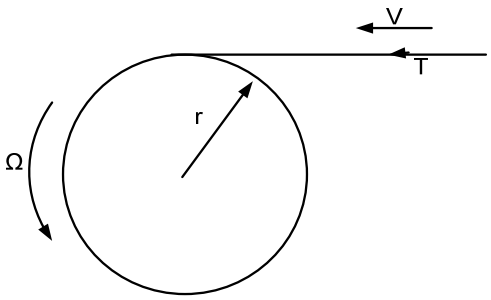

Figure 3. The mathematical description of the winding mechanism.

Static torque of spool:

$$M_s = T \cdot r \quad (4)$$

where: T–tension force in the wire; r–the radius of the spool.

$$M_s = \frac{T \cdot v}{\Omega} = \frac{k}{\Omega} \quad (5)$$

2.3. The dynamic relationships of winding mechanism

The relationships (6) describe the dynamic processes of winding mechanism in function of line are velocity of the wire, spool diameter and inertia which are also variable. [8].Based on this model was developed a system that ensure a high stability of the control system at high speed of the wire winding, make corrections in control system by estimating the radius and inertia of the spool [11].

$$\left.\begin{aligned} F_T(S) &= (V_{LM2}(S) - V_{LM1}(S)) \cdot \frac{E \cdot S_{cond.}}{L_k(S)} \\ V_{LM2} &= \omega_{M2}(S) \cdot \frac{R_T(S)}{i_{red.}} \\ \omega_{M2}(S) &= M_{din}(S)\frac{1}{J_\Sigma(S)} \end{aligned}\right\} \quad (6)$$

where: F_T–tension force in the wire;
V_{LM1}–linear speed of the wire;
V_{LM2}–linear speed of the wire at spool;
$S_{cond.}$–the wire section;
L_k–working length of the wire drawing machine;
R_T–radius of the spool;
E–the elasticity coefficient of wire.

3. THE VECTOR CONTROL SYSTEM OF WINDING MECHANISM

In this section is represented the simplified structure of the winding control system, the elements of this drive are shown in Figure 4. The wire tension force adjusting at winding takes places in a direct way, using a transducer for its measure, in the wire.

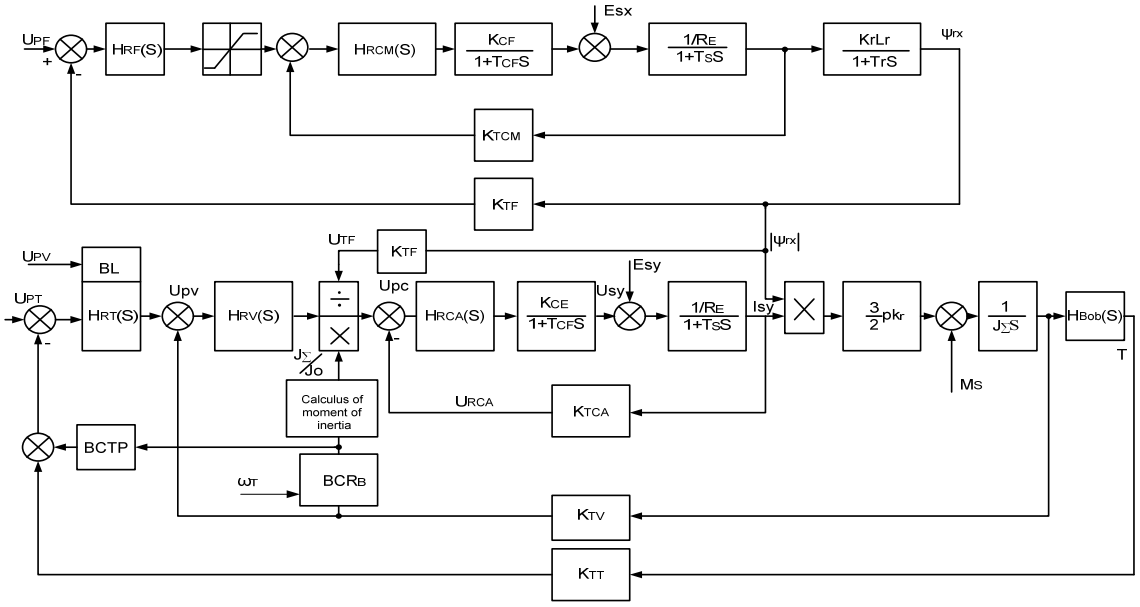

Figure 4. Simplified structural diagram of vector control system for adjusting winding speed and tension force [2], [10].

The diagram has three loops with subordinate adjustment of the active current, speed and of the wire strain force is outer loop. Changing the regulating modes is performed automatically after influence of the tension force controller over limit block. In case if wire is not, integral component of the regulator bring the regulator in saturation. The limit value is prescribed by the signal U_{pv}, and prescribes the speed of the spool when it is empty. The tension force will start to rise and the tension force regulator will exit from saturation and allow the contour of tension force regulator to work, considering that, the angular velocity of the spool is prescribed to be higher that the linear speed of the spool.

At wire breakage a reverse process will start, the signal from the tension force regulator exit will start to rise until saturation. The winding speed will also start to rise. To stop a full spool it is necessary to decrease the limit value of the tension regulator until it reaches nil. The multiplication and division device provides the granting of the speed loop at function with weakened magnetic flow or with changing the summary inertia at the motor shaft. The law of modification for the wire tension force is ensured by the correction block of tension force prescription [8], [10].

The corrections bloc of the prescribed tension force BCTP represents a proportional controller with factor(7):

$$k_{CPT} = k_R\left(1-\frac{R_{TB}}{R_B}\right) \tag{7}$$

where: k_R –reserve coefficient, decreasing the influence of the spool radius on the tension force, being chosen k_R=1,

R_{TB} –radius of the full spool;

R_B –radius of the empty spool.

BCRB–is block of the winding spool radius calculus.

3.1. The magnetic flow channel calculus

The structural diagram of the magnetic flow channel at vector control includes two loops of automatic regulation: the internal loop of the reactive current of magnetizing I_{sx}=I_m and the outer loop of the magnetizing flow (Figure 5).

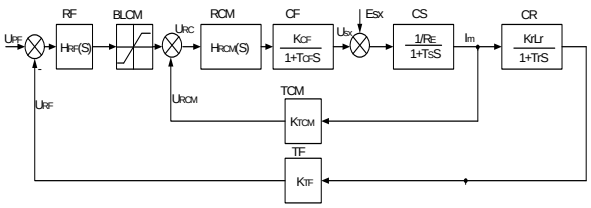

Figure 5. Structural diagram of the magnetic flow channel [9].

The turning system of coordinate x-y is oriented after the rotor magnetic flow $\psi_r = \psi_{rx} = |\psi_r|, (\psi_{ry} = 0)$, which ensure the simplest structure of the automatic control system.

The diagram from Figure.4 does not take into consideration the transformations ABC /α–β, α–β/x–y and reverse x–y/ α–β and α–β/ABC. In the outer loop the limit block of magnetizing current is introduced in (BLCM).

3.2. The magnetizing current loop calculus

Having determined the parameters of the motor, belonging to the winging mechanism, we make for the system regulation loops calculus. The frequency converter can be approximated with a first order element>

$$H_{CF}(S) = \frac{U_{SX}(S)}{U_c(S)} = \frac{k_{CF}}{1+T_{CF}S} \tag{8}$$

Where,

$$k_{CF} = \frac{U_{sx.N}}{U_{CN}} = \sqrt{\frac{2}{3}}\frac{U_s}{U_{CN}} \tag{9}$$

T_{CF}=0,005s –inner constant of the CF without a prescription integrator element.

If a Hall type current transducer is chosen, then it, can be described through a non inertial element.

$$k_{TCM} = \frac{U_{TCM.N}}{I_{SX.N}} \tag{10}$$

The RCM tuning is made, relative simply, based on module criteria the transfer function of the current closed loop is:

$$H^d_{d.c}(S) = \frac{1}{2T_{\mu c}S\left(T_{\mu c}S+1\right)} \tag{11}$$

where: $T_{\mu c}$ –the small constant (uncompensated by controller) of the current loop

The RCM regulation object

$$H_{ORC}(S) = H_{CF}(S)\cdot H_{CS}(S)\cdot H_{TCM}(S) = \frac{k_{CF}}{1+T_{CF}(S)}\cdot\frac{1/R_E}{1+T_S(S)}\cdot\frac{k_{TCM}}{1+T_{TCM}S} = \frac{k_{OR.C}}{\left(1+T_{\mu C}S\right)\left(1+T_SS\right)} \tag{12}$$

.....

where: $T_{\mu C} = T_{CF} = 0.005$;

$$k_{OR.C} = \frac{k_{CF}\cdot k_{TCM}}{R_E} \tag{13}$$

The current loop transfer function is:

$$H_{d.C}(S) = H_{RCM}(S) \cdot H_{OR.C}(S) \tag{14}$$

As a result, if the following equals is:

$$H_{d.C}(S) = H^{d}_{d.c}(S)$$

$$\mathrm{H}_{\mathrm{RCM}}(\mathrm{S}) = \frac{\mathrm{H}^{\mathrm{d}}_{\mathrm{dc}}(S)}{\mathrm{H}_{\mathrm{CRC}}(S)} \approx \frac{(1+T_S)S}{2k_{CRC}T_{\mu}S} \tag{15}$$

The RCM controller is PI type. The time constant of this controller compensates the big constant of the loop–the rotor constant $T_{IZ.C}=T_S$=0,248s.
The RCM integration constant is:

$$T_{I.C} = 2k_{OR.C} \cdot T_{\mu c} = 2\frac{k_{CF} \cdot k_{TCM}}{R_E} \cdot T_{\mu c} \tag{16}$$

The proportional coefficient of RCM:

$$k_{RCM} = \frac{T_{IZ.C}}{T_{I.C}} \tag{17}$$

The transfer function of current closed loop:

$$H_{BC}(S) = \frac{I_{SX}(S)}{U_{PC}(S)} = \frac{H_{d.c}(S)}{1+H_{d.c}(S)} = \\ = \frac{1/k_{TCM}}{2T^2_{\mu c}S^2 + 2T_{\mu c}S + 1} \tag{18}$$

where: $1/k_{TCM}$ –the inverse transfer function of the TCM, introduced in prescription current circuit $H_{OR.C}(S)$.

3.3. The magnetic flow loop calculus

The transfer function for the magnetic flow transducer

$$k_{TF} = \frac{U_{RF}(S)}{\psi_{rx}}\left[V/Wb\right] \tag{19}$$

The transfer function of magnetic flow loop:

$$\mathrm{H}_{\mathrm{CRF}}(\mathrm{S}) = \mathrm{H}_{\mathrm{SC}}(\mathrm{S}) \cdot \mathrm{H}_{\mathrm{CR}}(\mathrm{S}) \approx \\ \approx \frac{k_{CRF}}{(2T^2_{\mu}S^2 + 2T_{\mu}S + 1)(1+T_r S)} \tag{20}$$

where: $$k_{OR.F} = \frac{k_{TF} \cdot k_r \cdot L_r}{k_{TCM}} \tag{21}$$

For tuning of the RF magnetic flow controller, we use the same criteria of module with its desired function

$$H^{d}_{d.F}(S) = \frac{1}{2T_{\mu F}S\left(2T^2_{\mu c}S^2 + 2T_{\mu c}S + 1\right)} \tag{22}$$

The transfer function for the RF is similarly determined, gaining a PI controller

$$\mathrm{H}_{\mathrm{RF}}(\mathrm{S}) = \frac{\mathrm{H}^{\mathrm{d}}_{\mathrm{d.F}}(S)}{\mathrm{H}_{\mathrm{OR.F}}(S)} \approx \frac{(1+T_S)S}{k_{OR.F}T_{\mu F}S} \tag{23}$$

where: $T_{\mu F} = 2T_{\mu c} = 2T_{CF} = 0.01\ S$

The isodrom constant of the magnetic flow regulator, in this case is:

$$T_{IZ.F} = T_r = 0.813\,S$$

The RF integration constant:

$$T_I = k_{OR.F} \cdot T_{\mu F} \tag{24}$$

The proportional amplification constant:

$$k_{RF} = \frac{T_{IZ.F}}{T_{I.F}} \tag{25}$$

3.4. The vector control channel calculus

The vector control channel calculus of winding motor, has, the inner loop of the active stator current, connected in cascade, $I_{s\,y} = I_r$ with the RCA regulator and an outer speed loop (RV) with speed sensor (Figure 6).

This loop includes there DMD multiplication-division devices of the parameters at the RV exit, and another one at the current loop exit.

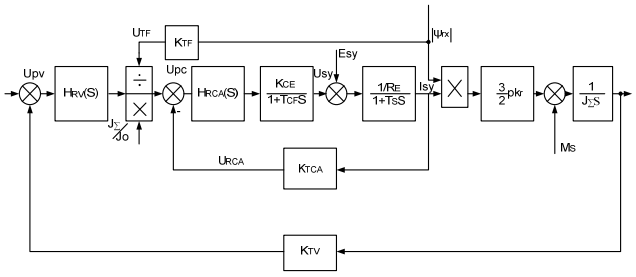

Figure 6. The simplified structural diagram of the speed vector control channel [8].

The division devise at the RV device is determined by the fact that this controller generates a prescription signal for the electromagnetic couple of motor, which is proportional with the ψ_r flow and the active stator current $I_{SA} \approx I_r$. As result, the prescription signal for the active stator current is:

$$U_{PCA} = \frac{U_{RV}}{U_{TF}} \tag{26}$$

The division device at the RV exit is meant for the torque correction of drive motor, according to variable inertia of the spool.

3.5. The loop of active stator current calculation

The active stator current sensor must be chosen with the same output signal $U_{TCA.N}$=3,5V at a nominal current of 3.5 A. The current, being twice as much, at the RCA entrance and voltage divider with a 0,5 coefficient is introduced:

$$k_{TCA} = \frac{U_{TCA.N}}{I_{CA.N}} \tag{27}$$

The transfer function is the same as in the reactive stator current case:

$$H_{CF}(S) = \frac{k_{CF}}{1 + T_{CF}S} \tag{28}$$

where: $k_{CF} = \frac{U_{sy.N}}{U_{CN}}; T_{CF} = 0.005\,S$

$T_{\mu C} = T_{CF} = 0.005\ S.-$ the uncompensated constant of the current loop.

Thanks to the current open loop, we get a current PI controller with transfer function:

$$H_{RCA}(S) = \frac{1 + T_{IZ.C}S}{T_{I.C}S} = \frac{1 + T_S S}{2k_{OR.A} \cdot T_{\mu C}S} \tag{29}$$

where: $T_{IZ.C} = T_S = 0.248\ S.$

$$T_{I.C} = 2k_{OR.A} \cdot T_{\mu C} \tag{30}$$

The amplification coefficient of RCA

$$k_{RCA} = \frac{T_{IZ.C}}{T_{IC}} \tag{31}$$

The stator current closed loop transfer function is:

$$H_{BC}(S) = \frac{1/k_{TCA}}{2T_{\mu C}S^2 + 2T_{\mu C} + 1} = \\ = \frac{2}{2T_{\mu C}S^2 + 2T_{\mu C} + 1} \tag{32}$$

3.6. The speed loop calculus

We pick a speed sensor with following transfer coefficient:

$$k_{TV} = \frac{U_{TC.V}}{\Omega_{rN}} \tag{33}$$

The inertia of the spool and of the driving motor is:

$$J_\Sigma = J_M + J_T = J_M + m_B \cdot \left(R_T^2 - R_{TO}^2\right)/i_R^2 \tag{34}$$

where: m_B=550kg; R_T=0,6m; R_{TO}=0,3m.

The speed control transfer functions of the object is:

$$H_{OR.V}(S) = H_{BC}(S) \cdot k_{TV} \cdot \Psi_r \frac{3}{2} p \cdot k_r / J_\Sigma S = \\ = \frac{k_{OR.V}}{S\left(T_{\mu C}^2 S^2 + 2T_{\mu C}S + 1\right)} \tag{35}$$

where $k_{OR.V} = 1.346$

If we start from this transfer function, the speed closed loop transfer function is:

$$H_{d.v}^d(S) = \frac{1}{T_{\mu V}S(2T_{\mu C}S^2 + 2T_{\mu C}S + 1)} \tag{36}$$

Then was got a pure proportional regulator for speed:

$$H_{RV} = \frac{H_{d.v}^d}{H_{OR.V}} = \frac{1}{k_{OR.V}T_{\mu V}} = \frac{1}{2k_{OR.V}T_{\mu C}} \tag{37}$$

The transfer function of speed closed loop with a proportional regulator is:

$$H_{BV}(S) = \frac{1/k_{TV}}{2T_{\mu C}S\left(T_{\mu C}^2 S^2 + 2T_{\mu C}S + 1\right) + 1} \tag{38}$$

But a pure proportional speed regulator does not provide a stationary error, reported to the motor load couple. The wire winding mechanism does not require a null stationary error, therefore we choose a PI speed regulator.

4. THE CONTROL SYSTEM WITH FREQUENCY CONVERTERS OF WIRE DRAWING MACHINE

In Figure 7 is given the diagram that is used to drive the wire drawing machine in the Tehelctro-SV company. In this system both motors are driven in vector control mode. Motor speed of wire drawing machine is done by the operator from the control panel via a potentiometer, the speed of winder motor is set by main converter that drive the motor of wire drawing machine through analog output MO, value of this signal depends on the transmission ratio of linear velocity of wire at output from wire drawing

machine and the linear speed of wire at input in the winding mechanism.

Further set of speed of the wire winding is achieved with the potentiometer connected to the analog input SI that show the position of the compensation arm, which also performs the tension force of the wire by using a cylinder with a compressed airflow. This signal is used as correction signal for PID controller from inside of the frequency converter.

Emergency stop of the wire drawing machine when for example the wire at entrance in the machine is entangled or is break and to exclude break of wire in the dies or in the annealing installation should be done in two stages:

1) Firstly winding mechanism at the same time with thermal processing installation must receive command to emergency stop.

2) Then when winder practically has zero speed, need to receive emergency stop command the control system of the wire drawing machine, this will exclude the influence of the moment of inertia of the spool with wire that will exclude wire breakage in the dies and in the annealing installation.

The PID control is a general process control method. By performing proportional, integral and differential operations on the difference between the feedback signal and the target signal, it adjust the output frequency and constitutes a feedback system to stabilize the controlled counter around the target value.

Set of PID controller from frequency converter of winding mechanism requires a very precisely calculation to ensure good stability of the system in a wide speed range and excluding wire breakage.

A very important step is to adjust the control system and calibration of the reaction loop in the frequency converter by set maximum and minimum value of signals (V/Hz) and their relative value in percentage to the basic signal, which is done using F4-13–F4-32 functions (for MD 380). Explanations of this stage of set are brought in Figure 8.

The PID set is a relative value and ranges from 0.0% to 100.0%. The PID feedback is also a relative value. The purpose of PID control is to make the PID set and PID feedback equal.

Start and stop of the wire driving machine is programmed in the converters to be carried out in 60sec. Dynamics of start and stop is smoothly, without shocks of the tension force in the wire.

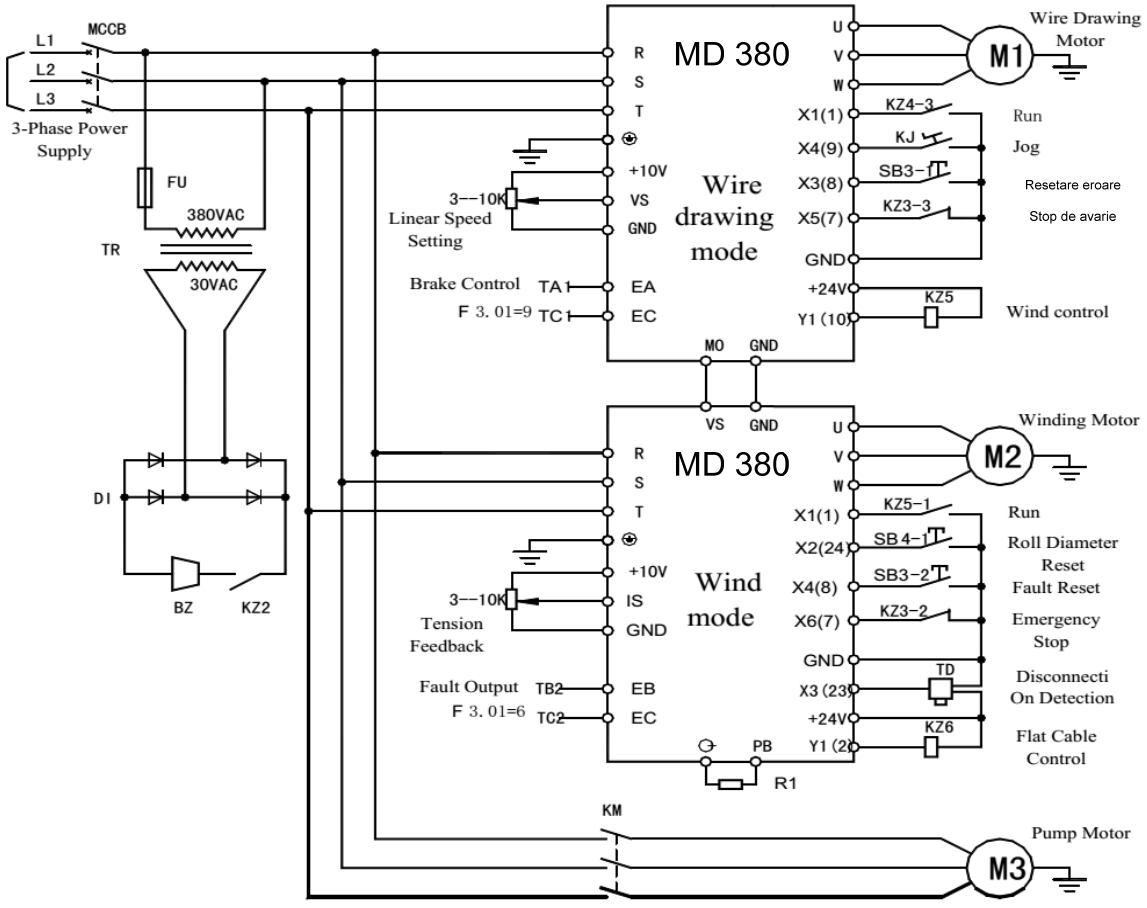

Figure 7. Typical diagram of wire drawing machine control system with frequency converters [9].

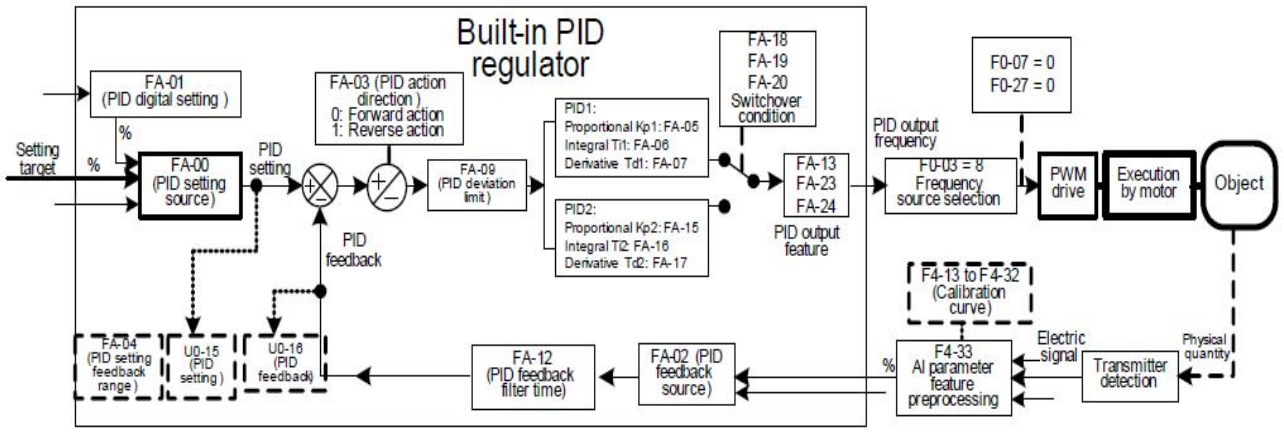

Figure 8. The PID controller setting into frequency converter [7].

4.1. Results analysis

After set of PID regulator was obtained the following values of coefficients: in the first was concluded that the best stability and high dynamic parameters can ensure the PI regulator with following coefficients kp=4 and ki=6. These coefficients have been obtained using results of modelling and Ziegler–Nichols tuning method. After setting of reaction loop has managed to reach of working speed up to 1200m/min, while it is processed the wire with diameter 1,3mm (at the entrance is wire with diameter 3mm). Initial spool weight is 110kg and final weight 550 kg with final diameter 600mm.

5. CONCLUSIONS

Based on the theoretical and practical methods was set the loop of the automatic control system of tension force from wire.

Based on the studies was identified the optimal method of control for winding mechanism driving with the asynchron motor and frequency converter.

The proposed control method of winding mechanism demonstrated high efficiency for wire driving machine and stability in wide range of operation speeds, high stability at acceleration, deceleration and emergency stop of the machine without mechanical shocks that can lead to break the processed wire.

The developed control system proves: the adequate behaving of the wiredrawing machine for different variations of the target signals and for different perturbations; the optimization of the dynamic and static processes vs. the quickness and exclusion of oscillations and overregulation of the controlled winding tension force. The practical research on this topic was made in Tehelectro-SV company, which is a factory of electrical wires and power cables.

Bibliography

1. Kalpakjian S., Schmid S. *Manufacturing engineering & technology. Prentice-Hall, 2006.*

2. Wright R.N. *Wire technology: process engineering and metallurgy. Elsevier, 2010.*

3. *Solutions for your wire drawing machine. www.automation.siemens.com/.../wire-drawing-machines.aspx*

4. *Wire Drawing Machines and Accessories http://morgan-koch.com/*

5. *Drawing technology. http://www.sampsistemi.com/drawing-technology/13146.html*

6. Abhro Mukherjee*. Industrial control of dancer-Less take up system for modern wire drawing machines with smart controllers. Regular paper J. Automation& Systems Engineering*

7. *User manual INOVANCE MD380 http://www.inovance.cn/UFile/201305151058003925.pdf*

8. Cazac V., Nuca I., Todos P., Nuca Iu. *Control system of the wiredrawing machine with annealing module. International Conference on Electromechanical and Power Systems, Chisinau, 13-15 Otober, 2011.*

9. Ivanov S. *Reglarea vectorială a sistemelor de acţionare electrică. Tipografia Universităţii din Craiova, 2000.*

10. Radionov A. A*. Avtomatizirovannyj electroprivod sovmeshhennogo prokatno-volokil'nogo provolochnogo stana. PHD abstract, Magnitogorsk, 2009.*

11. Krasil'nikov L. A*. Volochilshhik provolki. Izdanie, Moskva, Metalurgia, 1987, 320 page.*

Recommended for publication:16.03.2016.

IMPEDANCE METER WITH SIMULATED RESONANCE

Pavel Nicolaev, PhD student
Technical University of Moldova

INTRODUCTION

By using the method of simulated resonance for impedance measurement [1], it is possible developing of impedance meters with high metrological and operating characteristics and low cost [2, 3]. Among the technical characteristics available to these meters are listed: high measurement accuracy, simple structure and measurement algorithm, automated measurement process, ability to connect to PC, low weight and sizes [3].

Impedance-meter with simulated resonance is composed of three modules: signal source, measurement module and command module.

Signal source (SS) is an external energy source that provides power measurement circuit. This is a sinusoidal signal generator that comply the conditions:

- The known and stable value for frequency of generated signal;
- The possibility of automatic adjustment of signal level according to the measured impedance value.

In order to assure the high stability of the frequency of signal as a signal source is used a microcontroller-based digital generator with stabilization quartz.

Measurement module (MM) is the block of impedance-meter that performs the measurement of impedance components by means of the simulated resonance method. MM is based on a resonance measuring circuits (RMC), and the measurement process consists in its partial or full balancing. The balancing is according to the algorithm described in [4]. MM forms the signal of imbalance and the signal of reference for command module and the signal of level of amplitude for SS.

Command module (CM) provides automation of measurement through the following functions: fixing the amount of frequency of SS signal; automatic balancing of the RMC; storage, processing and display of results and assuring connection to PC. To assure balancing of the RMC, CM compares the phases of the reference signal and the imbalance signal from MM and depending on the amount of phase shift, it provides adjustment of impedance components reproduced by a metrological impedance simulator (MIS).

1. SIGNAL SOURCE OF THE IMPEDANCE METER

Signal source provides power for MM for the conversion of the measured impedance in active electrical size. According to the analysis [5] to comply with conditions of functional stability of the MIS and to achieve an effective balancing process, it is necessary to power the circuit to a stable source of current with internal impedance of active character. In practice, this can be achieved by using a stable source of voltage that has connected a high value resistor R_G at the output.

To assure the frequency and amplitude conditions, it is necessary to is use a digital generator with automatic adjustment of the amplitude. The block diagram of such a SS is shown in fig. 1.

The microcontroller μC assures forming of signal with pulse-width modulation (PWM) according to the sinusoidal signal law. The high stability of frequency the PWM signal is assured by the quartz element. By means of the "*Setting frequency*" bus is insured a multiplication coefficient corresponding to the clock frequency, and consequently it changes the frequency of the PWM signal. By means of the control unit, it insures the setting of frequency the measurement signal at one of wanted values.

Low-pass filters are set to the frequencies listed above respectively and they insure forming of the sinusoidal signal from PWM signal.

To assure an appropriate level of the measurement signal, SS has a block for automatic adjustment of the amplitude (AAA) which depending on the level of the signal from MM adjusts transfer coefficient of a programmable amplifier PA.

2. MEASUREMENT MODULE OF THE IMPEDANCE METER

The measurement module is the main block that insures the measurement of the unknown impedance and metrological characteristics of the device depends on its parameters. Due the simulated resonance, method of the impedance measurement is possible to develop a measurement module with

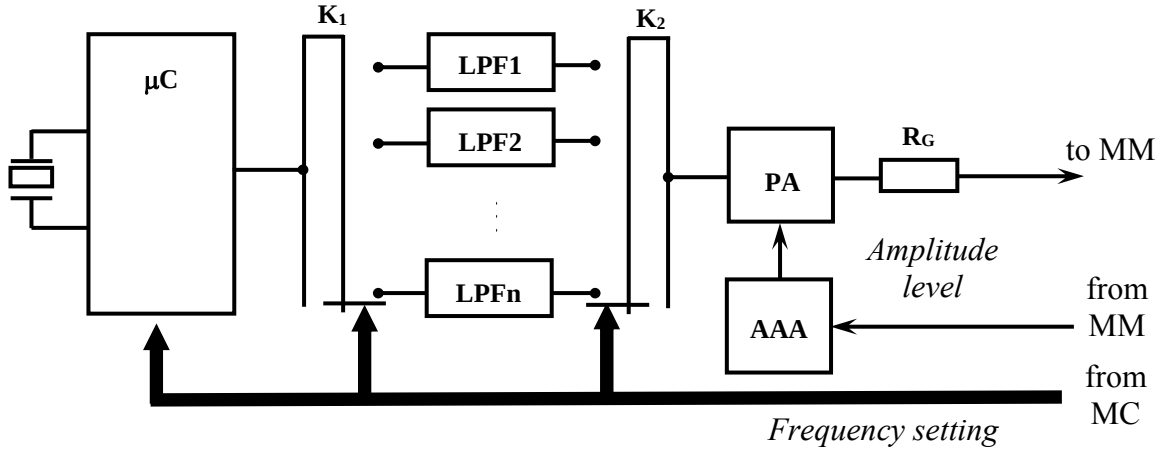

Figure 1. Block diagram of the signal source.

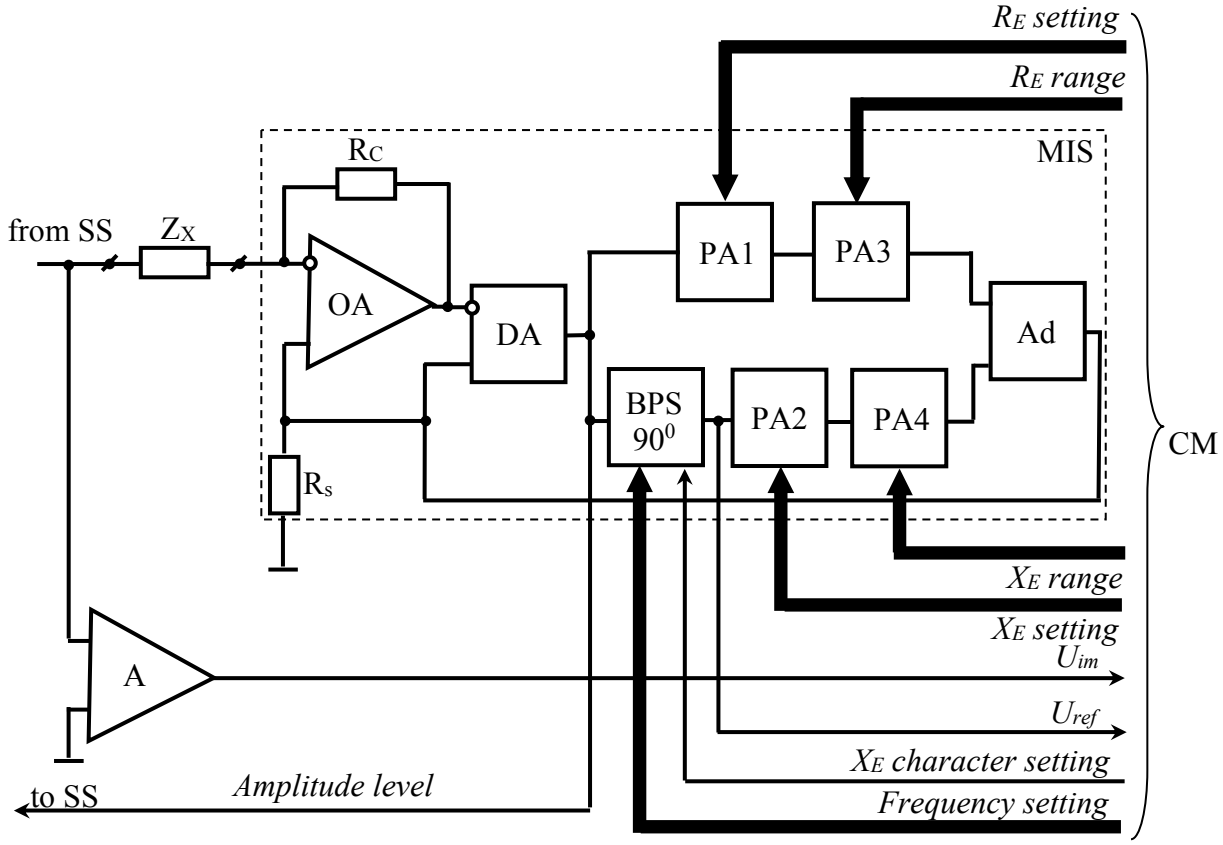

Figure 2. Block diagram of the measurement module.

higher characteristics than to other devices [6]. The block diagram of this module is shown in fig. 2.MM is based on a series-type RMC with a metrological impedance simulator (MIS) in its construction [7]. MIS insures reproduction of the reference impedance with adjustable value and character [8]. All MIS components are implemented on the basis of operational amplifiers (OA) [9]. For digital adjusting of the value and of the character for reference impedance, in MIS structure can be used the digital potentiometers or the digital programmable amplifiers (PA1, PA2) with the smooth and linear adjustment of the amplification coefficient [10].

According to MIS structure (fig. 2) the operational amplifier OA and the resistance R form a voltage-current converter. The resistance value R is selected according the condition of stability [5]. The differential amplifier DA has a unitary transfer coefficient and it assures summing the signal

applied to the non-inverting input with the signal applied to the inverting input [11].

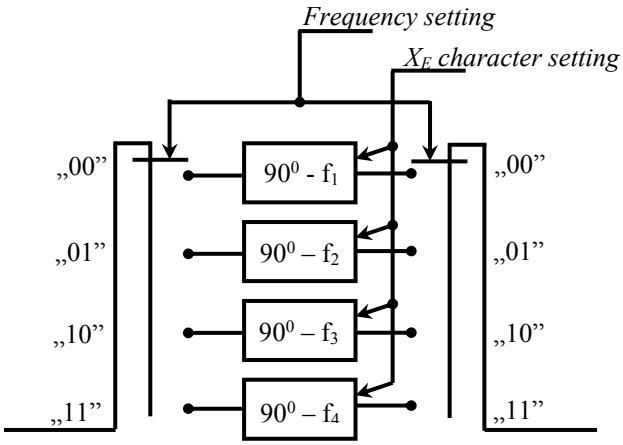

Figure 3. The structure of the block of phase shifters at 90^0

The formation of the reactive components in the circuit is performed by means of the block of phase shifters at 90^0 (BPS90^0) (fig. 3). This block consists from four phase shifters each of them is based on an operational amplifier (fig. 4) and assures a phase shift according to the relation:

$$\Delta\varphi = -2arctg\ 2\omega R_3 C_4 \qquad (1)$$

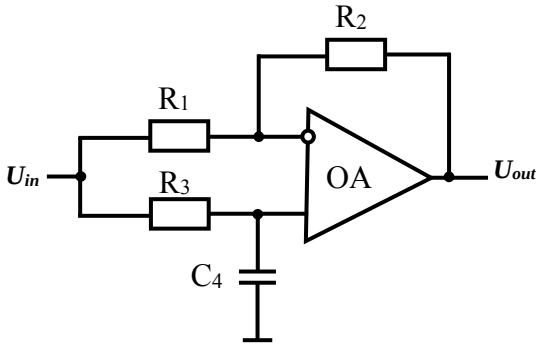

Figure 4. The circuit of the phase shifter based on OA

According to relation (1), if is selected the corresponding values for the elements of R_3 and C_1, the phase shift introduced by the circuit in fig. 4 will be 90^0 [12].

Whereas, that phase shift will be dependent of frequency, it takes 4 such phase shifters each of which is tuned to one of the frequencies of the SS signal according to the “Frequency setting " digital code from CM. To assure inductive character for reference impedance Z, the phase shift introduced by the phase shifter must be 90^0, but to assure capacitive character - 90^0. This is assured by switches K_1 and K_2 (fig. 5) through the digital code “ *X_E character setting*” from CM.

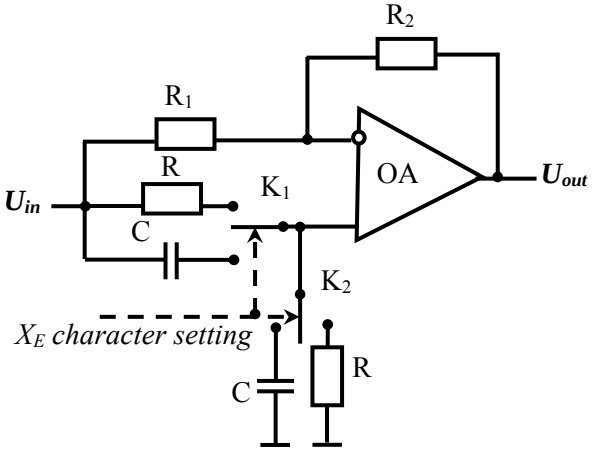

Figure 5. The circuit of the programmable phase shifter based on OA

The programmable amplifiers PA1 and PA2 in fig. 2, assure smooth adjustment to reference impedance components. To assure any character for active component of the reference impedance $\boldsymbol{Z_E}$, PA1 must assure an amplification factor in range of the values -1 ÷ +1. PA2 will assures an amplification factor in range of the values 0 ÷ +1 [13]. In addition, to could be conducted by CM, the adjustment of the amplification coefficient must be made via a digital code. The length of the digital code of adjustment for the reproduced impedance components determines the error of fixing the moment of resonance in RMC This error will be determined according to the relation:

$$\delta_{regl} = 2^{-N} \qquad (2)$$

where: N – the number of bits in the composition of the digital code.

The programmable amplifiers PA3 and PA4 (fig. 2) assure the adjustment of the range of values for the components of reference impedance, by assuring a stepped amplification coefficient. They can be realized based of OA for that amplification coefficient depends only on the values of the resistances in the feedback loop and does not depend on the OA parameters. In fig. 6 shows the structure of an PA with stepped adjustable coefficient based OA with inverting connection.

The adder Ad (fig. 2) assure the summation of the voltages from two branches of adjustment of components of the reference impedance. It is based on an AO and can be realized as an adder of the

direct voltages, as an adder of the inverted voltages or as a differential amplifier [9].

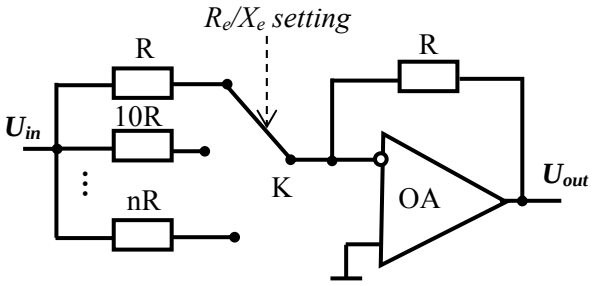

Figure 6. The circuit of the PA with stepped adjustable coefficient based OA.

To achieve the balancing process in measuring circuit, it is analyzed the evolution of the phase shift between the imbalance signal $\boldsymbol{U_{im}}$ and the reference signal $\boldsymbol{U_{ref}}$. The reference signal is formed by the IMS and it represents the voltage at the output of DPS90^0. The imbalance signal is obtained from MM input and to assure increased sensitivity, this signal is amplified by an amplifier A (fig. 2). CM realizes the process of determining the phase shift between these two signals and the balancing of the measuring circuit.

3. COMMAND MODULE OF THE IMPEDANCE METER

The command module is used to assure an automatic measurement process. This module assures the control of the functionality for entire device through the following functions:

- Assuring the user interface
- Fixing the frequency of signal from SS
- Balancing after the active component of RMC from MM;
- Balancing after the reactive component of RMC from MM;
- Processing results after balancing
- Transmission of results to the device interface.

The block diagram of the CM is shown in fig. 7. The basic element of the CM, which is the "brain" of the impedance meter, is the control unit (CU) based on the microcontroller. CM contains two comparators C_1 and C_1, to convert sinusoidal signals into a series of rectangular pulses, a dynamic D-type flop (DDF) which forms the signal *CE* for fixing the moment of resonance at balancing and a microcontroller USB (μC USB) that assures the interface between the CU and PC.

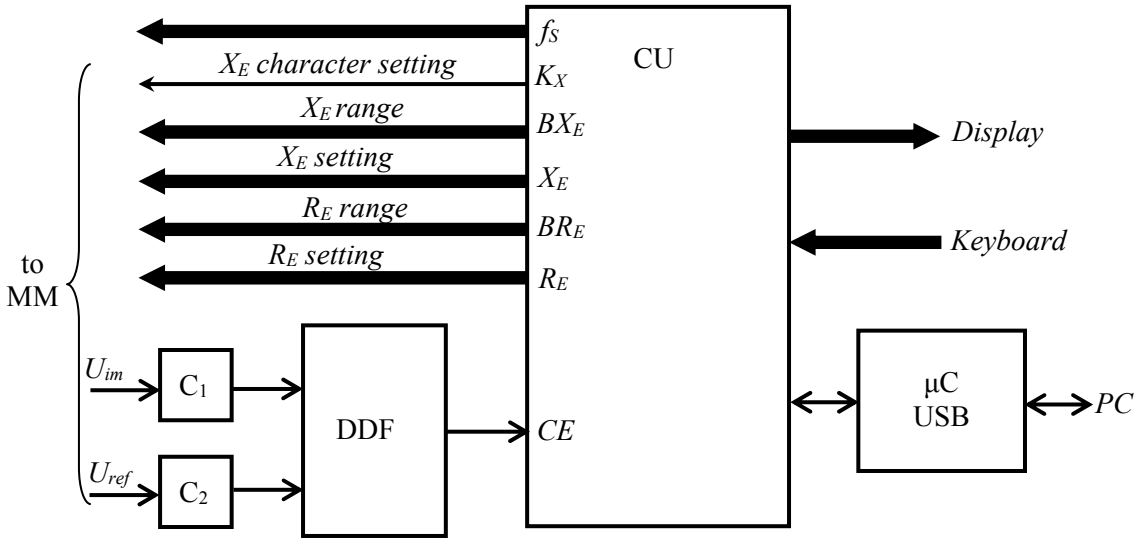

Figure 7. The block diagram of the command module.

According to the analysis [11], the balance process for RMC is achieved by varying the values of the components for the reference impedance and the tracking of the evolution of the phase shift between the imbalance signal and the reference signal. This is accomplished by using the DDF. The time diagrams for the input and output signals of the DDF is shown in fig. 8.

According to [12] the timing of balancing for RMC coincides with the appearance of a 0^0 (fig. 8 a) or 180^0 (fig. 8 b) phase shift between $\boldsymbol{U_{ref}}$ and $\boldsymbol{U_{im}}$. In the moment of these values of the phase shift, DDF changes its state, and the *CE* signal at its output is used as a signal for fixing the moment of the resonance in the balancing process.

CU assures the formation of the command signals for other modules and the automatic data processing. Once with the power connection, CU determines the type of the operator interface. Initially, it checks the connection to the PC via USB

port. If the impedance meter is not connected to the PC, CU will activate the ports at that are connected the display and the keyboard. After determining the user interface, CU asks the setting for the amount of the measurement signal frequency. This value of the frequency is encoded and transmitted to the corresponding blocks from SS and MM. At the same time, this frequency value is memorized and then it is used by CU for processing results.

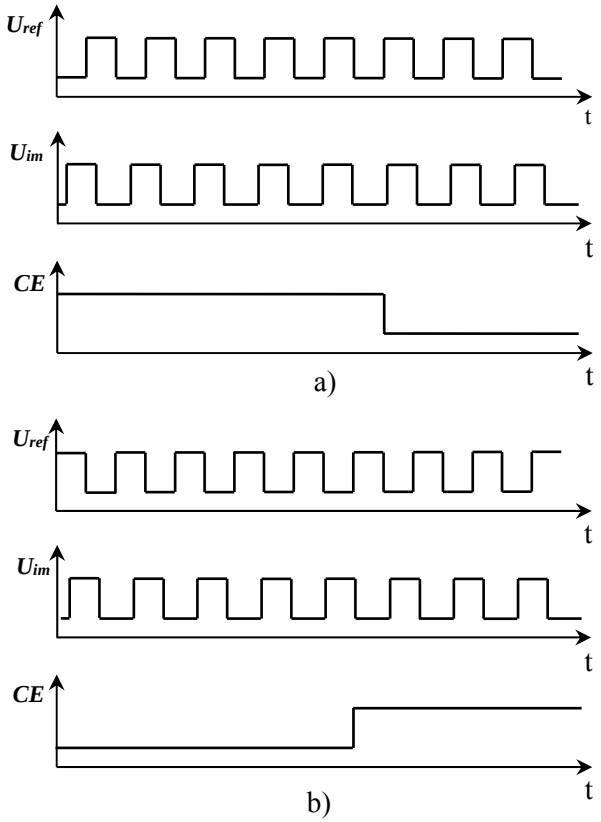

Figure 8. *T*he time diagrams for the signals of the DDF: *a) Fixing of the 0^0 phase shift between* $\mathbf{U_{ref}}$ *and* $\mathbf{U_{im}}$*; b) Fixing of the 180^0 phase shift between* $\mathbf{U_{ref}}$ *and* $\mathbf{U_{im}}$.

After setting the value of the measurement signal frequency, CU begins the process of balancing for RMC. According to [13] the balancing process realizes in two stages: the balancing of the active component and the balancing of the reactive component. As these two stages are independent of each other, they may be made as two separate processes.

In order to assure the balancing process of the active component, CU varies the value of the active component of the reproduced impedance through the channels „ *R_E setting*" and „*R_E range*" until the value of the *CE* signal changes. The algorithm for balancing of the active component is shown in fig. 9.

Initially, CU fixes the value zero for R_E and BR_E codes. Then CU reads the value of the *CE* signal and memorizes this value. Forwards, CU increments the value of the R_E code, reads again the value of *CE* signal and compares it with the memorized value. If the *CE* value is modified, CU will assure the balancing of the circuit and the respective values of R_E and BR_E codes will determine the value of active component of the reference impedance. If the CE value is not modified, CU will increment the value of the RE code until this value will be modified. If the value of R_E code reaches the maximum value and does not assure the modification of the CE signal, CU will change the value range and will repeat the process. To switch to a higher value of the range, CU assures the incrementing of the BR_E code. If CU exhausts all the values of the range and the balancing of the active component is not assured, CU will display *"The exceeded value of R_E"* on the interface of the impedance meter.

After ensuring the process of balancing of the active component or after displaying on the interface of the message *"The exceeded value of R_E"*, CU initiates the process of balancing of the reactive component (fig. 10). To do this, CU varies the value of the reactive component for the reference impedance through the channels „ *X_E setting"*, „ *X_E range*" and *„X_E character setting"*. As opposed to balancing process of the active component, for balancing of the reactive component is necessary and the setting of the character of the reference reactance. This is ensured by the CU through the K_X signal transmitted via the *„X_E character setting"* bus. Initially, CU checks the balancing of the reactive component, setting the inductive character of the reference reactance. ($K_X=0$). In this case the balancing process is similar to that shown in fig. 11, with the difference that the CU increments the value of the X_E and BX_E codes. If the balancing process of the reactive component is not ensured, CU will set the capacitive character of the reference reactance ($K_X=1$) and will repeat the same procedure as for the inductive character.

If CU does not ensure the balancing process after setting the capacitive character of the reference impedance, CU will display *"The exceeded value of X_E"* on the interface of the impedance meter [12].

If CU ensures the complete balancing of the RMC, it will initiate the procedure for processing the results and displaying them. If the operator interface is accomplished via PC, the procedure for processing the results can be made by computer using a special application. In this case, CU sends

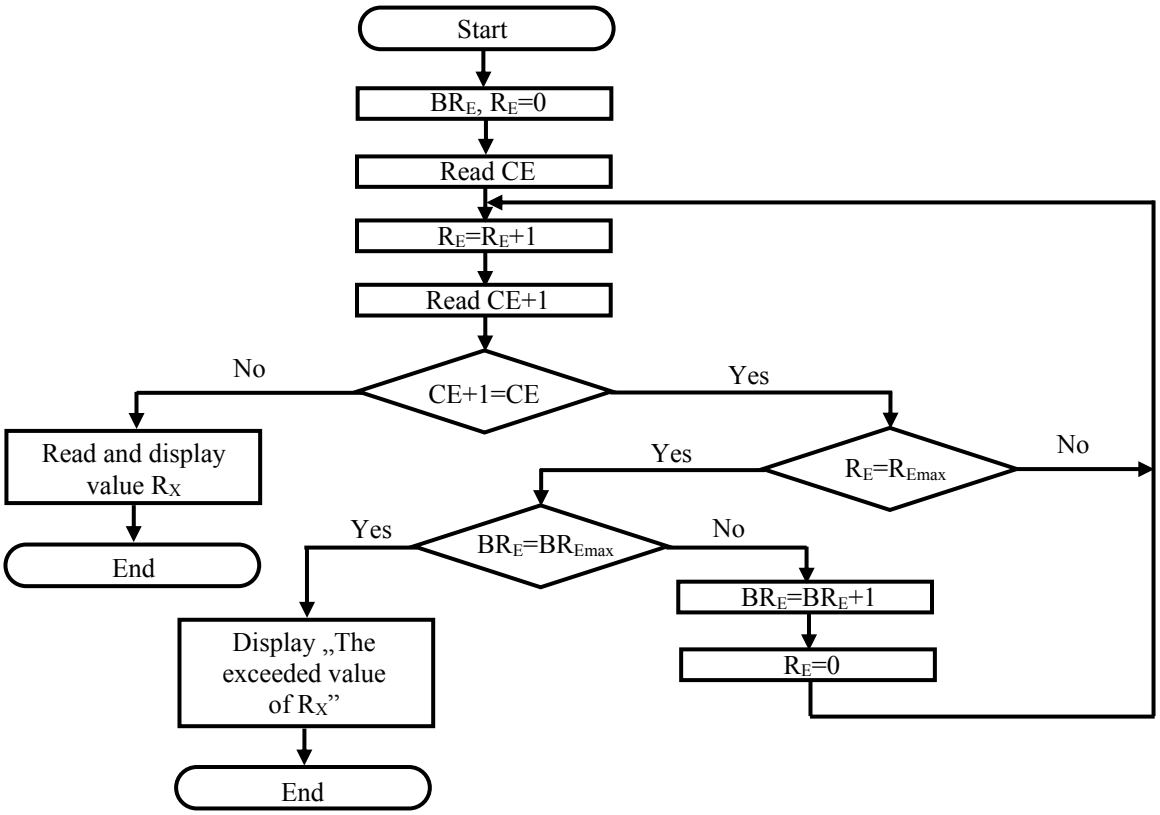

Figura 9. The measurement algorithm for the active component.

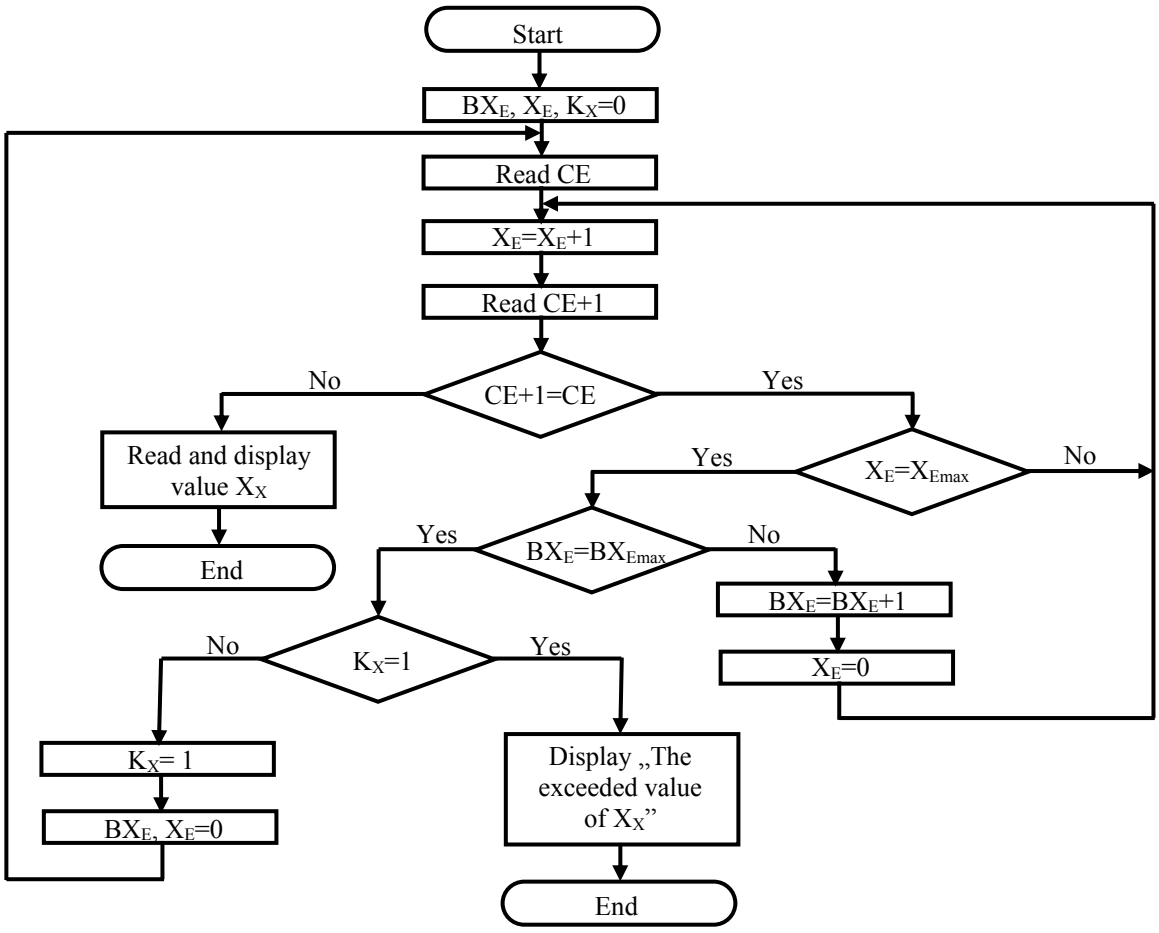

Figura 10. The measurement algorithm for the reactive component.

to the PC the values of the codes: R_E, BR_E, X_E, BX_E, K_X and f_S. If the results are indicated on the display of the impedance meter, then CU will ensure and the processing of the results [14].

CONCLUSIONS

The impedance measurement using the simulated resonance method ensures a high precision, simplicity of the measurement process and its automation. The high precision is determined by the precision of the metrological impedance simulator.

The use of impedance simulator with independent components adjustment ensures a simple measurement algorithm for impedances of any nature. The balancing of the measurement circuit is completely automatic, is realized in two stages: the balancing of the active component and the balancing of the reactive component. The impedance meter permits to measure the components of the impedance in Cartesian coordinates for four frequencies of the signal. The results can be indicated on the display of the impedance meter or on the PC.

Bibliography

1. **Nastas V., Nicolaev P.** *Măsurarea impedanţei în coordonate carteziene prin metoda rezonanţei simulate// Conference ICMCS, Chişinău, pag.65…68, 2009.*
2. **Nastas V., Nicolaev P**. *Methods and devices with simulated resonance for impedance measurement// Catalog of the European exhibition of creativity and innovation EUROINVENT 2013, Iaşi, Editura Universităţii Al. Ioan Cuza, 2013, pag 71.*
3. **Nastas V., Nicolaev P.,** *Impedancemeter with simulated resonance// The 6th International Conference on Electrical and Power Engineering, Vol. II, Iaşi, 2010, pag 297-300;*
4. **Nastas V.** *Application of the impedance simulators as measure of impedance. Annals of the University of Craiova, Electrical Engineering series, Nr. 33, Craiova, pag.159…163, 2009.*
5. **Nastas, V.** *Synthesis of Cartesian coordinates metrological impedance simulators// Moldavian Journal of the Physical Sciences, 2008, vol. 7, nr 4, pag. 481-490.*
6. **Nicolaev P.** *Optimizarea simulatorului de impedanţă în coordonate Carteziene// Conferinţa Tehnico-Ştiinţifică a colaboratorilor, doctoranzilor şi studenţilor UTM, 2009, vol I, pag. 109-110*
7. **Nicolaev P.** *Modelarea topologică a simulatoarelor de impedanţă în coordonate carteziene// International Conference Telecommunications, Electronics and Informatics 2010, vol. II, pag. 264-267*
8. **Nastas V.** *Metrological simulators of electrical passive quantities with algorithmic structure, Mold. J. Phys. Sci. Vol 9, Nr. 1, Chişinău, pag.85…102, 2010.*
9. **Dostal J.** *Operational amplifiers. ELSEVIER SPC, New York, 423 pag.,1981.*
10. **Nastas V., Nastas A.** *Convertor de impedanţă// Brevet de invenţie nr. 3154MD. BOPI nr. 9, 2006*
11. **Nastas V., Nicolaev P.** *Convertor de impedanţă// Brevet de invenţie nr. 248MD. BOPI nr. 7, 2010.*
12. **Nicolaev P.** *Defazor de 90^0 independent de frecvenţă.// Conferinţa Tehnico-Ştiinţifică a colaboratorilor, doctoranzilor şi studenţilor UTM, 2009, vol I, p. 111-112*
13. **Nicolaev P.** *Modelarea simulatorului de impedanţe flotante în programul Multisim. În: culegere de lucrări ştiinţifice la Conferinţa Tehnico-Ştiinţifică a colaboratorilor, doctoranzilor şi studenţilor UTM, 2008, vol I, p. 51-52*
14. **Nastas, V.** *Simulated resonance and its application for high - accuracy impedance measurement// Conference ICMCS, vol 2, Chişinău, pag. 312…315, 2002.*
15. **Nicolaev P**. *Măsurătoare de impedanţă cu rezonanţă simulată în coordopnate carteziene// Teza de doctor, Chişinău, 137 pag., 2016*
16. **Nastas, V.** *Precision measurement of the impedance components by method of simulated resonance// Conference SPIE, vol 5822, Bellingham, pag.181…191, 2004.*
17. **Nastas V., Nicolaev P.** *Eroarea sistematică a simulatorului metrologic de impedanţă. În: Meridian Ingineresc, 2013, nr 3, p. 37-42.*

Recommended for publication: 21.01.2016.

SYNTHESIS OF THE CONTROL ALGORITHM WITH THERMAL PROCESS IN THE OVEN

Irina Cojuhari, assoc. prof., PhD, Bartolomeu Izvoreanu, assoc. prof., PhD,
Ion Fiodorov, assoc. Prof., PHD, Dumitru Moraru, PhD student
Technical University of Moldova

INTRODUCTION

In the diverse technological processes can be necessary of control the thermal regime. The thermal processes represent the slow time - varying processes which can be characterized by the big inertia. In the most technical installations of thermal control are used the PID controllers, which are characterized by the good performance and robustness ensured in the automated system. By the its three components (proportional P, integrative I and derivative D), the typical controllers realize the basic functions as: adjusting the output value of the process in concordance with the tuning parameter of the P component, removing the errors in the stationary regime by the I component, predicting the future behavior of the process by the D component [6, 7].

The tuning of the controller in the control thermal systems is a difficult procedure. In the specialized literature are presented a lot of tuning methods the typical controllers: the empirical methods which are based on the classical methods of tuning the controller parameters developed by the Ziegler-Nichols and others, the graph-analytical methods and tuning methods which are based on the optimization techniques [2, 3, 8, 9].

The big number of these methods to be used require the known mathematical model of the industrial process. Knowing the mathematical model of the process requires using the identification procedures. Identification aims to obtain the mathematical model that would describe the static and dynamic characteristics of the industrial process.

In this paper is used the analytical and experimental methods of tuning the typical PID controller in the control thermal system, where control of the temperature is realized by the industrial controller TRM-151, OWEN firm [5, 7]. It was obtained the experimental curve of the oven and using the identification procedure was calculated the mathematical model of the oven. It is proposed to tune the PID controller by the maximum stability degree method with iteration and Ziegler-Nichols method. The obtained results are experimental verified by the installation and in the software package MATLAB.

1. DESCRIPTION OF THE DESIGNED SYSTEM

The principle scheme of the thermal control system is presented in the figure 1. The elements of the systems are: 1- the oven with heating element, 2 - the industrial controller TRM - 151, OWEN firm, 3 - the thermocouple temperature transducer TXK(L), 4 - interface AC3-M, 5 - PC. The oven is supplied with electrical energy from network of the alternative current 220 V. The oven was designed based on the following technical data: the oven volume V=500 cm^3, electrical power P=300 W, the maximal working temperature is T=400 °C.

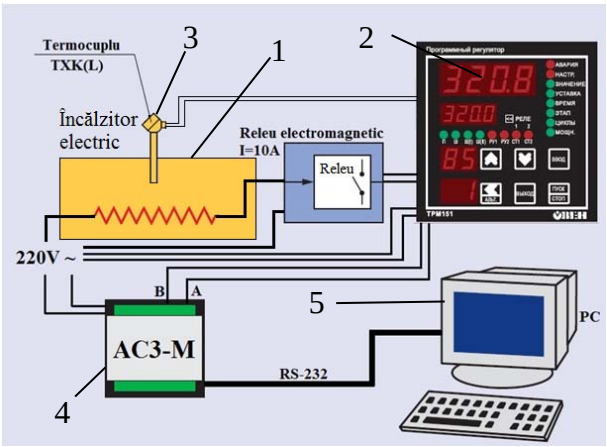

Figure 1. Principle scheme of the control system.

In the figure 2 is presented the structural block scheme of the control system, where $H_R(s)$ represents the transfer function of the controller, and $H_{PF}(s)$ - the transfer function of the control object (fixed part).

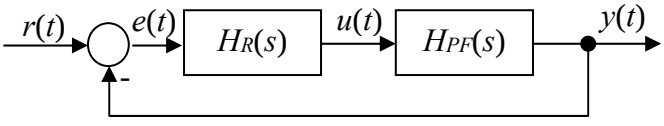

Figure 2. Block scheme of the control system.

2. IDENTIFICATION OF THE CONTROL OBJECT

To obtain the mathematical model of the oven was obtained the experimental curve of the temperature variation in the electrical oven, where the reference temperature was settled at the 207^0C. The experimental curve was registered by the TRM-151 and it is presented in the figure 3.

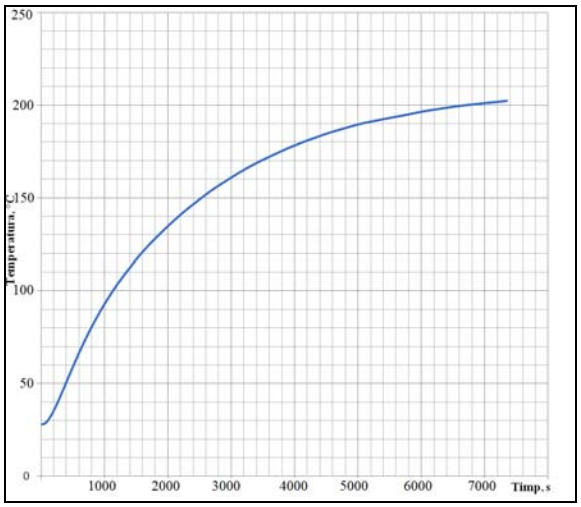

Figure 3. The experimental curve.

To estimate the model parameters of the control object was used the module Process Models from System Identification Toolbox from MATLAB and its interface is presented in the figure 4 and for identification was chosen the model object with inertia second order and time delay. In the figure 5 is presented the comparison between experimental curve - 1 with identified curve - 2.

Based on the identification procedure it was obtained the mathematical model described by the following transfer function:

$$H(s)=\frac{ke^{-\tau s}}{(T_1s+1)(T_2s+1)}=\frac{ke^{-\tau s}}{a_0s^2+a_1s+a_2}= \quad (1)$$

$$=\frac{207.06e^{-1.15s}}{(2125.9s+1)(34.034s+1)}=\frac{207.06e^{-1.15s}}{72352.88s^2+2159.93s+1}.$$

In the transfer function (1) are used the following notations: k transfer coefficient, T_1, T_2 - time constants, τ– time delay, $a_0=T_1T_2$, $a_1=T_1+T_2$, $a_2=1$.

In this paper is proposed to synthesize the standard control algorithm PID to the identified model object which is described by the following transfer function:

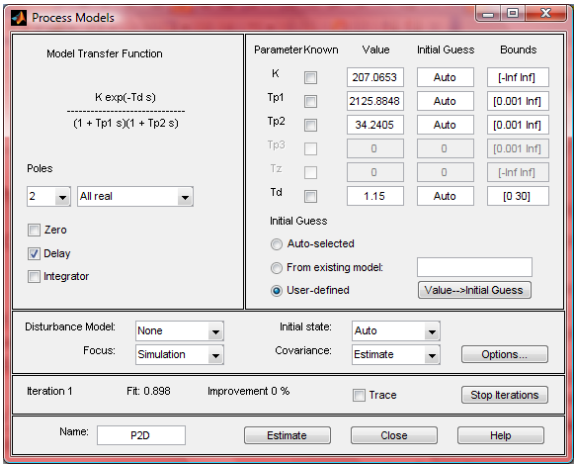

Figure 4. Identification interface by the package Process Models.

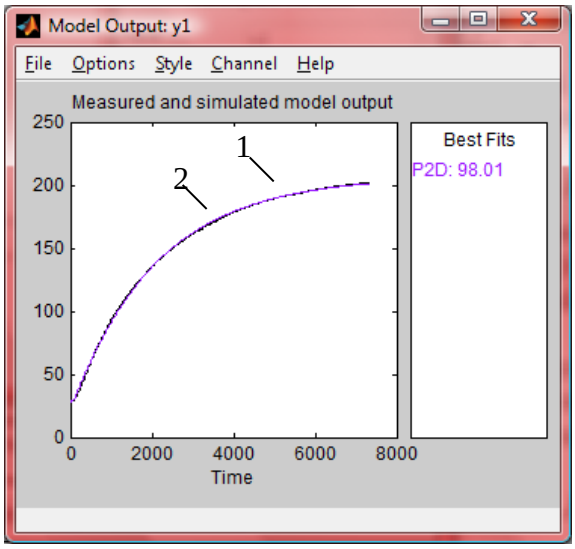

Figure 5. Comparison of the experimental curve with identified curve.

$$H_{PID}(s)=k_p+\frac{k_i}{s}+k_ds\,, \quad (2)$$

where k_p, k_i, k_d – represent the tuning parameters of the respectively controller.

3. METHODS OF TUNING THE PID CONTROLLER

3.1. The maximum stability degree method with iteration

The main problem in this method consists in ensuring for the respectively control laws the maximum stability degree of the designed control system. For the system structure which consists of fixed part with transfer function (1) and controller

with transfer function (2) was obtained the characteristic equation of the closed loop system and based on the procedure of the maximum stability degree method was obtained the system from four algebraic equations [10-12]:

$$c_0 J^3 - c_1 J^2 + c_2 J - c_3 = 0, \quad (3)$$

where $c_0 = \tau^3 a_0; c_1 = a_1\tau^3 + 9\tau^2 a_0,$

$$c_2 = a_2\tau^3 + 6\tau^2 a_1 + 18\tau a_0,$$

$$c_3 = 3a_2\tau^2 + 6\tau a_1 + 6a_0;$$

$$k_p = (1/k)\exp(-\tau J)(a_0\tau^2 J^4 - J^3(\tau^2 a_1 + 5\tau a_0) + \\ + J^2(\tau^2 + 3\tau a_1 + 3a_0) - \tau J - 1) = f_p(J); \quad (4)$$

$$k_i = (1/(2k))\exp(-\tau J)J^3(a_0\tau^2 J^2 - J(\tau^2 a_1 + 4\tau a_0) + \\ + \tau^2 + 2\tau a_1 + 2a_0) = f_i(J); \quad (5)$$

$$k_d = (1/(2k))\exp(-\tau J)(a_0\tau^2 J^3 - J^2(\tau^2 a_1 + 6\tau a_0) + \\ + J(\tau^2 + 4\tau a_1 + 6a_0) - 2\tau - 2a_1) = f_d(J). \quad (6)$$

In the maximum stability degree method [1] the tuning procedure of parameters the PID controller consists in determination the optimal stability degree from equation (3), but the tuning parameters of the controller are calculated from (4)-(5) equations. From application, the maximum stability degree method in case of tuning the PID controller was observed that this method doesn't ensure the stability of the system, in case when tuning parameters were obtained for the value of the optimal stability degree by the expression (3).

To expend the possibilities of using the maximum stability degree method was proposed to use the maximum stability degree method with iteration and the tuning procedure is describing below [10-12].

From expressions (4)-(6) can be observed that the tuning parameters of the PID controller k_p, k_i and k_d depend of the model object known parameters and of the unknown stability degree J of the control system: $k_p=f_p(J)$, $k_i=f_i(J)$, $k_d=f_d(J)$. From the relations (4)-(6) at the known values of model object parameters and at the variation the stability degree $J \geq 0$ in the respectively limits is effectuated the calculation and constructed the dependencies $k_p=f_p(J)$, $k_i=f_i(J)$, $k_d=f_d(J)$ for determination the tuning parameters of the PID controller. Next are chosen the sets of the parameters values J- k_p, k_i, k_d for the optimal and quasi optimal values of J and for every set is done the computer simulation of the control system with PID controller with chosen sets of tuning parameters. In final is chosen the transient process that satisfied the imposed performance.

3.2. The Ziegler-Nichols method based on the step response

The Ziegler-Nichols method based on the step response permits to tune the typical P, PI and PID algorithms by the following way: based on the step response (figure 6) of the open loop system when as input is applied the step signal, it is determinate the model object parameters k_f, L, T_f, a. The parameters L and T_f are calculated based on the experimental curve in the following way:

$$L = t_1;$$
$$T_f = t_2 - t_1; \quad (8)$$
$$a = k_f \frac{L}{T_f}.$$

Based on these parameters are done the calculations of tuning parameters for P, PI and PID algorithms by the following relations:

- For the control system with P controller – $k_p=1/a$.
- For the control system with PI controller – $k_p=0.9/a$, $T_i=3L$.
- For the control system with PID controller – $k_p=1{,}2/a$, $T_i=2L$, $k_d=L/2$.

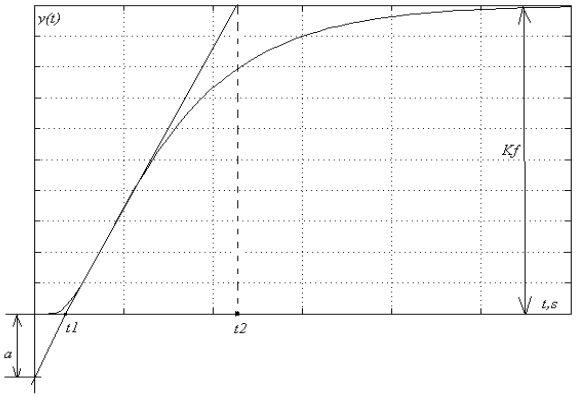

Figure 6. The response of he open loop system at the step signal.

4. COMPUTER SIMULATION

For analyzing the efficiency of tuning methods of the PID algorithm to the identified model object presented by the (1) transfer function, were done the respectively calculations of the tuning parameters based on the (4)-(6) expressions and were constructed the dependencies $k_p=f(J)$, $k_i=f(J)$, $k_d=f(J)$, which are presented in the figure 7. Based on the curves presented in the figure 7 were chosen the values sets J - k_p, k_i, k_d of the tuning parameters of the PID controller and these values are presented in the Table 1.

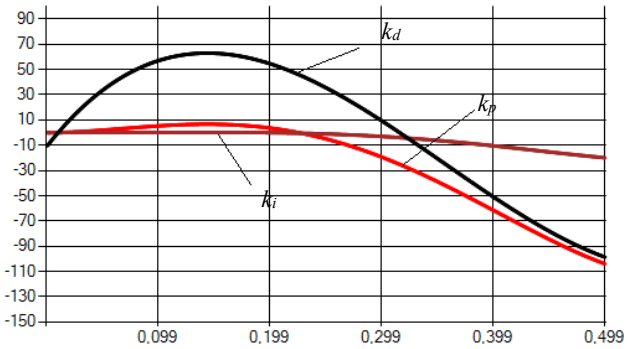

Figure 7. Dependencies $k_p = f_p(J)$, $k_i = f_i(J)$, $k_d = f_d(J)$ for the PID controller.

Next, it was done the calculation of the tuning parameters by the Ziegler-Nichols method based on the step response by the experimental curve (figure 8), using the expressions (8) were obtained the tuning parameters: $L = 189$; $T_f = 2211$; $k_f = 1.56$; $a = 0.13$ and the calculated parameters are presented in the Table 1.

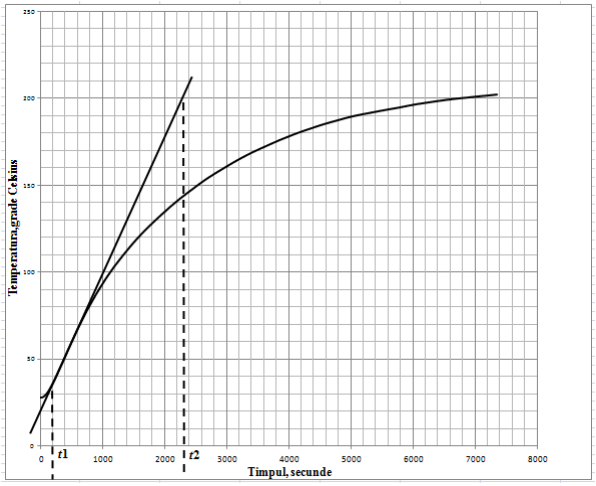

Figure 8. The calculation of the tuning parameters based on the experimental curve.

For verification the obtained results in case of tuning the PID controller to the model object (1) was done the computer simulation of the control system in the software package MATLAB and the simulation scheme is presented in the figure 9.

Transient processes of the control system are presented in the figure 10, where the numeration of the curves corresponds with iteration numeration from Tables 1, 2. In the Table 2 is presented the performance of the control system for the case of tuning the PID controller by the maximum stability degree method with iterations and Ziegler-Nichols method based on the step response.

Table 1. Tuning parameters of the PID controller.

Metoda acordare	**Nr. iter**	***J***	k_p	k_i	k_d
Metoda G.M.S.	1	0,02	0,39	0,002	10,038
	2	0,03	0,83	0,008	18,87
	3	0,19	4,12	0,004	55,76
Metoda Ziegler-Nichols			9.23	0.002	94.5

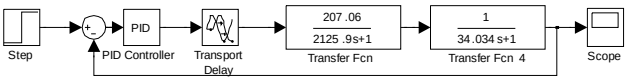

Figure 9. The simulation diagram of the control system.

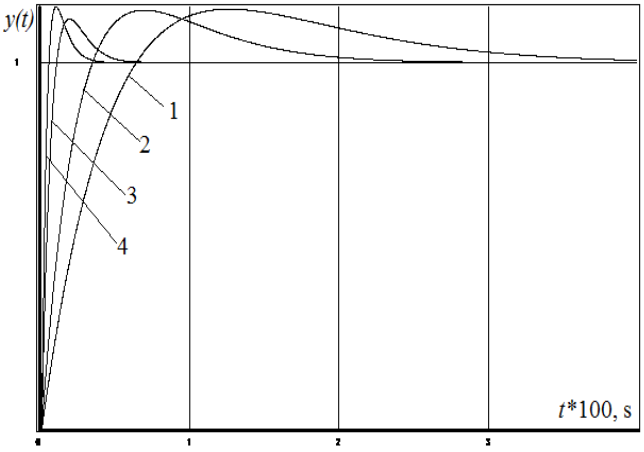

Figure 10. Transient processes of the control system.

From analyzing the transient processes from the figure 10, it can be observed that the best performance was obtained for the case of tuning the PID controller by the maximum stability degree method with iterations (curve 3).

Table 2. The performance of the control system.

Performance	**Nr. curve**	ε, %	t_c, s	σ, %	t_r, s	λ
Maxim. stabilit. degree method	1	5	57.5	14.5	249	1
	2	5	31.7	14.3	144.5	1
	3	5	10.1	11.8	33.6	1
Ziegler-Nichols	4	5	5.6	15	21.75	1

For analyzing the stability reserve of the control system with PID controller was obtained the poles distribution in the complex plane, that was

calculated in MATLAB (figure 11), where the numeration of the poles corresponds with numeration of the curves form Table 2.

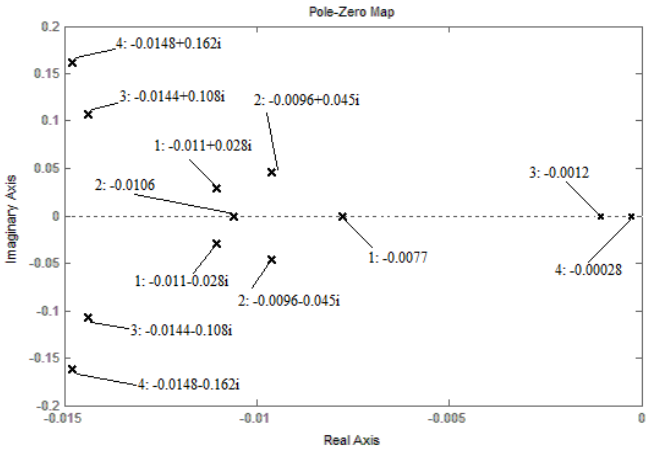

Figure 11. The poles distribution in complex plan of the control system.

Analyzing the poles distribution in the complex plane of the control system from figure 11 can be observed that in the case of tuning the PID controller by the maximum stability degree with iterations the system has the higher reserve stability with 4,2 times than the control system with PID controller tuned by the Ziegler-Nichols method.

From the calculation the values of the tuning parameters of the PID algorithm obtained by the maximum stability degree method with iterations and Ziegler-Nichols method, the parameters were settled in the industrial controller TRM-151 and were obtained the experimental curves of the system, figure 12: curve 1- in the case of tuning the PID controller by the maximum stability degree method with iterations, curve 2 - tuning the PID controller by the Ziegler-Nichols based on the step response. In the Table 3 are presented the performance of the control system for these two cases.

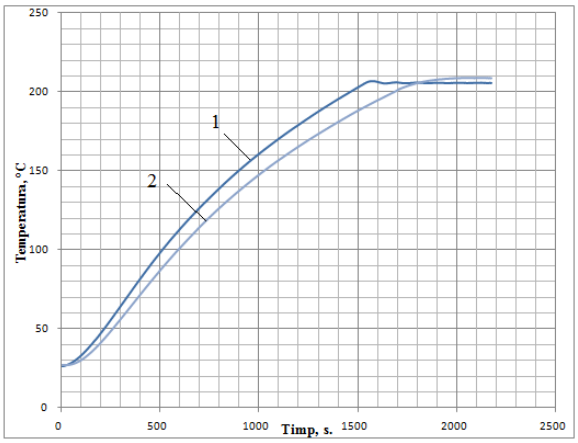

Figure 12. The transient experimental processes of the control system with PID.

Table 3. Performance of the control system.

Perform. of control system	**Nr. curve**	ε, %	t_c, s	σ, %	t_r, s	λ
Maxim. stabilit. degree method	1	5	1407	0	1407	0
Ziegler-Nichols	2	5	1625	0	1625	0

Analyzing the performance of the transient processes of the control system presented in the Table 3 can be observed that in the case of tuning the controller by the maximum stability degree method with iteration the settling time is lower with 14% than the control system with PID controller tuned by the Ziegler-Nichols method.

5. CONCLUSIONS

Analyzing the obtained results it can be done the following conclusions:

1. In the paper were compared the analytical and experimental methods of tuning the PID controller. As analytical method was chosen the maximum stability degree method and as the experimental method was chosen the Ziegler-Nichols method based on the step response.
2. There was designed the thermal control system in the electric oven, where the temperature control was realized by the industrial controller TRM-151, OWEN firm.
3. In case of using the analytical tuning method were used the identification procedures from the GUI System Identification Tool and was obtained the transfer function of the oven model with inertia second order and time delay.
4. To the identified model object was tuned the PID controller by the maximum stability degree method with iterations.
5. Based on the experimental transient process of the oven were obtained the tuning parameters of the PID controller by the Ziegler - Nichols method based on the step response.
6. From analyzing the performance of the control system with PID controller tuned by these methods, the best results were obtained for the case of tuning the PID controller by the maximum stability degree method with iterations.
7. The obtained results were verified by the

setting the tuning parameters in the industrial controller TRM-151. After, comparison of experimental results was observed that for the both methods were obtained the a periodical processes, without overshooting with stationary error equal with ±5%, but the transient process of the control system with PID controller tuned by the maximum stability degree method with iterations has the settling time lesser with 1,15 times than the system with PID controller tuned by the Ziegler-Nichols method based on the step response.

Bibliography

1. Zagarii G.I., Shubladze A. M. *Sintez sistem upravleniya na osnove kriteriya maximal'noi stepeni ustojchivosti. Moskva: Energoatomizdat, 98 s., 1988.*

2. Rotach' V. Ya. *Teoriya avtomaticheskogo upravleniya termoenergeticheskimi proczesami. Moskava: Energoatomizdat, 292 s., 1985.*

3. Lukas V. A. *Teoria avtomaticheskogo upravleniya. Moskva: Nedra, 416 s., 1990.*

4. *Diakonov V. P.* *MATLAB 6.5 SP1/ 7.0 Simulink 5/6 v matematike i modelirovanii. Moskva: SOLON-Press, 576 s., 2005.*

5. *OWEN, Katalog produkczii 2010. Oborudovaniya avtomatizaczii. s. 114-121.*

6. Dumitrache I. şi al. *Automatizări electronice. Bucureşti: EDP, 660 p., 1993.*

7. Lazăr C., Vrabie D., Carari S. *Sisteme automate cu regulatoare PID. Bucureşti: MATRIX ROM, 220 p., 2004.*

8. O'Dwyer A. *Handbook of PI and PID controller tuning rules. 2nd Edition. Imperial College Press, 545 p., 2006.*

9. Tan N., Atherton D. P. *Design of stabilizing PI and PID controllers. In: International Journal of Systems Science, Vol. 37. Issue 8, pp. 543-554, 2006.*

10. Izvoreanu B., Fiodorov I. *The Synthesis of Linear Regulators for Aperiodic Objects with Time Delay According to the Maximal Stability Degree Method. In: Preprints of the 4th IFAC Conference of Systems Structure and Control. Bucureşti: Editura Tehnică. V. 1, pp. 449 – 454, 1997.*

11. Izvoreanu B., Fiodorov I., Cojuhari I. *A Tuning Algorithm of Digital Controller to the Object's Models with Inertia and Time Delay. In: Proceedings of the 8-th International Conference on Development and Application Systems DAS-2006, Suceava, România, pp. 61-64, 2006.*

12. Izvoreanu B. *The Iterative Algorithm of Tuning Controllers to the Models Object with Inertia and Time Delay. In: Proceedings of the 3rd International Symposium on Electrical Engineering and Energy Converters ELS-2009. Suceava, România, pp. 189-192, 2009.*

Recommended for publication: 24.03.2016.

PROSPECTS FOR COOPERATION OF THE TECHNICAL UNIVERSITY OF MOLDOVA WITH ROMANIAN SPACE AGENCY IN THE FIELD OF SPACE TECHNOLOGIES

[1]Ion Bostan, academician, [2]Ioan-Marius Piso, Dr. eng., [1]Viorel Bostan, prof.Dr.Sc. [2]Alexandru Badea, Dr.eng., [1]Nicolae Secrieru, assoc.prof. Dr. [2]Gabriel Viorel Manciu, Eng.
[1]Technical University Of Moldova
[2]Romanian Space Agency

1. THE PREMISES OF COOPERATION

The rapid development of space technologies requires new paradigms of cooperation at regional and international scale in the field. The complex evolution of space technologies favours the expansion of research and innovation partnerships within educational and commercial projects attracting youth, accelerating also the dissemination of related technologies in the socio-economic, scientific and social environment.

For Moldovan researchers the research centres from Romania are the most valuable and accessible institutional structures able to develop partnerships for cooperation in the field of space technologies. These aspects of cooperation were discussed during the meeting in Bucharest on 2 April 2015 between PhD, DHC Marius-Ioan Piso - President of the Romanian Space Agency (ROSA) with the Academician Gh. Duca - President of the Academy of Sciences (ASM), Academician I. Bostan - Director of the National Centre of Space Technologies (CNTS), Technical University of Moldova (TUM), Academician I. Tighineanu - First Deputy Chairman of ASM.

The cooperation with the Romanian Space Agency is also of interest to the Republic of Moldova in terms of exchange of experience in the field of satellite technologies, Romania having launched into space its first satellite "Goliat" on 13 February 2012.

2. ROSA – ON THE TOP OF THE NATIONAL SPACE PROGRAMME

The Romanian Space Agency (ROSA) is the national and international coordinator of the activities of Romania in the field of space technologies. It has the statute of a public institution, is financed wholly from own revenues, being subordinated to the National Authority for Scientific Research and Innovation (A.N.C.S.I.) of the Ministry of National Education and Scientific Research [2-4]. The research directions coordinated by ROSA are focused on [4]:

- coordinating national research programs and space applications;
- promoting the development of Romania in the space field;
- representing the Romanian Government in international cooperation programs;
- research oriented on space issues.

As a coordinator of the national research programs and space applications, ROSA develops and coordinates the implementation of the National Space Program. Depending on its objectives, ROSA is authorized to establish research and development centres. As the representative of the Government, the Romanian Space Agency establishes cooperation agreements with international organizations such as the European Space Agency (ESA) and the Committee on Space Research (COSPAR) and bilateral agreements of cooperation at Romanian Government level. Together with the Ministry of Foreign Affairs, ROSA represents Romania at the meetings of the United Nations Committee on the Peaceful Uses of Outer Space and its subcommittees. ROSA coordinates the space activity of scientific and industrial communities, which include over 120 institutions, companies and businesses [4].

One of the most representative institutions, the **Institute of Space Sciences (ISS)** in Bucharest, has played a key role in Romania's accession to the ESA. Another mission of ISS refers to popularizing the research and development fields of ESA in Romania. ISS coordinates a wide range of research and development directions of which the following are worth mentioning [3]:

- Theoretical Physics and Mathematical Physics;
- High Energy Physics and Astrophysics;
- Astroparticle Physics and Cosmology;
- Microgravity, Space Dynamics and Nanosatellits;

- Solar-terrestrial interactions, magnetosphere physics and magnetosphere, solar wind and ionosphere-thermosphere coupling;
- Fundamental dynamic processes in collisionless plasmas; relationship to astrophysical and laboratory plasmas;
- Planetary and interplanetary disturbances and hazard in connection with space weather and electromagnetic phenomena associated with terrestrial tectonics;
- Development of experiments and equipment embarked on cosmic vehicles, in-flight calibration and associated software tools development;
- Advanced analysis and numerical simulation techniques with application to satellite data and images treatment; advanced methods for time series analysis;
- Distributed and Parallel Computing for Space and Ground-based Research and Applications;
- Human Performance and Space Biophysics, Biology and Medicine studies and experiments in benefit of Human Spaceflight and for societal terrestrial spin-off;
- Space Technologies Applications for Humans and Communitarian Health and Safety in critical situations on Earth;
- Systems Engineering and Knowledge Management applied to space-related activities.

Many of the directions mentioned are promoted within the **University Politehnica of Bucharest (UPB)**. The Research Centre for Aeronautics and Space was established in 2001 within UPB, which became an important component in space research. The Centre's mission is to maintain a balance between theoretical and applied investigations in the field of space technologies, with the objectives as follows:

- Development of scientific and practical cooperation with the involvement of SMEs, research institutes, university centres within distinct projects;
- Providing support to industrial units on exploiting new space technologies, improvement of human research potential in the field;
- Stimulation and development of research cooperation within the European Union initiatives.

Another institutional structure, the **Centre for Research and Advanced Studies (ASRC)**, develops theoretical and applied research projects in a variety of scientific and technological fields. ASRC tends to develop and apply innovative solutions in various areas of expertise through a multidisciplinary approach in order to solve problems arising from the social, industrial and ecological environments. ASRC can develop and analyse mathematical models, numerical methods and solutions, complex algorithms and innovative software tools for programming and visualization, as well as for the validation and substantiation of the results of various tests. ASRC areas of interest include fluid dynamics, geophysics, environment, structural analysis, biomathematics, telemedicine, virtual reality, space dynamics, artificial intelligence etc. ASRC has experience in initiating and promoting national and international projects and programs in the fields of Space, Aeronautics, Computer Science and Information Technology, Security.

Aerospace area is represented by **S.C. Aerostar S.A. (ASTAR)**, which has accumulated extensive experience with regard to repairing and modernization of military aircraft, production of light aircraft, hydraulic equipment for aviation and electronic equipment. In the field of GNSS - INS, ASTAR has gained experience in areas such as:

- development of hardware / software for GNSS-INS equipment;
- GPS and INS equipment integration in avionics;
- GPS / GALILEO equipment testing etc.

The Research, Development and Innovation Programme Space Technology and Advanced Research – STAR, for the period 2012-2019 [5], is the tool by which the Ministry of National Education - National Authority for Scientific Research (ANCS) ensures, through ROSA, a great support at national level to the implementation of the Agreement between Romania and the European Space Agency (ESA). The activities of many national programmes have been carried out under STAR [4-8]: CD-I AEROSPACE, CD-I SECURITY, CEEX, CORINT, INFOSOC, AMTRANS, AGRAL, RELANSIN, PNCDI-I/II, including international joint programmes with the European Space Agency (ESA), the United Nations Organization, organizational programmes in Food and Agriculture, PHARE Programme (1), bilateral and multilateral cooperation etc.

3. DEVELOPMENT OF SATELLITE TECHNOLOGIES IN THE REPUBLIC OF MOLDOVA

The starting of the project [1] in 2009 on developing the first Satellite of the Republic of Moldova has stimulated the initiation and development of a range of research and design activities in the field of satellite technologies. Given the funding opportunities of the project from the

State Budget, previously negotiated within the Supreme Council for Science and Technological Development of the ASM, and given the outlook of co-financing from extra budgetary sources, it was decided to develop a satellite with a mass of 10-12 kg, classified according to the European Scale as typo dimension - Microsatellite (MS).

The topic of the activities carried out in the period that followed was projected on three distinct directions:

The first direction - refers to the research, design and manufacture of microsatellite functional components related to its scientific purpose and objectives [1, 9]. The research and design activities devoted to the development of microsatellite on-board subsystems were based on the a priori concept adopted, including on the use of standardized functional COTS components available (Commercial Off The Shelf components) assembled on modular principle. This approach to the process of MS developing meets a number of advantages, including reduced costs and time to perform the MS research-assembly cycle, increased functional reliability of on-board subsystems and of the MS as a whole, simplified procedures and techniques of experimental testing and so on.

However, the theme of the activities included a wide spectrum of scientific research, experimental and construction-technological works, largely interdisciplinary, including at the junction of areas. Due to the achievement of the approved MS design concept based on the use of some functional COTS components (standardized, parametrically unified), their selection was based on an extensive study of ensuring the parametric compatibility, taking into account the mass limitations, dimension, accessibility and acquisition availability etc. Numerous undergraduate, postgraduate and doctoral students from different specialties and faculties were involved in the research and design process, thus ensuring the project an inter- and multidisciplinary educational character.

The second direction includes actions related to the establishment of the National Centre of Space Technologies (CNTS), with a network of interconnected ground stations so that:

- to ensure upward and downward connections of the MS during its flight, with ground infrastructure (especially when it is in the visible area of the Republic of Moldova);
- to ensure the determination, orientation and attitude control of the MS during orbit flight so that when entering into the visible area of the Republic of Moldova it is correctly oriented to capture images (the axis of the scanner lens to look in the nadir);
- to ensure the reception of satellite signals for their further processing;
- to allow the tracking and dialogue with foreign weather satellites etc.

CNTS establishment with a network of ground stations in the Republic of Moldova will open opportunities for expanding international cooperation and involving teams of researchers from the local academic community as partners in European projects in the field of space technology. But the main importance and purpose of such an infrastructure will be to ensure monitoring the MS flight after its release in the outer space.

The third direction of the research carried out relates to achieving the specific objectives with regard to remote sensing of the earth surface and providing various scientific and socio-economic space services as well as image capture of the land area of the territory of Moldova, prevention of flooding risks by determining the evolution of river hydrological status, monitoring the ecological status of forests, plantations and agricultural land, solving of various weather problems etc.

MS objectives bear an exclusive civil character, and the MS on-board subsystems developed using components purchased through non-disclosure commitments shall not be passed to third parties.

4. THE NATIONAL CENTRE OF SPACE TECHNOLOGIES (NSTC), THE REPUBLIC OF MOLDOVA

The first steps in researching engaged on projects in the field of satellite technologies have been taken with the launch of the State Programme *Capitalization of renewable energy resources in the conditions of Republic of Moldova and developing the Moldovan Satellite* - approved in 2009 for financing from the State Budget (coordinator Acad. I. Bostan) [1]. The programme provides for the development of the first satellite of the Republic of Moldova with four distinct projects in the field of developing satellite technologies (project leaders PhD, assoc.prof. Secrieru N., PhD, assoc.prof. V. Blaj, acad. V. Canter, acad. I. Bostan [1, 9].

To develop the research capacities, along with the formation in 2009 of scientific teams with some research and design experience in the field of satellite technologies, a comprehensive plan for the design and construction of the technical and material infrastructure was designed and implemented in 2009-2012 that aims at achieving the scientific goals and objectives of the satellite.

Figure 1. Laboratory of on-board subsystems for nano and microsatellites, NSTC, TUM.

***Figure* 2.** Laboratory of the Microsatellite assembly, NSTC, TUM.

Thus, in 2009 started the establishment of the National Centre of Space Technologies, which was formalized by TUM's Senate Decision no. 6 of 31.01.2012 with the following structure:

4.1. Laboratory of on-board subsystems for nano and microsatellites (SBNMS)

BNMS laboratory specializes in the research and development activities of on-board subsystems, including: the scanner for image capturing; MS electricity supply system by converting PV to solar energy; MS determination, orientation and attitude control systems in orbit flight; equipment for data reception and transmission; on-board computer, etc. The elaborations of MS on-board components are carried out based on alternatives, providing undergraduate, postgraduate and doctoral students with fairness of decision and competitive freedom of creation. Thus, based on alternative principles it is ensured the competition for ideas and innovative technical solutions of the teams of young researchers involved in educational projects of research and development of MS on-board subsystems.

Along with the elaborations made in the original variant [1, 9], research teams, based on case studies, propose variants of on-board COTS (commercial) components available together with compatibility, mass, dimension, and cost analyses, including the insurance of the interchangeability and reliability of the MS as a whole. SBNMS laboratory is equipped with modern computers, computer aided design stations applying modern design software in 3D and comparative analyses, including computer simulations of technological processes (Figure 1).

4.2. Laboratory of data and image processing (PDI)

PDI Laboratory is intended to familiarize undergraduate, postgraduate and doctoral students

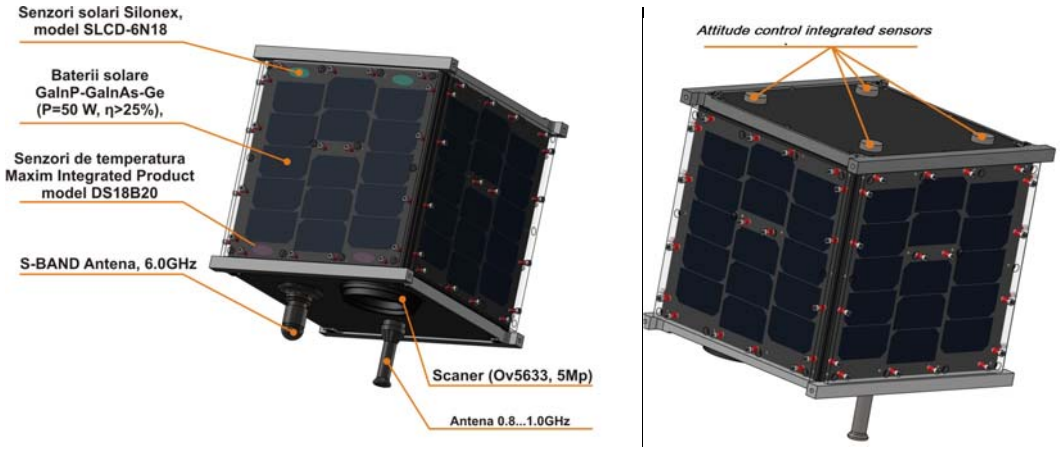

***Figure* 3.** The general view of the Microsatellite, developed at the Technical University of Moldova, Chişinău.

and young teachers with modern methods and techniques of data image and processing from the satellite, dissemination of processing results in different applications and fields. Within the research conducted in the PDI laboratory a special role is assigned to the study of processing peculiarities of satellite images jeopardized by geometric and radiometric distortions, as well as modern processing methods and techniques.

Figure 1 shows a post of geometric and frequency processing of satellite captured images.

4.3. Laboratory of on-board subsystems and MS assembly and testing (AEMS)

AEMS laboratory is endowed with equipment for the assembly of precision mechanics and electronic equipment for measurement (figure 2). figure 3 presents the general view of the MS developed at the Technical University of Moldova. The PV panels of the MS (figure 3) were designed at NSTC and manufactured using the photovoltaic cell GalnP-GalnAS-Ge (P = 50W, η> 25%) resistant to cosmic radiation. SILONEX Solar Sensors of SLCD-6N18 model, Temperature sensors Maxim Integrated Product of DS18B20 model, which are compatible with the MS attitude determination subsystem of MAI-200 model, are mounted in the PV panels.

At the same time, a Simulator (figure 4) is mounted in the AEMS in an isolated space, on a fixed foundation, for the experimental research in laboratory conditions of the MS kinematics and dynamics with sphere-space motion with a fixed point, which reproduces the rotary motion of the satellite around three axes of the orbital reference system. The Simulator also allows experimental research of the intervention of on-board systems on the MS orientation on the orbit, including the determination and calibration of physical efforts of the intervention developed by the two on-board systems [9] on the stability and dynamics of MS repositioning on the axes of the orbital coordinates system. The Simulator allows the experimental research of the MS in laboratory conditions and in vacuum medium of up to 10^{-6} bars (12 μm Hg).

Figure 4. The simulator with the Microsatellite mounted in the external gyroscope, NSTC, TUM.

The Simulator's nest with external gyroscope (figure 5) allows the MS rotation around the 0x, 0Y, and 0z axes in relation to the mobile coordinates system. The nest is equipped with two actuator drivers in order to communicate the MS the nutation motion with an angle of $\theta = 16°$ and precession motion at $\varphi = 360$ °. The planet gear carrier nest allows the study of MS kinematics and dynamics under the action of two MS on-board intervention systems, namely magneto torchers driven by the Earth's magnetic field and the inertial mechanism with three flywheels.

The original Simulator was designed within NSTC, TUM, and manufactured at factories in Chisinau.

4.4. Telemetry communications station (SCT)

The station is endowed with specialized equipment to ensure upward and downward linkages of the MS in orbit flight with the ground

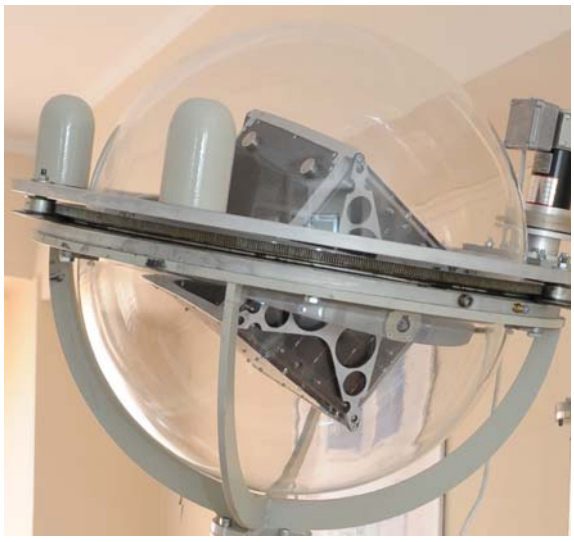

Figure 5. The Microsatellite mounted in the vacuumed planet gear carrier nest with spherical motion, NSTC, TUM.

infrastructure (figure 6). It is connected to a set of telemetry antennas and to the parabolic antenna with mixed purpose (figure 7) [1]. The telemetry

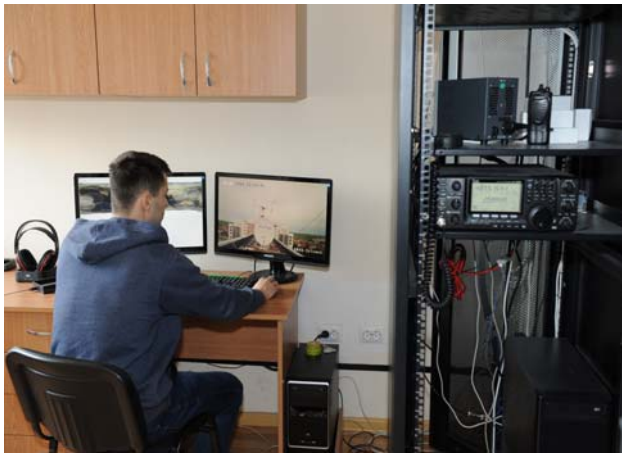

Figure 6. Laboratory of Telemetry Communications, NSTC, TUM.

Figure 7. The set of telemetry and parabolic antennas.

antennas and the parabolic antenna shown in Figure 7 are able to orient on two axes towards the MS in orbit flight through the actuator drivers of Rotor BIG-RAS HR model.

4.5. The design and manufacture platform

An autonomous design and manufacturing platform of components of the MS on-board subsystems affiliated to the CNTS. It is endowed with advanced stations of computer-aided design, computer simulation of the kinematic and dynamic processes of the MS in the stages of design, experimentation and in the prospect of MS launching. In the design process of functional components of the MS, to simulate the influence of cosmic perturbations on the MS positioning on the orbit, there were used softs like Solid Work, Catia, ANSYS, ABAQUS etc. The manufacture of the components of the MS basic functional subsystems is performed at the Centre of Advanced Technologies "*Etalon*", which is endowed with modern equipment, for example, machine tools of Motion Master TB-105 model having heads with 3 and 5 degrees of mobility, operated with the numerical control Fagor 8055M by applying the software SPUTH CAM and ASPIRE VECTRIC. For the manufacture of the plaques with printed wiring, the design and manufacturing platform is

Figure 8. 3D design platform, TUM.

endowed with equipment of LPKF-S103 model operating under the command of Soft Circuit PRO.

Figure 8 shows a computer-aided design and computer simulation station of the MS kinematics and dynamics at the stage of design, testing and commissioning; figure 9a - manufacturing of the components of the MS on-board subsystems at the Centre of Advanced Technologies "Etalon", and figure 9b – computer-aided design station for the prototyping of the plaques with printed wiring of the electronic modules.

NSTC is directly connected to the **Centre of Excellence and Communications of TUM**, endowed with extensive infrastructure for hosting a powerful network "Claud computing", which includes laboratories of research, design and simulation of informative, including satellite, communications systems. A successful collaboration was established with IBM, Romania, through workshops conformed to IBM Academic Initiative regarding the familiarization with design technologies like Model Drivon Systems developed with IBM Rational Rhapsody ILOG OPL-Operations Research.

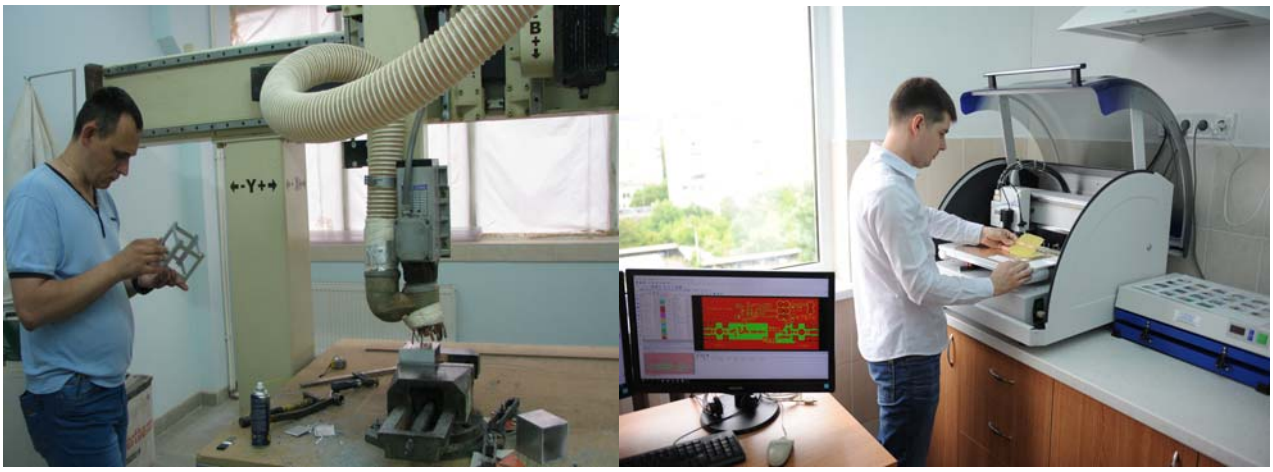

a) b)

***Figure* 9,a,b.** Manufacturing of the components of the Microsatellite's on-board subsystems, TUM.

SBNMS, PDI, AEMS and SCT laboratories are structures integrated in the NSTC, and the platform of design and manufacturing of the components of the MS on-board subsystems is affiliated as an autonomous structure with self-financing.

Bibliography

1. *Program de stat: Valorificarea resurselor regenerabile de energie în condiţiile Republicii Moldova şi elaborarea Satelitului Moldovenesc. Coordonator acad. Ion Bostan. AŞM: RAPORT privind activitatea Consiliului Suprem pentru Ştiinţă şi Dezvoltare Tehnologică şi rezultatele ştiinţifice principale obţinute în sfera ştiinţei şi inovării în anul 2012 (http://www.asm.md/administrator/fisiere/rapoarte/f170.pdf*)

2. *Space Activities in Romania, Romanian Space Agency, 2015. ISBN 978-973-0-20264-9.*

3. *Direcţii de cercetare şi dezvoltare ale Institutului Ştiinţe Spaţiale (http://www2.spacescience.ro/?page_id=3844)*

4. *Agenţia Spaţială Română (ROSA) (http://www2.rosa.ro/index.php/ro/rosa)*

5. Piso M.I., Racheru A., Simion I. *Space programme in Romania – Sharing between national and international activities. International Astronautical Congress 2008 IAC-08-E3.1.10, Sep. 2008.*

6. Crăciunescu V. *Romanian experience in developing a satellite based emergency response service. Copernicus User Forum on Emergency, Bruxelles, Comisia Europeană, 22 octombrie 2014.*

7. Crăciunescu V. *Satellite Based Service for Flood Monitoring in Romania. Simpozionul Internaţional „Sisteme Informaţionale Geografice", Ediţia a XXII-a, Chişinău, Academia de Ştiinţe a Moldovei, 24-25 octombrie 2014.*

8. Bratasanu D., Nedelcu I., Datcu M. *Interactive spectral band discovery for exploratory visual analysis of satellite images, IEEE JSTARS, Vol. 5, No. 11, 2012.*

9. Bostan I., Cantzer V., Secrieru N., Bodean G., Candraman S. *Research, Design and Manufacture of Functional Components of The Microsatellite „Republic of Moldova". In: 2nd International Communication Colloquium, Aahen, 2014, p. 19-30.*

10. Bostan I., Piso I.M., Bostan V., Badea A., Secrieru N., Trusculescu M., Candraman S., Margarint A. *Perspectivele cooperării Universităţii Tehnice a Moldovei cu agenţia spaţială Română în domeniul tehnologiilor Satelitare. In: Academos, nr. 2 (70), 2016, p. 70-77.*

11. Bostan I., Piso I.M., Bostan V., Badea A., Secrieru N., Trusculescu M., Candraman S., Margarint A., Melnic V. *Arhitectura reţelei staţiilor terestre de comunicaţii cu sateliţi. In: Academos, nr. 2 (70), 2016, p. 70-77.*

Recommended for publication: 18.02.2016.

ARCHITECTURE OF THE GROUND STATIONS - SATELLITES COMMUNICATION NETWORK

[1]Ion Bostan, academician, [2]Ioan-Marius Piso, Dr. eng., [1]Viorel Bostan, prof.Dr.Sc., [2]Alexandru Badea, prof. Dr.eng., [1]Nicolae Secrieru, assoc.prof. Dr., [2]Marius Trusculescu, Dr. eng., [1]Sergiu CANDRAMAN, PhD student, [1]Andrei Margarint, PhD student

[1]Technical University Of Moldova

[2]Romanian Space Agency

1. INTRODUCTION

Space technologies have an important role in the development of different branches of the economy, especially agriculture, geodesy and surveying, ecology and environmental monitoring, prevention and mitigation of floods and other natural disasters etc. In recent years the number of universities that initiate and develop projects in the field of development and launching of pico-nano-microsatellites into space for scientific, socio-economic, commercial purposes etc. is increasing.

Small satellites are built and launched into space with minimal costs, but generally they can ensure an intense exchange of data with ground stations distributed territorially. Ground stations are usually isolated and have limited radio visibility periods between the station and the satellite, including possessing low temporal resolution. A more effective solution would be to create a network of interconnected ground stations that can communicate with remote control. Such networks of ground stations allow monitoring a wide range of satellites, such as educational and commercial satellites for several universities. Development of such networks requires the construction of ground stations located on the territory in a dispersed way with an appropriate antenna system capable of ensuring a good quality and functionality of the communication.

The authors promote the idea of ground stations connection via a computer network in a complex infrastructure, including its connection via the Internet to the Romanian Space Agency (ROSA) and the European Space Agency (ESA), which would help increase usability and efficiency of satellite communications. In this paper we present the concept of development of ground stations network of satellite communication and technical solutions aimed at ensuring reliable "*satellite-ground infrastructure*" communication with remote control and connection to ROSA and ESA.

2. ARCHITECTURE OF THE GROUND STATIONS NETWORK OF SATELLITE COMMUNICATIONS

The project *Connecting the Infrastructure of the National Centre of Space Technologies with the Educational Global Network for Satellite Operations*, conducted during the years 2015-2016, is a continuation of the efforts made for the realization of the State Program "Development of the Moldovan Satellite". The new project's objective is to make the connection of the research centres in Moldova to the pan-European research thematic infrastructure, such as ESFRI (European Scientific Forum for Research Infrastructure) ERICs (European Research Infrastructure Centres), ETPs (European Technology Platforms) etc.[1,2,3].

The idea of connecting ground stations (Figure 1) through a virtual network of computers was developed within the project, which allows considerable extension of the radio visibility period of a satellite and, consequently, increasing the amount of data sent. Another opportunity is the simultaneous reception of data from a satellite via several ground stations, and storing them in the command centre, where the data packages will merge. This system allows improving the quality of "*satellite - ground stations*" communication by reducing the bit error rate (BER). Specialized laboratories (SBNMS, PDI, AEMS, SCT), established within the National Centre of Space Technologies (NSTC), TUM, Chisinau, together with the network of ground stations, form the ground infrastructure of satellite communications with the architecture shown in Figure 1 [1-3]. MS in orbit flight through the actuator drivers of Rotor BIG-RAS/HR model.

An important role in the ground infrastructure is assigned to the ground station with parabolic antenna (Figure 1d) for the reception of images from the MS on the orbit. The parabolic antenna, with a diameter D = 4.3 m, through two separate actuator drivers fitted with drivers, can revolve

around two axes in individual regime commanded on the server computer. The kinematic chain of the two actuator drivers is fitted with mechanical torsions to exclude the gear backlash, thus increasing kinematic (angular) accuracy of parabolic antenna orientation towards the MS in orbit flight. MS in orbit flight through the actuator drivers of Rotor BIG-RAS/HR model.

Ground stations endowed with specialized equipment ensure the upward and downward links of the microsatellite (MS) (Figure 1b) in orbit flight with the ground infrastructure (Figure 1c, d). The station is connected to a set of telemetry antennas, and to the parabolic antenna with mixed purpose [1-3], which are able to orient on two axes.

An important role in the ground infrastructure is assigned to the ground station with parabolic antenna (Figure 1d) for the reception of images from the MS on the orbit. The parabolic antenna, with a diameter

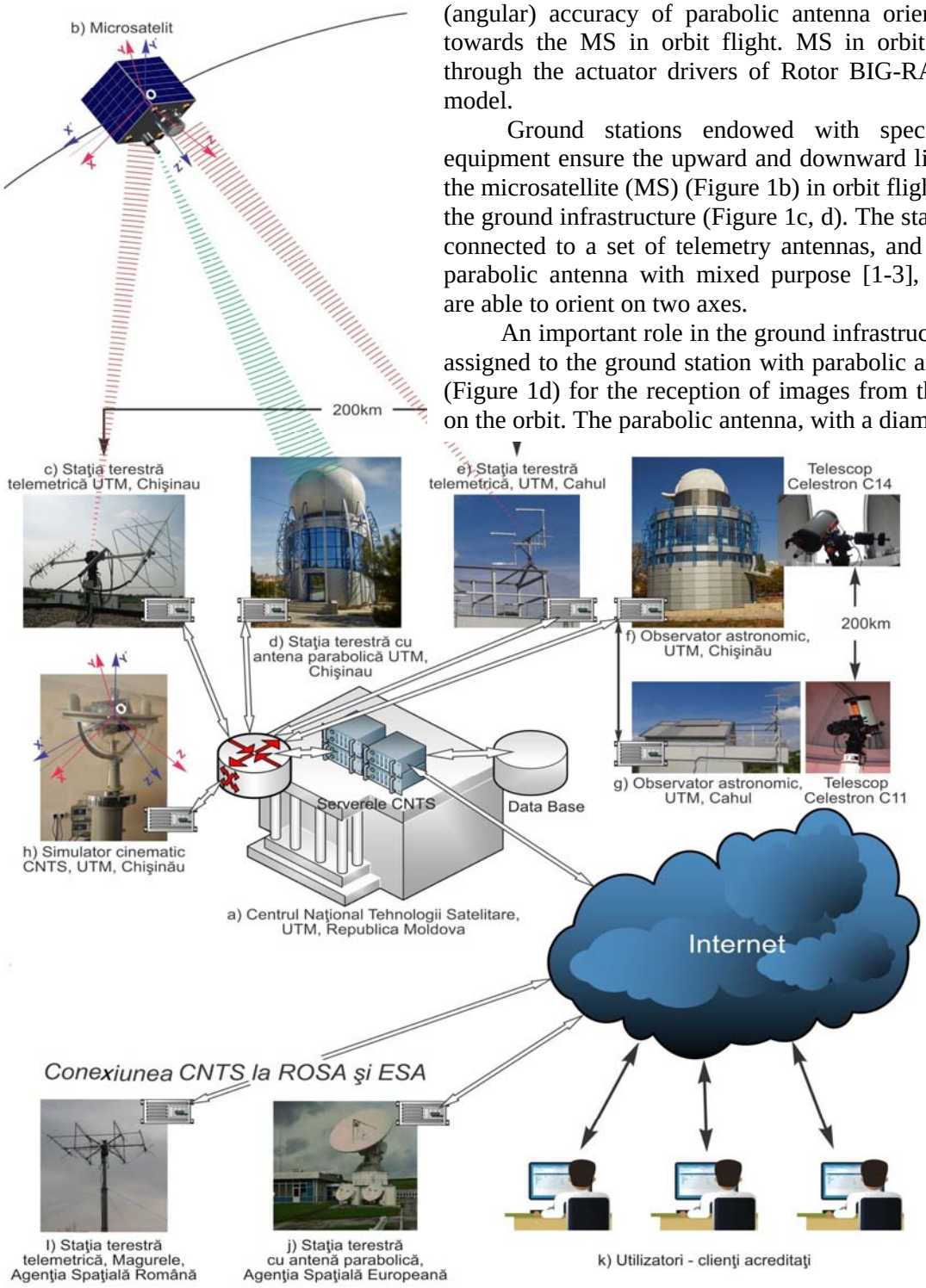

Figure 1. Architecture of ground stations network developed at TUM, Chisinau, with connections to ROSA and ESA.

a) Space Technology Center, NSTC Servers; b) Microsatellite; c) Telemetry ground station of TUM, Chisinau; d) Ground station with parabolic antenna of TUM, Chisinau; e) Telemetry ground station of TUM, Cahul; f) Astronomic observatory with Celestron C14 Telescope, Chisinau; f) Astronomic observatory with Celestron C14 Telescope, Cahul; h) Kinematic simulator of the NSTC, TUM, Chisinau; NSTC connection to ROSA and ESA; i) Telemetry ground station, Magurele, Romanian Space Agency; j) Ground station with parabolic antenna, European Space Agency; k) Users - accredited clients.

Figure 2. Ground station with parabolic antenna, 9 Studentilor str., Chisinau

D = 4.3 m, through two separate actuator drivers fitted with drivers, can revolve around two axes in individual regime commanded on the server computer. The kinematic chain of the two actuators drivers is fitted with mechanical torsions to exclude the gear backlash, thus increasing kinematic (angular) accuracy of parabolic antenna orientation towards the MS in orbit flight.

For the installation and operation of the ground station with parabolic antenna with mobility on two axes (elevation and azimuth) a building was built in the area adjacent to the location of NSTC (9 Studentilor str., Chisinau) with a foundation of 16

Figure 4. Astronomic observatory of TUM, 9 Studentilor str., Chisinau

Figure 3. The parabolic antenna of the ground station, 9 Studentilor str., Chisinau.

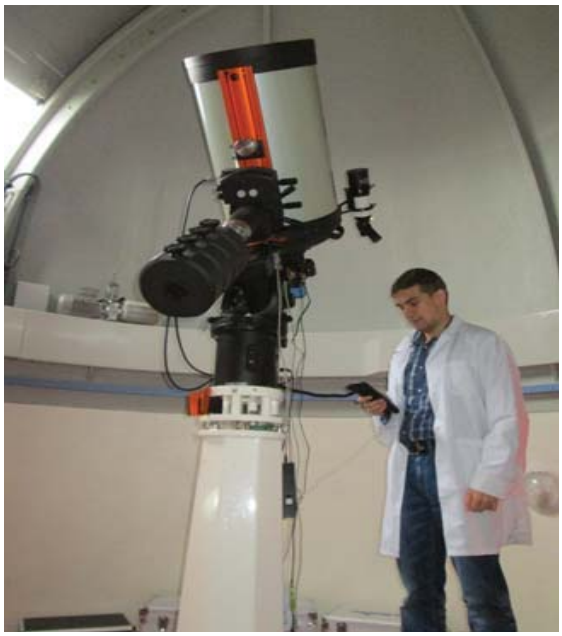

Figure 5. Celestron C14 telescope of the Astronomic observatory, UTM, Chisinau.

m. The resistance structure of this ground station was reinforced vertically with two membranes of reinforced concrete to take over reactive torque load generated by dynamic movements of elevation and on the azimuth of the parabolic antenna weighing about 2 t. On the second floor of the building the tracking points of the MS flight is located connected via optical fibre to the support point in Cahul, Branza commune, and to NSTC, Chisinau.

To expand the area of monitoring and altitude control of the MS flight (about 200 km away) a support point equipped with a telemetry antenna was built in the commune of Branza, Cahul (Figure

1e). Ground infrastructure also includes an astronomical observatory located in Chisinau, equipped with a telescope model Celestron C14 and an astronomical observatory located in the support point of commune Branza, Cahul equipped with a telescope model Celestron C14.

Celestron telescopes' both servers are connected to NSTC via optical fibre. Thus, the infrastructure created with two telescopes interconnected and connected to NSTC virtually allows real-time recording of the MS positioning in flight from two land points. All components of the ground infrastructure (Figure 1a, c, d, e, f, g, h) are interconnected by optical fibre, and NSTC has

Figure 6. Astronomic observatory, com. Branza, Cahul.

connections with the telemetry ground station in Magurele, Romania, extending to the European Space Agency, based on the implemented project [1-3].

3. REMOTE CONTROL OF SATELLITE OMMUNICATION GROUND STATIONS

The network of ground stations, whose architecture is shown in Figure 1, is designed and constructed so as to ensure the communication among stations regionally / worldwide via the Internet. Ground stations can communicate via client applications with server components based on TCP / IP protocol (Figure 8). The architecture developed (Figure 1) enables centralizing the data received from a satellite by different ground stations in the same database. Client applications can only

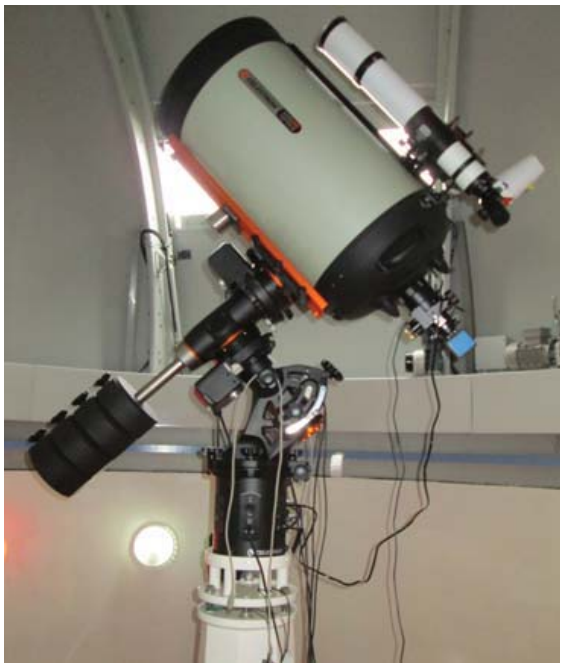

Figure 7. Celestron C14 telescope of the Astronomic observatory, com. Branza, Cahul.

communicate with the server, Server components having the administrative role. The Server component is the only link of the system which provides access to the database and is able to communicate with all client applications in the system. In order to implement the remote control of ground stations, the "*client-server*" classical architecture was taken as the basis consisting of three parts: a VPN server and a separate network device that interconnects the main server and the clients in a secure manner; the main high-performance server that manages the entire network and provides a web interface for end users; a number of clients PCs worldwide connected to the VPN network. Clients can be of two categories: the first category - only to access the web interface, and the second category - to connect the ground station to the network for its joint use [3-4].

Currently, the VPN server runs on the computer MikroTik Cloud Router with advanced performance - a high level of flexibility and a wide range of possibilities. The main server is running on the "*blade*" type server Sun Microsystems, and Ubuntu Server LTS is used as operating system and provides a range of personalized services developed for the remote control of ground stations. For the purpose of redundancy, a second *"blade*" type server is installed, identical to the main one. The client computer can be any type of PC, from a low-performance SBC to a "*high-end*" desktop computer. The choice depends on the purpose of the end user, which may consist of access to the web interface and / or connection to the ground station.

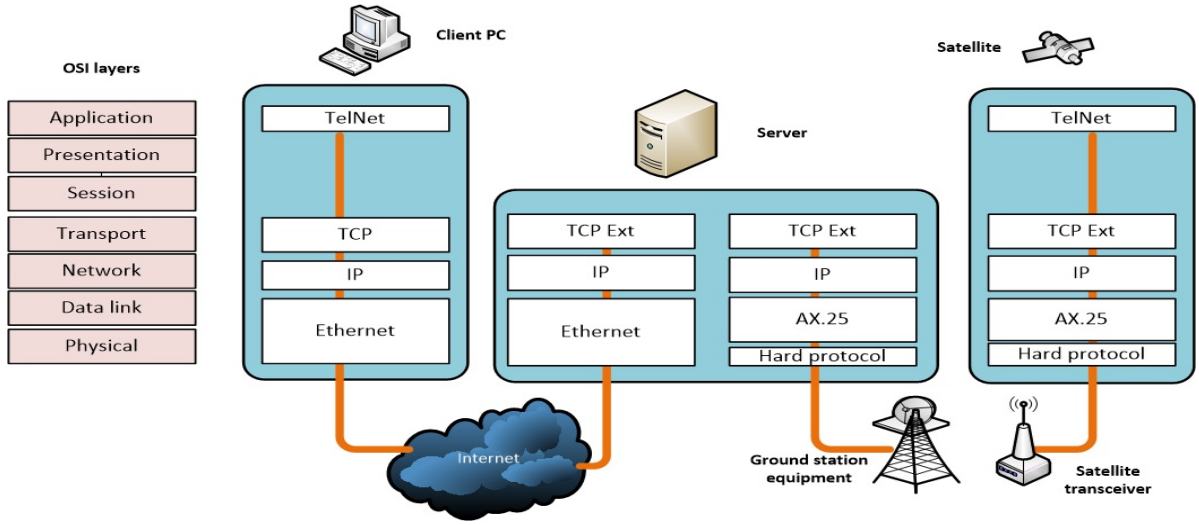

Figure 8. OSI levels for educational missions through small satellites.

At the current stage of implementation, the client software for the connection to the ground station has been tested successfully on a Raspberry PC SBC module and a desktop PC, which is running an Ubuntu distribution, but it can run any other operating system: Microsoft Windows, Mac OS X, GNU / Linux and even on BSD derivatives.

The Software "*server-side*" component was developed at NSTC that provides the following services and/or certain functional destinations [3-4]:

- **Main DB –** the main database for storing data necessary for current operations (data stored for a short period of time);
- **Scheduler** – monitors the main DB for current data, making decisions based on previously acquired data - appealing the **Launcher** or sending data to the **DB archive**; maintaining and updating TLEs and future observations based on updated information;
- **DB archive –** database in which previous data is stored in the long term;
- **Web Client –** GUI component, enables end users to interact with the system in order to schedule new observations or remove old ones, view information about the connected ground stations etc. (only accessed by clients of the VPN network);
- **Web Server –** ensures the functionality of the Web Client component and access to databases;
- **Launcher –** is the service that communicates with clients (those with the ground station connected), sending them commands required to fulfil specific tasks based on some parameters provided by Scheduler;
- **Ground Station –** is the end point of the system that receives and executes the requested commands.

Also, the "*Client-side*" component (Figure 9 (a, b)) was developed within NSTC which is more complex than the "*server-side*" component, including the actual control of the stations (rotor, transceiver) [3 - 4]:

- **Worker –** the main service that controls all the others and sends commands to several executors;
- **Hamlib –**open-source sub-components (rotctld and rigctld);
- **Rotctld –** is responsible for the communication and control of rotors of various types. **Rigctld** can control several types of transmitters-receivers, offering the possibility of change / configuration;
- **Rotor –** is able to control different types of rotors, including those for telemetry antennas with low angular accuracy, and those with large angular accuracy, for parabolic antennas;
- **RF-Freq –** controls / adjusts the operating frequency for different transceivers;
- **GNU Radio –** open-source component with very wide communication possibilities with different types of telecommunications hardware, enabling the reception of signals with advanced post-processing and also sending signals with the desired pre-processing;
- **RF-Audio –** GNU Radio reception and processing via a transceiver audio channel;
- **SDR-Date.** GNU Radio for raw data processing, coming from DST connected devices;
- **VPN network –** client-server communication via secured VPN network tunnel;

Server Link – the client receives all commands from the server-side component.

4. DATA MANAGEMENT FOR INFORMATION RETRIEVAL IN GROUND STATIONS NETWORKS

Monitoring ground stations are not built typically parallel because, on the one hand, the beam of radio waves from the satellite is

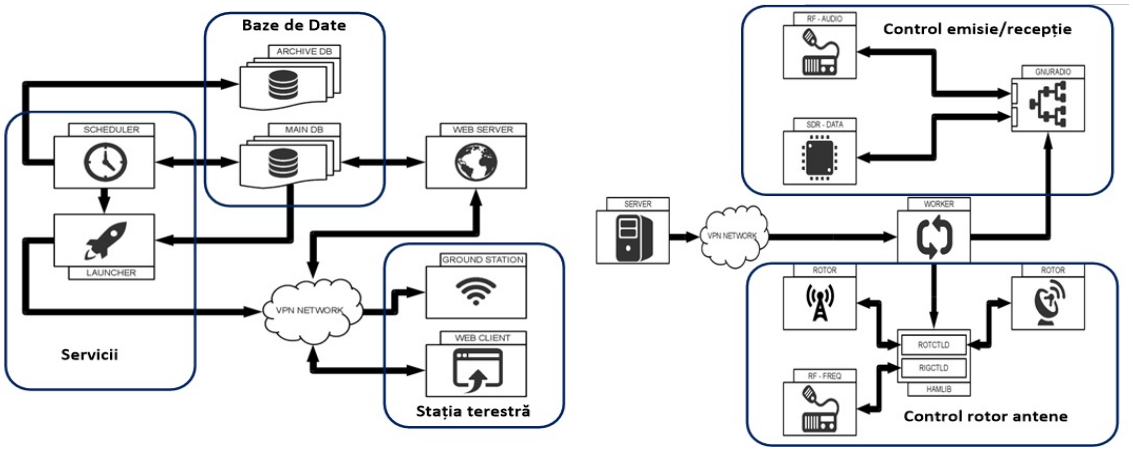

a) b)

Figure 9. Server (a) and Client (b) components of remote control of the ground stations.

relatively narrow and, on the other hand, the development of several backup ground stations for a space agency can be very expensive. Networks of educational ground stations can share resources to ensure simultaneously the reception of the data stream from a single satellite. The reception from a "downlinks" satellite offers both opportunities and challenges. The opportunity is to get redundant data from ground stations, and the challenge lies in the need to develop a system that requires the use of appropriate methods of management and data synchronization.

Data management has evolved from the idea of combining multiple data streams from the same satellite, received at a number of geographically distributed ground stations. Theoretically, these data streams received in parallel by ground stations should be identical, but in reality they differ for several reasons (Figure 7):

1. The interaction time of each satellite and ground station differs depending on the route. When two routes overlap, the ground stations being geographically spaced apart, there is a small period of time during which only one of them will be in contact with the satellite. Thus, each station receives different sets of data frames.

2. The received data can be corrupted, resulting in bit errors or even lack of frames / packages caused by atmospheric disturbances, low signal / noise level, technological or constructive inaccuracies of the receiver. These errors can lead to a situation where there are received several data streams in an identical fraction on the overlapping routes of ground stations, when there occures a small part of different information, data being thus corrupted or lost. The idea was to combine in automatic regime data streams, received differently by the network of ground stations and to form a single data stream, ensuring their proper management.

A satellite operator would thus have to monitor only the single data stream consisting of streams information received in the network. Combining multiple data streams from the same satellite, received by geographically distributed ground stations, arise a series of new problems:

- Arranging data frames in the correct order on a single time scale (worldwide). Due to the unsynchronized time from the ground stations and transmission delays in space and on Earth, temporal ordering of the packages can be modified / distorted;
- Identification of similar data packages, if redundant packages have been received from the satellite at the ground network;
- Removing data gaps using redundant information.

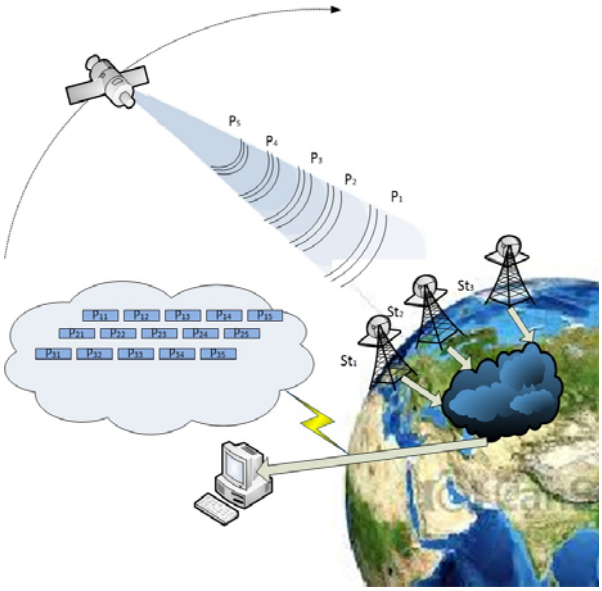

Figure 10. Scheme of data reception in the ground stations network.

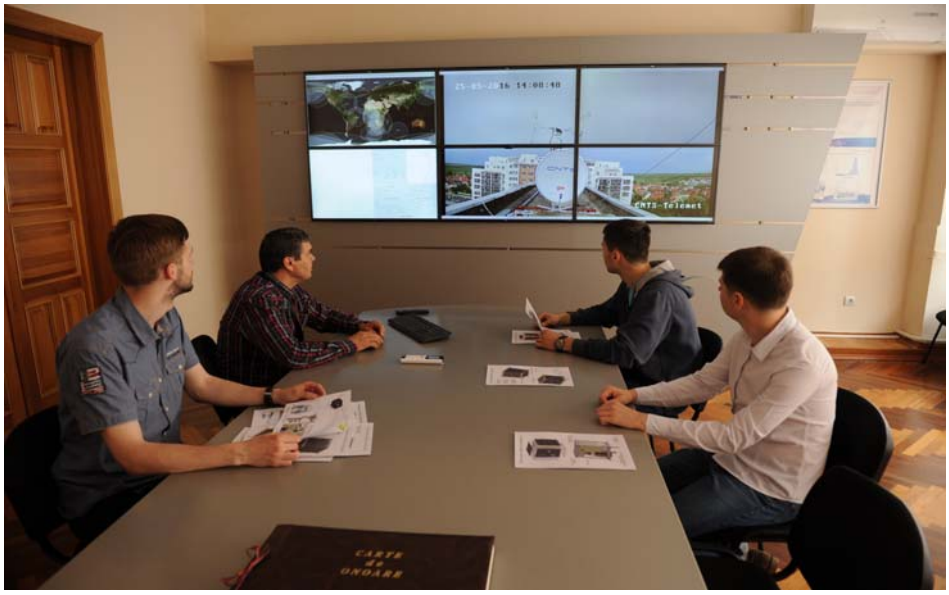

Figure 11. Monitoring the flight of satellites, NSTC, TUM, Chisinau

The complex data management problem was reduced to two separate sub-problems. Firstly, ground stations of the network must be synchronized between them, to command data frames received on a common time scale worldwide. This supposes both synchronizing computer clocks and timing of subsequent data streams. Secondly, the information in the synchronized data streams must be combined to make up for the missing data.

5. TESTING THE REMOTE CONTROL OF THE GROUND STATIONS UNDER REAL CONDITIONS

The project on the creation of the ground infrastructure NSTC with ground stations interconnected and remotely controlled being performed in premiere (within NSTC), needed a series of checks and tests under real conditions of communication with a range of satellites.

Through the competition of researchers from the Institute of Space Sciences, ROSA, Bucharest, there were conducted a series of test procedures in several thematic stages. At the first stage, the equipment was adjusted both to facilitate the remote control of the antennas and of the radio reception / transmission component of telemetry ground stations in Rascani campus of TUM (Figure 1c), the support point in the south in Cahul (Figure 1e), and Magurele of ROSA (Bucharest) (Figure 1l). At the second stage, local control systems and "*Client-side*" software were installed at all ground stations and local control procedures were carried out. At the next stage, the "*server-side*" software component was installed on the NSTC servers and there were performed the "*client-server*" interaction procedures of remote control of ground stations. Subsequently, verification procedures were applied regarding the interaction / connection of the stations with separate and concomitant communication with different educational microsatellites.

All these actions were conducted and coordinated from one centre of monitoring the flight of satellites (Figure 11), which has different ways of control: semi-automatic, automatic with a single station / all stations and automatically planned for a series of satellites. The "*server-side*" software component ensures the merging of multiple data streams from the same satellite received at geographically dispersed ground stations.

An important testing experiment of the "*microsatellite - ground infrastructure*" communication with remote control was conducted at NSTC, TUM. The experiment was performed with an electronic module of microsatellite with functions of image capture and transmission of telemetry data and images launched with a HAB (high altitude balloon) helium balloon in the stratosphere. The flight lasted more than three hours and reached an altitude of 28 667 m. The flight of the electronic module was monitored by the telemetry ground station from the National Centre of Space Technologies, Rascani campus of TUM, with remote access from the control tower of Chisinau International Airport [6-7].

During the experiment of communication with the electronic module installed on HAB, it was also tested the function of the ground station of tracking the balloon using on-board GPS data. In order to ensure the telemetry of the module (internal and environment temperature, module supply voltage and the current consumed etc.), including for receiving and transmitting images, a mobile station was equipped on a car that followed the balloon. The mobile unit, fitted with a 3G modem, was sending data to the server. Ground stations used the appellatives ER1TUM / ER5TUM, officially recognized by the Centre of Radio Frequencies from the Republic of Moldova. Images captured by the module were saved on the SD card and at the same time sent to the ground station.

HAB flight was controlled by the National Centre of Space Technologies, including from the control tower of Chisinau International Airport. Analysing the telemetry data and images transmitted to the ground station a minimum of errors (about 0.3% packet losses) was found which confirms the correctness of technical solutions that laid at the basis of these developments.

CONCLUSIONS

The concept of NSTC infrastructure development with a network of interconnected ground stations promoted within the project *Connecting the infrastructure of the National Centre of Space Technologies to the Educational Global Network for Satellite Operations*, call for competition *Connecting centres of excellence in Moldova to the European research infrastructure* [1] was carried out in full.

Elaborations under the project on connecting NSTC and ground stations in Moldovass in a common network with connection to ROSA and ESA will be available to researchers in international cooperation partnerships in the field of space technologies. The project is part of provisions of the Grant Agreement Nr. 2014 / 346-992 of 24.9.2014 of the European Commission *Financial support for Moldova's participation in the European Union's research and innovation Framework Programme HORIZON 2020*.

Connection of NSTC and of the network of ground stations in Moldova to the Global Network GENSO (Global Educational Network for Satellite Operations) provides premises for expanding international cooperation in the field of satellite technologies, particularly with ROSA, that will stimulate the development of educational projects in the field by involving undergraduate, postgraduate and doctoral students, and young researchers. At the same time, new prospects will open for widening the diapason of interdisciplinary investigations and development of new space products and technologies. This will create a secure foundation for expanding cooperation internationally.

Bibliography

1. *Conectarea Centrelor de Excelență din Moldova la Infrastructura de cercetare a UE. http://www.h2020.md/sites/h2020/fi les/Newsletter-rom-fi n.pdf*

2. Bostan I., Secrieru N., Candraman S., Margarint A., Barbovschi A. *National space technologies center infrastructure connection to global educational network for satellite operation. În: Meridian Ingineresc, nr. 2, 2015, Chișinău.*

3. Bostan I., Secrieru N., Candraman S., Margarint A., Barbovschi A. *Connecting the infrastructure of National Centre of Space Technologies to Global Educational Network for Satellite Operations. In: Proceeding of the 5th International Conference "Telecommunications, Electronics and Informatics", May 20-23, 2015, Chișinău, Vol. 1.*

4. Margarint A., Barbovschi A. *Automation of satellite tracking for worldwide ground stations. In: Proceeding of the 5th Int. Conf. "Telecommunications, Electronics and Informatics", May 20-23, 2015, Chișinău, Vol. 1, p. 421-422.*

5. Levineț N., Ilco V., Secrieru N. *Satellite telemetry data reception an processing via soft ware defined radio. In: Meridian Ingineresc Nr.2, 2015, Chișinău, p. 72-76.*

6. Bostan I., Cantzer V., Secrieru N., Bodean G., Candraman S. *Research, Design and Manufacture of Functional Components of The Microsatellite "Republic of Moldova". - In: 2nd International Communication Colloquium, Aahen, 2014, p. 19-30.*

7. Bostan I., Dulgheru V., Secrieru N., Bostan V., Sochirean A., Candraman S., Gangan S., Margarint A., Grițcov S. *Dispozitive mecatronice, tehnologii industriale și satelitare. În: Academos, nr. 1 (32), 2014, p. 21-25.*

8. Bostan I., Piso I. M., Bostan V., Badea A., Secrieru N., Trusculescu M., Candraman S., Margarint A., Melnic V. *Arhitectura rețelei stațiilor terestre de comunicații cu sateliți. In: Academos, nr. 2 (70), 2016, p. 70-77.*

Recommended for publication: 26.04.2016.

CREATIVITY IN GROUPS: WHY BRAINSTORMING DOESN'T WORK

I hate to be the bearer of bad news, but study after study has shown that when it comes to producing the best, most useful ideas, brainstorming *just doesn't work*. People in brainstorming groups have been found by researchers to produce fewer *and* lower quality ideas than when working alone.

Here's why researchers believe this is the case…

1. **Social loafing:** Research in the area of "*social loafing*" shows that when people are in groups, they are less likely to fully commit themselves because others will pick up the slack (bystander effect anyone?)

2. **Production blocking:** When other people are talking, the rest of the brainstorming group has to wait. This causes some people to lose focus of their ideas, dissuade themselves from mentioning them, or just plain out forget some of the insights they just fleshed out.

3. **Evaluation apprehension:** Simply put, although many brainstorming groups try to leave evaluation out until later, contributors *know* that other people are judging their ideas when the state them. When you are by yourself, you have more time to build an idea before presenting it to anyone.

If that's the case, then why even bother with brainstorming?

There are 2 big reasons…

The **first** is that research (particularly from professor Ben Jones) has shown that *collaboration* is indeed an important part in coming up with brilliant ideas. Data on collaboration seems to point to scientists today doing more collaboration, and reveals that in many instances, two "so-so" ideas are made great by collaboration.

The **second** has to do with the way that groups work. When everyone feels like they've contributed, group projects tend to be more successful. In other words:

People who have participated in the creative stage are likely to be more motivated to carry out the group's decision.

Since not all creative work can be done alone, some sort of collaboration is necessary in order to make sure no ideas get passed up, and to ensure that the entire group feels involved in actually putting the ideas into action.

So what is the answer to this dilemma?

Well, according to brand new research (2012), the internet may be the savior for brainstorming. Specifically, the use of *Electronic Brainstorming* was found to be more effective in coming up with the best non-redundant ideas in groups.

How does it work?

First, it follows the older rules of '*Brainwriting*,' which includes the following:

1. Don't criticize.
2. Focus on quantity.
3. Combine and improve ideas produced by others.
4. Write down any idea that comes to mind, no matter how wild.

The difference is that instead of using things like post-it notes (that '*Brainwriting*' suggests), things like internet chat rooms or instant messaging are utilized.

It seems to work well because it allows members to see ideas flowing all at once, but it solves some of the problems with face-to-face brainstorming. When it's done online, each person doesn't have to wait for the others to stop talking *and* they are less worried about being evaluated.

I prefer to use tools like Campfire for this, but any group chat software should do the trick.

The Character Traits of Creative People

Since creativity seems to thrive with individuals and sometimes collaboration rather than group work, what sort of traits are often found in especially creative people?

As with all creativity research (since it is a very large and complex topic), the results are a bit muddy, but a collection of the research seems to point to a few traits that are found regularly in creative people.

Below we'll discuss a few that are *more common* in those people with creative skills (note that this does **not** mean that all creative people have these traits!)

1. Creative people are eccentric

Breaking news: the sun is hot! Everyone saw this coming, but more interesting is looking at what ways creative people are more eccentric. One interesting finding from Harvard is that creative people tend to have lower "*latent inhibition*" defined as:

…an animal's unconscious capacity to ignore stimuli that experience has shown are irrelevant to its needs. Thus, creative people tend to be able (maybe through a combination of nature + nurture?) to take in more detail due to their ability to not block out "irrelevant" details.

Perhaps this is why most of us see a red wheelbarrow, and creative poets can visualize a Red Wheelbarrow.

2. Creative people often feel "*isolated*"

Despite the hollow cries of introverts everywhere, creativity is not necessary associated with being an introvert *or* an extrovert. Creative people have personality traits of all types, and being outgoing is not limiting to creativity. One thing that recent research has looked into though, is if creative people have a feeling of "*isolation*" among peers, even when they can make friends and colleagues easily.

This may be caused by their inability to relate to regular conversation as easily, or that their conversational partners cannot follow their "*more creative*" train of thought (if that sounds arrogant, don't worry, I'll be taking them down a peg later on). There has also been some research on especially creative people and social rejection, indicating that a feeling of rejection of peers **and** a desire to feel different (thus, embracing the rejection) may spur on more creative activities.

Lastly, creative people seem to be less trustworthy of others (on average) than non-creatives, which may play a part in this feeling of isolation.

3. Creative people are both smart + responsible *and* irresponsible + immature

There are numerous studies that show creativity positively correlates with intelligence, but after a certain point, the correlation dips off. Conversely, some research conducted on creative geniuses has shown that immaturity often goes hand-in-hand with creativity (as you might be able to imagine).

The thing is, there is a very fine balance between this responsible + irresponsible nature in very creative people…

Without discipline, creative works cannot be achieved, and creative people are known for long extended blocks of work (being "*wrapped up in*" a project). Conversely, the immaturity shown in many creative people likely goes hand-in-hand with their ability to produce novel ideas.

4. Creative people are often arrogant

Is it easy to get along with creative people? Although research on "*agreeableness*" and creativity shows no strong correlation either way, newer research that examines subsets of agreeableness points to a new finding…

As it turns out, while not *all* creative people are this way, there is strong negative association with humility and creativity, meaning creative people tend to be braggarts. This could likely stem from reinforcement and the ego, with successful creative people constantly being told how creative they are.

5. Creative people are a bit… *crazy*

If this section felt too much like ego-stroking, well… it's time to take creative people down a peg! There has been a plethora of research that shows creative people are a tad crazy… and kind of mean. For instance, many studies show that creative people are better liars than their peers, and other research has shown that creative people were:

- More likely to cheat on a game in the lab
- Better at justifying their dishonesty afterwards

…and get this: Creativity was more closely associated with *dishonesty* than intelligence! (Remember how I said that creativity only coincides with intelligence up to a certain point?)

Other research has shown that creative thinking is unusually high in criminals and lawbreakers. Most troubling (and direct) of all, a few studies have found that creative people score higher on psychoticism, which includes traits like less empathy, being cold, and egocentricity. Worse yet, the advantage that creative people have (discussed above) in having lower levels of "latent inhibition" may open them up for a variety of mental illnesses. There, now creative people can hop off their high-horse.

Column written by professor Valeriu Dulgheru, Ph.D. Dr. Sc. from Technical University of Moldova

PERSONALITIES OF THE SCIENTIFIC UNIVERSE: Aurel Vlaicu

Flying by air was a matter of concern for people from ancient times. Mythology presents us Icarus, the hero who created for himself wings like birds, with feathers and wax. The Bible also describes an aircraft that brings to mind to the spacecraft.

By the year 200 BC there were made in China some kites that could lift a man into the air. One of these men was even the prince Yuan Huangtou. The famous Leonardo da Vinci sketched a flying machine with wings and even one similar, in principle, with helicopters from nowadays.

In this area, the flight with a device that is heavier than air, Romanians have made numerous contributions. One Romanian was Aurel Vlaicu.

Aurel Vlaicu was born on November 6, 1882 in Binţinţi locality, located between Orastie and Sebes, in a family with eight children of the Mayor Dumitru Vlaicu. Aurel was the eldest and the handiest. He built his house in the shed belonging to a real machine shop. He saw paper flying kites handled by village children and explained to his brothers and friends how it will look the flying machine that he will build.

After graduating the primary school in his village he is enrolled at the reformed High-School of Orastie, where he was noted for his technical skills. He repaired watches of his teachers and he devised a threshing machine. He continued his secondary education at Sibiu, where he was a colleague of Octavian Goga. Here he has invented a turbine factory that was taken over by Rieger in order to be produced in series.

In 1902, after finishing high school, he joined the Polytechnic School in Budapest, and one year later, in 1903, was transferred to the Polytechnic School in Munich because here there were treated better the mechanical disciplines. As a student, he built the model of the first flying machine remaining in the school lab. He obtained his engineering diploma in 1907, then he was concentrated to a submarine unit in the Adriatic Sea, which belonged to the Austro-Hungarian navy.

In 1908, he was employed as an engineer at Opel's engine plant Rüsselheim with the intention to build an engine for the flying machine that he dreamt at since his childhood. The factory management put more conditions on Aurel Vlaicu that he could not accept, so in 1909 he returned home. He was helped financially by his father, Dumitru Vlaicu, by his brothers and other friends and built a glider plane that he tried on pasture land of Binţinţi village. He named it "Beetle". Moreover. In one of the trials he boarded his sister Valeria on the glider plane. It was a world first: the first woman to fly a glider. The hang gliding demonstrations continued in Sibiu and Brasov. Being encouraged by these results and supported by several officials, including Spiru Haret, he came to Bucharest in 1910 where he built Vlaicu I. For the engine choice he was advised by Traian Vuia. He obtained the patent for a "flying machine with an arrow-shaped body". On June 17, 1910 Aurel Vlaicu makes a test flight on the pitch at Cotroceni. Here's what the inventor said after approximately one year after this flight, "A great joy, but I felt it when I flew for the first time at Cotroceni. I did not then raised more than four meters. However, neither the Alps weren`t taller than the height that I rose to. Those four meters were then for me a remarkable record, a record that made my machine famous. I flew and this was the main thing ". He flew at the moment only 50 meters. This day, June 17 was important for Aurel Vlaicu. This day, June 17, is important for the aviation in Romania.

Aurel Vlaicu flew his machine, between Piatra Olt and Slatina to carry an order of battle in military manoeuvres organized by the Romanian Army. It was the first aircraft used by the Romanian army.

In 1911, he built the flying machine Vlaicu II that did demonstrations at Blaj and then in Sibiu and in Brasov. On this occasion it reached a speed of 90 km / hour and the ceiling height of 1,000 m.

With the same device, he participated in 1912 in a competition in Austria where he won the First Prize in throwing the target. In this contest, attended 40 pilots from seven countries, including the famous French pilot Roland Garros. Here's what the press wrote: „*Beautiful and brave flights conducted by the Romanian Aurel Vlaicu on an original airplane, built by himself with two propellers, among them being sited the pilot*

himself. Whenever his car twisted in a place, the head seemed to come over, the world rewarded the Romanian pilot with thunderous ovations, with unimaginable enthusiastic acclamations".

With the same device he participated in the summer of 1913 to the Second Balkan War for aerial observation missions.

He wanted that his experience cumulated to be used to build a new device called Vlaicu III, which had a full metal structure, and he wanted to cross the Carpathians with it. Originally, he wanted to make this flight in August 1913 to participate in the festivities organized by the Transylvanian Association for Romanian Literature and Culture of the Romanian People – ASTRA at Orăștie, but he considered that Vlaicu II device is quite worn off and postponed until the completion of the new Vlaicu III airplane. Meanwhile other pilots announced their intention to do for the first time the flight across the Carpathians. Under these circumstances, it was decided to fly the old device so that on September 13, 1913 he departed from Bucharest. He stops at Ploiesti to power the airplane and takes off for Brasov. He has never arrived. Near the city of Campina, on the outskirts of village Brăneşti, the plane crashes and the constructor loses his life.

Column written by professor eng .Gheorghe Manolea PhD, University of Craiova ,Doctor Honoris Causa of Technical University of Moldova from Chisinau

↵ (11 points)

TITLE OF ARTICLE, MAXIMUM 3 ROWS, ON THE ENTIRE WIDTH OF THE PAGE, (R_TIMES 14 POINTS, BOLD, CENTER, ALL CAPS)

↵ (11 points)

Aurel Bradu, dr.prof. (The name(s) of Authors(s), R_Times, 11 points, bold, Italic, center)

University... (Name of the institution where the Author works, R_Times, 11 points, italic, normal, center)

↵ (11 points)

↵ (11 points)

INTRODUCTION (R_TIMS 13 POINTS, BOLD, CENTER, ALL CAPS)

↵ (11points)

<Tab> The paper may contain an introduction of 20 lines maximum describing the general aspects the background of issues dealt with.

↵ (11 points)

↵ (11 points)

1. TITLE OF THE FIRST CHAPTER, NUMBERED IN ARABIC NUMERALS (R_TIMS 13 POINTS, BOLD, CENTER, TWO COLUMNS, ALL CAPS)

↵ (11 points)

<Tab> In front of each chapter title leave an empty space of two lines. The text of the paper (R_Times, 11 points, normal) begins after chapter titles, after leaving a blank line (↵ 11 points).

↵ (11 points)

1.1. Sample of subtitle with 2 indexes (R_Times 13 points, bold, justify)

↵ (11 points)

<Tab> In front of the text of each title of sub-chapter with two indexes leave a one line empty space. In the text, each new paragraph is marked by the introduction of a „<Tab>".

↵(11 points)

1.1.1.Sample of subtitle with 3 indexes (R_Times 12 points, bold, justify)

<Tab> If the work contains subtitles with three indexes, their text begins directly after subtitle without space. To emphasize the importance of certain words ***within the text they can be entered only by marking them with bold text*** *(without underlining).*

↵ (11 points)

↵ (11 points)

2. INSTRUCTIONS FOR PAPER TYPEWRITING

↵(11 points)

2.1. General aspects

↵(11 points)

<Tab> The works that do not comply with the instructions exactly will be rejected. Paper typewriting is binding in word processor Microsoft Word for Windows '95 / '97 / '98 / '2000, Version 6.0, Version 7.0, Windows NT. Only fonts R_ Times ***(****normal,* ***bold,*** italic, *ALL CAPS, or* ***ALL CAPS)*** *are used for typewriting****.*** *The paper is submitted in one copy, laser or ink get printed, and is accompanied by a floppy disk that will contain „doc files" of the paper and summary****.***

↵ (11 points)

2.2. Page skeleton:

↵(11 points)

<Tab> Page skeleton is the following: Top: 2,0 cm; Bottom: 2,0 cm; Left: 2,0 cm; Right: 2,0 cm; Header: 1,75 cm; Footer: 0

↵(11 points)

2.3. Typewriting format of the paper text:

2.3.1. Writing in two-column format. *The paper text, computing relations, figures and tables are inserted on two columns under this sample:*

Number of Columns: 2; Width: 8.15 cm; Spacing: 0.7 cm.

<Tab> Where the text must contain embedded tables or figures that exceed the column width specified above, to maintain their clarity, you can enter on the page a work area in a single column (between two „session break").

↵(11 points)

2.3.2. The format of writing paragraphs

<Tab> Text of the paper is drawn at a single line (single), all paragraphs are left / right aligned (justify).

2.3.3. Header

<Tab> The „Header" contains the full title of the paper (R_Times, 11 points, ***bold****,* italic*, centered),* ***unless it exceeds one line, situation in which the title is written partially followed by....***

↵(11 points)

2.3.4. Fonts

<Tab> The text of the paper shall be written using only font R_Times, 11 points, normal, (eventual ***R_Times, 11 points, bold,*** *if special highlights of text passages are necessary).* ***Font R_TIMES, BOLD, ALL CAPS*** *are used only for the title and the chapter titles of the paper.*

↵(11 points)

2.3.5. Paper pagination

<Tab> ***THE PAPER IS NOT PAGINATED, as it follows to be inserted in the journal.***

2.4. Figures, tables and mathematical formulas

2.4.1. Figures

<Tab> All figures are inserted in the file „paper.doc". The maximum width of an inserted figure to the text (one column) cannot exceed the column width. All figures are numbered in Arabic numerals and presented according to the sample below. Before and after each figure inserted into the text leave one blank line. If images are inserted, they will be scanned with a minimum resolution of 300 dpi (600 dpi preferable), and will be edited such as to have good contrast. ***It is not allowed sticking photos or drawings on separate sheets. If the figures have annotations*** *in the form of numbers or letters* ***they should have a height of letters equivalent to font*** *R_Times, 11 points, normal,* ***and under the title of figure the legend is inserted with necessary explanations.***

Figure 1. Systematic unitary concept of „R1 integrated in the environment...". *1 – unity; 2 – ensemble...*

↵(11 points)

2.4.2. Tables. *Tables are numbered in Arabic numerals and presented according to the sample below.*

Table 1. Sample of titrating a table.

↵(6 points)

Features /Measurements	***Determ. Nr.1***	***Determ. Nr.2***	***Determ. Nr.3***

↵(11 points)

<Tab> Before and after each table included in the text leave one blank line... All grid lines forming the table have the same thickness (1 point). In the Table the text/figures are written using R_Times font, 11 points, and normal, ***except the head of the table.***

↵(11 points)

2.4.3. Mathematical formulas. *All mathematical formulas are written* ***COMPULSORY*** *with the equation editor of the word processor* ***Microsoft Word for Windows '95/, 97/, 98/, 2000, (Version 6.0, / Version 7.0, 2000), bold, italic, centered according to the sample below.***

↵(6 points)

$$A^2+B^2=C^2 \quad (1)$$

↵(6 points)

2.5. Reference. *Before Reference leave two blank lines... (11 points). Between the title „Reference" and bibliographic references themselves leave one blank line.* References are written according to the sample below:

Reference

(R_Times, 11 points, italic (in bold only the surname and name of author), justify. Sources in Cyrillic characters will be transliterated)

↵(11 points)

1. Nicolescu, A., Stanciu, M. *Static capacity and elastic deformations of the guides // TCMM Conference, Chişinău, pages 141...148, 1996.*

2. Nicolescu, A., Enciu, G. *Design of industrial robots. Meridian Ingineresc No.1, Chişinău, pag.11...20, 1995.*

3. Nicolescu A*. Industrial robot // Patent no. 1344MD. BOPI no. 10, 1999.*

ABSTRACTS

<Tab> ***For each paper submitted to be published in the journal****, it is mandatory to draw up an abstract in ROMANIAN, ENGLISH, FRENCH and RUSSIAN. The abstract should contain a maximum of 10 lines and will be presented following the sample.*

Nicolescu A. **Design of industrial robots.** This paper.....

<Tab> Abstracts are drawn SEPARATELY ***from the paper and are submitted all in one file.***